

R. H. C. LIBRARY	
CLASS	CTCE
No.	Eat
ACC. No.	119,811
DATE ACQ.	1974

Force Fields and Vibrational Absorption Intensities

in Aromatic Molecules

by Valerie Joy Eaton, B. Sc.

A Thesis

presented to the Faculty of Science

of the University of London

in candidature for

the Degree of Doctor of Philosophy

Department of Chemistry,
Royal Holloway College,
(University of London),
Englefield Green,
Surrey.

September 1973

ProQuest Number: 10096796

All rights reserved

INFORMATION TO ALL USERS

The quality of this reproduction is dependent upon the quality of the copy submitted.

In the unlikely event that the author did not send a complete manuscript and there are missing pages, these will be noted. Also, if material had to be removed, a note will indicate the deletion.



ProQuest 10096796

Published by ProQuest LLC(2016). Copyright of the Dissertation is held by the Author.

All rights reserved.

This work is protected against unauthorized copying under Title 17, United States Code.
Microform Edition © ProQuest LLC.

ProQuest LLC
789 East Eisenhower Parkway
P.O. Box 1346
Ann Arbor, MI 48106-1346

University of London

Regulations for

INTERNAL STUDENTS

proceeding to

HIGHER DEGREES

35.1 A thesis ... shall be either a record of original work or an ordered and critical exposition of existing knowledge.

An excellent treatise of the relevant theory and methods has already been presented by my colleague, Dr. R.A.R. Pearce.

It was felt, therefore, that the emphasis of this thesis should be, rather, a detailed account of the origins of the conceptual and experimental details underlying this work.

ABSTRACT

A general quadratic force field, using the overlay technique developed by Schachtschneider and Snyder^[34], was determined for the in-plane vibrations of Benzene and fifteen Fluorine substituted Benzenes by the cyclic refinement of the initial guesses for the force constants, known as the perturbation method. It was necessary to assume a Kekulé' type C-C/C-C interaction relation $(R_i R_{i+1}) = -(R_i R_{i+2}) = (R_i R_{i+3})$, as first introduced by Scherer and Overend^[5]. Removal of this constraint gave rise to linear relationships between the force constants, and satisfactory convergence onto one force field was not obtained. The appropriate force constants of the derived field are compared with those obtained by Duinker^[9, 10] for the in-plane vibrations of Benzene. Although the model used is similar to his, the transferability condition is a severe extra constraint, and the extent of agreement is better than anticipated.

Reassignments of the fundamentals were made for most of the molecules, and spectra were re-examined, where necessary, to obtain Raman polarisation data, and vapour phase infra red band contours.

Biphenyl is known to be planar in the crystal and twisted in solution. The force field for Biphenyl and two deuterated analogues was refined to minimise $(\nu_{\text{obs}} - \nu_{\text{calc}})$. Assuming that the force field does not change with geometry, the vibrational frequencies were calculated for angles of twist in the range $0^\circ < \theta < 90^\circ$ and an estimate obtained for the dihedral angle of the molecule in solution.

Similar calculations were tried for 4,4' difluoro Biphenyl, but as there is insufficient frequency data available, the results were inconclusive.

The combination bands arising from the out-of-plane deformations of the C-H bonds of eight Fluorine substituted Benzenes were investigated, to measure the absolute infra red intensities, and, by a least squares analysis, to derive values for bond moments and bond moment derivatives. Regrettably, studies were limited to 1,4 difluoro Benzene, and, because of experimental difficulties, the intensities measured were so inaccurate that it was impossible to obtain reliable values for the parameters.

A valuable new technique is currently being developed by other workers. In a solution spectrum, bands arising from a γ_{CH} deformation are observed to shift in frequency, and to broaden when CH_3CN is added to the solution. The effects of this phenomenon were investigated for all eight molecules.

ACKNOWLEDGEMENTS

Sincere gratitude is expressed for the advice and guidance given by Dr. D. Steele during the preparation of this thesis and for the personal interest he has taken in this work.

The receipt of a College Scholarship, and a University Studentship are gratefully acknowledged.

Thanks are also due to Dr. R.A.R. Pearce and Dr. R.M. Barrett for the many hours of helpful discussion.

CONTENTS

Page No.

PART I. The Force Fields of the Fluorine
Substituted Benzenes

Chapter One	Some Aspects of Force Constant Calculations for the Planar Normal Modes of Benzene.	15
Chapter Two	Some General Aspects.	53
Chapter Three	The Vibrational Frequencies and other Input Data.	66
Chapter Four	The Force Fields.	129
Chapter Five	Discussion of the Force Fields.	138

PART II. The Dihedral Angle of Biphenyl and some
of its Derivatives.

Chapter Six	The Dihedral Angle of Biphenyl and some of its Derivatives.	153
-------------	--	-----

PART III. Absolute Infra Red Intensities for
some Combination Bands of the Fluorine
Substituted Benzenes.

Chapter Seven	Absolute Infra Red Intensities for some Combination Bands of the Fluorine Substituted Benzenes.	189
References		242

Chapter One : Some Aspects of Force Constant Calculations
for the Planar Normal Modes of Benzene.

Section	1.1	Introduction	15
	1.2	Nomenclature and Related Matters for the Benzene Molecule	18
	1.3	The Force Constant Display Method	25
	1.4	Whiffen's Benzene Force Field	32
	1.5	Duinker's Benzene Force Field	39

Chapter Two : Some General Aspects.

Section	2.1	Potential Function	53
	2.2	Anharmonicity	54
	2.3	Errors in the Observed Data	55
	2.4	Some of the More Important Methods of Overcoming the Indeterminacy in the Force Field	56
	2.5	Additional Data Obtained from Isotopic Molecules	58
	2.6	Band Contour Data Obtained from I.R. Vapour-Phase Studies	59
	2.7	Raman Polarisation Data	62
	2.8	Application of the Product, Sum and Inequality Rules to Molecules which are not Isotopically Related	63

Chapter Three : The Vibrational Frequencies and other Input Data.

Section	3.1	Geometry	66
	3.2	Masses	69
	3.3	Symmetry Point Groups	69
	3.4	Internal Coordinates	73
	3.5	Redundancies	77
	3.6	Transformation from Internal Coordinates to Symmetry Coordinates	78
	3.7	The Vibrational Assignments	95

Chapter Four : The Force Fields.

Section 4.1	Introduction	129
4.2	Scaling of Force Constants	130
4.3	Absolute/Percentage Weighting	133
4.4	Statistical Dispersion	134
4.5	Problems arising during the Force Constant Refinement Process	135

Chapter Five : Discussion of the Force Fields.

Section 5.1	Selection of the Parameters for the Modified Valence Force Field	138
5.2	The Force Fields Obtained using the Constraint $(R_i R_{i+1}) = -(R_i R_{i+2}) = (R_i R_{i+3})$	141
5.3	The Effects of Lifting the Constraint $(R_i R_{i+1}) = -(R_i R_{i+2}) = (R_i R_{i+3})$	142
5.4	Choice between the Two Alternative Solutions for the B_{2u} Species.	149

Chapter Six : <u>The Dihedral Angle of Biphenyl and some of its Derivatives.</u>	
Section 6.1 Introduction	153
6.2 Theoretical Predictions	155
6.3 The Initial Calculations	160
6.4 A Discussion of the Observed and Calculated Frequency Shifts for Biphenyl on a Change of State.	161
6.5 The Frequency Shifts Observed for D ₂ Biphenyl and D ₁₀ Biphenyl on a Change of State.	163
6.6 A Discussion of the Observed and Calculated Frequency Shifts for 4,4' Difluoro Biphenyl	163
6.7 The Perturbation of Vibrational Energy Levels	177
6.8 The Refining of the Force Field for Biphenyl, D ₂ Biphenyl and D ₁₀ Biphenyl, and the Estimate for the Dihedral Angle	178
6.9 The Refining of the Force Field for 4,4' Difluoro Biphenyl	186
Chapter Seven : <u>Absolute Infra Red Intensities for some Combination Bands of the Fluorine Substituted Benzenes.</u>	
Section 7.1 Introduction	189
7.2 Absolute Intensities of Combination Bands	198
7.3 A Discussion of the γ_{CH} Combination Bands observed for the Fluorine substituted Benzenes	202
7.4 Computation of $\left(\frac{\partial^2 \mu}{\partial q_i \partial q_j} \right)$	232

TABLES

Page No.

Table 1.1	Comparison of the Symbolisms used by Whiffen, Duinker and Eaton for the Benzene Force Field	19
1.2	Symmetry Properties of the Planar Normal Coordinates of Benzene under the Symmetry Operations of the Point Group D_{6h}	22
1.3	Planar Symmetry Coordinates for Benzene, including E_{1u} Redundancy	24
1.4	The 37 Planar Latin Force Constants	36
1.5	Whiffen's 26 Planar Latin Force Constants by Removal of Explicit Mention of the 7 Force Constants in Italic Brackets	36
1.6	Whiffen's 19 Parameter Benzene Force Field	36
1.7	Duinker's 13 Parameter Benzene Force Field	36
1.8	Transformation from Internal to Symmetry Force Constant Representation	38
Table 2.1	Band Types	60
Table 3.1	Orientation of the Cartesian Axes	70
3.2	The Symmetry Point Groups and the Symmetry Species of the In-Plane Vibrations of the Fluorine Substituted Benzenes	72
3.3	Atoms Involved in a C-C Stretch	74
3.4	Atoms Involved in a C-X Stretch, X = H or F	75
3.5	Atoms Involved in an Angle Bend	75
3.6	Atoms Involved in an In-Plane Angle Bend	75
3.7 - 3.13	The U Matrices	80
3.14- 3.30	The Fundamental Vibrations and their Symmetry Assignments	96
3.31	Fundamental Frequencies of Hexafluoro Benzene	125
3.32	Infra Red Active Binary Summations for D_{6h}	126
3.33	Raman Active Binary Summations for D_{6h}	126
3.34	Possibilities for Assignment of Summation Bands of Hexafluoro Benzene	127

	<u>Page No.</u>
Table 4.1 A Comparison of the two Common Sets of Units	132
Table 5.1 $(R_i R_{i+1}) = -(R_i R_{i+2}) = (R_i R_{i+3})$ - the Kekulé-type C-C/C-C interaction relation	144
5.2 $(R_i R_{i+1}), (R_i R_{i+2}), (R_i R_{i+3})$ included as separate parameters	146
5.3 Comparison of the Force Constants for the In-Plane Vibrations of Benzene of Eaton and Duinker	148
Table 6.1 The 20 Parameter S.V.F.F. used to Calculate the In-Plane Vibrational Frequencies of Biphenyl	165
6.2 The Initial Values of the 37 Parameter M.V.F.F. for Biphenyl, D_2 Biphenyl and D_{10} Biphenyl	167
6.3 The Convergence of the In-Plane Force Field	168
6.4 The Convergence of the Out-of-Plane Force Field	169
6.5 The Final Values of the 37 Parameter M.V.F.F. for Biphenyl, D_2 Biphenyl and D_{10} Biphenyl	171
6.6 The Calculated Frequencies for the $B_{1g}, B_{1u}, B_{2u}, B_{2g}$ species of Biphenyl at each stage of the Perturbation	172
6.7 The Observed Frequencies used in the Calculations	173
Table 7.1 The Observed Frequencies in cm^{-1} used for the Out-of-Plane Vibrations	218
7.2 The Absolute Intensity of the 1862 cm^{-1} Band of 1,4 Difluoro Benzene	230
7.3 The Absolute Intensity of the 1736 and 1757.5 cm^{-1} Bands of 1,4 Difluoro Benzene	230
7.4 The Absolute Intensity of the $1736, 1757.5$ and 1772 cm^{-1} Bands of 1,4 Difluoro Benzene	230
7.5 The Absolute Intensity of the 1631.5 cm^{-1} Band of 1,4 Difluoro Benzene	231

FIGURES

Page No.

Figure 1.1	Numbering of the Atoms and Orientation of the Axes in Benzene	20
1.2	Force Constant Display Graph for the A_{1g} Species	28
1.3	Force Constant Display Graph for the B_{1u} Species	29
1.4	Force Constant Display Graph for the B_{2u} Species	30
1.5	Definition of Redundant Coordinate Representation around Carbon Atom C_i	
Figure 2.1	The Orientation of x, y, z Axes in a C_{2v} Molecule	59
Figure 3.1	Geometry of Fluoro Benzene	67
3.2	Numbering of Atoms Involved in an Angle Bend	67
3.3	Numbering of Atoms Involved in an In-Plane Angle Bend	76
3.4	Numbering of the Atoms	46
3.5	Definition of Redundant Coordinate Representation around Carbon Atom C_i	47
3.6	C_s Symmetry Point Group	79
3.7	C_{2v} Symmetry Point Group	81
3.8	C_{2v} Symmetry Point Group	83
3.9	C_{2v} Symmetry Point Group	85
3.10	D_{2h} Symmetry Point Group	87
3.11	D_{3h} Symmetry Point Group	89
3.12	D_{6h} Symmetry Point Group	92
Figure 6.1	Relationships Between Vibrations of Different Symmetry Species in the D_{2h} , D_2 and D_{2d} Configurations	158
6.2	Numbering of the Carbon Atoms	159
6.3	Demonstrating the Motions Associated with Certain Interaction Force Constants 6.4 and 6.5 Calculated	166
	Frequency vs Dihedral Angle	184
		185

SPECTRA

Figure 7.1	Fluoro Benzene	209
7.2	1,2 Difluoro Benzene	211
7.3	1,3 Difluoro Benzene	213
7.4	1,4 Difluoro Benzene	215
7.5	1,3,5 Trifluoro Benzene	217
7.6	1,2,3,4 Tetrafluoro Benzene	219
7.7	1,2,3,5 Tetrafluoro Benzene	221
7.8	1,2,4,5 Tetrafluoro Benzene	223
7.9	1,4 Difluoro Benzene/ $\text{CH}_3\text{CN}/\text{CCl}_4$ - 1862 cm^{-1} Band	226
7.10	1,4 Difluoro Benzene - 1862 cm^{-1} Band	227
7.11	1,4 Difluoro Benzene/ $\text{CH}_3\text{CN}/\text{CCl}_4$ - 1736 cm^{-1} Band	228
7.12	1,4 Difluoro Benzene - 1736 cm^{-1} Band	229

PART 1

The Force Fields of the Fluorine-Substituted

Benzenes

CHAPTER ONESome Aspects of Force Constant Calculations for the Planar Normal Modes of BenzeneSection 1.1 Introduction

Over the past twenty-five years, the force field of Benzene has been the subject of some intensive research. Because there is not sufficient frequency data available on Benzene and its isotopic species to determine the most general harmonic force field, a number of different sets of force constants have been published. The most important of these calculations may be summarised into four main groups.

Calculations by Crawford and Miller^[1], using a modified valence force field with a number of interaction constants set to zero, were revised and modified by Whiffen^[2], and then further revised by Albrecht^[3].

Calculations based on a Urey Bradley model, by Califano and Crawford^[4], were revised and modified by Scherer and Overend^[5], and further revised by Scherer^[6].

Recently, Scherer^[6, 7] published an alternative modified valence force field, which differs considerably from Whiffen's.

Although all of these force fields give a satisfactory fit to frequency data on Benzene and most of its deuterated isotopic species, and can be transferred (with the necessary additions) to other aromatic molecules derived from Benzene, they lead to incorrect calculated values for the Coriolis zeta constants of Benzene and Hexadeutero Benzene relating the two components of the E_{2g} species vibration ν_6 which have been reported by Callomon et al^[8], and so the problem was re-examined by Mills^[9] and Duinker^[10], using a modified valence force field based on the hybrid orbital model, developed by Mills^[11]. While this is considered

to be the most reliable force field for the in-plane vibrations of Benzene, a close examination of the work done by Whiffen is very necessary, as the framework of the problem and its solution is presented there.

The vibrational problem for planar molecules can be considerably simplified by factorising the Secular Matrix to separate the in-plane and out-of-plane vibrations. Following Herzberg^[12], the x and y axes lie in the plane of the molecule, and the z axis is perpendicular to it. When these axes are reflected at the plane,

$$x \xrightarrow{\sigma(xy)} x \quad y \xrightarrow{\sigma(xy)} y \quad z \xrightarrow{\sigma(xy)} -z$$

An in-plane internal coordinate R_i (i.e. a bond stretch, an angle bend, or an in-plane angle bend) involves motion in the x and y directions only. On reflection at the plane,

$$R_i \xrightarrow{\sigma(xy)} R_i$$

An out-of-plane internal coordinate (i.e. an out-of-plane angle bend, a torsion or a special torsion) involves motion in the z direction only. On reflection at the plane,

$$R_j \xrightarrow{\sigma(xy)} -R_j$$

On reflection at the plane, the terms involving R_i and R_j in the Kinetic and Potential Energy expressions change sign,

$$g_{i,j}^{-1} \dot{R}_i \dot{R}_j \xrightarrow{\sigma(xy)} -g_{i,j}^{-1} \dot{R}_i \dot{R}_j$$

$$f_{i,j} dR_i dR_j \xrightarrow{\sigma(xy)} -f_{i,j} dR_i dR_j$$

Since the Kinetic and Potential Energies must be invariant under all symmetry operations

$$g_{i,j}^{-1} = 0 \quad f_{i,j} = 0$$

If P_i is the momentum conjugate with R_i , then since

$$g_{i,j} P_i P_j \xrightarrow{\sigma(xy)} -g_{i,j} P_i P_j$$

it also follows that $g_{i,j} = 0$

Therefore the G and F matrices can each be factored into two blocks, G_{xy} and G_z , and F_{xy} and F_z . Thus

$$\begin{vmatrix} G_{xy} & 0 \\ 0 & G_z \end{vmatrix} \begin{vmatrix} F_{xy} & 0 \\ 0 & F_z \end{vmatrix} = \begin{vmatrix} G_{xy} F_{xy} & 0 \\ 0 & G_z F_z \end{vmatrix}$$

When the in-plane vibrations are considered, only the G_{xy} and F_{xy} matrix need to be constructed.

Radcliffe and Steele^[13] fitted a 15 parameter force field to the fundamental frequencies of the out-of-plane vibrations of Benzene, Fluoro Benzene, 1,4 difluoro Benzene and their fully deuterated analogues, which formed the starting field for the calculations of Pearce^[14], who then fitted a 23 parameter force field to the out-of-plane vibrations of 20 Fluorine substituted Benzenes.

The work reported in this thesis is concerned with the other half of the problem - the fitting of a force field to the in-plane vibrations of this set of Fluorine substituted Benzenes (less the three molecules 1,2,3-, 1,3,5-D₁- and 1,3,5-D₂-trifluoro Benzene).

Section 1.2 Nomenclature and Related Matters for the Benzene Molecule

Both in this work and that of Duinker^[10], Whiffen^[2] has been followed in the conventions used for the orientation of the axes, the definition of the internal displacement coordinates, and, with one reservation, explained in detail later, the symmetry coordinates.

Nomenclature

The correct symbolism for the description of internal force constants is of the form

$$f_{r_o R_o \beta_j} (\alpha_{j+1} - \alpha_{j-1})$$

and is explicit and unambiguous. It is, however, very cumbersome to write, and a printer's nightmare. Whiffen introduced a set of Latin force constants, which were adopted, or rather adapted, by Duinker.

In this work, it was necessary to specify not only the substituent involved in the deformation, but also the environment. Use of the formal symbolism would have been exceedingly complex and so a condensed form of symbolism was introduced^[15].

Diagonal force constants are represented by the symbol for the coordinate alone. The substituent is in parentheses. Post superscripts show the substituents in the ortho position.

Interaction force constants are represented by enclosing the symbols for the two internal deformation coordinates in parentheses. The relative positions of the coordinates are indicated by subscripts on the symbols. Each subscript refers to the carbon atom of the ring, either to which the the substituent involved in the motion is attached, which forms the central atom of the α , or is the first atom counting clockwise of R.

Duinker	Whiffen	Subscript on f	Eaton
D	\tilde{D}	ΔR_j^2	R^{HH}
d	\tilde{d}_o	$\Delta R_j \Delta R_{j+1}$	$(R_i R_{i+1})$
-d	\tilde{d}_m	$\Delta R_j \Delta R_{j+2}$	$(R_i R_{i+2})$
d	\tilde{d}_p	$\Delta R_j \Delta R_{j+3}$	$(R_i R_{i+3})$
E	E	Δr_j^2	$r^{HH}(H)$
	e_o	$\Delta r_j \Delta r_{j+1}$	$(r_i(H) r_{i+1}(H))$
	e_m	$\Delta r_j \Delta r_{j+2}$	\circ
	e_p	$\Delta r_j \Delta r_{j+3}$	
F	\tilde{F}	$R_o^2 \alpha_j^2$	$\alpha(H)$
f_o	f_o	$R_o^2 \alpha_j \alpha_{j+1}$	$(\alpha_i \alpha_{i+1})$
G	G	$r_o^2 \beta_j^2$	$\beta^{HH}(H)$
g_o	g_o	$r_o^2 \beta_j \beta_{j+1}$	$(\beta_i(H) \beta_{i+1}(H))$
g_m	g_m	$r_o^2 \beta_j \beta_{j+2}$	$(\beta_i(H) \beta_{i+2}(H))$
g_p	g_p	$r_o^2 \beta_j \beta_{j+3}$	$(\beta_i(H) \beta_{i+3}(H))$
h_o	\tilde{h}_o	$\Delta r_j (\Delta R_j + \Delta R_{j-1})$	$(r_i(H) R_i)$
	\tilde{h}_m	$\Delta r_j (\Delta R_{j+1} + \Delta R_{j-2})$	
	\tilde{h}_p	$\Delta r_j (\Delta R_{j+2} + \Delta R_{j-3})$	
i_o	\tilde{i}_o	$R_o \alpha_j (\Delta R_j + \Delta R_{j-1})$	$(\alpha_i R_i)$
j_o	\tilde{j}_o	$r_o \beta_j (\Delta R_j - \Delta R_{j-1})$	$(\beta_i(H) R_i)$
	\tilde{j}_m	$r_o \beta_j (\Delta R_{j+1} - \Delta R_{j-2})$	$(\beta_i(H) R_{i+1})$
	\tilde{j}_p	$r_o \beta_j (\Delta R_{j+2} - \Delta R_{j-3})$	
k	\tilde{k}	$R_o \alpha_j \Delta r_j$	$(\alpha_i r_i(H))$
	\tilde{k}_o	$R_o \alpha_j (\Delta r_{j+1} + \Delta r_{j-1})$	
	l_o	$r_o \beta_j (\Delta r_{j+1} - \Delta r_{j-1})$	
	l_m	$r_o \beta_j (\Delta r_{j+2} - \Delta r_{j-2})$	
n_o	\tilde{n}_o	$r_o R_o \beta_j (\alpha_{j+1} - \alpha_{j-1})$	$(\beta_i(H) \alpha_{i+1})$

} as
Duinker

TABLE 1.1 Comparison of the symbolisms used by Whiffen, Duinker and Eaton, for the Benzene force field.

Table 1 shows, for the Benzene force field, the formal symbolism, the Latin force constants introduced by Whiffen, Duinker's adaptation of these, and the symbolism adopted in this work.

Orientation of the Axes and Numbering of the Atoms

In the equilibrium configuration, Benzene has a regular planar hexagonal structure with symmetry D_{6h} . In accordance with the recommendations of Mulliken^[16], the z axis is chosen to coincide with the C_6 axis, and the y axis passes through carbon atoms 1 and 4, if the carbon atoms are numbered 1 to 6 in clockwise order as viewed from a point on the positive axis.

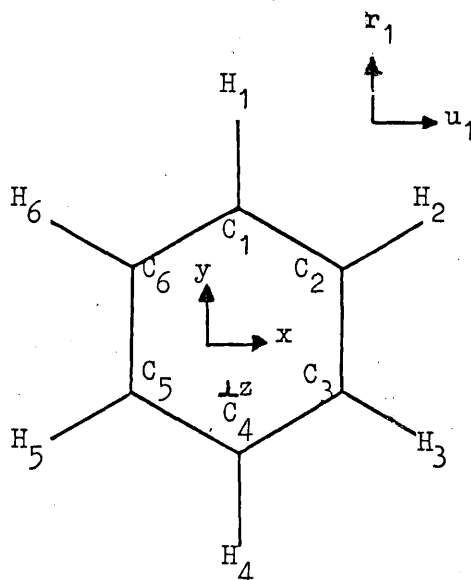


Fig. 1.1

Definition of the Internal Deformation Coordinates

The CARTESIAN coordinates for motion of the i^{th} carbon atom from its equilibrium position in the radial, the z , and the mutually perpendicular direction counted positive in a clockwise sense may be taken as \bar{R}_i , Z_i and U_i and likewise for the H atoms \bar{r}_i , z_i and u_i .

The VALENCY or INTERNAL DEFORMATION coordinates, known thereafter as INTERNAL COORDINATES, are defined in Wilson, Decius and Cross^[17], Chapter 4. The in-plane deformations are

- R_i stretching of the $C_i - C_{i+1}$ bond
- r_i stretching of the $C_i - H_i$ bond
- α_i increase of the ring angle $C_{i-1} - C_i - C_{i+1}$
- β_i bending of the $C_i - H_i$ bond relative to the external bisector of the $C_{i-1} - C_i - C_{i+1}$ angle. β_i is defined to be positive when the H atom moves towards the C_{i-1} atom.

The internal coordinates can be expressed in terms of the right-handed system \bar{R}, Z, U as

$$R_i = (2^{-1})(\bar{R}_i + \bar{R}_{i+1}) - (3^{\frac{1}{2}} 2^{-1})(U_i - U_{i+1})$$

$$r_i = \bar{r}_i - \bar{R}_i$$

$$\alpha_i = (3^{\frac{1}{2}} 2^{-1})(\bar{R}_{i-1} - 2\bar{R}_i + \bar{R}_{i+1}) + (2^{-1})(U_{i-1} - U_{i+1})$$

$$\beta_i = U_i - u_i + (3^{\frac{1}{2}} 4^{-1} \rho)(\bar{R}_{i-1} \bar{R}_{i+1}) + (4^{-1} \rho)(U_{i-1} + 2U_i + U_{i+1})$$

where $\rho = r_0/R_0$

R_0 is the $C_i - C_{i+1}$ distance

r_0 is the $C_i - H_i$ distance.

TABLE 1.2 Symmetry Properties of the Planar Normal Coordinates of Benzene under the Symmetry Operations of the Point Group D_{6h}

	E	$2C_6$	$2C_3$	C_2	$3C_2'$	$3C_2''$	i	$2S_3$	$2S_6$	σ_h	$3\sigma_d$	$3\sigma_v$
A_{1g}	1	1	1	1	1	1	1	1	1	1	1	1
A_{2g}	1	1	1	1	-1	-1	1	1	1	1	-1	-1
E_{2g}	2	-1	-1	2	0	0	2	-1	-1	2	0	0
B_{1u}	1	-1	1	-1	1	-1	-1	1	-1	1	-1	1
B_{2u}	1	-1	1	-1	-1	1	-1	1	-1	1	1	-1
E_{1u}	2	1	-1	-2	0	0	-2	-1	1	2	0	0

Normal Coordinate Representation

The planar vibrational normal coordinate representation is

$$\Gamma(Q)_v = 2a_{1g} + a_{2g} + 4e_{2g} + 2b_{1u} + 2b_{2u} + 3e_{1u}$$

The rotational normal coordinate representation is

$$\Gamma(Q)_r = a_{2g} + e_{1g}$$

The translational normal coordinate representation is

$$\Gamma(Q)_t = a_{2u} + e_{1u}$$

Removal of the Redundant Coordinate

The elimination of the redundancy in the E_{1u} species, which arises because there are only 21 independent planar symmetry coordinates, has led to complications. If the four redundancy symmetry coordinates are denoted S_{18} , S'_{19} , S_{20} , S'_{21} , the redundancy is then removed by the orthogonal transformation

$$\begin{bmatrix} S_{19} \\ S_r \end{bmatrix} = \frac{1}{\sqrt{2}} \begin{bmatrix} +1 & -1 \\ +1 & +1 \end{bmatrix} \begin{bmatrix} S'_{19} \\ S'_{21} \end{bmatrix} \quad (1)$$

where S_r is the redundant coordinate, identically equal to zero.

Crawford and Miller^[1] used this transformation, but their use of the same notation for the symmetry coordinates before and after transformation leads to confusion. Whiffen^[2] used the coordinates S_{18} , S'_{19} and S_{20} directly, which amounts to using a non-orthogonal matrix.

In order to obtain the correct relation between the signs of observed and calculated zeta constants $\sum_{ja,jb}^z$, it is important to follow the convention recommended by Boyd and Longuet-Higgins^[18] which requires that

$$C_6(S_{ja} + i S_{jb}) = e^{-i\Theta} (S_{ja} + S_{jb}) C_6 \quad (2a)$$

where $\Theta = +2\pi/6$ for an E_1 species, and $+4\pi/6$ for an E_2 species.

Whiffen's Table 1^[2] implies that the coordinates (S_{ja}, S_{jb}) $i = 18, 19$ and 20 all transform under all the symmetry operations of the point group like the components of the dipole moment (μ_y, μ_x) instead of $(\mu_y, -\mu_x)$.

Whiffen's definition of the E_{2g} species coordinates S_6 , S_7 , S_8 and S_9 do not follow the convention as they satisfy $\Theta = -4\pi/6$. Mills^[9] thought to reverse the signs of these coordinates (whenever possible) for all isotopic species. In the sym Trideutero Benzene molecule, the E_{1u}

Planar symmetry coordinates for Benzene; including E_{1u} redundancy [9]

D_{6h} Class	Sym. Coord.	coefficient for i =							Int. Coord.
		1	2	3	4	5	6	N	
A_{1g}	S_1	1	1	1	1	1	1	$6^{-\frac{1}{2}}$	R_i
	S_2	1	1	1	1	1	1	$6^{-\frac{1}{2}}$	r_i
A_{2g}	S_3	1	1	1	1	1	1	$6^{-\frac{1}{2}}$	β_i
B_{1u}	S_{12}	-1	1	-1	1	-1	1	$6^{-\frac{1}{2}}$	α_i
	S_{13}	-1	1	-1	1	-1	1	$6^{-\frac{1}{2}}$	r_i
B_{2u}	S_{14}	-1	1	-1	1	-1	1	$6^{-\frac{1}{2}}$	R_i
	S_{15}	-1	1	-1	1	-1	1	$6^{-\frac{1}{2}}$	β_i
E_{2g}	S_{7a}	-2	1	1	-2	1	1	$12^{-\frac{1}{2}}$	r_i
	S_{7b}	0	-1	1	0	-1	1	2^{-1}	r_i
	S_{8a}	-1	2	-1	-1	2	-1	$12^{-\frac{1}{2}}$	R_i
	S_{8b}	-1	0	1	-1	0	1	2^{-1}	R_i
	S_{9a}	0	-1	1	0	-1	1	2^{-1}	β_i
	S_{9b}	2	-1	-1	2	-1	-1	$12^{-\frac{1}{2}}$	β_i
	S_{6a}	-2	1	1	-2	1	1	$12^{-\frac{1}{2}}$	α_i
	S_{6b}	0	-1	1	0	-1	1	2^{-1}	α_i
E_{1u}	S_{18a}	0	1	1	0	-1	-1	2^{-1}	β_i
	S_{18b}	2	1	-1	-2	-1	1	$12^{-\frac{1}{2}}$	β_i
	S'_{19a}	-1	0	1	1	0	-1	2^{-1}	R_i
	S'_{19b}	1	2	1	-1	-2	-1	$12^{-\frac{1}{2}}$	R_i
	S_{20a}	-2	-1	1	2	1	-1	$12^{-\frac{1}{2}}$	r_i
	S_{20b}	0	1	1	0	-1	-1	2^{-1}	r_i
	S'_{21a}	-2	-1	1	2	1	-1	$12^{-\frac{1}{2}}$	α_i
	S'_{21b}	0	1	1	0	-1	-1	2^{-1}	α_i

Whiffen removes the E_{1u} redundancy, and uses coordinates

S_{18a} , S_{18b} , S'_{19a} , S'_{19b} , S_{20a} , S_{20b}

Duinker reverses all the signs of the E_{2g} species.

Table 1.3

and E_{2g} species of D_{6h} merge to form the E' species of D_{3h} , and if all the seven pairs of (S_{ja}, S_{jb}) coordinates are to form a correct basis for the E' species without modification they must be chosen in the way that Whiffen chose them - so that they contravene the convention in the E_{2g} species. Applying the operation C_6 a second time to both sides of (1) gives (since $C_6^2 = C_3$)

$$C_3(S_{ja} + i S_{jb}) = e^{-i2\Theta} (S_{ja} + i S_{jb}) C_3 \quad (2b)$$

If the coordinates in the E_{2g} species are chosen to satisfy $\Theta = +2\pi/3$ in (2a) then $2\Theta = +4\pi/3 = -2\pi/3 \pmod{2\pi}$ in (2b) which contravenes the convention for the D_{3h} point group. There is no solution to this paradox: if the E_{2g} coordinates are chosen to satisfy the convention in D_{6h} , they will not satisfy it in D_{3h} and vice versa. It is easier to retain Whiffen's definitions of the symmetry coordinates and to reverse the sign of all calculated zeta constants in the E_{2g} species before comparing with the "observed" values, which are obtained by analysing a spectrum making use of certain selection rules in order to deduce the energy levels from the spectra. However the energy level formulae and the selection rules are based on the assumption that the convention has been correctly followed in defining the coordinates and the zeta constant, and reversing the convention proves to be equivalent to reversing the sign of the effective zeta constant.

Duinker^[10] preferred to reverse the signs of the E_{2g} species.

Section 1.3 The Force Constant Display Method

Before describing in detail the work of Whiffen^[2] and Duinker/Mills^[9,10] it is necessary to show that because the frequency data is not sufficient

to uniquely define the symmetry (and hence the internal) force constants, it is the way the constraints on the force field were chosen that led to two completely different force fields.

If the problem of determining the force constant parameters of an assumed type of field from vibrational data is expressed in a suitable symmetry coordinate basis set, then for a species of order 2, there is a simple way of representing the family of acceptable solutions. [26,27,28,29]

If the vibrational data for a 2 x 2 species of both Benzene and Hexadeutero Benzene is considered, then, to obtain information additional to that derived from the Benzene vibrational data, the isotopic substitution must produce changes in the vibrational frequencies of that species. The product rule (explained in a later chapter), which relates the frequencies to the nuclear masses and geometry, implies that there are only three independent pieces of vibrational data. The experimental frequencies will be subject to experimental uncertainties and will also either be uncorrected for anharmonicity or have been corrected using a correlation factor of some specific uncertainty. To produce the best fit of parameters to data, a least squares analysis is therefore required.

A second, much more serious difficulty arises because of the quadratic nature of the problem. The secular equation may be written

$$\begin{vmatrix} G_{11} F_{11} + G_{12} F_{12} - \lambda, & G_{11} F_{12} + G_{12} F_{22} \\ G_{12} F_{11} + G_{22} F_{12}, & G_{12} F_{12} + G_{22} F_{22} - \lambda \end{vmatrix} = 0$$

The G elements and the roots λ are known. In conjugation with a third equation for the isotopically substituted molecules the F_{ij} are derivable from a quadratic equation in G and λ . Thus two sets of equations are found, both acceptable on mathematical grounds. The force constant display graphs show, for each isotopic species, the complete family of

force fields which reproduce the two vibration wavenumbers as a function of one free parameter, which we take to be the interaction force constant. The two sets of curves should intersect for the same value of F_{12} . Their failure to do so is a measure of the incompatibility of the two sets of frequencies to a quadratic force field. Whether the solution is well-determined or whether it still leaves a large ambiguity in the parameters depends on the angle under which the ellipses for the isotopic molecules intersect.

In matrix notation, the frequency parameters λ_k are the eigenvalues of GF or

$$\begin{aligned} \left| \begin{array}{c} GF - E \lambda \\ \hline GF L = L \Lambda \end{array} \right| &= 0 \end{aligned} \quad (1)$$

GF is not symmetric. Because G is a positive definite symmetric matrix, the lower triangular matrix A can be calculated such that

$$AA^t = G \quad (2)$$

(1) transforms to

$$(A^t F A) A^{-1} L = A^{-1} L \Lambda \quad (3)$$

From (3) it follows that the eigenvalues of $(A^t F A)$ are the same as those of GF. Furthermore, $A^t F A$ is symmetric; therefore the matrix that diagonalizes $A^t F A$ is an orthogonal matrix P. P is chosen to be

$$\begin{aligned} P &= \begin{bmatrix} \cos \psi & -\sin \psi \\ \sin \psi & \cos \psi \end{bmatrix} \\ A^t F A P &= P \Lambda \quad \text{or} \\ F &= (A^{-1})^t P \Lambda P^t A^{-1} \end{aligned} \quad (4)$$

A whole family of solutions F_{1-1} , F_{1-2} , F_{2-2} (all of which reproduce the two frequencies), can be calculated in a systematic way by calculating the right hand side of (4) for a range of ψ values, inserting for the diagonal elements of Λ , the values λ_1 (obs) and λ_2 (obs).

Of the six symmetry species for Benzene, three are of order 2. An estimate of the symmetry force constants for these species can be obtained.

A_{1g} species

The coordinates involved are $S_1(R)$ and $S_2(r)$. The observed frequencies are 3073 and 993 cm^{-1} for Benzene and 2303 and 945 cm^{-1} for Hexadeutero Benzene. Because the product rule fails for the observed wavenumbers, the intersection between the two pairs of curves do not lie one above the other, and so a vertical line cannot be drawn in through the two points of intersection, which would define an acceptable force field for both isotopic species. As the intersections occur at a small angle, satisfactory compromise solutions are given by force fields in the following ranges:-

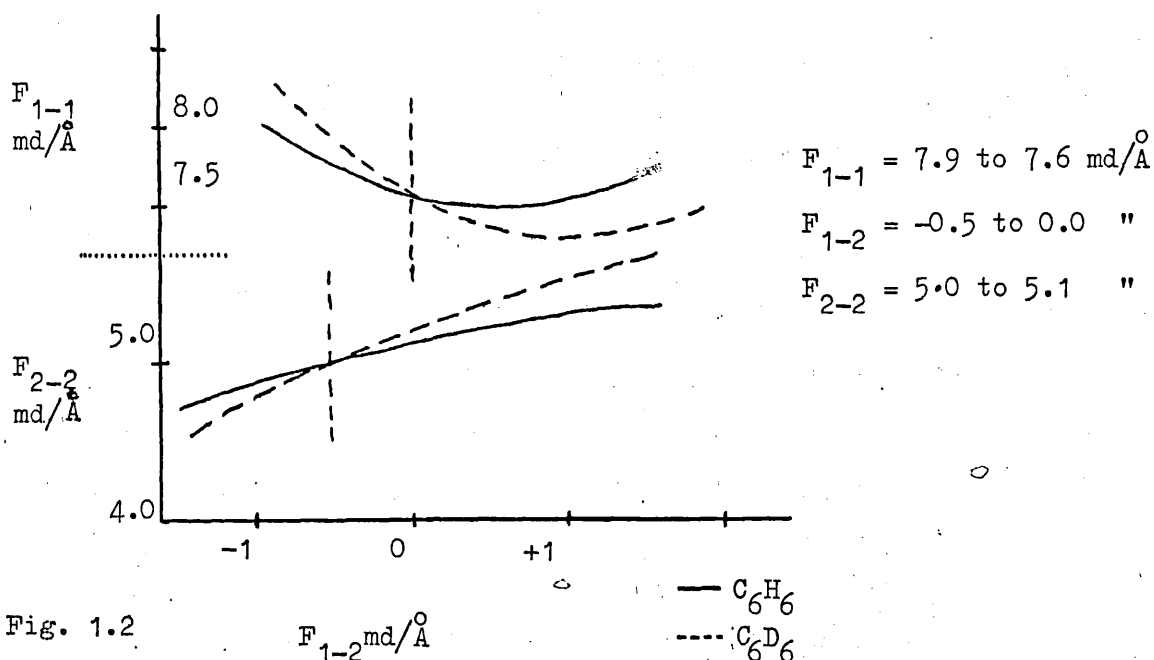


Fig. 1.2

B_{1u} species

The coordinates involved are $S_{12}(\alpha)$ and $S_{13}(r)$. The observed frequencies are 3057 and 1010 cm^{-1} for Benzene, and 2285 and 970 cm^{-1} for Hexadeutero Benzene. Again the intersections occur at a narrow angle, and acceptable force fields are given by constants in the following ranges.

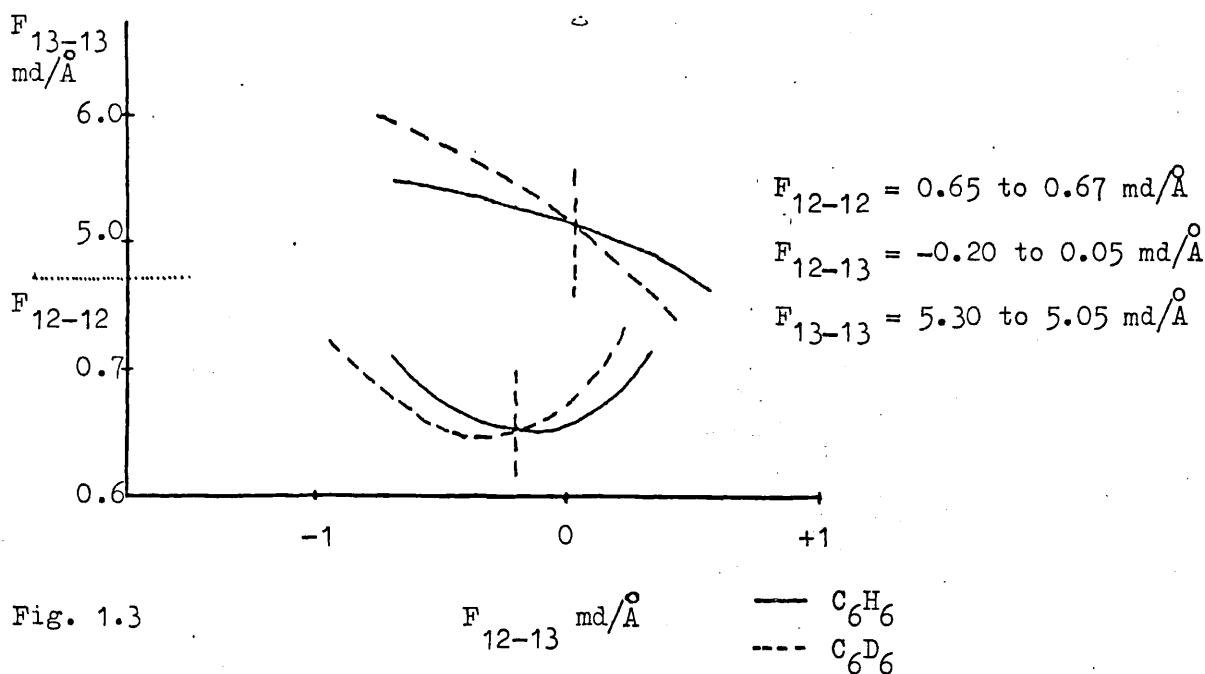


Fig. 1.3

B_{2u} species

The coordinates involved are $S_{14}(R)$ and $S_{15}(\beta)$. Displacements in S_{14} carry the structure of the molecule towards one or other of the two Kekulé structures and it is generally assumed that such displacements will correspond to a lower force constant than normally expected for a C-C ring. Following the Mair and Hornig assignment^[19], rather than that of Ingold^[20,21] the observed frequencies are 1309 and 1146 cm^{-1} for Benzene and 1282 and 824 cm^{-1} for Hexadeutero Benzene. The intersections

between the Benzene and Hexadeutero Benzene curves occur at a sharper angle, which implies two distinct alternative solutions to the force field, corresponding to the interactions on the left and the right of the figure respectively.

These solutions are:-

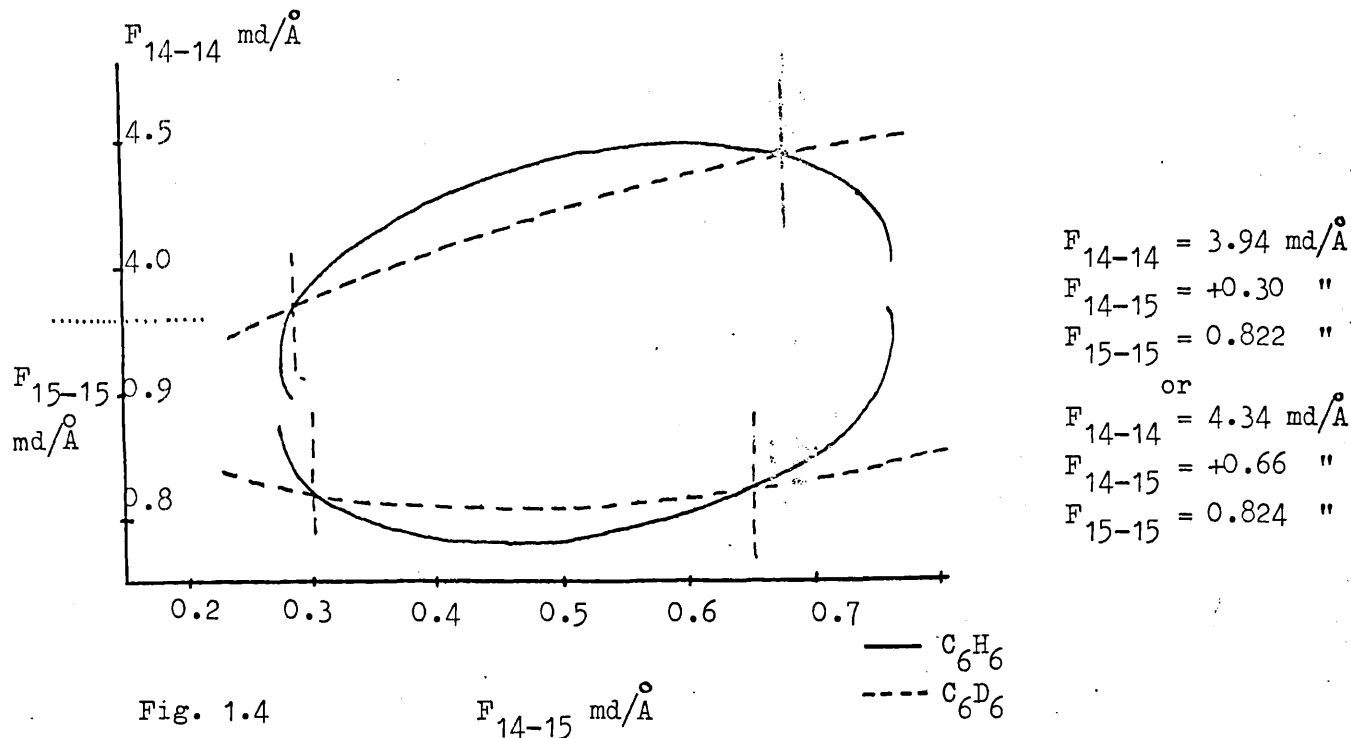


Fig. 1.4

Whiffen^[2] chose the first solution, because of the smaller interaction force constants, and Duinker^[9,10] chose the second because the values are consistent with his calculated values for the E_{2g} species.

The other three species are as follows:-

A_{2g} species

As there is only one coordinate in the symmetry species, no ambiguity arises. The motion represents twisting of the H atoms against the ring. In Benzene the frequency occurs at 1350 cm^{-1} ; in Hexadeutero Benzene at 1059 cm^{-1} . The two frequencies fix F_{3-3} at $0.863 \text{ md}/\text{\AA}$.

E_{2g} species

The four pairs of coordinates involved are $S_6(\alpha)$, $S_7(r)$, $S_8(R)$ and $S_9(\beta)$ and the most general harmonic force field contains 10 independent force constants. The force field is thus very much under-determined by the available data. In addition there is no simple method of plotting out the acceptable family of solutions to the force field in the manner used for the (2 x 2) species: indeed the data available leave free parameters in the force field, so that the family of acceptable force fields must be several-fold infinite. Additional information, not available to Whiffen, is given by data on the Coriolis constant $\xi_{6a,6b}$ (denoted ξ_6 for brevity) for both Benzene and Hexadeutero Benzene.

E_{1u} species

After eliminating the redundancy, this species contains the three coordinates $S_{18}(\beta)$, $S_{19}(\alpha \text{ and } R)$ and $S_{20}(r)$ and there are thus six independent force constants in the most general harmonic force field. The wavenumbers of the fundamentals of Benzene and Hexadeutero Benzene leave considerable freedom in the choice of these six force constants and, as for the E_{2g} species, there is no simple way of representing the family of acceptable solutions to the force field analogous to the force constant display graphs for the (2 x 2) species. Duinker found, from trial calculations, that one well-determined zeta constant for any one of the three fundamentals of this species would greatly limit the family of acceptable force fields.

Until about five years ago, Whiffen's field was accepted as the best approximation which could be made on the frequency data available for Benzene and its deuterium substituted analogues, and transference of the force constants to other systems invariably produced good frequency data.

However, when a first order Coriolis constant ξ_6 for one of the e_{2g} vibrations of both Benzene and Hexadeutero Benzene was reported by Callomon et al^[8], the field failed to reproduce the data. As this zeta constant provides a considerable restriction on the possible form of the normal vibrations in the E_{2g} species, which are of particular interest, Duinker and Mills^[9, 10] were prompted to re-examine the problem as a whole. An attempt is now made to describe the approach used in these two studies.

Section 1.4 Whiffen's Benzene Force Field^[2].

Following the nomenclature of Crawford and Miller (1949)^[1] for the planar force constants, the potential energy V , expressed in symmetry coordinates, is given by

$$\begin{aligned}
 2V = & \Lambda_1 s_1^2 + \Lambda_2 s_{14}^2 + \Lambda_3 (s_{8a}^2 + s_{8b}^2) + 2\Lambda_4 (s_{19a}^2 + s_{19b}^2) \\
 & + \Omega_1 s_2^2 + \Omega_2 s_{13}^2 + \Omega_3 (s_{7a}^2 + s_{7b}^2) + \Omega_4 (s_{20a}^2 + s_{20b}^2) \\
 & + \Gamma_1 s_3^2 + \Gamma_2 s_{15}^2 + \Gamma_3 (s_{9a}^2 + s_{9b}^2) + \Gamma_4 (s_{18a}^2 + s_{18b}^2) \\
 & + \Sigma_2 s_{12}^2 + \Sigma_3 (s_{6a}^2 + s_{6b}^2) \\
 & + 2\xi_1 s_1 s_2 + 2\xi_3 (s_{7a} s_{8a} + s_{7b} s_{8b}) + 2^{3/2} \xi_4 (s_{19a} s_{20a} + s_{19b} s_{20b}) \\
 & + 2\chi_3 (s_{6a} s_{8a} + s_{6b} s_{8b}) \\
 & + 2\pi_3 (s_{6a} s_{9a} + s_{6b} s_{9b}) \\
 & + 2\mu_2 s_{14} s_{15} + 2\mu_3 (s_{8a} s_{9a} + s_{8b} s_{9b}) + 2^{3/2} \mu_4 (s_{18a} s_{19a} + s_{18b} s_{19b}) \\
 & + 2\psi_2 s_{12} s_{13} + 2\psi_3 (s_{6a} s_{7a} + s_{6b} s_{7b}) \\
 & + 2\tau_3 (s_{7a} s_{9a} + s_{7b} s_{9b}) + 2\tau_4 (s_{18a} s_{20a} + s_{18b} s_{20b}) \\
 & + \text{out-of-plane terms}
 \end{aligned}$$

Because there are far too many parameters in the E_{2g} and E_{1u} classes to be determined from the frequency data, it is necessary to set parameters which are expected to be small to zero

$$\xi_3 \quad E_{2g} \quad r_i/R_i$$

$$\xi_4 \quad E_{1u} \quad r_i/R_i$$

$$\psi_3 \quad E_{2g} \quad r_i/\alpha_i$$

$$\tau_3 \quad E_{2g} \quad r_i/\beta_i$$

$$\tau_4 \quad E_{1u} \quad r_i/\beta_i$$

In order to put all C-H stretching coordinates on the same terms when the symmetry classes become combined in the partially deuterated compounds, it is also necessary to set

$$\xi_1 \quad A_{1g} \quad r_i/R_i$$

$$\psi_2 \quad B_{1u} \quad r_i/\alpha_i$$

equal to zero, and to neglect all interactions with C-H stretching coordinates. The errors are probably less than those caused by the neglect of anharmonicity.

The General Quadratic Force Field for Benzene can be described by 37 planar Latin constants whereas there are only 26 planar Greek constants which are sufficient for an exact description. 4 of the Latin constants, namely

$$\begin{array}{l} 1 \quad (\beta_i r_i) \\ 1_p \quad (\beta_i r_{i+3}) \\ n \quad (\beta_i \alpha_i) \\ n_p \quad (\beta_i \alpha_{i+3}) \end{array}$$

are zero, since non-zero values are inconsistent with D_{6h} symmetry for the molecule. There are also 3 independent relationships between the valency coordinates which allow a reduction in 3 independent parameter combinations. These relationships are:

$$\begin{aligned}\alpha_i + \alpha_{i+1} + \alpha_{i+2} + \alpha_{i+3} + \alpha_{i+4} + \alpha_{i+5} &= 0 \\ (2\alpha_i + \alpha_{i+1} - \alpha_{i+2} - 2\alpha_{i+3} - \alpha_{i+4} + \alpha_{i+5}) &= 3^{\frac{1}{2}} (-R_i + R_{i+2} + R_{i+3} - R_{i+5}) \\ 3^{\frac{1}{2}}(\alpha_{i+1} + \alpha_{i+2} - \alpha_{i+4} - \alpha_{i+5}) &= (-R_i - 2R_{i+1} - R_{i+2} + R_{i+3} + 2R_{i+4} + R_{i+5})\end{aligned}$$

There are many ways in which the 33 non-zero Latin constants may be reduced to 26, but it seems best to remove explicit mention of the terms which are likely to be small, namely, those governed by

$$\begin{aligned}f_m & (\alpha_i \alpha_{i+2}) \\ f_p & (\alpha_i \alpha_{i+3}) \\ i_m & (\alpha_i R_{i+1}) \\ i_p & (\alpha_i R_{i+2}) \\ n_m & (\beta_i \alpha_{i+2}) \\ k_m & (\alpha_i r_{i+2}) \\ k_p & (\alpha_i r_{i+3})\end{aligned}$$

If the following relationships between Latin and Greek constants are considered

$$\begin{aligned}6 \tilde{h}_o &= \xi_1 + \xi_3 + 6^{\frac{1}{2}} \xi_4 - 2 \cdot 3^{\frac{1}{2}} \psi_2 + 3 \cdot 3^{\frac{1}{2}} \psi_3 \\ 6 h_m &= \xi_1 - 2 \xi_3 \\ 6 \tilde{h}_p &= \xi_1 + \xi_3 - 6^{\frac{1}{2}} \xi_4 + 2 \cdot 3^{\frac{1}{2}} \psi_2 - 3 \cdot 3^{\frac{1}{2}} \psi_3 \\ \tilde{k} &= -\psi_2 + 2 \psi_3\end{aligned}$$

$$\tilde{k}_o = -\Psi_2 + \Psi_3$$

$$6l_o = -3^{\frac{1}{2}} \tau_3 + 3^{\frac{1}{2}} \tau_4$$

$$6l_m = 3^{\frac{1}{2}} \tau_3 + 3^{\frac{1}{2}} \tau_4$$

it can be seen that these terms, under the restrictions imposed above, are zero. Thus there are 19 non-zero planar Latin force constants describing the G.Q.F.F.

With the tilda set of force constants, the planar force field may be expressed as

$$\begin{aligned} 2V = & \tilde{D} \sum \Delta R_i^2 + 2\tilde{d}_o \sum \Delta R_i \Delta R_{i+1} + 2\tilde{d}_m \sum \Delta R_i \Delta R_{i+2} + 2\tilde{d}_p \sum \Delta R_i \Delta R_{i+3} \\ & + E \sum \Delta r_i^2 + 2e_o \sum \Delta r_i \Delta r_{i+1} + 2e_m \sum \Delta r_i \Delta r_{i+2} + 2e_p \sum \Delta r_i \Delta r_{i+3} \\ & + G r_o^2 \sum \beta_i^2 + 2g_o r_o^2 \sum \beta_i \beta_{i+1} + 2g_m r_o^2 \sum \beta_i \beta_{i+2} + 2g_p r_o^2 \sum \beta_i \beta_{i+3} \\ & + \tilde{F} R_o^2 \sum \alpha_i^2 + 2\tilde{f}_o R_o^2 \sum \alpha_i \alpha_{i+1} + 2\tilde{i}_o R_o \sum \alpha_i (\Delta R_i + \Delta R_{i-1}) \\ & + 2\tilde{h}_o \sum \Delta r_i (\Delta R_i + \Delta R_{i-1}) + 2\tilde{h}_m \sum r_i (\Delta R_{i+1} + \Delta R_{i-2}) + 2\tilde{h}_p \sum \Delta r_i (\Delta R_{i+2} + \Delta R_{i-3}) \\ & + 2\tilde{j}_o r_o \sum \beta_i (\Delta R_i - \Delta R_{i-1}) + 2\tilde{j}_m r_o \sum \beta_i (\Delta R_{i+1} - \Delta R_{i-2}) + 2\tilde{j}_p r_o \sum \beta_i (\Delta R_{i+2} - \Delta R_{i-3}) \\ & + 2\tilde{k}_o R_o \sum \alpha_i \Delta r_i + 2\tilde{k}_m R_o \sum \alpha_i (\Delta r_{i+1} + \Delta r_{i-1}) + 2\tilde{n}_o r_o R_o \sum \beta_i (\alpha_{i+1} - \alpha_{i-1}) \\ & + 2l_o r_o \sum \beta_i (\Delta r_{i+1} - \Delta r_{i-1}) + 2l_m r_o \sum \beta_i (\Delta r_{i+2} - \Delta r_{i-2}) \end{aligned}$$

The summations are normally over the values $i = 1, 6$ except for cases such as $\sum \beta_i \beta_{i+3}$ where only three terms are involved, since values of $i > 3$ would give the same quantities with the factors in reverse order.

Numbering the atoms in a clockwise fashion, β_i is defined to be positive if the motion corresponds to the displacement of H towards the C_{i-1} atom.

Thus the negative sign in the β interactions occurs because the bracketed terms, although equivalent, have opposite signs.

	R	r	α	β
R	D d _o d _m d _p	h _o h _m h _p	i _o i _m i _p	j _o j _m j _p
r		E e _o e _m e _p	k k _o k _m k _p	(1) l _o l _m (l _p)
α			F f _o f _m f _p	(n) n _o n _m (n _p)
β				G g _o g _m g _p

Table 1.4 The 37 planar Latin force constants.

	R	r	α	β
R	d d _o d _m d _p	h _o h _m h _p	i _o {i _m } {i _p }	j _o j _m j _p
r		E e _o e _m e _p	k k _o {k _m } {k _p }	l _o l _m
α			F f _o {f _m } {f _p }	n _o {n _m }
β				G g _o g _m g _p

Table 1.5 Whiffen's 26 planar Latin force constants by removal of explicit mention of the 7 force constants in italic brackets.

	R	r	α	β
R	D d _o d _m d _p		i _o	j _o j _m j _p
r		E e _o e _m e _p		
α			\tilde{F} \tilde{f}_o	\tilde{n}_o
β				G g _o g _m g _p

Table 1.6 Whiffen's 19 parameter Benzene force field.

	R	r	α	β
R	D d		i _o	j _o
r		E	k	
α			F f _o	n _o
β				G g _o g _m g _p

Table 1.7 Duinker's 13 parameter Benzene force field.

Whiffen aimed to reproduce the observed frequencies of Benzene and its deuterated derivatives to within 2%. He used the frequencies of Benzene and Hexadeutero Benzene given in the summarizing paper of Herzfeld, Ingold and Poole (1946)^[20]. It was after much of the work was completed that the alternative suggestions of Mair and Hornig (1949)^[19] regarding the inactive B_{2u} frequencies came to his attention - that the carbon frequency of Benzene lies at 1311 cm^{-1} and not at 1648 cm^{-1} and that the hydrogen deformation is at 1147 cm^{-1} and not at 1110 cm^{-1} . Whiffen therefore calculated sets of values for the 19 non-zero planar Latin force constants for both alternative assignments.

In many of the symmetry classes, an ambiguity arises in the choice of solutions of quadratic equations and two or possibly more equally satisfactory sets of force constants can be obtained. One basis for making a choice between the alternative sets would be to calculate the frequencies of the partially deuterated Benzenes with each combination of sets and compare for the best fit with experimental values. This would be tedious and it is not certain that a clear decision would result. A second basis of choice is that the force constants must be physically reasonable. Because of the apparent success of the S.V.F.F., Whiffen felt that the forces principally arise from the stretching of valency bonds and the distortion of valency angles, and that a description in these terms must give a reasonably good force field, and that the interaction constants which must be added to give the exact field must be small. Thus, for example, in the B_{2u} species, where the force constant display graph defines two solutions, Whiffen excluded the set with the higher interaction force constant, and chose the set which gave the lower value for F_{14-15} .

Table 1.8 Transformation from internal to symmetry force constant representation [9]

$F_{2,2}$	=	$E + 2e_o + 2e_m + e_p$
$F_{13,13}$	=	$E - 2e_o + 2e_m - e_p$
$F_{7,7}$	=	$E - e_o - e_m + e_p$
$F_{20,20}$	=	$E + e_o - e_m - e_p$
$F_{3,3}$	=	$G + 2g_o + 2g_m + g_p$
$F_{15,15}$	=	$G - 2g_o + 2g_m - g_p$
$F_{9,9}$	=	$G - g_o - g_m + g_p$
$F_{18,18}$	=	$G + g_o - g_m - g_p$
$F_{1,1}$	=	$D + 2d_o + 2d_m + d_p$
$F_{14,14}$	=	$D - 2d_o + 2d_m - d_p$
$F_{8,8}$	=	$D - d_o - d_m + d_p$
$F_{19,19}$	=	$\frac{1}{2}(D + d_o - d_m - d_p + F + f_o - f_m - f_p) - 3^{\frac{1}{2}}(i_o - i_p)$
$F_{12,12}$	=	$F - 2f_o + 2f_m - f_p$
$F_{6,6}$	=	$F - f_o - f_m + f_p$
$F_{1,2}$	=	$2h_o + 2h_m + 2h_p$
$F_{7,8}$	=	$h_o - 2h_m + h_p$
$F_{19,20}$	=	$(\frac{3}{2})^{\frac{1}{2}}(h_o - h_p) - (\frac{1}{2})^{\frac{1}{2}}(k + k_o - k_m - k_p)$
$F_{12,13}$	=	$k - 2k_o + 2k_m - k_p$
$F_{6,7}$	=	$k - k_o - k_m + k_p$

Table 1.8 (continued)

$$\begin{aligned}
 F_{14,15} &= 2j_o - 2j_m + 2j_p \\
 F_{8,9} &= (3)^{\frac{1}{2}} (-j_o + j_p) \\
 F_{18,19} &= \left(\frac{1}{2}\right)^{\frac{1}{2}} (j_o + 2j_m + j_p) - \left(\frac{3}{2}\right)^{\frac{1}{2}} (n_o + n_m) \\
 F_{6,9} &= (3)^{\frac{1}{2}} (-n_o + n_m) \\
 \\
 F_{7,9} &= (3)^{\frac{1}{2}} (-l_o + l_m) \\
 F_{18,20} &= (3)^{\frac{1}{2}} (+l_o + l_m) \\
 \\
 F_{6,8} &= i_o - 2i_m + i_p
 \end{aligned}$$

Section 1.5 Duinker's Benzene Force Field

Duinker^[10] used a modified valency force field based on the hybrid orbital model. He selected a set of internal force constants, including all the diagonal force constants and some interaction force constants, chosen on arguments of orbital following and rehybridisation of the carbon atom orbitals. The model of chemical bonds formed from overlapping atomic orbitals on the individual atom can be used in a qualitative way to predict the signs of stretch-bend interaction force constants^[23,24]. Changes of interbond angle about a central atom lead to changes of hybridisation in the bonding orbitals on the central atom, due to orbital-following of the bending coordinate. In s-p hybrid orbitals, an increase in p-content results in a longer bond, and an increase in s-content a shorter bond. Thus, if, for example, increasing a particular bond angle results in an increase in s-content for a particular bond, one

would expect that constraining an increase in the angle would lead to a shortening of the bond, and so one expects a positive value for the stretch-bend interaction constant. If this argument can be used to express the angle bending force constants and interaction force constants in terms of a smaller number of parameters, then it may be possible to solve the GFF for underdetermined systems such as Benzene. Mills^[22] outlined the theory as follows:-

It is necessary first to estimate the change in bond length which one expects to result from constraining a certain change in bond angle, denoted $(\partial R_i / \partial \theta_j)$ where R_i and θ_j are respectively bond length and bond angle coordinates in the valency representation. This may be written as the product of two derivatives

$$(\partial R_i / \partial \theta_j) = (\partial \lambda_i / \partial \theta_j) (\partial R_i / \partial \lambda_i) \quad (1)$$

where λ_i is a hybridisation parameter defining the s-p hybridisation of the central atom orbital in the R_i bond. So that there are no complications from the presence of d orbitals, the model is restricted to central atoms from the first row of the periodic table e.g. C, where the four central atom valency orbitals are constructed as linear combinations of s and p atomic orbitals only. Following Coulson^[23], λ_i is defined by the equation

$$\psi_i = \frac{s + \lambda_i p}{1 + \lambda_i^2} \quad (2)$$

where ψ_i is the wavefunction of the s-p atomic hybrid on the central atom, and s and p denote atomic orbital functions, the latter being directed along the bond. The condition of orthogonality between atomic orbitals on the central atom gives the following relations for every pair of orbitals^[23]

$$\lambda_i \lambda_k \cos \alpha_{ik} + 1 = 0 \quad (3)$$

where α_{ik} is the angle between the directed orbitals ψ_i and ψ_k . There are six equations of the type (3) between the fourvalency orbitals of a first row atom, and by differentiating these equations, the derivatives $(\partial\lambda_i/\partial\theta_j)$ in (1) can be determined. The orthogonality relations (3) prevent orbital following in certain bending coordinates, but allow it in others; one expects to find stretch-bend interactions only in the second case.

The derivatives $(\partial R_i/\partial\lambda_i)$ might be estimated from information on equilibrium geometry. For example, the trend in the C-H bond lengths of methane ($r_e(\text{CH}) = 1.095\text{\AA}$, $\lambda^2 = 3$), ethylene or Benzene ($r_e(\text{CH}) = 1.084\text{\AA}$, $\lambda^2 = 2$) and acetylene ($r_e(\text{CH}) = 1.06\text{\AA}$, $\lambda^2 = 1$) may be used to make a rough estimate of $(\partial r/\partial\lambda)_{\text{CH}}$, giving the approximate value $+0.03\text{\AA}$. Alternatively the derivatives $(\partial R_i/\partial\lambda_i)$ may be left in the theory as adjustable parameters (one for each type of bond), in recognition of the fact that this whole treatment is a naïve simplification of the origin of interaction force constants. The latter approach has been found to be the more useful; this also allows the model to represent the possibility of only partial orbital following in the bending coordinate. However, considerations of equilibrium geometry indicate a positive sign for $(\partial R_i/\partial\lambda_i)$ in almost all cases, and suggest an order of magnitude for this derivative, these expectations being further supported by theoretical arguments^[23].

When both the factors on the right-hand side of (1) are known, the derivative $(\partial R_i/\partial\theta_j)$ may be simply related to the interaction force constant F_{ij} between the valency coordinates R_i and θ_j . Consider the three relevant terms in the internuclear potential energy function

$$V = \frac{1}{2} F_{ii} \delta R_i^2 + F_{ij} \delta R_i \delta \theta_j + \frac{1}{2} F_{jj} \delta \theta_j^2 \quad (4)$$

To find the change in R_i induced by constraining a change in the angle θ_j , the derivative $(\partial V/\partial R_i)$ is formed from the appropriate value of θ_j , and set equal to zero.

$$(\partial V/\partial R_i) = F_{ii} \delta R_i + F_{ij} \delta \theta_j = 0$$

whence
$$\delta R_i = - (F_{ij}/F_{ii}) \delta \theta_j \quad (5)$$

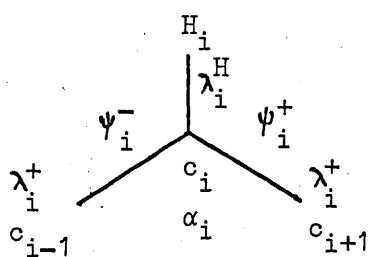
Thus
$$F_{ij} = - \left(\frac{\partial R_i}{\partial \theta_j} \right) \cdot F_{ii} \quad (6)$$

This equation relates a stretch-bend interaction force constant to the corresponding diagonal stretching constant, and may thus be used to reduce the number of parameters in the force field. Even if $(\partial R_i/\partial \lambda_i)$ is left in as an adjustable parameter in equation (1), this will only give one parameter for each bond type, and in general there will still be a reduction in the number of parameters from the number in the GFF. This model is called the Hybrid Orbital Force Field (HOFF).

It will now be attempted to show how this model was applied to Benzene. Before terms of the form $(\partial \lambda_i/\partial \alpha_i)$ can be evaluated, the redundancy between the angle displacements around a carbon atom must be removed by defining three new coordinates as linear combinations of $\Delta \alpha_i$, $\Delta \psi_i^+$, $\Delta \psi_i^-$

$$\begin{aligned} S_1 &= 6^{-\frac{1}{2}} [2\Delta \alpha_i - \Delta \psi_i^+ - \Delta \psi_i^-] \\ S_2 &= 2^{-\frac{1}{2}} [\Delta \psi_i^+ - \Delta \psi_i^-] \\ S_r &= 3^{-\frac{1}{2}} [\Delta \alpha_i + \Delta \psi_i^+ + \Delta \psi_i^-] \end{aligned} \quad (7)$$

where
$$\begin{aligned} S_1 &= (3/2)^{\frac{1}{2}} \alpha_i \\ S_2 &= 2^{\frac{1}{2}} \beta_i \end{aligned}$$



$$\begin{aligned} \lambda_i^H \lambda_i^+ \cos \psi_i^+ + 1 &= 0 \\ \lambda_i^H \lambda_i^- \cos \psi_i^- + 1 &= 0 \\ \lambda_i^+ \lambda_i^- \cos \alpha_i + 1 &= 0 \end{aligned} \quad (8)$$

Fig. 1.5

Differentiation of the orthogonality conditions (8) gives

$$\lambda_i^H \cos \psi_i^+ \Delta \lambda_i^+ + \lambda_i^+ \cos \psi_i^+ \Delta \lambda_i^H - \lambda_i^H \lambda_i^+ \sin \psi_i^+ \Delta \psi_i^+ = 0$$

$$\lambda_i^H \cos \psi_i^- \Delta \lambda_i^- + \lambda_i^- \cos \psi_i^- \Delta \lambda_i^H - \lambda_i^H \lambda_i^- \sin \psi_i^- \Delta \psi_i^- = 0$$

$$\lambda_i^- \cos \alpha_i \Delta \lambda_i^+ + \lambda_i^+ \cos \alpha_i \Delta \lambda_i^- - \lambda_i^+ \lambda_i^- \sin \alpha_i \Delta \alpha_i = 0$$

These equations determine whether orbital following of a bending coordinate may occur or not. Substituting the appropriate displacements $\Delta \alpha_i$, $\Delta \psi_i^+$, $\Delta \psi_i^-$ into these equations gives three equations in three unknowns, $\Delta \lambda_i^+$, $\Delta \lambda_i^-$, $\Delta \lambda_i^H$.

Using the notation S_1 and S_2 to denote the two bending coordinates $S_1(r)$ and $S_2(R)$, unit change in S_1 can be effected by taking

$$\Delta \alpha_i = 2.6^{-\frac{1}{2}}$$

$$\Delta \psi_i^+ = \Delta \psi_i^- = -6^{-\frac{1}{2}} \text{ from inspection of (7), which gives}$$

$$\Delta \lambda_i^H = 2$$

$$\Delta \lambda_i^H = \Delta \lambda_i^+ = -1$$

We can now evaluate the derivatives

$$(\partial \lambda_i^+ / \partial S_1) = (\partial \lambda_i^- / \partial S_1) = -1$$

$$\text{or } (\partial \lambda_i^+ / \partial \alpha_i) = (\partial \lambda_i^- / \partial \alpha_i) = [-1/2.6^{-\frac{1}{2}}] = -(3/2)^{\frac{1}{2}} \quad (9)$$

$$(\partial \lambda_i^H / \partial S_1) = 2$$

$$\text{or } (\partial \lambda_i^H / \partial \alpha_i) = [2/2.6^{-\frac{1}{2}}] = 6^{\frac{1}{2}}$$

Combination of (9) and (6) gives two expressions

$$(\alpha_i R_i) = (3/2)^{\frac{1}{2}} (\partial R / \partial \lambda)_{CC} \cdot R_i$$

$$(\alpha_i r_i) = -2(3/2)^{\frac{1}{2}} (\partial r / \partial \lambda)_{CH} \cdot r_i$$

Unit change in S_2 can be effected by taking

$$\Delta \psi_i^+ = -\Delta \psi_i^- = 2^{-\frac{1}{2}}$$

We can now evaluate the derivatives

$$(\partial \lambda_i^+ / \partial S_2) = -(\partial \lambda_i^- / \partial S_2) = -3^{\frac{1}{2}}$$

$$\text{or } (\partial \lambda_i^+ / \partial \beta_i) = -(\partial \lambda_i^- / \partial \beta_i) = -6^{\frac{1}{2}} \quad (10)$$

$$(\partial \lambda_i^H / \partial S_2) = 0 \text{ or } (\partial \lambda_i^H / \partial \beta_i) = 0$$

Combination of (10) and (6) gives

$$(\beta_i R_i) = 6^{\frac{1}{2}} (\partial R / \partial \lambda_i) \cdot R_i$$

On this basis, Duinker included the stretch-bend interactions

$(\beta_i R_i)$, $(\alpha_i R_i)$ and $(\alpha_i r_i)$ as parameters in the force constant refinement.

Bend-bend interaction force constants cannot be related to bending diagonal force constants in the manner outlined above, but quantitatively, if, during a distortion of the molecule from the equilibrium position due to displacement in the β coordinates maximum overlap between the bonding orbitals of adjacent C atoms is retained, one might expect that any distortion of coordinates which favours a clockwise rotation of the orbitals around one carbon atom, will favour an anticlockwise rotation of the orbitals around the neighbouring atoms. Using these tentative arguments, Duinker felt justified in including the following bend-bend interaction force constants $(\beta_i \beta_{i+1}) + ve$, $(\beta_i \alpha_{i+1}) + ve$, $(\alpha_i \alpha_{i+1}) -ve$. Following Scherer and Overend^[5], he introduced a "Kekulé" parameter to allow for C-C stretch interactions

$$(R_i R_{i+1}) = -(R_i R_{i+2}) = (R_i R_{i+3})$$

In order to make a first guess at the Benzene force field in an internal coordinate representation, for use in a force constant refinement calculation, Duinker used these internal force constants to consider the symmetry force constants, species by species and attempt to deduce the sign and order of magnitude of the interaction force constants where possible.

A_{1g} species

Since some following of +S₁ and -S₂ might be achieved by putting more p character into the C_i-H_i bond and more s into the C_i - C_{i+1} band, F₁₋₂ was expected to be small and positive. As explained later, this parameter had to be constrained.

B_{1u} species

This involves one stretch-bend interaction ($\alpha_i r_i$)

$$S_{12} = R_0 6^{-\frac{1}{2}} (-\alpha_1 + \alpha_2 - \alpha_3 + \alpha_4 - \alpha_5 + \alpha_6)$$

Defining $\Delta\Theta = -\alpha_1 = +\alpha_2 = -\alpha_3 = +\alpha_4 = -\alpha_5 = +\alpha_6$

$$S_{12} = R_0 6^{\frac{1}{2}} \Delta\Theta$$

Application of (9) gives

$$(\partial \lambda_{H_2}^H / \partial S_{12}) = R_0^{-1}$$

From (1), the displacement in r (C₂-H₂) with a small displacement Δx in S₁₂ can be written as

$$\Delta r_{H_2} = (\partial r_H / \partial \lambda_H) \cdot (\partial \lambda_H / \partial S_{12}) \cdot \Delta x$$

$$\text{or } S_{13} = 6^{-\frac{1}{2}} (-r_1 + r_2 - r_3 + r_4 - r_5 + r_6)$$

$$= 6^{\frac{1}{2}} \cdot R_0^{-1} (\partial r_H / \partial \lambda_H) \cdot \Delta x$$

$$\text{From (6) } F_{12-13} = -6^{\frac{1}{2}} \cdot R_0^{-1} (\partial r_H / \partial \lambda_H) \cdot F_{13-13}$$

Calculations on methylhalogenides and formaldehyde indicate that

$$(\partial r_H / \partial \lambda_H) \text{ is } \sim +0.025 \overset{\circ}{\text{A}}. \quad \text{Using } F_{13-13} = 5.1 \text{ md}/\overset{\circ}{\text{A}}, F_{12-13} = -0.99 \text{ md}/\overset{\circ}{\text{A}}.$$

B_{2u} species

This involves one stretch-bend interaction ($\beta_i R_i$)

$$S_{15} = r_o \cdot 6^{-\frac{1}{2}} (-\beta_1 + \beta_2 - \beta_3 + \beta_4 - \beta_5 + \beta_6)$$

Defining $\Delta\theta = -\beta_1 = +\beta_2 = -\beta_3 = +\beta_4 = -\beta_5 = +\beta_6$

$$S_{15} = r_o \cdot 6^{\frac{1}{2}} \cdot \Delta\theta$$

If Δx is a small displacement in S_{15} , then application of (9) and (1)

gives $\Delta R_1 = (\partial R_1 / \partial \lambda_c) \cdot (\partial \lambda_c / \partial S_{15}) \cdot \Delta x = 2 \cdot r_o^{-1} (\partial R_c / \partial \lambda_c) \cdot \Delta x$.

S_{14} can now be written as

$$S_{14} = 6^{-\frac{1}{2}} (-R_1 + R_2 - R_3 + R_4 - R_5 + R_6) = -2 \cdot 6^{\frac{1}{2}} \cdot r_o^{-1} (\partial R_c / \partial \lambda_c) \cdot \Delta x$$

From (6) $F_{14-15} = 2 \cdot 6^{\frac{1}{2}} \cdot r_o^{-1} (\partial R_c / \partial \lambda_c) \cdot F_{14-14}$

Taking $(\partial R_c / \partial \lambda_c) = 0.03 \overset{\circ}{\text{A}}$ and $F_{14-14} = 4.34 \text{ md } / \overset{\circ}{\text{A}}$, then $F_{14-15} = +0.57 \text{ md } / \overset{\circ}{\text{A}}$.

E_{2g} species

There are six interaction force constants. The hybrid orbital model makes no predictions regarding F_{7-8} , a stretch-stretch interaction between $S_7(r)$ and $S_8(R)$, and F_{6-9} , a bend-bend interaction between $S_6(\alpha)$ and $S_9(\beta)$. Application of (10) to the interaction between $S_7(r)$ and $S_9(\beta)$ predicts $F_{7-9} = 0$. Expected signs and estimate values for the three stretch-bend interactions are derived as follows:-

F_{6-7} is the interaction between $S_6(\alpha)$ and $S_7(r)$

$$S_6 = 12^{-\frac{1}{2}} \cdot R_o (-2\alpha_1 + \alpha_2 + \alpha_3 - 2\alpha_4 + \alpha_5 + \alpha_6)$$

Defining $\Delta\theta = -\frac{1}{2}\alpha_1 = +\alpha_2 = +\alpha_3 = -\frac{1}{2}\alpha_4 = +\alpha_5 = +\alpha_6$

From (1) and (9) a small displacement Δx in S_6 induces

$$\Delta r_2 = (\partial r_H / \partial \lambda_H) \cdot (\partial \lambda_H / \partial S_6) \cdot \Delta x$$

$$S_7 = 12^{-\frac{1}{2}} (-2r_1 + r_2 + r_3 - 2r_4 + r_5 + r_6) = 6^{\frac{1}{2}} \cdot R_0^{-1} (\partial r_H / \partial \lambda_H) \cdot \Delta x$$

$$\text{From (6) } F_{6-7} = -6^{\frac{1}{2}} \cdot R_0^{-1} (\partial r_H / \partial \lambda_H) \cdot F_{7-7}$$

If $(\partial r_H / \partial \lambda_H)$ is given the value from formaldehyde of 0.025 \AA , and using

$$F_{7-7} = 5.158 \text{ md / \AA}, \text{ then } F_{6-7} = -0.02 \text{ md / \AA}.$$

F_{6-8} is the interaction between $S_6(\alpha)$ and $S_8(R)$. S_6 can be expressed as above. From (1) and (9) a small displacement Δx in S_6 induces

$$\Delta R_2 = -(\partial R_2 / \partial \lambda_{c_2}) \cdot 2^{-3/2} \cdot R_0^{-1} \cdot \Delta x$$

$$\Delta R_1 = (\partial R_2 / \partial \lambda_{c_2}) \cdot 2^{-5/2} \cdot R_0^{-1} \cdot \Delta x$$

$$S_8 = 12^{-\frac{1}{2}} (-R_1 + 2R_2 - R_3 - R_4 + 2R_5 - R_6) = -12^{\frac{1}{2}} (\partial R_2 / \partial \lambda_{c_2}) \cdot 2^{-5/2} \cdot R_0^{-1} \cdot \Delta x$$

$$\text{From (6) } F_{6-8} = 12^{\frac{1}{2}} (\partial R_2 / \partial \lambda_{c_2}) \cdot 2^{-5/2} \cdot R_0^{-1} \cdot F_{8-8}$$

For 100% orbital following of S_6 , taking $(\partial R_2 / \partial \lambda_{c_2}) = 0.06 \text{ \AA}$ and

$$F_{8-8} = 6.427 \text{ md / \AA} \text{ then } F_{6-8} = 0.40 \text{ md / \AA}.$$

F_{8-9} is the interaction between $S_8(R)$ and $S_9(\beta)$

$$S_9 = r_0 \cdot 2^{-1} (-\beta_2 + \beta_3 - \beta_5 + \beta_6)$$

Defining $\Delta \theta = -\beta_2 = +\beta_3 = +\beta_5 = +\beta_6$

$$S_9 = 2r_0 \Delta \theta$$

From (1) and (10) a small displacement in S_9 induces

$$\Delta R_2 = 6^{\frac{1}{2}} \cdot 2^{-1} \cdot r_0^{-1} (\partial R_2 / \partial \lambda_{c_2}^+) \cdot \Delta x$$

$$\Delta R_1 = -6^{\frac{1}{2}} \cdot 2^{-2} \cdot r_0^{-1} (\partial R_2 / \partial \lambda_{c_2}^+) \cdot \Delta x$$

$$S_8 = 12^{-\frac{1}{2}} (-R_1 + 2R_2 - R_3 - R_4 + 2R_5 - R_6) = 3 \cdot 2^{-\frac{1}{2}} \cdot r_0^{-1} (\partial R_2 / \partial \lambda_{c_2}^+) \cdot \Delta x$$

From (6) $F_{8-9} = -3.2^{-\frac{1}{2}} \cdot r_o^{-1} (\partial R_2 / \partial \lambda^+ c_2) \cdot F_{8-8}$

For 100% orbital following, taking $(\partial R_2 / \partial \lambda^+ c_2) = 0.03 \text{ \AA}$ and $F_{8-8} = 6.427 \text{ md/\AA}$ then $F_{8-9} = -0.42 \text{ md/\AA}$.

E_{1u} species

After the redundancy has been eliminated, there are three interaction force constants involved. Application of (10) to the interaction between

$S_{18}(\beta)$ and $S_{20}(r)$ predicts $F_{18-20} = 0$.

F_{18-19} is the interaction between $S_{18}(\beta)$ and $S_{19}(R)$

$$S_{18} = r_o \cdot 2^{-1} (+\beta_2 + \beta_3 - \beta_5 - \beta_6)$$

Defining $\Delta\Theta = +\beta_2 = +\beta_3 = -\beta_5 = -\beta_6$.

$$S_{18} = 2r_o \Delta\Theta$$

$$S_{19} = 2^{\frac{1}{2}} \cdot S'_{19} = 2^{-\frac{1}{2}} (-R_1 + R_3 + R_4 - R_6)$$

Remembering that for $(\partial R_1 / \partial S_{18})$, only one end of the bond contributes to the change of length, and using (1) and (10), a small displacement Δx in S_{18} induces

$$S_{19} = -2 \cdot 3^{\frac{1}{2}} \cdot r_o^{-1} (\partial R_{1-2} / \partial \lambda c_2^-) \cdot \Delta x$$

From (6) $F_{18-19} = 2 \cdot 3^{\frac{1}{2}} \cdot r_o^{-1} (\partial R_{1-2} / \partial \lambda c_2^-) \cdot F_{19-19}$

Taking $(\partial R_{1-2} / \partial \lambda c_2^-) = +0.03 \text{ \AA}$, and $F_{19-19} = 3.67 \text{ md/\AA}$, $F_{18-19} = +0.155 \text{ md/\AA}$.

F_{19-20} is the interaction between $S_{19}(\alpha)$ and $S_{20}(r)$

Invoking the redundancy $S_{19} = 2^{\frac{1}{2}} S'_{21}$

$$S_{19} = 6^{-\frac{1}{2}} \cdot R_o (2\alpha_1 + \alpha_2 - \alpha_3 - 2\alpha_4 - \alpha_5 + \alpha_6)$$

Defining $\Delta \Theta = \frac{1}{2}\alpha_1 = \alpha_2 = -\alpha_3 = \frac{1}{2}\alpha_4 = -\alpha_5 = \alpha_6$

$$S_{19} = 2.6^{\frac{1}{2}} \cdot R_o \Delta \Theta$$

From (1) and (9) a small displacement Δx in S_{19} induces

$$\Delta r_1 = R_o^{-1} (\partial r_1 / \partial \lambda_{H_1}) \text{ and } \Delta r_2 = 2^{-1} R_o^{-1} (\partial r_1 / \partial \lambda_{H_1}) \cdot \Delta x$$

$$S_{20} = 12^{-\frac{1}{2}} (-2r_1 - r_2 + r_3 + 2r_4 + r_5 - r_6) = 12^{-\frac{1}{2}} \cdot 2^{-1} \cdot R_o^{-1} (\partial r_1 / \partial \lambda_{H_1}) \cdot \Delta x$$

$$\text{From (6) } F_{19-20} = 12^{\frac{1}{2}} \cdot 2^{-1} \cdot R_o^{-1} (\partial r_1 / \partial \lambda_{H_1}) \cdot F_{20-20}$$

For 100% following of S_{19} , taking $(\partial r_1 / \partial \lambda_1) = 0.025 \overset{\circ}{\text{A}}$ and $F_{20-20} = 5.15 \overset{\circ}{\text{md/A}}$, then $F_{19-20} = 0.15 \overset{\circ}{\text{md/A}}$.

Duinker sought a set of internal force constants to give the best fit to the following observed data.

- 1) the vibrational frequencies of the planar modes of Benzene and Hexadeutero Benzene given by Brodersen [25].
- 2) The Coriolis zeta interaction coefficients, relating the two degenerate components of the ring angle bending vibration ν_6 in E_{2g} for Benzene and Hexadeutero Benzene.
- 3) the vibrational frequencies of the planar normal modes of sym Trideutero Benzene.

The force constant display graphs determine the symmetry force constants for the A_{1g} , B_{1u} and B_{2u} species. The one force constant for the A_{2g} species is unambiguously defined. Having selected a set of 12 internal force constants, Duinker used this limited amount of knowledge to estimate them.

Although two well-defined solutions for the three force constants F_{14-14} , F_{14-15} , F_{15-15} are obtained from the force constant display graph for the

B_{2u} species, both giving the expected sign and order of magnitude for j_o , calculations show the higher interaction force constant $F_{14-15} = +0.66 \text{ md/\AA}$ to be consistent with the E_{2g} species. Neglecting j_m, j_p

$$B_{2u} \quad F_{14-15} = 2j_o = 0.66$$

$$E_{2g} \quad F_{8-9} = -3^{\frac{1}{2}} j_o \sim -0.42$$

giving $j_o = 0.33 \text{ md/\AA}$.

Having already defined $d = d_o = -d_m = d_p$, the symmetry force constants for the C-C stretch become

$$A_{1g} \quad F_{1-1} = D + d = 7.9 \text{ to } 7.6$$

$$B_{2u} \quad F_{14-14} = D - 5d = 4.34$$

giving $D \cong 7.07 \text{ md/\AA}$ and $d \cong 0.55 \text{ md/\AA}$

Neglecting l_o, l_m, l_p the symmetry force constants for the C-H stretch become

$$A_{1g} \quad F_{2-2} = E = 5.0 \text{ to } 5.1$$

$$B_{1u} \quad F_{13-13} = E = 5.30 \text{ to } 5.05$$

giving $E = 5.1 \pm 1 \text{ md/\AA}$.

Neglecting g_m and g_p , the symmetry force constants for the C-H bend become

$$A_{2g} \quad F_{3-3} = G + 2g_o = 0.863 \text{ md/\AA}$$

$$B_{2u} \quad F_{15-15} = G - 2g_o = 0.824 \text{ md/\AA}$$

giving $G = 0.843 \text{ md/\AA}$ and $g = 0.01 \text{ md/\AA}$.

l_o and l_m were neglected. An accurate zero order guess cannot be obtained from the display graphs for the parameters F, f_o, k, i_o, n_o and h_o so they were treated as adjustable parameters in a least squares procedure, constraining j_o, D, d, E, G, g_o to the values obtained from the display

graphs. A very reasonable fit to the vibrational and Coriolis data was obtained in all the symmetry species except E_{1u} . A large number of adjustment calculations were performed, varying the important parameters at random within the range that was calculated from the display graphs. F_{18-18} is the parameter governing the 1482 cm^{-1} Benzene frequency in E_{1u} . The symmetry diagonal force constants associated with C-H bending are

$$A_{2g} \quad F_{3-3} \quad = G + 2g_o + 2g_m + g_p$$

$$E_{2g} \quad F_{9-9} \quad = G - g_o - g_m + g_p$$

$$B_{2u} \quad F_{15-15} \quad = G - 2g_o + 2g_m - g_p$$

$$E_{1u} \quad F_{18-18} \quad = G + g_o - g_m - g_p$$

g_m and g_p were therefore included as variable parameters in the force constant adjustment calculations.

Calculations were performed in which all 14 parameters $E, G, D, F, d, i_o, j_o, k, g_o, g_m, g_p, n_o, h_o, f_o$, were allowed to change their value independently, but these showed a strong tendency towards singularity, because h_o is not well defined by the data. This parameter, therefore, was constrained to zero, as were k and f_o , and convergence was obtained on a set of 11 parameters. Calculations were repeated for different constrained values of k and f_o , the optimum solution being obtained when $f_o \cong -0.05 \text{ md/\AA}$ and $k \cong -0.01 \text{ md/\AA}$. It makes little difference whether f_o and k are included or not. Because of the large difference between C-H stretching frequencies and all other fundamentals, the former can be treated separately to a good approximation, and they are nearly independent of all other parameters of the force field except the diagonal C-H

stretching force constants. This is the main reason why $k = (r_i \alpha_i)$ and $h_0 = (r_i R_i)$ could not be well-determined.

Duinker maintained that the effects of anharmonicity increase with frequency and so are normally distributed. He therefore calculated the errors on a percentage instead of an absolute basis, where the highest frequencies have a relatively higher statistical weight.

CHAPTER TWOSome General AspectsSection 2.1 Potential Function

As a first approximation, molecular vibrations may be treated independently of rotation and electronic motions [17, 30]. V , the potential energy due to distortion of the atoms, which are considered to be charged point masses, from their equilibrium position during vibration, may be expressed as a power series in some complete set of displacement coordinates - chosen to be R_i , the set of internal coordinates.

$$V = V_0 + \sum_i \left(\frac{\partial V}{\partial R_i} \right)_0 dR_i + \frac{1}{2} \sum_{ij} \left(\frac{\partial^2 V}{\partial R_i \partial R_j} \right)_0 dR_i dR_j + \frac{1}{6} \sum_{ijk} \left(\frac{\partial^3 V}{\partial R_i \partial R_j \partial R_k} \right)_0 dR_i dR_j dR_k$$

+ higher terms

V_0 defines the zero of the potential energy scale, and is independent of the displacement coordinates or momenta. It is convenient to define $V_0 = 0$.

If the internal coordinates R_i are independent, then since the displacements are defined from the equilibrium position $\partial V / \partial R_i = 0$. If redundancies exist through geometrical necessity, or if the force field is of a Urey-

Bradley type and defined in terms of interatomic interactions, then the R_i are not independent, though it is always possible to transform the

coordinate systems so that sufficient independent coordinates exist to

define the problem. The meaning of linear terms in the potential

function when the coordinates are dependent has been the subject of much debate [17, 31, 32] and it appears that their inclusion in the potential

function is unnecessary [33], being only of importance for vibrations

belonging to the fully symmetric species. In order to limit the

mathematical difficulties, and to retain a physical picture, the harmonic approximation is used, that is, only small displacements from the equilibrium configuration are considered, and cubic and terms of a higher degree in dR_i are neglected since $dR_i dR_j dR_k \ll dR_i dR_j$ for small dR_i . The potential function now reduces to the general quadratic form

$$2V = \sum_{ij} f_{ij} dR_i dR_j$$

where the coefficients f_{ij} are the harmonic internal force constants defined by

$$f_{ij} = \left(\frac{\partial^2 V}{\partial R_i \partial R_j} \right)_0$$

Section 2.2 Anharmonicity

The harmonic potential field represents a $3N-5$ dimensional hypersurface with a minimum which is quite deep compared with kT at the equilibrium configuration. Because the energy necessary to break a chemical bond is finite, terms of higher than second order must be important for large displacements. The validity of the harmonic approximation depends upon the masses and the kinds of bonds. Although it is found experimentally from the occurrence and positions of the combination and overtone bands in the spectra that anharmonicity cannot always be neglected, it is probably better to neglect the anharmonic effects and consider the observed frequencies to be harmonic, as it is usually impossible to include those factors which may be involved, let alone to consider the possibility of unknown interactions. Anharmonicity causes a deformation of the potential surface. The vibrational frequencies which are calculated using an harmonic potential energy function are called the normal frequencies, and the force field which

fits these data represents an average potential energy over the amplitudes of the vibrations.

The anharmonicity of a vibration is strongly correlated with the amplitudes in the vibrational mode, so the effect is largest for motions in which a hydrogen atom plays an important part. If the anharmonicity factors for a C-H and the corresponding C-D stretching or bending mode were equal, their frequencies could be reproduced by the same force field. It was observed by Duinker^[10] that a force field which reproduces a frequency in which a H atom moves with appreciable amplitude always gives a value for the corresponding D mode which is too high owing to the lower anharmonicity factors for D modes.

Section 2.3 Errors in the Observed Data

Vibrational frequencies do not represent ideal pieces of information because they are observed, and hence encumbered with error, and the theoretical relation between the observables and the force constants of the system may be obscure. Errors can be caused by the following:-

1. random errors on the accurate measurement of vibrational band positions are usually very small and have little effect on subsequent calculations. When measuring the position of a diffuse band, however, they may become appreciable. These errors may be correctly taken into account by suitable weighting of the observed data.
2. the effect of anharmonicity, resonance perturbations, liquid phase interactions, solute-solvent interactions or other unknown disturbing factors.

3. coarse errors can arise from

- (i) the incorrect designation of fundamentals to their symmetry classes.
- (ii) the incorrect assignments of frequencies as fundamentals.
- (iii) allocation of frequencies of a given symmetry to incorrect atomic displacements.

Thus the normal vibrational frequencies need to be reproduced only within the limits to which they are actually known when due allowance has been made for these errors.

Section 2.4 Some of the More Important Methods of Overcoming the Indeterminacy in the Force Field

There exists a fundamental problem in the calculation of force constants from observed vibrational frequencies. In an N-atomic asymmetric molecule there are $\frac{1}{2}(3N-6)(3N-5)$ independent force constant parameters and $3N-6$ fundamental vibrational frequencies, some of which are inactive in molecules of high symmetry. Although the number of independent parameters is reduced considerably when the molecule possesses symmetry, for Fluorine substituted Benzenes it always exceeds the number of observed frequencies. As outlined in Chapter One, two different ways of reducing the number of parameters in a M.V.F.F. for the Benzene molecule have been tried.

1. Whiffen's approach was to eliminate a sufficient number of unimportant cross terms from the complete potential function.
2. Duinker used an approximate model of the force field based on a physical picture and containing only a limited number of force constants.

The Overlay Procedure, developed by Schachtschneider and Snyder^[34] assumes that similar internal coordinate deformations in similar environments in different molecules require the same force. This is supported by a vast amount of chemical evidence on bond reactivities and physical properties, and implies that internal transference of force constants is possible between similar molecules or between similar groupings in different molecules. Such a pseudo isotopic treatment usually leads to a sufficient number of frequencies being available to solve for all the entries in the force field being used, the resulting force constants having an internal consistency. A favourable case for application of this technique should be a set of substituted Benzene molecules with a common substituent, where several of the molecules are of high symmetry.

Another method of solving for an excess of parameters is to supplement the vibrational frequency data with data which are functions of the force field, available from other sources. These include

- (i) data on isotopic molecules
- (ii) Coriolis coupling coefficients between two degenerate vibrations of a doubly degenerate symmetry species, obtainable from high-resolution vibration-rotation spectra.
- (iii) centrifugal distortion constants, from U.V., I.R. and microwave spectra.
- (iv) mean square amplitudes of vibration from electron diffraction measurements.
- (v) I.R. band shapes and intensities.
- (vi) Raman intensities and polarisation data..

Data from sources (i), (v), (vi) were found to be very useful.

Section 2.5 Additional Data Obtained from Isotopic Molecules

The existence of isotopically substituted molecules whose vibrational spectra have been assigned is of considerable help in providing additional information which can be used in force field calculations since, to a high degree of approximation, the force field remains unchanged in isotopic molecules while the change of mass causes frequency displacement, providing more information about the molecule without introducing any new unknowns. The amount of information about a given molecule is not proportional to the number of isomers assigned because of the limitations of a number of rules (see [17] Chapter 8 or [35] Chapter 7). The Redlich-Teller product rule states that for two isotopic molecules, the ratio of the product of the frequencies belonging to a given symmetry species is independent of the potential constants of the molecule. If there are three or more isotopic molecules, then the sum rule is involved. The existence of higher order isotope rules has also been recognised [36, 37, 38], which further limits the amount of independent data available from larger molecules.

If the isotopic substitution has only negligible effect on certain modes i.e. the coordinates of the isotopically substituted nucleus do not contribute to the molecular representation of the species, then this will give no new data.

Although the product rule only holds for harmonic frequencies and anharmonic frequencies may be considered to produce independent pieces of information, due consideration must be given to the weight that such information carries.

Section 2.6 Band Contour Data Obtained from I.R. Vapour-Phase Studies [12]

The Fluorine substituted Benzenes are all volatile, which allows vapour phase band contour data to be used in vibrational assignments - an extremely important aid not generally available for the other halogeno systems. All the molecules of C_{2v} and C_s symmetry are asymmetric tops, which means that the three principal moments of inertia are different $I_A < I_B < I_C$. The three principal axes are chosen such that C has the largest, B the intermediate and A the smallest moment of inertia. It is important to notice that for the Fluorine substituted Benzenes, the C axis is parallel to out-of-plane motions, whilst the A and B axes cut the plane of the molecule. Thus a band with a type C contour can be assigned to an out-of-plane mode, whilst type A and B bands can be assigned to the correct in-plane species after careful study of the appropriate group table. A good example is afforded by Fluoro Benzene and Pentafluoro Benzene. The orientation of x, y, z axes in a C_{2v} molecule is as shown.

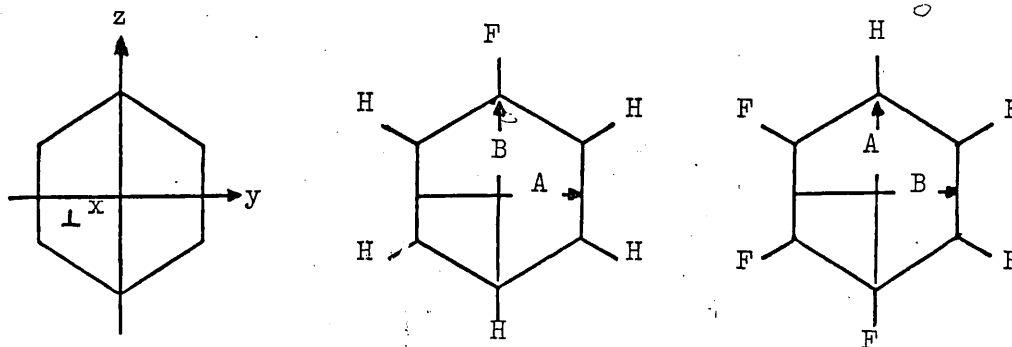


Fig. 2.1

Translation along the z axis belongs to the B_2 species whilst translation along the y axis belongs to the A_1 species. Thus in Fluoro Benzene, a type A contour can be assigned to the A_1 species, but in Pentafluoro Benzene it would be assigned to the B_2 species.

Table 2.1 BAND TYPES

Molecule	Symmetry Species	Band Type
<u>Symmetric Top Molecules</u>		
Benzene	E_{1u}	\perp
	A_{2u}	"
1,3,5 trifluoro Benzene	E'	\perp
	A''_2	"
Hexafluoro Benzene	E_{1u}	\perp
	A_{2u}	"
<u>Asymmetric Top Molecules</u>		
Fluoro Benzene	A_1	A
	B_2	B
	B_1	C
1,2 difluoro Benzene	A_1	A
	B_2	B
	B_1	C
1,3 difluoro Benzene	B_2	A
	A_1	B
	B_1	C
1,4 difluoro Benzene	B_{1u}	A
	B_{2u}	B
	B_{3u}	C
1,2,4 trifluoro Benzene	A'	} A B
	A''	
1,2,3,4 tetrafluoro Benzene	A_1	A
	B_2	B
	B_1	C

/continued

Table 2.1 BAND TYPES (continued)

1,2,3,5 tetrafluoro Benzene	A ₁	A
	B ₂	B
	B ₁	C
1,2,4,5 tetrafluoro Benzene	B _{2u}	A
	B _{1u}	B
	B _{3u}	C
Pentafluoro Benzene	B ₂	A
	A ₁	B
	B ₁	C

The characteristic band contours are as follows:-

Type A bands have a strong Q branch and prominent P and R branches.

The principal feature of a type B band is a central minimum with two strong, well-split Q branches with broad P and R branches which are often difficult to detect.

Type C bands show a very strong Q branch and relatively broad P and R structure.

For molecules of D_{6h}, D_{3h}, D_{2h} symmetry, as the asymmetry has decreased towards the symmetric rotor limit (A → B or C → B), the appropriate band types merge.

A number of causes of distortion of band contours from the expected exist. Two of the more important are hot band structure and inadequate resolution.

Since anharmonicity almost invariably leads to a convergence of vibrational levels which differ only in a single vibrational quantum number then it follows that the 1 → 2 band centre will be to lower frequencies

than the $0 \rightarrow 1$ centre. In the case of low frequency fundamentals the excited vibrational states will have appreciable equilibrium populations and the transitions to higher energies from these excited levels (hot band transitions) will give band structure additional to that of the $0 \rightarrow 1$. This is generally observed only if sharp Q branches exist, when the effect observed is a series of additional sharp Q branches rapidly diminishing in intensity on the low frequency side.

With molecules of large moments of inertia, since $B \propto \frac{1}{I_A}$, the instrumental resolving power may be inadequate to resolve the band structure into P, Q and R branches. In such a case a type B band may appear to have a broad central absorption purely as a result of instrumental overlap of the two branches. Considerable care must be exercised in drawing conclusions when this situation might prevail.

Calculations have been done on the overall band contours to be expected for the three band types for various relative values of the principal moments of inertia^[39], and the fraction of intensity in the Q branch and separation between the P and R maxima have been computed^[40].

Section 2.7 Raman Polarisation Data

Raman polarisation data is extremely important for the assignment of vibrational frequencies to their symmetry species. One experimental technique commonly employed with laser excitation is to have the polarised exciting beam travelling perpendicular to the axis of observation, with the plane of polarisation perpendicular to the axis of observation, and to measure the polarisation perpendicular to and along the plane of polarisation of the incident beam. Defining $\bar{\alpha}'$ as the mean polarisability tensor derivative,

β' as the anisotropy, and ρ as the depolarisation ratio, then

$$\rho = \frac{I^{E_{\parallel}}}{I^{E_{\perp}}} = \frac{3\beta'^2}{45\alpha'^2 + 4\beta'^2}$$

Thus $\rho_{\max} = 0.75$.

α' vanishes except for transitions between states, the direct product of which belongs to the fully symmetric species, and so $\rho = 0.75$ for all transitions other than those in which the vibrational mode excited has the full symmetry of the molecule. Thus Raman polarisation measurements offer an unequivocal means of recognising transitions belonging to the fully symmetric species in liquids or gases. Few generalities can be made about the relative values of α'^2 and β'^2 except for in spherical top molecules when all principal polarisabilities are equivalent in a state in which spherical symmetry is retained and therefore for the fully symmetric species β' , and hence ρ , are identically zero.

Section 2.8 Application of the Product, Sum and Inequality Rules to Molecules which are not Isotopically Related [35]

It is not usually a simple matter to assign vibrational absorption or emission bands to the principal types of vibrations involved. With some simple molecules sufficient information can be obtained from band contours, rotational fine structure and Raman polarisation data to achieve this. More generally, mode type assignments are made from these band characteristics supplemented by information on related molecules.

Redlich-Teller Product Rule

This rule relates the product of the harmonic frequencies of a given species of a molecule to the product of the corresponding frequencies of some isotopically related molecule, for which the force constant matrix is

identical. If the rule is applied to two molecules RX and RY, where X and Y are not isotopes of one another, then, provided the force fields are identical, a first order correction can be made to allow for the changes in the RX(Y) stretching and bending force constants. Ignoring the interaction constants between the R-X(Y) bonds and $R, \left\{ \frac{GF(RX)}{GF(RY)} \right\}^{\frac{1}{2}}$ will be higher by a factor $\left(\frac{\prod_{f_{R(X)}}}{\prod_{f_{R(Y)}}} \right)^{\frac{1}{2}}$, where the product is over the force constants for internal modes involved in a possible representation of the symmetry species.

Sum Rule

If several isotopic molecules can be geometrically superimposed with appropriate signs in such a way that the atoms vanish in all positions then the corresponding linear combination of the sums of the squares of the frequencies will vanish in the harmonic approximation. These sums may be taken independently over the frequencies of the symmetry classes of the subgroup arising from the symmetry elements common to all superimposition of the molecules. It is inherent in the superimposition nature of the rule that anharmonicities will partially cancel and it appears that changes in force constants are also partially compensated for as long as the rates of change of force constants with perturbing influence are uniform throughout the series under consideration.

Rayleigh's Rule and the Inequality Rule

Rayleigh's Rule states that increasing any mass in a periodically vibrating system without changing the force field must decrease all frequencies. Thus the j^{th} highest frequency of any symmetry species of a deuterated molecule must be below the j^{th} highest frequency of the normal molecule.

The Inequality Rule is an extension of this. If, for two molecules, RX and RY, the mass of the substituent X is greater than that of the substituted Y, then in any given symmetry class of RX containing "a" modes associated with the RX bond, the j^{th} highest frequency lies between the j^{th} and $(j + a)^{\text{th}}$ highest frequencies of the equivalent symmetry class of RY. For isotopic substitution this is an exact rule as its derivation does not depend on a quadratic assumption, the only requirement being an invariance of the force field. It can be successfully applied to nonisotopically related molecules despite the lack of any correction or compensating factors for force constant change.

CHAPTER THREEThe Vibrational Frequencies and Other Input DataSection 3.1 Geometry

The most drastic assumption made in this work is in assuming a regular hexagonal geometry for all of the Fluorine substituted Benzenes, using the following bond lengths.

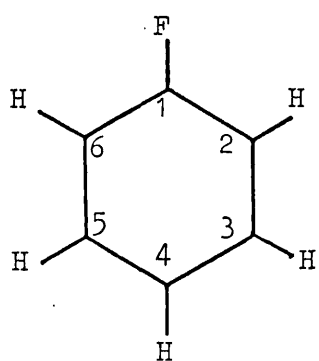
C-F	1.327 Å
C-C	1.397 Å
C-H	1.084 Å

Structural data seems to be limited to Benzene^[41], Fluoro Benzene^[42], 1,2 and 1,3 difluoro Benzene^[43], and Hexafluoro Benzene^[44]. The most comprehensive work is that of Nygaard et al^[42] on Fluoro Benzene. Two effects of Fluorine substitution observed were an opening to 123° of the carbon ring angle adjacent to the Fluorine substituent, and a decrease in the bond lengths of the C-C bonds next to the C-F bond. However, in Hexafluoro Benzene, the C-C bond lengths are very similar to those in Benzene. It is difficult to make any logical variations in the assumed C-C lengths and it was decided to retain the Benzene geometry throughout. Although second order changes in geometry might only lead to secondary corrections to calculated principal force constants if a general quadratic potential field is being evaluated, it need not even be a good approximation when other, simpler force fields are being used. Estimates of the effects of possible geometry errors were made by Pearce^[14] in his study of the out-of-plane vibrations of Fluorine substituted Benzenes. Variations of up to 3% were found, but most frequencies altered by much less, and this lies within the acceptable error margin between observed and computed frequencies.

The structural data to be found in the literature can be summarized as follows:-

Fluoro Benzene [42]

Nygaard et al were fortunate in being able to prepare three



C(1)-C(2)	1.383 $\overset{\circ}{\text{Å}}$ (+0.003)	$\widehat{\text{C}(6)\text{C}(1)\text{C}(2)}$	123.4 $^{\circ}$
C(2)-C(3)	1.395 $\overset{\circ}{\text{Å}}$ (+0.001)	$\widehat{\text{C}(1)\text{C}(2)\text{C}(3)}$	117.9 $^{\circ}$
C(3)-C(4)	1.397 $\overset{\circ}{\text{Å}}$ (+0.001)	$\widehat{\text{C}(2)\text{C}(3)\text{C}(4)}$	120.5 $^{\circ}$
C(1)-F	1.354 $\overset{\circ}{\text{Å}}$ (-0.006)	$\widehat{\text{C}(3)\text{C}(4)\text{C}(5)}$	119.8 $^{\circ}$
C(2)-H(2)	1.081 $\overset{\circ}{\text{Å}}$ (+0.005)	$\widehat{\text{C}(1)\text{C}(2)\text{H}(2)}$	120.0 $^{\circ}$
C(3)-H(3)	1.083 $\overset{\circ}{\text{Å}}$ (+0.004)	$\widehat{\text{C}(4)\text{C}(3)\text{H}(3)}$	119.9 $^{\circ}$
C(4)-H(4)	1.080 $\overset{\circ}{\text{Å}}$ (+0.004)		

Fig. 3.1

isotopes 3-D, 4-D and 2,4,6-D₃ Fluoro Benzene, and also a mixture of ¹³C substituted isotopes, and so have sufficient microwave data to elucidate the structure, which has three significant differences from that of Benzene - the C(1) - C(2) distance is 0.01 $\overset{\circ}{\text{Å}}$ shorter, the $\widehat{\text{C}(6)\text{C}(1)\text{C}(2)}$ angle is 3.4 $^{\circ}$ larger and the $\widehat{\text{C}(1)\text{C}(2)\text{C}(3)}$ angle is 2 $^{\circ}$ smaller - arising from the C(1) atom being "pushed" approximately 0.04 $\overset{\circ}{\text{Å}}$ towards the ring centre. The Fluorine substitution is expected to cause only minimal changes in the opposite part of the molecule. This is shown in the quite normal C-C and C-H distances and the practically regular angles. H(2) and H(6) are slightly attracted by the Fluorine atom.

The changes in geometry can be explained quantitatively^[45]. Fluorine, being highly electronegative, withdraws electrons from the carbon atom, leaving it with a positive charge. The carbon atom loses a 2p electron, in preference to a 2s electron, as these are less tightly bound. The C-C H.A.O's will contain more 2s character, which causes the bond length to contract and the C(1) angle to open.

1,2 difluoro Benzene and 1,3 difluoro Benzene [43]

Nygaard et al did not prepare isotopes of these molecules, and so they had to assume an undistorted Benzene skeleton with

$$\text{C-C } 1.397 \overset{\circ}{\text{Å}}$$

$$\text{C-H } 1.084 \overset{\circ}{\text{Å}}$$

$$\overset{\wedge}{\text{CCC}} \ 120^\circ$$

Using this approximation to simplify the calculations, they calculated C-F bond lengths of $1.318 \overset{\circ}{\text{Å}}$ in 1,2 difluoro Benzene, and $1.308 \overset{\circ}{\text{Å}}$ in 1,3 difluoro Benzene.

Hexafluoro Benzene [44]

This was studied by a least squares analysis of electron diffraction data giving

$$\text{C-C } 1.394 \pm 0.07 \overset{\circ}{\text{Å}}$$

$$\text{C-F } 1.327 \pm 0.007 \overset{\circ}{\text{Å}}$$

The C-F bond length is significantly shorter than in Fluoro Benzene.

The C-C bond length is perhaps $0.01 \overset{\circ}{\text{Å}}$ shorter than in Benzene, but it is not outside the error limits. The same bond length is also found in Hexachloro and Hexabromo Benzene. The equilibrium conformation does not seem to deviate significantly from the planar form, a result also obtained for Benzene and Hexachloro Benzene.

It is difficult to see how any accurate microwave studies with the precision of the Fluoro Benzene work can be done for the other molecules of interest which possess permanent dipole moments, as even if deuterium

1,2,4 trifluoro Benzene

1,2,3,4 tetrafluoro Benzene

1,2,3,5 tetrafluoro Benzene

Pentafluoro Benzene

analogues are prepared, since the molecule has fewer H atoms, there are

not many different isotopes and so less microwave data. Also, since the separation of the rotational lines decreases with increasing moment of inertia $B \propto \frac{1}{I_A}$, the measurements are less accurate. Perhaps the study of ^{13}C isotopes will be extended beyond Fluoro Benzene.

Section 3.2 Masses [46]

The atomic weights used in the calculations were (in atomic mass units)

Hydrogen	1.00797
Deuterium	2.01410
Carbon	12.01115
Fluorine	18.99840

Section 3.3 Symmetry Point Groups

The labelling of the symmetry species and the orientation of the cartesian axes are in accordance with the recommendations of Mulliken [16].

They are:-

1. For planar C_{2v} molecules

The z axis is the C_2 axis (the z axis is always the axis of highest symmetry).

The x axis is perpendicular to the molecular plane.

2. For planar D_{2h} molecules

The x axis is perpendicular to the molecular plane.

The z axis passes through the maximum number of atoms.

3. For planar D_{3h} molecules

The z axis is the C_3 axis, and therefore perpendicular to the molecular plane.

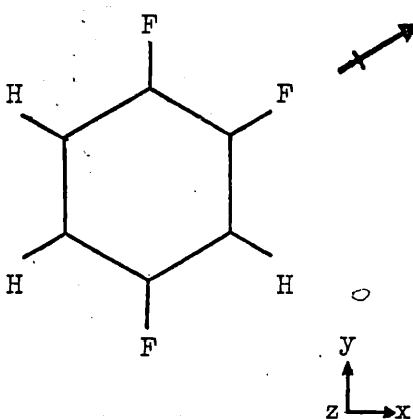
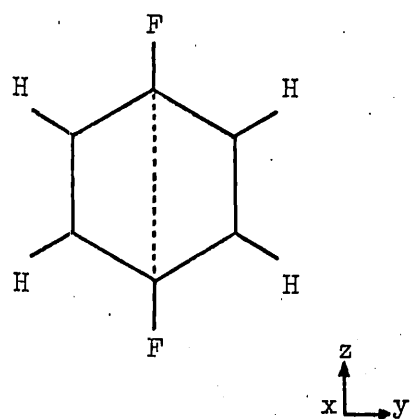
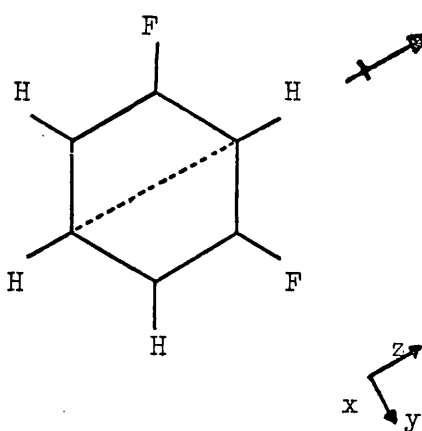
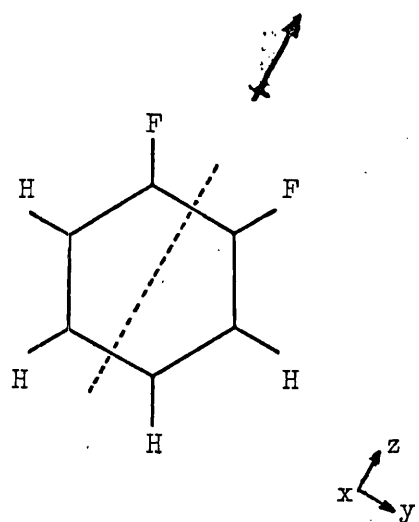
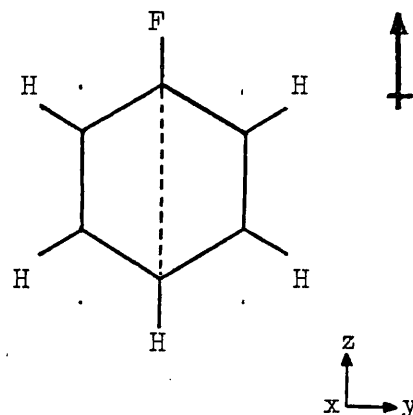
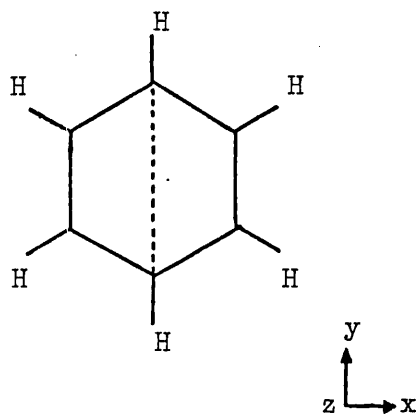
Table 3.1 Orientation of the Cartesian Axes C_2 axis shown

Table 3.1 (continued)

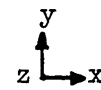
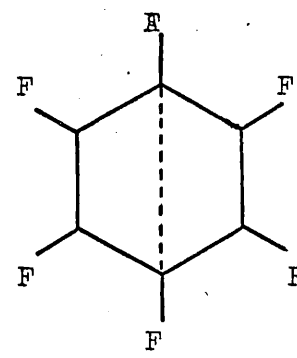
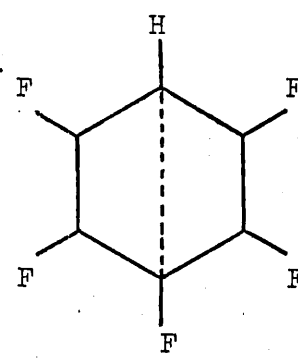
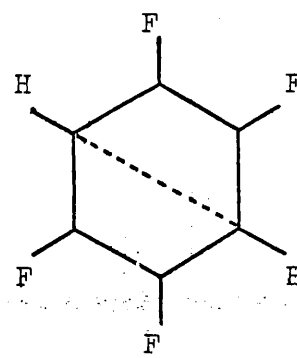
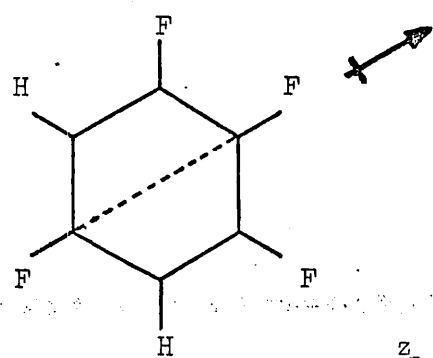
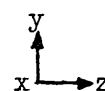
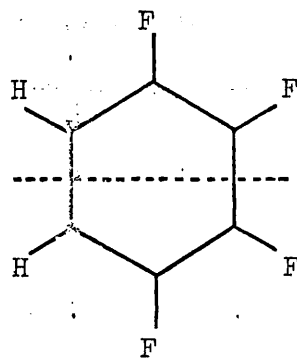
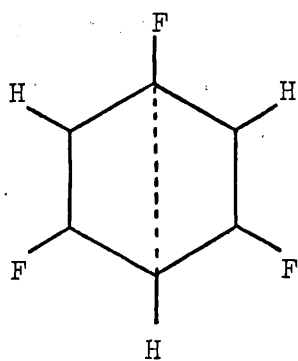


Table 3.2 The Symmetry Point Groups and the Symmetry Species of the In-Plane Vibrations of the Fluorine Substituted Benzenes

Molecule	Point Group	Symmetry Species
Benzene	D_{6h}	$2A_{1g} + 1A_{2g} + 2B_{1u} + 2B_{2u} + 4E_{2g} + 3E_{1u}$
Hexadeutero Benzene	D_{6h}	$2A_{1g} + 1A_{2g} + 2B_{1u} + 2B_{2u} + 4E_{2g} + 3E_{1u}$
Fluoro Benzene	C_{2v}	$13A_1 + 11B_2$
Fluoro Pentadeutero Benzene	C_{2v}	$13A_1 + 11B_2$
1,2 difluoro Benzene	C_{2v}	$13A_1 + 11B_2$
1,3 difluoro Benzene	C_{2v}	$13A_1 + 11B_2$
1,4 difluoro Benzene	D_{2h}	$7A_g + 5B_{3g} + 6B_{1u} + 6B_{2u}$
1,4 difluoro Tetradeutero Benzene	D_{2h}	$7A_g + 5B_{3g} + 6B_{1u} + 6B_{2u}$
1,2,4 trifluoro Benzene	C_s	$24A'$
1,3,5 trifluoro Benzene	D_{3h}	$5A_1' + 3A_2' + 8E'$
1,3,5 trifluoro Trideutero Benzene	D_{3h}	$5A_1' + 3A_2' + 8E'$
1,2,3,4 tetrafluoro Benzene	C_{2v}	$13A_1 + 11B_2$
1,2,3,5 tetrafluoro Benzene	C_{2v}	$13A_1 + 11B_2$
1,2,4,5 tetrafluoro Benzene	D_{2h}	$7A_g + 5B_{3g} + 6B_{1u} + 6B_{2u}$
Pentafluoro Benzene	C_{2v}	$13A_1 + 11B_2$
Pentafluoro Deutero Benzene	C_{2v}	$13A_1 + 11B_2$
Hexafluoro Benzene	D_{6h}	$2A_{1g} + 1A_{2g} + 2B_{1u} + 2B_{2u} + 4E_{2g} + 3E_{1u}$

3. (continued)

The x and y axes are degenerate and one of them must coincide with one of the C_2 axes.

4. For planar D_{6h} molecules

The z axis is the C_6 axis and therefore perpendicular to the molecular plane.

The x and y axes are degenerate and one of them must coincide with one of the C_2' axes.

The C_2' axes and the σ_v planes pass through the greatest number of atoms.

5. For planar C_s molecules

The xy plane is the σ_h plane and therefore the z axis is perpendicular to the molecular plane.

Section 3.4 Internal Coordinates

The instantaneous position of each atom is defined by three Cartesian coordinates denoted generally by q . The Cartesian coordinate system is not a convenient system to define the internal vibrations of a molecule. The $3N$ degrees of freedom - one independent motion along each coordinate x, y, z for all N atoms of the molecule - can be redefined as three corresponding to translation of the molecule as a whole, as three corresponding to rotation of the molecule as a whole, and the remaining $3N-6$ degrees of freedom as internal changes in the positions of the atoms in the molecule with no overall translation or rotation.

These internal changes form the complete set of Internal Coordinates of the molecule, that is, a set which is sufficient to describe all possible deformations and which is internally consistent - any symmetry element of the system must transform members of the set into equivalent members which must also be in the set.

Changes in the internal coordinates of a molecule refer to changes in the bond parameters, which are usually bond lengths and bond angles, and are more convenient to use when describing the vibrations of a molecule than displacements of the atoms in x, y or z directions.

The force constants are evaluated in terms of the internal coordinates as only in this form are they transferable between similar molecules of different symmetry.

Fluorine substituted Benzenes are described by a set of 24 internal coordinates, designated

R_i $i = 1,6$ increase in the length of the $C_i - C_{i+1}$ bond.

r_i $i = 1,6$ increase in the length of the $C_i - H_i$ bond.

$R\alpha_i$ $i = 1,6$ increase in the ring angle $C_{i-1} - C_i - C_{i+1}$, scaled with the

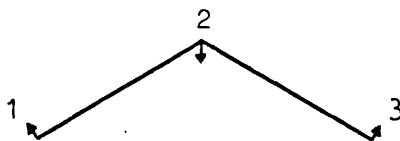


Fig. 3.2 Numbering of the atoms in an angle bend.

equilibrium length of the C-C bond, R .

Table 3.3 Atoms involved in a C-C stretch

Internal coordinate	Atom	
	1	2
R_1	1	2
R_2	2	3
R_3	3	4
R_4	4	5
R_5	5	6
R_6	6	1

Table 3.4 Atoms involved in a C-X stretch, X = H or F

Internal coordinate	Atom	
	1	2
r_1	1	7
r_2	2	8
r_3	3	9
r_4	4	10
r_5	5	11
r_6	6	12

Table 3.5 Atoms involved in an Angle Bend

Internal coordinate	Atom		
	1	2	3
$R\alpha_1$	6	1	2
$R\alpha_2$	1	2	3
$R\alpha_3$	2	3	4
$R\alpha_4$	3	4	5
$R\alpha_5$	4	5	6
$R\alpha_6$	5	6	1

Table 3.6 Atoms involved in an In-Plane Angle Bend

Internal coordinate	Atom			
	1	2	3	4
$r\beta_4$	7	6	2	1
$r\beta_2$	8	1	3	2
$r\beta_3$	9	2	4	3
$r\beta_4$	10	3	5	4
$r\beta_5$	11	4	6	5
$r\beta_6$	12	5	1	6

$r \beta_i$ $i = 1, 6$ increase in the angle between C_i-H_i bond and the external bisector of the $C_{i-1} - C_i - C_{i+1}$ angle, scaled with the product of the equilibrium length of the C-H bond, r .

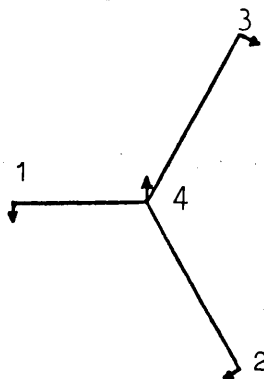


Fig. 3.3 Numbering of atoms in an In-Plane Angle Bend.

β_i is defined to be positive if the motion corresponds to the motion of H towards the C_{i-1} atom.

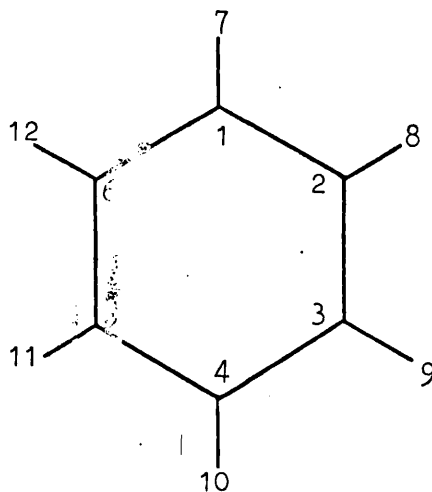
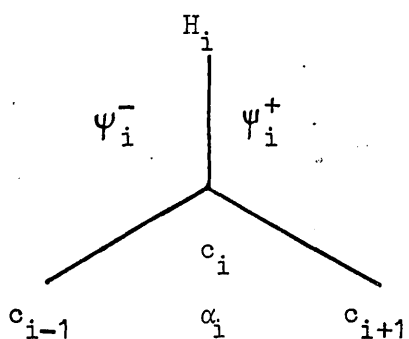


Fig. 3.4 Numbering of the atoms.

Section 3.5 Redundancies

It is usually necessary to introduce a complete set containing more than $3N-6$ internal coordinates to define the $3N-6$ fundamental vibrations. Because the internal coordinates are not independent, redundancies will occur. By definition, no internal coordinate can be arbitrarily excluded from a complete set. When the secular equation is solved, the redundant coordinates give rise to zero eigen values, which implies no vibrational motion of the atoms. The associated eigen vectors are also zero, giving zero vibrational frequencies.

The redundancies which occur in all the Fluorine substituted Benzenes arise because the sum of the deformations of the three angles in the plane of the nuclei must be zero.



$$\alpha_i = -\psi_i^- - \psi_i^+$$

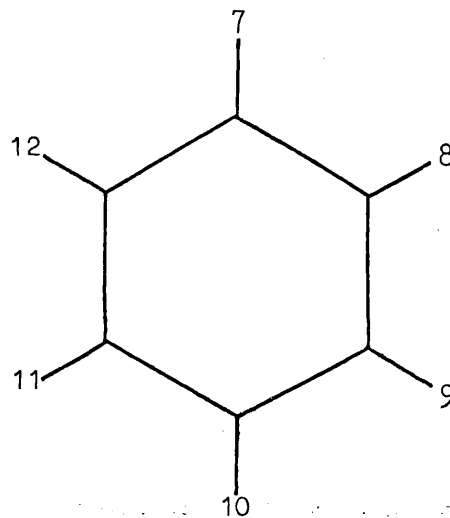
Fig. 3.5

Redundancies can also arise when the Secular Equation is expressed in Symmetry Coordinates. A complete set of coordinates must be generated and this set can overdefine the secular matrix. If the redundant symmetry coordinates can be identified, they are not included. However the symmetry coordinates which give rise to zero eigen values are usually linear combinations of the original symmetry coordinates and are not always obvious on inspection. It is not normally necessary to

remove the redundant coordinates as the programmes are designed to evaluate the eigen values and eigen vectors by diagonalisation of the matrices, so zero eigen values are acceptable. If the secular equation is set up in the form $|\mathbf{F}-\mathbf{G}^{-1}\mathbf{\Lambda}| \mathbf{L} = 0$, \mathbf{G} will be singular if redundancies are present, and therefore cannot be inverted. This can give rise to problems when calculating the Cartesian Displacements of the atoms in a normal mode. Gussoni and Zerbi^[46] have given a method of removing redundancies.

Section 3.6 Transformations from Internal Coordinates to Symmetry Coordinates

Having set up the \mathbf{G} and \mathbf{F} matrices in internal coordinates, they are now expressed in symmetry coordinates. For the Fluorine substituted Benzenes, there are 7 different transformations from internal to symmetry coordinates depending on the symmetry and structure of the molecule. The following tables give the \mathbf{U} (or transformation) matrices. The symmetry elements for the molecules are also shown.

Fig. 3.6 C_S Symmetry Point Group1,2,4 trifluoro Benzene σ_h - Molecular Plane

Molecule	Atoms						Bond lengths	
	7	8	9	10	11	12	r'	r
1,2,4 trifluoro Benzene	F	F	H	F	H	H	CF	CH

Table 3.7 U Matrix - C_s Symmetry

Symmetry		Coefficient for i =						N Factor	Internal Coordinate	
Species	Coord	1	2	3	4	5	6			
A'	S ₁	+1						1	R_i	
	S ₂		+1					1	R_i	
	S ₃			+1				1	R_i	
	S ₄				+1			1	R_i	
	S ₅					+1		1	R_i	
	S ₆							+1	1	R_i
	S ₇	+1							1	r'_i
	S ₈		+1						1	r'_i
	S ₉			+1					1	r_i
	S ₁₀				+1				1	r'_i
	S ₁₁					+1			1	r_i
	S ₁₂							+1	1	r_i
	S ₁₃	+1							1	$R\alpha_i$
	S ₁₄		+1						1	$R\alpha_i$
	S ₁₅			+1					1	$R\alpha_i$
	S ₁₆				+1				1	$R\alpha_i$
	S ₁₇					+1			1	$R\alpha_i$
	S ₁₈							+1	1	$R\alpha_i$
	S ₁₉	+1							1	$r'\beta_i$
	S ₂₀		+1						1	$r'\beta_i$
	S ₂₁			+1					1	$r\beta_i$
	S ₂₂				+1				1	$r'\beta_i$
	S ₂₃					+1			1	$r\beta_i$
	S ₂₄							+1	1	$r\beta_i$

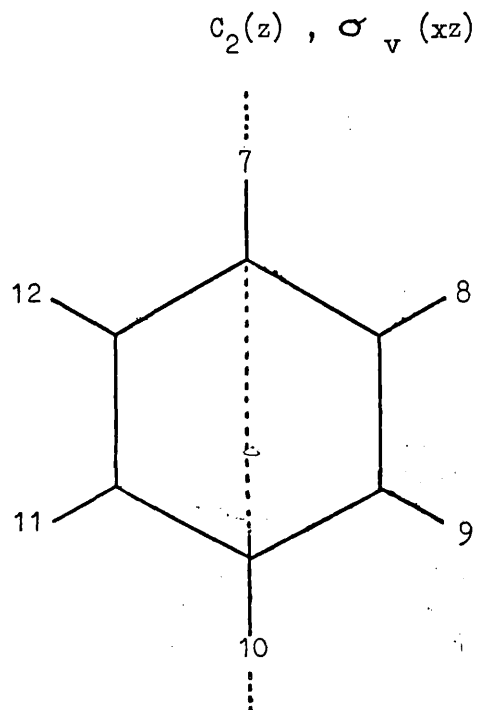
Fig. 3.7 C_{2v} Symmetry Point Group

Fluoro Benzene

Fluoro Pentadeutero Benzene

Pentafluoro Benzene

Pentafluoro Deutero Benzene

 $\sigma_v(yz)$ - Molecular Plane

Molecule	Atoms						Bond Lengths	
	7	8	9	10	11	12	r'	r
Fluoro Benzene	F	H	H	H	H	H	CF	CH
Fluoro Pentadeutero Benzene	F	D	D	D	D	D	CF	CH
Pentafluoro Benzene	H	F	F	F	F	F	CH	CF
Pentafluoro Deutero Benzene	D	F	F	F	F	F	CH	CF

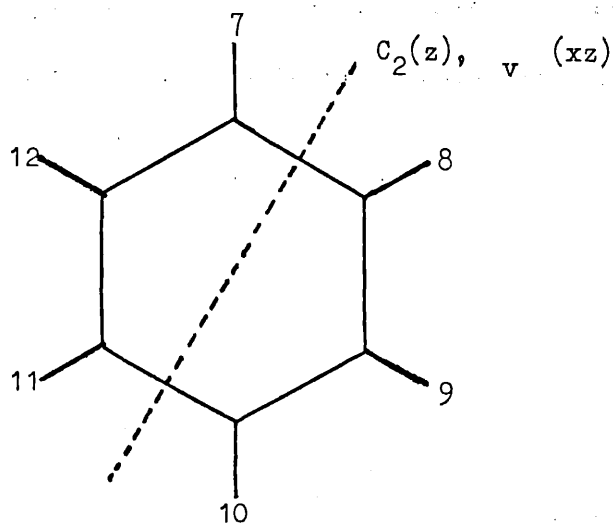
Table 3.8 U Matrix - C_{2v} Symmetry

Symmetry		Coefficient for i =						N Factor	Internal Coordinate		
Species	Coord	1	2	3	4	5	6				
A ₁	S ₁	+1						+1	$2 \frac{1}{\sqrt{2}}$	R _i	
	S ₂		+1					+1	$2 \frac{1}{\sqrt{2}}$	R _i	
	S ₃			+1	+1				$2 \frac{1}{\sqrt{2}}$	R _i	
	S ₄	+1							1	r' _i	
	S ₅		+1					+1	$2 \frac{1}{\sqrt{2}}$	r _i	
	S ₆			+1			+1		$2 \frac{1}{\sqrt{2}}$	r _i	
	S ₇					+1			1	r _i	
	S ₈	+1							1	Rα _i	
	S ₉		+1					+1	$2 \frac{1}{\sqrt{2}}$	Rα _i	
	S ₁₀			+1			+1		$2 \frac{1}{\sqrt{2}}$	Rα _i	
	S ₁₁					+1			1	Rα _i	
	S ₁₂		+1						-1	$2 \frac{1}{\sqrt{2}}$	rβ _i
	S ₁₃			+1			-1		$2 \frac{1}{\sqrt{2}}$	rβ _i	
B ₂	S ₁	+1						-1	$2 \frac{1}{\sqrt{2}}$	R _i	
	S ₂		+1				-1		$2 \frac{1}{\sqrt{2}}$	R _i	
	S ₃			+1	-1				$2 \frac{1}{\sqrt{2}}$	R _i	
	S ₄		+1					-1	$2 \frac{1}{\sqrt{2}}$	r _i	
	S ₅			+1		-1			$2 \frac{1}{\sqrt{2}}$	r _i	
	S ₆		+1					-1	$2 \frac{1}{\sqrt{2}}$	Rα _i	
	S ₇			+1		-1			$2 \frac{1}{\sqrt{2}}$	Rα _i	
	S ₈	+1							1	r'β _i	
	S ₉		+1					+1	$2 \frac{1}{\sqrt{2}}$	rβ _i	
	S ₁₀			+1			+1		$2 \frac{1}{\sqrt{2}}$	rβ _i	
	S ₁₁					+1			1	r'β _i	

Fig. 3.8 C_{2v} Symmetry Point Group

1,2 difluoro Benzene

1,2,3,4 tetrafluoro Benzene

 $\sigma_v(yz)$ - Molecular Plane

Molecule	Atoms						Bond Lengths	
	7	8	9	10	11	12	r'	r
1,2 difluoro Benzene	F	H	F	H	H	H	CF	CH
1,2,3,4 tetrafluoro Benzene	H	F	H	F	F	F	CH	CF

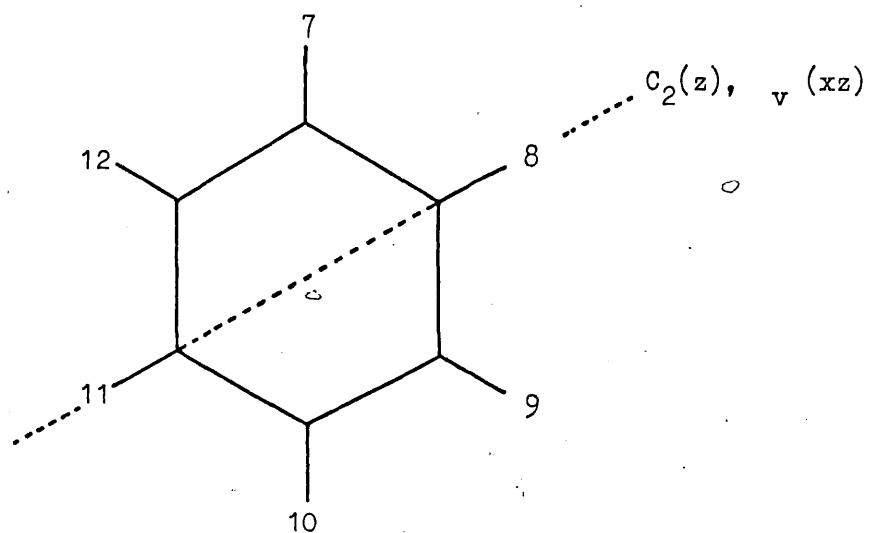
Table 3.9 U Matrix - C_{2v} Symmetry

Symmetry		Coefficient for i =						N Factor	Internal Coordinate
Species	Coord	1	2	3	4	5	6		
A ₁	s ₁	+1						1	R _i
	s ₂		+1				+1	$2^{-\frac{1}{2}}$	R _i
	s ₃			+1		+1		$2^{-\frac{1}{2}}$	R _i
	s ₄				+1			1	R _i
	s ₅	+1	+1					$2^{-\frac{1}{2}}$	r _i
	s ₆			+1				$2^{-\frac{1}{2}}$	r _i
	s ₇				+1	+1		$2^{-\frac{1}{2}}$	r _i
	s ₈	+1	+1					$2^{-\frac{1}{2}}$	Ra _i
	s ₉			+1				$2^{-\frac{1}{2}}$	Ra _i
	s ₁₀				+1	+1		$2^{-\frac{1}{2}}$	Ra _i
	s ₁₁	+1	-1					$2^{-\frac{1}{2}}$	r _i β _i
	s ₁₂			+1				$2^{-\frac{1}{2}}$	rβ _i
	s ₁₃				+1	-1		$2^{-\frac{1}{2}}$	rβ _i
B ₂	s ₁		+1				-1	$2^{-\frac{1}{2}}$	R _i
	s ₂			+1		-1		$2^{-\frac{1}{2}}$	R _i
	s ₃	+1	-1					$2^{-\frac{1}{2}}$	r _i
	s ₄			+1			-1	$2^{-\frac{1}{2}}$	r _i
	s ₅				+1	-1		$2^{-\frac{1}{2}}$	r _i
	s ₆	+1	-1					$2^{-\frac{1}{2}}$	Ra _i
	s ₇			+1			-1	$2^{-\frac{1}{2}}$	Ra _i
	s ₈				+1	-1		$2^{-\frac{1}{2}}$	Ra _i
	s ₉	+1	+1					$2^{-\frac{1}{2}}$	r _i β _i
	s ₁₀			+1				$2^{-\frac{1}{2}}$	rβ _i
	s ₁₁				+1	+1		$2^{-\frac{1}{2}}$	rβ _i

Fig. 3.9 C_{2v} Symmetry Point Group

1,3 difluoro Benzene

1,2,3,5 tetrafluoro Benzene

 $\sigma_v(yz)$ - Molecular Plane

Molecule	Atom						Bond Lengths	
	7	8	9	10	11	12	r'	r
1,3 difluoro Benzene	F	H	F	H	H	H	CF	CH
1,2,3,5 tetrafluoro Benzene	H	F	H	F	F	F	CH	CF

Table 3.10 U Matrix - C_{2v} Symmetry

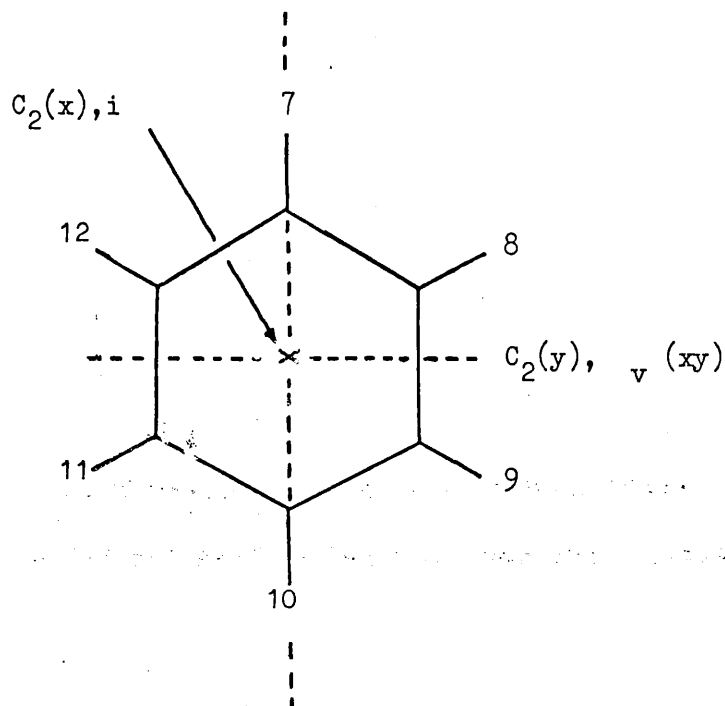
Symmetry		Coefficient for i =						N factor	Internal Coordinate
Species	Coord	1	2	3	4	5	6		
A ₁	S ₁	+1	+1					$2^{-\frac{1}{2}}$	R _i
	S ₂			+1			+1	$2^{-\frac{1}{2}}$	R _i
	S ₃				+1	+1		$2^{-\frac{1}{2}}$	R _i
	S ₄		+1					1	r _i
	S ₅	+1		+1				$2^{-\frac{1}{2}}$	r' _i
	S ₆				+1		+1	$2^{-\frac{1}{2}}$	r _i
	S ₇					+1		1	r _i
	S ₈		+1					1	Rα _i
	S ₉	+1		+1				$2^{-\frac{1}{2}}$	Rα _i
	S ₁₀				+1	+1	+1	$2^{-\frac{1}{2}}$	Rα _i
	S ₁₁					+1		1	Rα _i
	S ₁₂	+1		-1				$2^{-\frac{1}{2}}$	r'β _i
	S ₁₃				+1		-1	$2^{-\frac{1}{2}}$	rβ _i
B ₂	S ₁	+1	-1					$2^{-\frac{1}{2}}$	R _i
	S ₂			+1			-1	$2^{-\frac{1}{2}}$	R _i
	S ₃				+1	-1		$2^{-\frac{1}{2}}$	R _i
	S ₄	+1		-1				$2^{-\frac{1}{2}}$	r' _i
	S ₅				+1		-1	$2^{-\frac{1}{2}}$	r _i
	S ₆	+1		-1				$2^{-\frac{1}{2}}$	Rα _i
	S ₇				+1		-1	$2^{-\frac{1}{2}}$	Rα _i
	S ₈		+1					1	rβ _i
	S ₉	+1		+1				$2^{-\frac{1}{2}}$	r'β _i
	S ₁₀				+1		+1	$2^{-\frac{1}{2}}$	rβ _i
	S ₁₁					+1		1	rβ _i

Fig. 3.10 D_{2h} Symmetry Point Group

1,4 difluoro Benzene

1,4 difluoro Tetradeutero Benzene

1,2,4,5 tetrafluoro Benzene

 $\sigma_h(yz)$ - Molecular Plane

Molecule	Atom						Bond lengths	
	7	8	9	10	11	12	r'	r
1,4 difluoro Benzene	F	H	H	F	H	H	CF	CH
1,4 difluoro Tetradeutero Benzene	F	D	D	F	D	D	CF	CH
1,2,4,5 tetrafluoro Benzene	H	F	F	H	F	F	CH	CF

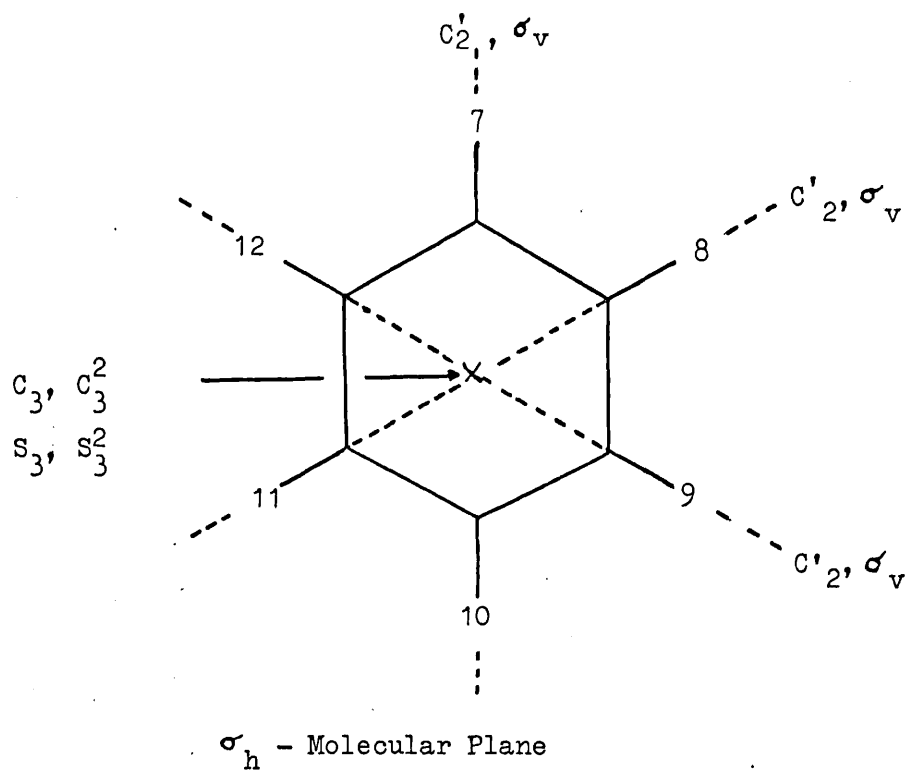
Table 3.11 U Matrix - D_{2h} Symmetry

Symmetry		Coefficient for i =						N factor	Internal Coordinate	
Species	Coord	1	2	3	4	5	6			
A_{1g}	S_1	+1		+1	+1		+1	2^{-1}	R_i	
	S_2		+1				+1	$2^{-\frac{1}{2}}$	R_i	
	S_3	+1			+1			$2^{-\frac{1}{2}}$	r'_i	
	S_4		+1	+1			+1	+1	2^{-1}	r_i
	S_5	+1			+1				$2^{-\frac{1}{2}}$	$R\alpha_i$
	S_6		+1	+1			+1	+1	2^{-1}	$R\alpha_i$
	S_7		+1	-1			+1	-1	2^{-1}	$r\beta_i$
B_{3g}	S_1	+1		-1	+1		-1	2^{-1}	R_i	
	S_2		+1	-1		+1	-1	2^{-1}	r_i	
	S_3	+1		-1		+1	-1	2^{-1}	$R\alpha_i$	
	S_4	+1			+1			$2^{-\frac{1}{2}}$	$r'\beta_i$	
	S_5		+1	+1			+1	+1	2^{-1}	$r\beta_i$
B_{2u}	S_1	+1		+1	+1		-1	2^{-1}	R_i	
	S_2		+1				-1	$2^{-\frac{1}{2}}$	R_i	
	S_3		+1	+1			-1	-1	2^{-1}	r_i
	S_4		+1	+1			-1	-1	2^{-1}	$R\alpha_i$
	S_5	+1				-1			$2^{-\frac{1}{2}}$	$r'\beta_i$
	S_6		+1	-1			-1	+1	2^{-1}	$r\beta_i$
B_{1u}	S_1	+1		-1	-1		+1	2^{-1}	R_i	
	S_2	+1				-1		$2^{-\frac{1}{2}}$	r_i	
	S_3		+1	-1			-1	+1	2^{-1}	r_i
	S_4	+1				-1			$2^{-\frac{1}{2}}$	$R\alpha_i$
	S_5		+1	-1			-1	+1	2^{-1}	$R\alpha_i$
	S_6	+1		+1			-1	-1	2^{-1}	$r\beta_i$

Fig. 3.11 D_{3h} Symmetry Point Group

1,3,5 trifluoro Benzene

1,3,5 trifluoro Trideutero Benzene



Molecule	Atoms						Bond Lengths		
	7	8	9	10	11	12	r'	θ	r
1,3,5 trifluoro Benzene	F	H	F	H	F	H	CF		CH
1,3,5 trifluoro Trideutero Benzene	F	D	F	D	F	D	CF		CH

The symmetry coordinates for the E' species are given by Duinker. It is perhaps instructive to see how these were obtained. First a set of orthogonal basis functions are chosen, and the effects of symmetry transformations calculated.

E	σ_h	c_3	s_3	c_3^2	s_3^2	c_2'	σ_v	c_2'	σ_v	c_2'	σ_v
(R_2+R_5)	(R_4+R_1)	(R_6+R_3)	(R_5+R_2)	(R_3+R_6)	(R_1+R_4)	(R_5+R_2)	(R_3+R_6)	(R_1+R_4)	(R_5+R_2)	(R_3+R_6)	(R_1+R_4)
(R_3+R_4)	(R_5+R_6)	(R_1+R_2)	(R_4+R_3)	(R_5+R_6)	(R_1+R_2)	(R_4+R_3)	(R_2+R_1)	(R_5+R_6)	(R_4+R_3)	(R_2+R_1)	(R_5+R_6)
r_1	r_3	r_5	r_1	r_5	r_3	r_1	r_5	r_3	r_1	r_5	r_3
r_4	r_6	r_2	r_4	r_2	r_6	r_4	r_2	r_6	r_4	r_2	r_6
α_1	α_3	α_5	α_1	α_5	α_3	α_1	α_5	α_3	α_5	α_3	α_5
α_4	α_6	α_2	α_4	α_2	α_6	α_4	α_2	α_6	α_4	α_2	α_6
$(\beta_3-\beta_5)$	$(\beta_5-\beta_1)$	$(\beta_1-\beta_3)$	$(-\beta_5+\beta_3)$	$(\beta_1-\beta_3)$	$(\beta_5-\beta_1)$	$(-\beta_5+\beta_3)$	$(-\beta_3+\beta_1)$	$(-\beta_1+\beta_5)$	$(-\beta_3+\beta_1)$	$(-\beta_1+\beta_5)$	$(-\beta_3+\beta_1)$
$(-\beta_2+\beta_6)$	$(-\beta_4+\beta_2)$	$(-\beta_6+\beta_4)$	$(\beta_6-\beta_2)$	$(-\beta_6+\beta_4)$	$(-\beta_4+\beta_2)$	$(\beta_6-\beta_2)$	$(\beta_4-\beta_6)$	$(\beta_2-\beta_4)$	$(\beta_4-\beta_6)$	$(\beta_2-\beta_4)$	$(\beta_4-\beta_6)$

From the formulae
$$S_a^{\Gamma} = \sum_j U_{aj} R_j$$

$$U_{a_i} = \sum_s \frac{(a_{ij}^s \chi^{\Gamma}(s) U_{aj}^{\Gamma})}{n_i}$$

and the entries in the character table for the E' species

E	$2C_3$	$3C_2'$	σ_h	$2S_3$	$3\sigma_v$
2	-1	0	2	-1	0

$$2 \{2(R_2+R_5)-(R_4+R_1)-(R_6+R_3)\} = (-R_1+2R_2-R_3-R_4+2R_5-R_6)$$

$$2 \{2(R_3+R_4)-2(R_6-R_1)-(R_5+R_6)+(R_2+R_3)-(R_1+R_2)+(R_4+R_5)\} = (-R_1+R_3+R_4-R_6)$$

$$2 \{2r_1-r_3-r_5\} = (2r_1-r_3-r_5)$$

$$2 \{2r_4-r_6-r_2\} = (-r_2+2r_4-r_6)$$

$$2 \{2\alpha_1-\alpha_3-\alpha_5\} = (2\alpha_1-\alpha_3-\alpha_5)$$

$$2 \{2\alpha_4-\alpha_6-\alpha_2\} = (-\alpha_2+2\alpha_4-\alpha_6)$$

$$2 \{2(\beta_3-\beta_5)-(\beta_5-\beta_1)-(\beta_1-\beta_3)\} = (\beta_3-\beta_5)$$

$$2 \{2(-\beta_2+\beta_6)-(-\beta_4+\beta_2)-(-\beta_6-\beta_4)\} = (-\beta_2+\beta_6)$$

Table 3.12 U Matrix - D_{3h} Symmetry

Symmetry		Coefficient for i =						N factor	Internal Coordinate
Species	Coord	1	2	3	4	5	6		
A ₁ '	S ₁	+1	+1	+1	+1	+1	+1	$6^{-\frac{1}{2}}$	R _i
	S ₂	+1		+1		+1		$3^{-\frac{1}{2}}$	r' _i
	S ₃		+1		+1		+1	$3^{-\frac{1}{2}}$	r _i
	S ₄	+1		+1		+1		$3^{-\frac{1}{2}}$	Ra _i
	S ₅		+1		+1		+1	$3^{-\frac{1}{2}}$	Ra _i
A ₂ '	S ₁	+1	-1	+1	-1	+1	-1	$6^{-\frac{1}{2}}$	R _i
	S ₂	+1		+1		+1		$3^{-\frac{1}{2}}$	r'β _i
	S ₃		+1		+1		+1	$3^{-\frac{1}{2}}$	rβ _i
E'	S ₁	-1	+2	-1	-1	+2	-1	$12^{-\frac{1}{2}}$	R _i
	S ₂	-1		+1	+1		-1	2 ⁻¹	R _i
	S ₃	+2		-1		-1		$6^{-\frac{1}{2}}$	r' _i
	S ₄		+2		-1		-1	$6^{-\frac{1}{2}}$	r _i
	S ₅	+2		-1		-1		$6^{-\frac{1}{2}}$	Ra _i
	S ₆		+2		-1		-1	$6^{-\frac{1}{2}}$	Ra _i
	S ₇			+1		-1		$2^{-\frac{1}{2}}$	r'β _i
	S ₈		-1				+1	$2^{-\frac{1}{2}}$	rβ _i

Table 3.13 U Matrix - D_{6h} Symmetry

Symmetry		Coefficient for i =						N factor	Internal Coordinate
Species	Coord	1	2	3	4	5	6		
A _{1g}	S ₁	+1	+1	+1	+1	+1	+1	$6^{-\frac{1}{2}}$	R _i
	S ₂	+1	+1	+1	+1	+1	+1	$6^{-\frac{1}{2}}$	r _i
A _{2g}	S ₁	+1	+1	+1	+1	+1	+1	$6^{-\frac{1}{2}}$	rβ _i
E _{2g}	S ₁	-1	+2	-1	-1	+2	-1	$12^{-\frac{1}{2}}$	R _i
	S ₂	-2	+1	+1	-2	+1	+1	$12^{-\frac{1}{2}}$	r _i
	S ₃	-2	+1	+1	-2	+1	+1	$12^{-\frac{1}{2}}$	Rα _i
	S ₄		-1	+1		-1	+1	2^{-1}	rβ _i
B _{1u}	S ₁	-1	+1	-1	+1	-1	+1	$6^{-\frac{1}{2}}$	r _i
	S ₂	-1	+1	-1	+1	-1	+1	$6^{-\frac{1}{2}}$	Rα _i
B _{2u}	S ₁	-1	+1	-1	+1	-1	+1	$6^{-\frac{1}{2}}$	R _i
	S ₂	-1	+1	-1	+1	-1	+1	$6^{-\frac{1}{2}}$	rβ _i
E _{1u}	S ₁	-1		+1	+1		-1	2^{-1}	R _i
	S ₂	-2	-1	+1	+2	+1	-1	$12^{-\frac{1}{2}}$	r _i
	S ₃		+1	+1		-1	-1	2^{-1}	rβ _i

Section 3.7 The Vibrational Assignments

Vibrational spectra and assignments for all the molecules considered have been reported in the literature, and form a good basis for the calculations of the force fields. Apparent discrepancies between the frequencies used in the calculations and those quoted in the appropriate reference arise in two ways:

- a) If the spectra have been re-run, then these frequencies are used instead.
- b) Whereas, in the literature, the assignment of bands which are infra red active is, for consistency, that of the liquid phase, it is preferred in this work to use vapour phase data when available.

On passing from the gas phase to condensed phase, molecules show several changes in their spectral characteristics e.g. frequency maxima, intensities, band shapes etc. The changes observed in the condensed phase are due either to a chemical effect or the dielectric effect. Chemical effects arise from intermolecular interactions, whilst the dielectric effect modifies the local field strength of the light which interacts with the molecule in question. In the dilute gas phase, intermolecular interactions are minimised, so it is in this phase that the most 'pure' information can be obtained. This does not imply that information derived from other phases is inferior, it is simply different.

The observed frequencies (obs. $\bar{\nu}$) and their weighting factors (w) are given, and three sets of results - the calculated frequencies (calc. $\bar{\nu}$), and the difference between the observed and calculated frequencies ($d\bar{\nu}$), together with the weighted square error (WSQ ER) and the weighted average frequency error ($|d\bar{\nu}|$). All frequencies are given in units of cm^{-1} .

BENZENE

			39 (ABS)		37 (ABS)		37(%)	
	obs. \bar{v}	w	calc. \bar{v}	d \bar{v}	calc. \bar{v}	d \bar{v}	calc. \bar{v}	d \bar{v}
A _{1g}	3073.5	1.0	3081.5	+8.0	3080.3	+6.8	3084.4	+10.9
	992.8	1.0	982.6	-10.2	982.4	-10.4	984.3	-8.5
A _{2g}	1350	1.0	1356.2	+6.2	1354.7	+4.7	1357.1	+7.1
E _{2g}	3055	1.0	3055.2	+0.2	3056.2	+1.2	3056.2	+1.2
	1600	1.0	1599.3	-0.7	1599.8	-0.2	1604.5	+4.5
	1177	1.0	1182.8	+5.8	1182.3	+5.3	1187.7	+10.7
	607	1.0	604.4	-2.6	604.8	-2.2	603.3	-3.7
B _{1u}	3057	1.0	3051.8	-5.2	3052.6	-4.4	3051.8	-5.2
	1010	1.0	1008.9	-1.1	1008.8	-1.2	1007.3	-2.7
B _{2u}	1309	1.0	1312.6	+3.6	1315.2	+6.2	1311.6	+2.6
	1146	1.0	1147.0	+1.0	1146.6	+0.6	1147.4	+1.4
E _{1u}	3068	1.0	3070.8	+2.8	3070.5	+2.5	3073.0	+5.0
	1482	1.0	1491.2	+9.2	1493.6	+11.6	1495.6	+13.6
	1037	1.0	1026.2	-10.8	1024.4	-12.6	1026.1	-10.9
d \bar{v}			4.8		5.0		6.3	
WSQER			1.173 x 10 ⁻³		1.358 x 10 ⁻³		1.813 x 10 ⁻³	

TABLE 3.14

The fundamental frequencies of Benzene have been the subject of much discussion. Accurate measurements of the frequencies in the gas and liquid phases were made by Brodersen and Langseth^[25]. The fundamental frequencies given in their work are used here. Their assignments are based on those of Ingold and co-workers, who published a long series of papers entitled "The Structure of Benzene", summarised in Part XXI^[20], but using the Mair and Hornig assignments for the B_{2u} species.

Because a set of degenerate frequencies represents only one observation, one member only of the set is used in the calculations.

HEXADEUTERO BENZENE

			39 (ABS)		37 (ABS)		37 (%)	
	obs. $\bar{\nu}$	w	calc. $\bar{\nu}$	$\bar{\nu}$	calc. $\bar{\nu}$	$\bar{\nu}$	calc. $\bar{\nu}$	$\bar{\nu}$
A _{1g}	2303	1.0	2292.1	-10.9	2296.0	-7.0	2295.4	-7.6
	945.5	1.0	934.6	-10.9	932.3	-13.2	935.7	-9.8
A _{2g}	1059	1.0	1054.9	-4.1	1053.9	-5.1	1055.6	-3.4
E _{2g}	2275	1.0	2280.2	+5.2	2280.8	+5.8	2280.1	+5.1
	1558	1.0	1571.6	+13.6	1571.0	+13.0	1575.8	+17.8
	868	1.0	842.1	-25.9	842.3	-25.7	846.6	-21.4
	579	1.0	579.4	+0.4	579.5	+0.9	578.1	-0.9
B _{1u}	2285	1.0	2283.0	-2.0	2280.1	-4.9	2281.0	-4.0
	970	1.0	954.0	-16.0	955.4	-14.6	953.3	-16.7
B _{2u}	1282	1.0	1269.4	-12.6	1270.7	-11.3	1274.4	-7.6
	824	1.0	839.0	+15.0	839.5	+15.5	835.4	+11.4
E _{1u}	2286	1.0	2284.1	-1.9	2287.5	+1.5	2286.2	+0.2
	1333	1.0	1316.7	-16.3	1316.3	-16.7	1318.7	-14.3
	814	1.0	811.6	-2.4	810.4	-3.6	812.6	-1.4
$\bar{\nu}$			9.8		9.9		8.7	
WSQER			4.786 x 10 ⁻³		4.678 x 10 ⁻³		5.989 x 10 ⁻³	

TABLE 3.15

The frequencies and assignments are those of Brodersen and Langseth^[25], and are similar to those of Foil A. Miller^[51].

The first complete assignment of Fluoro Benzene was that of Smith et al^[52]. Scott et al^[53] rejected the band at 876 cm^{-1} as a b_2 fundamental, and assigned it instead to 1157 cm^{-1} . Whiffen^[54] reassigned the b_2 fundamental at 1236 cm^{-1} to 1290 cm^{-1} .

The very strong infra red liquid band at 1220 cm^{-1} , and the moderate, polarised Raman line at 1217 cm^{-1} firmly support the assignment of the a_1 fundamental at 1220 cm^{-1} . Calculations consistently predict this frequency to lie at $\sim 1245\text{ cm}^{-1}$.

FLUORO BENZENE

			39 (ABS)		37 (ABS)		37 (%)	
	obs. \bar{v}	w	calc. \bar{v}	$d\bar{v}$	calc. \bar{v}	$d\bar{v}$	calc. \bar{v}	$d\bar{v}$
A ₁	3091	0.3	3084.9	-6.1	3084.3	-6.7	3087.2	-3.8
	3067	0.3	3071.2	+4.2	3071.2	+4.2	3072.9	+5.9
	3053	0.3	3053.5	+0.5	3054.4	+1.4	3053.9	+0.9
	1597	1.0	1607.9	+10.9	1608.3	+11.3	1611.7	+14.7
	1499	1.0	1498.8	-0.2	1499.7	+0.7	1500.1	+1.1
	1220	1.0	1244.7	+24.7	1244.4	+24.4	1246.5	+26.5
	1156	1.0	1159.9	+3.9	1160.2	+4.2	1163.7	+7.7
	1020	1.0	1020.0	+0.0 ^c	1018.8	-1.2	1018.8	-1.2
	1009	1.0	1000.8	-8.2	1000.1	-8.9	1001.4	-7.6
	806	1.0	800.7	-5.3	801.7	-4.3	801.7	-4.3
	520	1.0	511.0	-9.0	511.7	-8.3	512.0	-8.0
B ₂	3078	0.3	3081.4	+3.4	3081.4	+3.4	3083.2	+5.2
	3067	0.3	3059.7	-7.3	3060.4	-6.6	3060.7	-6.3
	1597	1.0	1604.5	+7.5	1604.2	+7.2	1608.3	+11.3
	1460	1.0	1465.8	+5.8	1467.5	+7.5	1467.1	+7.1
	1323	1.0	1319.3	-3.7	1320.4	-2.6	1320.1	-2.9
	1290	1.0	1292.9	+2.9	1293.2	+3.2	1292.8	+2.8
	1156	1.0	1154.5	-1.5	1154.0	-2.0	1155.6	-0.4
	1066	1.0	1062.2	-3.8	1060.8	-5.2	1061.7	-4.3
	615	1.0	617.8	+2.8	617.8	+2.8	616.1	+1.1
	405	1.0	410.1	+5.1	410.8	+5.8	410.5	+5.5
$d\bar{v}$ WSQER			5.6 2.866×10^{-3}		5.8 2.938×10^{-3}		6.2 5.141×10^{-3}	

TABLE 3.16

FLUORO PENTADEUTERO BENZENE

			39 (ABS)		37 (ABS)		37 (%)	
	obs. $\bar{\nu}$	w	calc. $\bar{\nu}$	d $\bar{\nu}$	calc. $\bar{\nu}$	d $\bar{\nu}$	calc. $\bar{\nu}$	d $\bar{\nu}$
A ₁	2295	1.0	2298.2	+3.2	2300.4	+5.4	2299.8	+4.8
	-	0.0	2286.8	-	2289.3	-	2288.4	-
	-	0.0	2281.6	-	2280.6	-	2280.7	-
	1577	1.0	1592.2	+15.2	1592.0	+15.0	1595.1	+18.1
	1391	1.0	1384.8	-6.2	1381.5	-9.5	1382.8	-8.2
	1163	1.0	1166.5	+3.5	1168.4	+5.4	1169.9	+6.9
	959	1.0	952.9	-6.1	952.3	-6.7	952.8	-6.2
	878	1.0	852.8	-25.2	852.4	-25.6	855.5	-22.5
	818	1.0	816.3	-1.7	816.3	-1.7	818.4	+0.4
	756	1.0	747.3	-8.7	747.7	-8.3	747.8	-8.2
	504	1.0	499.8	-4.2	500.5	-3.5	500.6	-3.4
B ₂	2295	0.3	2295.8	+0.8	2296.5	+3.5	2296.9	+1.9
	-	0.0	2281.7	-	2283.1	-	2282.2	-
	1566	1.0	1577.8	+11.8	1576.5	+10.5	1581.1	+15.1
	1311	1.0	1325.5	+14.5	1324.4	+13.4	1324.9	+13.9
	1281	0.2	1268.5	-12.5	1269.2	-11.8	1271.7	-9.3
	1034	1.0	1031.9	-2.1	1031.3	-2.7	1033.2	-0.8
	844	1.0	839.3	-4.7	839.7	-4.3	839.9	-4.1
	808	1.0	809.4	+1.4	809.1	+1.1	808.5	+0.5
	590	1.0	593.3	+3.3	593.6	+3.6	591.7	+1.7
	388	1.0	391.2	+3.2	391.8	+3.8	391.4	+3.4
	d $\bar{\nu}$		7.1		7.5		7.2	
WSQER		3.488 x 10 ⁻³		3.567 x 10 ⁻³		5.524 x 10 ⁻³		

TABLE 3.17

The only reported spectra and assignments of Fluoro Pentadeutero Benzene are those of Steele et al.^[55], and these were used without modification.

1,2 DIFLUORO BENZENE

			39 (ABS)		37 (ABS)		37 (%)	
	obs. \bar{v}	w	calc. \bar{v}	d \bar{v}	calc. \bar{v}	d \bar{v}	calc. \bar{v}	d \bar{v}
A ₁	3081	0.3	3084.7	+3.7	3084.1	+3.1	3086.9	+5.9
	3060	0.3	3065.8	+5.8	3066.3	+6.3	3067.1	+7.1
	1625	1.0	1619.2	-5.8	1619.4	-5.6	1622.5	-2.5
	1514	1.0	1511.6	-2.4	1511.7	-2.3	1510.7	-3.3
	1313	0.3	1301.4	-11.6	1301.5	-11.5	1300.1	-12.9
	1277	1.0	1285.2	+8.2	1286.7	+9.7	1287.9	+10.9
	1155	1.0	1149.7	-5.3	1149.4	-5.6	1148.8	-6.2
	1025	1.0	1021.9	-3.1	1020.6	-4.4	1021.7	-3.3
	762	1.0	765.3	+3.3	765.3	+4.3	766.0	+4.0
	565	1.0	573.6	+8.6	573.1	+8.1	572.2	+7.2
	287	1.0	289.2	+2.2	289.3	+2.3	289.2	+2.2
	B ₂	3081	0.3	3081.0	+0.0	3081.0	+0.0	3082.5
3060		0.3	3055.0	-5.0	3055.8	-4.2	3055.5	-4.5
1609		1.0	1614.6	+5.6	1615.6	+6.6	1618.4	+9.4
1464		1.0	1467.9	+3.9	1469.3	+5.3	1468.0	+4.0
1292		0.5	1274.2	-17.8	1275.3	-16.7	1277.4	-14.6
1214		1.0	1219.2	+5.2	1218.7	+4.7	1219.5	+5.5
1103		1.0	1095.1	-6.9	1094.4	-8.6	1097.7	-5.3
857		1.0	854.1	-2.9	853.7	-3.3	853.3	-3.7
546		1.0	547.8	+1.8	545.9	-0.1	546.3	+0.3
440		1.0	437.0	-3.0	438.7	-1.3	439.9	-0.1
d \bar{v}			5.3		5.4		5.4	
WSQER			1.400 x 10 ⁻³		1.532 x 10 ⁻³		2.278 x 10 ⁻³	

TABLE 3.18

Spectra and assignments for 1,2-difluoro Benzene have been reported by Nonnenmacher and Mecke^[56], Scott et al^[57] and Green et al^[58]. The frequencies used in this work are those of Green, with two reassignments. Calculations consistently place 1625 cm^{-1} as the a_1 and 1609 cm^{-1} as the b_2 fundamental. Experimental evidence is inconclusive for either set of assignments.

From an investigation of the microwave spectra, Hatta and Kozima^[59] assigned the lowest a_1 fundamental as $255 \pm 10\text{ cm}^{-1}$. Scott assigned the lowest a_1 fundamental to a vvw Raman band at 240 cm^{-1} which was not detected when the Raman spectrum was re-examined by Pearce^[14]. An examination, by Pearce, of the gas phase infra red spectrum showed a confused contour centred at 283 cm^{-1} . It cannot be a type B contour as this would indicate a b_2 fundamental, the lowest of which is observed to be at 440 cm^{-1} ^[57] and calculated by Scherer^[57]. Also there is no strong Q branch and therefore it cannot be the b_1 fundamental observed in the Raman spectrum at 298 cm^{-1} . The liquid phase infra red spectrum shows only one band centred at 287 cm^{-1} ; too far removed from 298 cm^{-1} to be the b_1 fundamental. Scherer calculated the lowest a_1 fundamental to be at 319 cm^{-1} . This suggests that the lowest a_1 fundamental is at 287 cm^{-1} and that the value given by Hatta and Kozima is low.

1,3 DIFLUORO BENZENE

			39 (ABS)		37 (ABS)		37 (%)	
	obs. \bar{v}	w	calc. \bar{v}	d \bar{v}	calc. \bar{v}	d \bar{v}	calc. \bar{v}	d \bar{v}
A ₁	3096	1.0	3094.1	-1.9	3094.4	-1.6	3095.1	-0.9
	3087	1.0	3085.5	-1.5	3085.1	-1.9	3087.5	+0.5
	-	0.0	3058.8	-	3059.6	-	3059.5	-
	1608	1.0	1611.0	+5.6	1612.6	+4.6	1615.3	+7.3
	1456	1.0	1451.9	+3.9	1459.9	+3.9	1456.0	+0.0
	1286	1.0	1281.8	-4.2	1282.6	-3.4	1283.0	-3.0
	1066	1.0	1071.6	+5.6	1070.3	+4.3	1074.0	+8.0
	1008	1.0	1011.0	+3.0	1009.8	+1.8	1010.7	+2.7
	735	1.0	731.9	-3.1	732.3	-2.7	732.2	-2.8
	524	1.0	521.7	-2.3	522.9	-1.1	523.1	-0.9
	331	1.0	329.4	-1.6	329.4	-1.6	329.1	-1.9
B ₂	3087	0.3	3077.8	-9.2	3078.3	-8.7	3079.2	-7.8
	1608	1.0	1612.9	+4.9	1612.8	+4.8	1615.9	+7.9
	1493	1.0	1489.6	-3.4	1489.5	-3.5	1488.5	-4.5
	-	0.0	1307.0	-	1308.9	-	1308.4	-
	-	0.0	1261.1	-	1259.8	-	1261.7	-
	1158	1.0	1152.5	-5.5	1152.1	-5.9	1151.8	-6.2
	1123	1.0	1133.2	+10.2	1132.9	+9.9	1133.9	+10.9
	954	1.0	945.6	-8.4	947.2	-6.8	946.1	-7.9
	514	1.0	504.8	-9.2	505.2	-8.8	505.7	-8.3
	478	1.0	479.8	+1.8	481.1	+3.1	480.4	+2.4
d \bar{v} WSQER			4.7 1.130 x 10 ⁻³	4.4 0.968 x 10 ⁻³	4.7 2.593 x 10 ⁻³			

TABLE 3.19

Spectra and assignments for 1,3 difluoro Benzene have been reported by Ferguson et al^[60], and revisions made by Green et al^[58].

Green's assignments are used in this work, with the exception of the b_2 fundamentals at 1265 cm^{-1} and 1290 cm^{-1} for which there does not appear to be enough evidence.

1,4 DIFLUORO BENZENE

			39 (ABS)		37 (ABS)		37 (%)	
	obs. $\bar{\nu}$	w	calc. $\bar{\nu}$	d $\bar{\nu}$	calc. $\bar{\nu}$	d $\bar{\nu}$	calc. $\bar{\nu}$	d $\bar{\nu}$
A _{1g}	3084	0.8	3087.3	+3.3	3086.9	+2.9	3089.3	+5.3
	1617	1.0	1615.0	-2.0	1615.4	-1.6	1618.1	+1.1
	1245	1.0	1251.7	+6.7	1251.3	+6.3	1253.3	+8.3
	1142	1.0	1142.8	+0.8	1143.3	+1.3	1146.2	+4.2
	849	0.5	838.1	-10.9	837.6	-11.4	838.8	-10.2
	451	0.3	440.0	-11.0	440.6	-10.4	441.4	-9.6
B _{3g}	-	0.0	3070.3	-	3071.3	-	3070.8	-
	1617	1.0	1611.5	-5.5	1610.4	-6.6	1611.1	-5.9
	1285	1.0	1283.5	-1.5	1283.6	-1.4	1283.1	-1.9
	635	1.0	645.1	+10.1	644.1	+9.1	641.8	+6.8
	451	0.3	458.1	+7.1	459.7	+8.7	456.9	+5.9
B _{2u}	3088	0.3	3085.9	-2.1	3085.8	-2.2	3087.9	-0.1
	1425	1.0	1420.7	-4.3	1422.3	-2.7	1424.5	-0.5
	1285	1.0	1281.9	-3.1	1281.9	-3.1	1281.7	-3.3
	1083	1.0	1077.6	-5.4	1076.9	-6.1	1073.4	-9.6
	352	1.0	350.0	-2.0	350.3	-1.7	351.7	-0.3
B _{1u}	-	0.0	3072.7	-	3073.3	-	3073.2	-
	1511	1.0	1507.9	-3.1	1507.1	-3.9	1505.8	-5.2
	1225	1.0	1231.5	+6.5	1231.5	+6.5	1233.1	+8.1
	1012	1.0	1021.7	+9.7	1020.3	+8.3	1019.9	+7.9
	740	1.0	740.0	+0.0	742.4	+2.4	743.3	+3.3
d $\bar{\nu}$			5.0		5.1		5.1	
WSQER			1.205 x 10 ⁻³		1.158 x 10 ⁻³		2.680 x 10 ⁻³	

TABLE 3.20

Spectra and assignments for 1,4 difluoro Benzene have been reported by Ferguson et al^[61]. Stojiljkovic and Whiffen^[62] made a number of reassignments based on a comparison with 1,4 dichloro, 1,4 dibromo and 1,4 diiodo Benzene. Steele et al^[63] examined the liquid phase far infra red spectrum and assigned a band at 352 cm^{-1} as the lowest b_{2u} fundamental. An examination, by Pearce^[14], of the gas phase far infra red spectrum confirmed this assignment by the observation of a band with a type B contour at 346 cm^{-1} .

The a_g and b_{3g} fundamentals are Raman active. There is a moderate Raman band at 451 cm^{-1} which is tentatively assigned as the lowest fundamental for both species. The two very strong polarised Raman bands at 840 cm^{-1} and 858.5 cm^{-1} make it difficult to assign the a_g fundamental.

1,4 DIFLUORO TETRADEUTERO BENZENE

			39 (ABS)		37 (ABS)		37 (%)	
	obs. $\bar{\nu}$	w	calc. $\bar{\nu}$	$\delta\bar{\nu}$	calc. $\bar{\nu}$	$\delta\bar{\nu}$	calc. $\bar{\nu}$	$\delta\bar{\nu}$
A _g	2313	1.0	2299.2	-13.8	2302.2	-10.8	2301.3	-11.7
	1595	1.0	1607.6	+12.6	1607.8	+12.8	1609.9	+14.9
	1229	1.0	1238.6	+9.6	1237.2	+8.2	1240.0	+11.0
	847	0.5	832.9	-14.1	833.4	-13.6	836.6	-10.4
	780	1.0	787.2	+7.2	786.3	+6.3	787.2	+7.2
	453	1.0	438.5	-14.5	439.1	-13.9	439.8	-13.2
B _{3g}	2304	1.0	2293.1	-10.9	2293.6	-10.4	2292.3	-11.7
	-	0.0	1585.1	-	1583.1	-	1584.9	-
	1008	1.0	1005.5	-2.5	1005.6	-2.4	1004.0	-4.0
	614	1.0	618.0	+4.0	617.8	+3.8	615.8	+1.8
	-	0.0	427.2	-	428.5	-	426.0	-
B _{2u}	2310	1.0	2297.7	-12.3	2301.3	-8.7	2299.7	-10.3
	1328	1.0	1331.9	+3.9	1329.9	+1.9	1335.1	+7.1
	1287	1.0	1267.2	-19.8	1267.3	-19.7	1269.1	-17.9
	802	1.0	804.6	+2.6	804.9	+2.9	800.6	-1.4
	348	1.0	345.8	-2.2	346.1	-1.9	347.5	-0.5
B _{1u}	2277	1.0	2294.6	+17.6	2293.8	+16.8	2293.7	+16.7
	1435	1.0	1431.6	-3.4	1426.9	-8.1	1426.5	-8.5
	1130	1.0	1122.7	-7.3	1126.4	-3.6	1126.0	-4.0
	859	1.0	864.3	+5.3	863.9	+4.9	864.7	+5.7
	685	1.0	689.1	+4.1	690.8	+5.8	691.4	+6.4
$\delta\bar{\nu}$ WSQER			8.2 3.617×10^{-3}		7.6 3.085×10^{-3}		8.1 6.077×10^{-3}	

TABLE 3.21

The only reported spectra and assignments for 1,4 difluoro Tetradeutero Benzene are those of Gates et al^[64]. Steele et al^[63] examined the liquid phase far infra red spectrum and assigned the lowest b_{2u} fundamental to a band at 348 cm^{-1} . Gates et al explained the two moderate polarised Raman bands at 828 cm^{-1} and 867 cm^{-1} as an a_g fundamental in resonance with an overtone, which would put the fundamental above 828 cm^{-1} . An examination, by Pearce^[14], of the gas phase infra red spectrum showed type A contours at 859 cm^{-1} and 1439 cm^{-1} .

If the weak Raman band at 1595 cm^{-1} is assigned as the a_g fundamental, then there is no Raman band corresponding to the b_{3g} fundamental calculated to lie at $\sim 1583 \text{ cm}^{-1}$. Similarly, there is no Raman band corresponding to the lowest b_{3g} fundamental calculated to be at $\sim 428 \text{ cm}^{-1}$.

1,2,4 TRIFLUORO BENZENE

			39 (ABS)		37 (ABS)		37 (%)	
	obs. \bar{v}	w	calc. \bar{v}	d \bar{v}	calc. \bar{v}	d \bar{v}	calc. \bar{v}	d \bar{v}
	3094	1.0	3093.9	-0.1	3094.3	+0.3	3094.9	+0.9
	3094	0.3	3086.6	-7.4	3086.3	-7.7	3088.5	-5.5
	3062	0.3	3071.4	+9.4	3072.2	+10.2	3072.0	+10.0
	1629	1.0	1627.0	-2.0	1626.5	-2.5	1627.1	-1.9
	1629	1.0	1620.0	-9.0	1620.6	-8.4	1621.9	-7.1
	1522	1.0	1513.6	-8.4	1512.6	-9.4	1510.5	-11.5
	1443	1.0	1444.5	+1.5	1445.0	+2.0	1444.9	+1.9
	1312	1.0	1316.3	+4.3	1316.0	+4.0	1316.1	+4.1
	1287	1.0	1278.2	-8.8	1278.9	-8.1	1279.1	-7.9
	1250	1.0	1258.3	+8.3	1258.9	+8.9	1259.4	+9.4
A ₁	1203	1.0	1212.7	+9.7	1212.2	+9.2	1212.3	+9.3
	1144	1.0	1147.2	+3.2	1147.7	+3.7	1146.9	+2.9
	1099	1.0	1099.6	+0.6	1099.1	-0.7	1099.5	+0.5
	966	1.0	962.4	-3.6	962.5	-3.5	961.6	-4.4
	782	1.0	786.2	+4.2	786.6	+4.6	786.9	+4.9
	729	1.0	732.8	+3.8	732.9	+3.9	733.3	+4.3
	587	1.0	590.1	+3.1	588.4	+1.4	587.0	+0.0
	503	1.0	506.1	+3.1	507.6	+4.6	507.4	+4.4
	441	1.0	436.6	-4.4	437.4	-3.6	438.4	-2.6
	340	1.0	338.5	-1.5	338.8	-1.2	340.0	+0.0
	284	1.0	288.2	+4.2	288.2	+4.2	287.7	+3.7
d \bar{v}			4.8		5.0		4.6	
WSQER			1.357 x 10 ⁻³		1.373 x 10 ⁻³		2.514 x 10 ⁻³	

TABLE 3.22

The only reported spectra and assignments for 1,2,4 trifluoro Benzene are by Ferguson et al^[66]. The gas phase infra red spectrum was examined by Pearce^[14]. Type A contours were found at 966 cm^{-1} , 782 cm^{-1} and 729 cm^{-1} . In the far infra red spectrum, Pearce observed a type B contour at 340 cm^{-1} , and a very weak type A contour at 284 cm^{-1} .

Thus the reassignments made, based on the calculations, are the replacement of bands at 835 cm^{-1} and 1376 cm^{-1} with a band at 1287 cm^{-1} and another at 1629 cm^{-1} .

1,3,5 TRIFLUORO BENZENE

			39 (ABS)		37 (ABS)		37 (%)	
	obs. $\bar{\nu}$	w	calc. $\bar{\nu}$	d $\bar{\nu}$	calc. $\bar{\nu}$	d $\bar{\nu}$	calc. $\bar{\nu}$	d $\bar{\nu}$
A ₁ '	-	0.0	3095.8	-	3095.8	-	3096.8	-
	1350	1.0	1343.3	-6.7	1343.5	-6.5	1343.5	-6.5
	1010	1.0	1017.5	+7.5	1015.7	+5.7	1017.1	+7.1
	578	1.0	565.2	-12.8	566.7	-11.3	567.5	-10.5
A ₂ '	-	0.0	1298.9	-	1300.8	-	1300.8	-
	-	0.0	1181.4	-	1180.5	-	1178.6	-
	-	0.0	552.7	-	555.3	-	553.0	-
E'	-	0.0	3093.0	-	3093.5	-	3093.9	-
	1620	0.5	1620.0	+0.0	1618.9	-1.1	1621.0	+1.0
	1475	1.0	1467.8	-7.2	1466.2	-8.8	1461.1	-13.9
	1122	1.0	1130.8	+8.8	1130.5	+8.5	1131.5	+9.5
	993	1.0	989.3	-3.7	990.7	-2.3	992.5	-0.5
	500	1.0	502.5	+2.5	503.3	+3.3	504.1	+4.1
	326	1.0	322.9	-3.1	322.8	-3.2	322.4	-3.6
d $\bar{\nu}$ WSQER			5.8 0.990 x 10 ⁻³		5.6 0.889 x 10 ⁻³		6.3 2.985 x 10 ⁻³	

TABLE 3.23

Spectra and assignments for 1,3,5 trifluoro Benzene have been reported by Nielsen et al^[66] and by Scherer et al^[68]. Nielson's assignments were revised by Ferguson^[67]. Scherer's values were used in this work without modification.

1,3,5 TRIFLUORO TRIDEUTERO BENZENE

			39 (ABS)		37 (ABS)		37 (%)	
	obs. $\bar{\nu}$	w	calc. $\bar{\nu}$	d $\bar{\nu}$	calc. $\bar{\nu}$	d $\bar{\nu}$	calc. $\bar{\nu}$	d $\bar{\nu}$
A ₁ '	2309	1.0	2310.1	+1.1	2310.9	+1.9	2310.5	+1.5
	1344	1.0	1343.0	-1.0	1343.1	-0.9	1343.2	-0.8
	966	1.0	965.0	-1.0	963.2	-2.8	964.8	-1.2
	575	1.0	565.1	-1.9	566.6	-8.4	567.4	-7.6
A ₂ '	-	0.0	1265.1	-	1264.8	-	1265.4	-
	-	0.0	950.1	-	951.1	-	954.7	-
	-	0.0	507.1	-	509.4	-	504.3	-
E'	2308	1.0	2308.1	+0.1	2310.1	+2.1	2308.2	+0.2
	1606	0.5	1607.5	+1.5	1606.1	+0.1	1608.2	+2.2
	1420	1.0	1412.0	-8.0	1407.2	-12.8	1405.3	-14.7
	1046	1.0	1045.9	-0.1	1048.2	+2.2	1047.6	+1.6
	792	1.0	782.9	-9.1	783.4	-8.6	785.2	-6.8
	484	1.0	490.6	+6.6	491.3	+7.3	491.9	+7.9
	322	1.0	321.1	-0.9	321.1	-0.9	320.7	-1.3
d $\bar{\nu}$ WSQER			3.6		4.5		4.2	
			0.688 x 10 ⁻³		0.898 x 10 ⁻³		2.565 x 10 ⁻³	

TABLE 3.24

The assignments and frequencies for 1,3,5 trifluoro Trideutero Benzene were taken from the paper of Scherer et al.^[68] and used without modification.

1,2,3,4 TETRAFLUORO BENZENE

			39 (ABS)		37 (ABS)		37 (%)	
	obs. \bar{v}	w	calc. \bar{v}	d \bar{v}	calc. \bar{v}	d \bar{v}	calc. \bar{v}	d \bar{v}
A ₁	-	0.0	3086.6	-	3086.3	-	3088.6	-
	1634	1.0	1632.9	-1.1	1634.6	+0.6	1636.5	+2.5
	1525	1.0	1523.8	-1.2	1525.1	+0.1	1523.6	-1.4
	1331	1.0	1330.1	-0.9	1330.0	-1.0	1330.6	-0.4
	1271	1.0	1274.4	+3.4	1274.6	+3.6	1274.2	+3.2
	1165	1.0	1165.2	+0.2	1164.8	-0.2	1164.4	-0.6
	1050	1.0	1044.1	-5.9	1041.5	-8.5	1041.2	-8.8
	684	1.0	683.2	-0.8	683.1	-0.9	683.3	-0.7
	458	1.0	453.6	-4.4	453.0	-5.0	453.6	-4.4
	325	1.0	322.5	-2.5	323.0	-2.0	324.5	-0.5
	279	1.0	273.9	-5.1	273.3	-5.7	274.5	-4.5
B ₂	-	0.0	3071.5	-	3072.2	-	3072.0	-
	1634	1.0	1639.3	+5.3	1640.5	+6.5	1638.8	+4.8
	1517	1.0	1512.9	-4.1	1512.9	-4.1	1509.8	-7.2
	1278	1.0	1278.5	+0.5	1279.2	+1.2	1278.3	+0.3
	1243	1.0	1249.1	+6.1	1250.1	+7.1	1252.5	+9.5
	991	1.0	990.3	-0.2	988.6	-2.4	989.7	-1.3
	748	1.0	759.5	+11.6	759.3	+11.3	759.8	+11.8
	604	1.0	603.2	-0.8	604.2	+0.2	603.4	-0.6
	490	1.0	492.1	+2.1	491.7	+1.7	492.4	+2.4
	291	1.0	286.5	-4.5	286.5	-4.5	285.3	-5.7
	d \bar{v}		3.2		3.5		3.7	
WSQERR		0.818 x 10 ⁻³		0.981 x 10 ⁻³		4.719 x 10 ⁻³		

TABLE 3.25

The only reported spectra and assignments for 1,2,3,4 tetrafluoro Benzene are by Steele^[69].

A re-examination, by Pearce^[14], of the gas phase infra red spectrum showed a type B contour at 684 cm^{-1} and a type A contour at 748 cm^{-1} . The far infra red gas phase spectrum showed a type B contour at 279 cm^{-1} .

The Raman spectrum was examined again as polarisation data was not reported by Steele.

The reassignments are as follows:-

a_1 class

The fundamental expected to lie at about 1211 cm^{-1} is assigned to a weak, polarised Raman line at 1271 cm^{-1} . The tentative assignment of the lowest fundamental as 268 cm^{-1} can be fixed at 278 cm^{-1} .

b_2 class

Calculations suggest that the fundamental at 1607 cm^{-1} should be higher, at 1634 cm^{-1} . The 1402 cm^{-1} band is excluded, and both the 1278 cm^{-1} and 1243 cm^{-1} bands with type A contours included. The assignment of the lowest fundamental as 310 cm^{-1} is too low and is replaced by the weak, depolarised Raman line observed at 604 cm^{-1} .

1,2,3,5. TETRAFLUORO BENZENE

			39 (ABS)		37 (ABS)		37 (%)	
	obs. \bar{v}	w	calc. \bar{v}	d \bar{v}	calc. \bar{v}	d \bar{v}	calc. \bar{v}	d \bar{v}
A ₁	3090	1.0	3094.9	+4.9	3095.1	+5.1	3095.8	+5.8
	1642	1.0	1637.5	-4.5	1638.7	-3.3	1639.4	-2.6
	1531	1.0	1525.6	-5.4	1524.8	-6.2	1520.1	-10.9
	1384	1.0	1374.9	-9.1	1374.8	-9.2	1373.8	-10.2
	1247	1.0	1250.7	+3.7	1250.6	+3.6	1249.5	+2.5
	1130	1.0	1132.9	+2.9	1132.7	+2.7	1133.3	+3.3
	1002	1.0	996.6	-5.4	997.3	-4.7	999.0	-3.0
	788	1.0	796.3	+8.3	795.6	+7.6	796.3	+8.3
	578	1.0	570.9	-7.1	572.2	-5.8	572.9	-5.1
	445	1.0	441.2	-3.8	441.1	-3.9	442.1	-2.9
	310	1.0	304.5	-5.5	304.6	-5.4	304.7	-5.3
B ₂	-	0.0	3093.0	-	3093.5	-	3094.0	-
	1642	1.0	1633.0	-9.0	1632.8	-9.2	1632.2	-9.8
	1466	1.0	1462.8	-3.2	1462.6	-3.4	1462.4	-3.6
	1273	1.0	1286.2	+13.2	1286.2	+13.2	1286.2	+13.2
	1179	1.0	1172.3	-6.7	1173.3	-5.7	1171.2	-7.8
	1056	1.0	1054.2	-1.8	1052.1	-3.9	1053.2	-2.8
	638	1.0	640.7	+2.7	640.7	+2.7	639.5	+1.5
	505	1.0	511.6	+6.6	512.3	+7.3	512.7	+7.7
	334	1.0	329.3	-4.7	329.5	-4.5	330.1	-3.9
	-	0.0	277.6	-	277.2	-	276.8	-
	d \bar{v} WSQER			5.8 1.788 x 10 ⁻³		5.7 1.735 x 10 ⁻³		5.8 4.920 x 10 ⁻³

TABLE 3.26

The only reported spectra and assignments for 1,2,3,5 tetrafluoro Benzene are by Steele^[69].

A re-examination, by Pearce^[14] of the gas phase infrared spectrum showed a type A contour at 788 cm^{-1} , and type B contours at 638 cm^{-1} and 505 cm^{-1} , which confirms Steele's work.

The gas phase infra red spectrum shows a type A contour at 1249 cm^{-1} and a type B contour at 1273 cm^{-1} .

Reassignments are as follows:-

a₁ class

The polarised Raman band at 1384 cm^{-1} is used instead of the polarised Raman band at 1404 cm^{-1} . From the observed band contour, the missing fundamental is assigned as 1247 cm^{-1} . From the calculations, the moderately strong infra red liquid band at 445 cm^{-1} is chosen rather than the band of similar strength at 471 cm^{-1} .

b₂ class

The fundamental placed at 1240 cm^{-1} is assigned to a band at 1273 cm^{-1} with type B contour. The lowest fundamental seems to be higher than 258 cm^{-1} as calculations put it at $\sim 277\text{ cm}^{-1}$.

1,2,4,5 TETRAFLUORO BENZENE

			39 (ABS)		37 (ABS)		37(%)	
	obs. $\bar{\nu}$	w	calc. $\bar{\nu}$	d $\bar{\nu}$	calc. $\bar{\nu}$	d $\bar{\nu}$	calc. $\bar{\nu}$	d $\bar{\nu}$
A _{1g}	3097	1.0	3093.6	-3.4	3094.0	-3.0	3094.5	-2.5
	1641	1.0	1639.0	-2.0	1638.5	-2.5	1636.0	-5.0
	1374	1.0	1373.3	-0.7	1372.1	-1.9	1372.0	-2.0
	748	1.0	756.2	+8.2	756.3	+8.3	756.2	+8.2
	487	1.0	486.3	-0.7	486.2	-0.8	485.9	-1.1
	280	1.0	282.0	+2.0	281.8	+1.8	278.8	-1.2
B _{3g}	-	0.0	1625.4	-	1626.5	-	1627.3	-
	1196	1.0	1196.3	+0.3	1197.2	+1.2	1195.8	-0.2
	1120	1.0	1125.0	+5.0	1126.2	+6.2	1126.0	+6.0
	637	1.0	633.7	-3.3	632.3	-4.7	630.8	-6.2
	418	1.0	416.5	-1.5	417.5	-0.5	419.1	+1.1
B _{2u}	3088	1.0	3094.1	+6.1	3094.5	+6.5	3095.1	+7.1
	1435	1.0	1444.9	+9.9	1446.3	+11.3	1447.8	+12.8
	1224	1.0	1227.1	+3.1	1224.9	+0.9	1225.0	+1.0
	700	1.0	711.6	+11.6	710.6	+10.6	712.4	+12.4
	3455	1.0	343.3	-2.2	343.7	-1.8	345.1	-0.4
B _{1u}	1534	1.0	1527.1	-6.9	1526.2	-7.8	1525.1	-8.9
	1277	1.0	1283.5	+6.5	1282.3	+5.3	1281.5	+4.5
	1161	1.0	1164.5	+3.5	1166.3	+5.3	1164.8	+3.8
	853	1.0	865.1	+12.1	865.5	+12.5	864.0	+11.0
	299	1.0	295.4	-3.6	295.8	-3.2	298.2	-0.8
d $\bar{\nu}$ WSQER			4.6 1.311 x 10 ⁻³		4.8 1.488 x 10 ⁻³		4.8 2.546 x 10 ⁻³	

TABLE 3.27

The only reported spectra and assignments for 1,2,4,5 tetrafluoro Benzene are by Ferguson et al^[70]. Steele and Whiffen^[71] made some reassignments on the basis of a comparison with Pentafluoro Benzene.

A re-examination, by Pearce^[14], of the gas phase infra red spectrum showed type B contours at 1435 cm^{-1} , 1224 cm^{-1} and 700 cm^{-1} and type A contours at 1277 cm^{-1} , 1161 cm^{-1} and 853 cm^{-1} .

An extension of the range showed a type B contour at 345.5 cm^{-1} , and a weaker band at 299 cm^{-1} .

Thus all b_{2u} and b_{1u} fundamentals can be easily assigned.

The Raman spectrum was re-examined, and the a_{1g} and b_{3g} fundamentals reassigned. The highest a_{1g} fundamental must lie $\sim 1600\text{ cm}^{-1}$ and is assigned as 1643 cm^{-1} . Of the two bands 1374 cm^{-1} and 1338 cm^{-1} the very strong one at 1374 cm^{-1} is chosen. The weak band at 832 cm^{-1} is excluded, and the lowest fundamental is assigned to a weak, polarised Raman band at 280 cm^{-1} .

The highest b_{3g} fundamental is difficult to assign as the very weak band at 1611 cm^{-1} does seem rather low, compared with separations of the two fundamentals $\sim 1600\text{ cm}^{-1}$ in other molecules. The lowest fundamental is not as low as 202 cm^{-1} , and is assigned to a band at 418 cm^{-1} .

PENTAFLUORO BENZENE

			39 (ABS)		37 (ABS)		37(%)	
	obs. \bar{v}	w	calc. \bar{v}	d \bar{v}	calc. \bar{v}	d \bar{v}	calc. \bar{v}	d \bar{v}
A ₁	3097	1.0	3093.8	-3.2	3094.2	-2.8	3094.8	-2.2
	1645	1.0	1646.8	+1.8	1647.7	+2.7	1644.9	-0.1
	1512	1.0	1521.9	+9.9	1524.0	+12.0	1523.0	+11.0
	1414	1.0	1402.3	-11.7	1402.0	-12.0	1402.1	-11.9
	1293	1.0	1289.9	-3.1	1289.7	-3.3	1288.5	-4.5
	1079	1.0	1074.4	-4.6	1071.7	-7.3	1072.1	-6.9
	718	1.0	731.1	+13.1	730.4	+12.4	731.2	+13.2
	578	1.0	576.6	-1.4	577.8	-0.2	578.2	+0.2
	474	1.0	475.7	+1.7	474.8	+0.8	475.0	+1.0
	329	1.0	327.8	-1.2	328.1	-0.9	329.2	+0.2
	275	0.5	277.1	+2.1	276.6	+1.6	274.1	-0.9
B ₂	1645	1.0	1641.3	-3.7	1643.3	-1.7	1642.9	-2.1
	1535	1.0	1532.1	-2.9	1532.6	-2.4	1529.9	-5.1
	1275	1.0	1273.8	-1.2	1272.8	-2.2	1272.9	-2.1
	1178	1.0	1185.5	+7.5	1186.2	+8.2	1184.4	+6.4
	1142	1.0	1136.3	-5.7	1137.2	-4.8	1136.7	-5.3
	958	1.0	955.8	-2.2	952.9	-5.1	954.6	-3.4
	688	1.0	684.6	-3.4	685.5	-2.5	685.0	-3.0
	436	1.0	434.8	-1.2	434.2	-1.8	435.2	-0.8
	304	1.0	302.7	-1.3	302.9	-1.1	304.3	+0.3
	275	0.5	272.8	-2.2	272.1	-2.9	273.9	-1.1
d \bar{v} WSQER			4.1 1.406 x 10 ⁻³	4.2 1.581 x 10 ⁻³	3.9 2.567 x 10 ⁻³			

TABLE 3.28

The only reported spectra and assignments for Pentafluoro Benzene are by Steele and Whiffen^[77]. A re-examination, by Pearce^[14], of the gas phase infra red spectrum showed a type B contour at 718 cm^{-1} and a type A contour at 958 cm^{-1} . The gas phase far infra red spectrum showed a type B contour at 329 cm^{-1} and a type A contour at 304 cm^{-1} .

A tentative reassignment of the lowest a_1 and b_2 fundamentals places them both at 275 cm^{-1} .

PENTAFLUORO DEUTERO BENZENE

			39 (ABS)		37 (ABS)		37(%)	
	obs. \bar{v}	w	calc. \bar{v}	d \bar{v}	calc. \bar{v}	d \bar{v}	calc. \bar{v}	d \bar{v}
A ₁	2315	1.0	2308.4	-6.6	2310.0	-5.0	2308.6	-6.4
	1644	1.0	1640.9	-3.1	1642.0	-2.0	1639.3	-4.7
	1527	1.0	1519.3	-7.7	1521.2	-5.8	1520.2	-6.8
	1405	1.0	1394.9	-10.1	1394.0	-11.0	1394.8	-10.2
	1288	1.0	1280.7	-7.3	1280.3	-7.7	1279.3	-8.7
	1075	1.0	1067.9	-7.1	1065.1	-9.9	1065.5	-9.5
	705	1.0	716.7	+11.7	716.2	+11.2	717.0	+12.0
	578	1.0	576.1	-1.9	577.2	-0.8	577.7	-0.3
	467	1.0	473.9	+6.9	473.0	+6.0	473.2	+6.2
	325	1.0	327.3	+2.3	327.6	+2.6	328.7	+3.7
	-	0.0	277.1	-	276.5	-	274.0	-
B ₂	1644	1.0	1641.2	-2.8	1643.2	-0.8	1642.9	-1.1
	1515	1.0	1518.1	+3.1	1518.1	+3.1	1516.0	+1.0
	1267	1.0	1262.7	-4.3	1261.0	-6.0	1260.8	-6.2
	1146	1.0	1144.2	-1.8	1144.2	-1.8	1144.0	-2.0
	1024	1.0	1017.4	-6.6	1017.9	-6.1	1016.5	-7.5
	873	1.0	875.6	+2.6	875.0	+2.0	877.6	+4.6
	631	1.0	629.0	-2.0	629.6	-1.4	627.9	-3.1
	435	1.0	434.3	-0.7	433.7	-1.3	434.7	-0.3
	-	0.0	302.3	-	302.6	-	303.9	-
	-	0.0	272.8	-	272.1	-	273.9	-
d \bar{v} WSQER			4.5 1.277 x 10 ⁻³		4.4 1.331 x 10 ⁻³		5.0 3.723 x 10 ⁻³	

TABLE 3.29

In this paper on Pentafluoro Benzene, Steele and Whiffen^[71] also reported some assignments for Pentafluoro Deutero Benzene.

The only reassignment made was to reject the moderate infra red band at 1175 cm^{-1} in favour of the moderate band at 1146 cm^{-1} .

HEXAFLUOROBENZENE

			39 (ABS)		37 (ABS)		37 (%)	
	obs. $\bar{\nu}$	w	calc. $\bar{\nu}$	d $\bar{\nu}$	calc. $\bar{\nu}$	d $\bar{\nu}$	calc. $\bar{\nu}$	d $\bar{\nu}$
A _{1g}	1490	1.0	1490.8	+0.8	1490.7	+0.7	1488.1	-1.9
	559	1.0	558.5	-0.5	560.0	+1.0	559.4	+0.4
A _{2g}	-	0.0	774.4	-	775.9	-	777.6	-
E _{2g}	1655	1.0	1653.0	-2.0	1654.9	-0.1	1651.8	-3.2
	1157	1.0	1158.6	+1.3	1158.8	+1.8	1157.7	+0.7
	443	1.0	445.3	+2.3	443.6	+0.6	444.2	+1.2
	264	1.0	273.6	+9.6	272.8	+8.8	270.5	+6.5
B _{1u}	1323	1.0	1327.3	+4.3	1328.1	+5.1	1326.2	+3.2
	-	0.0	609.8	-	610.3	-	611.7	-
B _{2u}	1253	1.0	1258.0	+5.0	1255.5	+2.5	1255.4	+2.4
	-	0.0	270.5	-	269.8	-	275.0	-
E _{1u}	1530	1.0	1542.7	+12.7	1546.2	+16.2	1545.6	+15.6
	1007	0.5	1012.0	+5.0	1007.1	+0.1	1008.2	+1.2
	315	1.0	315.5	+0.5	315.8	+0.8	317.2	+2.2
d $\bar{\nu}$			4.0		3.4		3.5	
WSQER			0.770 x 10 ⁻³		0.903 x 10 ⁻³		3.200 x 10 ⁻³	

TABLE 3.30

Spectra and assignments have been reported for Hexafluoro Benzene by Delbouille^[72, 73] and by Steele and Whiffen^[74].

The Raman spectrum was re-examined, and the two inactive e_{2u} fundamentals were assigned as 640 cm^{-1} and 145 cm^{-1} . The frequencies used were taken from Steele and Whiffen.

TABLE 3.31

<u>Fundamental Frequencies of Hexafluoro Benzene</u>		
<u>cm⁻¹</u>	<u>class</u>	<u>Justification</u>
145	e_{2u}	Raman, w, in violation of selection rules
195	b_{2g}	
217	a_{2u}	I.R.(g), Raman, vw, in violation of selection rules
264	e_{2g}	Raman dp, m
270	b_{2u}	
315	e_{1u}	I.R.(g), vvs, also Raman dp, vw, in violation of selection rules
370	e_{1g}	Raman dp, m
443	e_{2g}	Raman dp, ms
559	a_{1g}	Raman p, s
606	b_{1u}	
640	e_{2u}	Raman p at 1280 cm^{-1}
714	b_{2g}	Raman p at 1429 (l) or 1436 (g)
770	a_{2g}	
1007	e_{1u}	I.R.(l) shows 994 vvs and 1019 vvs. Fermi resonance of e_{1u} fundamental at $\sim 1007\text{ cm}^{-1}$ with $370 + 640 = 1010\text{ cm}^{-1}$
1157	e_{2g}	Raman dp, m
1253	b_{2u}	$1157 + 1253 = 2410$ $1655 + 1253 = 2908$ $2 \times 1253 = 2506$
1323	b_{1u}	$1655 + 1323 = 2978$ $1157 + 1323 = 2480$
1490	a_{1g}	Raman p, ms
1530	e_{1u}	I.R.(l), vvvs
1655	e_{2g}	Raman dp, m

TABLE 3.32 Infra-red active Binary Summations for D_{6h}

	a_{1g}	e_{2g}	a_{2g}	b_{2g}	e_{1g}
e_{1u}	e_{1u}	e_{1u}	e_{1u}	ia	e_{2u}
b_{1u}	e_a	e_{1u}	ia	e_{1u}	ia
b_{2u}	ia	e_{1u}	ia	ia	ia
a_{2u}	a_{2u}	ia	ia	ia	e_{1u}
e_{2u}	ia	a_{2u}	ia	a_{2u}	e_{1u}




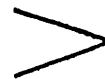
TABLE 3.33 Raman active Binary Summations for D_{6h}

	a_{1g}	a_{2g}	b_{2g}	e_{1g}	e_{2g}
a_{1g}	a_{1g}	ia	ia	e_{1g}	e_{2g}
a_{2g}		a_{1g}	ia	e_{1g}	e_{2g}
b_{2g}			a_{1g}	e_{2g}	e_{1g}
e_{1g}				$a_{1g} + e_{2g}$	e_{1g}
e_{2g}					$a_{1g} + e_{2g}$

	a_{2u}	b_{1u}	b_{2u}	e_{1u}	e_{2u}
a_{2u}	a_{1g}	ia	ia	e_{1g}	e_{2g}
b_{1u}		a_{1g}	ia	e_{2g}	e_{1g}
b_{2u}			a_{1g}	e_{2g}	e_{1g}
e_{1u}				$a_{1g} + 3e_{2g}$	e_{1g}
e_{2u}					$a_{1g} + e_{2g}$

TABLE 3.34 Possibilities for assignment of Summation Bands of

Hexafluoro Benzene

416	$145 + 264 = 409$		
466	$145 + 315 = 460(R)$		
482			
514	$145 + 370 = 515$		$264 + 270 = 534$
553			
569			
583	$264 + 315 = 579$		$145 + 443 = 588$ $217 + 370 = 587$
648			
717	$270 + 443 = 713$		
755	$315 + 443 = 758$		
776	$217 + 559 = 776$		$195 + 606 = 801$
841	$195 + 640 = 835$		
849	$145 + 714 = 859$		
872	$315 + 559 = 874$		$264 + 506 = 870$
885			
965			
1010	$370 + 640 = 1010$		
1044	$443 + 606 = 1049$		
1086	$315 + 770 = 1085$		$443 + 640 = 1083$
1160			
1248			
1266	$264 + 994 = 1258$		
1277	$264 + 1019 = 1283$		
1304	$606 + 714 = 1320$		$145 + 1157 = 1302$
1348	$640 + 714 = 1354$		
1365	$370 + 994 = 1364$		$370 + 1019 = 1389$
1402			$270 + 1157 = 1427$
1442	$443 + 994 = 1437$		
1470	$315 + 1157 = 1472$		$443 + 1019 = 1462$
1488			
1510	$264 + 1253 = 1517$		$195 + 1323 = 1518$
1552	$559 + 994 = 1553$		
1565			
1575	$559 + 1019 = 1578$		$264 + 1323 = 1587$
1600			
1693	$443 + 1253 = 1696$		
1710	$217 + 1490 = 1707$		

/continued

1765	$443 + 1323 = 1766$	}	$606 + 1157 = 1763$	$770 + 994 = 1764$
			$770 + 1019 = 1789$	$264 + 1530 = 1794$
1806	$640 + 1157 = 1797$	}	$315 + 1490 = 1805$	$145 + 1655 = 1800$
1838				
1897	$370 + 1530 = 1900$	}	$270 + 1655 = 1925$	
1940				
1976	$315 + 1655 = 1970$		$443 + 1530 = 1973$	
2040	$714 + 1323 = 2037$			
2087	$559 + 1530 = 2089$			
2150	$994 + 1157 = 2151$			
2173	$1019 + 1157 = 2176$			
2261	$606 + 1655 = 2261$		$770 + 1530 = 2300$	
2408	$1157 + 1253 = 2410$			
2480	$994 + 1490 = 2484$		$1157 + 1323 = 2480$	
2500	$1253 + 1253 = 2506$			
2580				
2686	$1019 + 1655 = 2674$		$1157 + 1530 = 2687$	
2850				
2909	$1253 + 1655 = 2908$			
2976	$1323 + 1655 = 2978$			
3024	$1490 + 1530 = 3020$			
3179	$1530 + 1655 = 3185$			

CHAPTER FOUR

The Force Fields

Section 4.1 Introduction

The Potential Energy expression (Section 2.1) is completely general. It does not differentiate between the different substituents on different molecules, and can therefore show the force constants only in the most general terms.

The G.V.F.F. for the series of molecules being studied can be constructed, which includes all possible types of interaction between all the different types of internal coordinates, but excludes any effects from atoms which are not involved in the internal coordinate defining a particular force constant. If a force field containing every parameter defined were to be calculated, it would not necessarily reproduce the G.V.F.F. of each molecule since it is an overlay force field, based on the assumption that similar internal coordinate deformations in similar environments in different molecules should require the same force. It is important to realise that it is the force field which is transferable between molecules, and not individual force constants, since a force constant is defined only in terms of the force field of which it is a member.

When the data set is not large enough to calculate the G.V.F.F., certain interaction force constants are ignored. Such a field is only an approximation, but provided that the force constants to be ignored are chosen on a correct basis it should satisfactorily reproduce the observed vibrational frequencies. The choice of which interaction force constants are to be included in the Benzene force field has been made in

two ways, as explained in Chapter 1. The H.O.F.F., which was used by Duinker, is a method of calculating stretch/angle bend interaction force constants from the diagonal stretch force constants, and, as he found, no predictions can be made concerning many of the interaction force constants. In the M.V.F.F., those interaction force constants which might be expected to be significant are included, but care must be taken that any assumptions made are valid. Califano [48] has pointed out the fallacies in two common assumptions. The first and more serious is that the force constants for the interaction of a C-H stretch with any other coordinate can be neglected. This is based on the fact that since C-H stretching frequencies are usually much greater than the others, it is possible to factorise the secular equation and calculate the C-H stretching frequencies separately^[17]. This is a mathematical procedure without any chemical basis and cannot be applied to C-D stretches since these frequencies are much closer to the others and the interaction force constants cannot be neglected. But the force constants for the C-H stretches should be transferable to C-D stretches and vice versa, and the above assumption is not valid. The second assumption often made is that interactions between coordinates become less important the further apart they are in the molecule. This is a reasonable approximation for some large molecules, but not for systems containing conjugated bonds, like Benzene, where resonance structures become important.

Section 4.2 Scaling of Force Constants

It was necessary to assume that all the molecules have the same bond lengths and angles since in the Harmonic Oscillator approximation

$$2V = \sum_{i,j} f_{i,j} dR_i dR_j$$

where dR_i and dR_j are expressed in Angstroms and V , the Potential Energy, in millidyne Angstroms. If the internal coordinates are scaled by appropriate bond lengths to be unitless, all the force constants have to be similarly scaled, by a scaling factor

$$(R_{12} \cdot R_{23})^{\frac{1}{2}} \text{ for an angle bend } d\alpha$$

and by r_{14} for an in-plane angle bend $d\beta$.

Thus all the force constants are expressed in units of force per unit length, that is millidynes per Angstrom. This scaling of the force constants was implicit in all the calculations. So that the force constants are transferable between molecules, either the approximation is made that all molecules have the same geometry, so that the internal coordinates to which they refer contain bonds of constant length, or, the true geometries are used, and the force constants are scaled via the specification matrix Z .

It is important to realise that there are two distinct sets of units commonly used in the literature. Force constants can be expressed in units of

$$\begin{array}{l} \text{N/m (md/\AA)} \quad \text{or} \\ 10^2 \text{ N/m(md/\AA)}, 10^{-8} \text{ N/rad (md/rad)}, 10^{-18} \text{ Nm/rad}^2 (\text{md } \overset{\circ}{\text{A}}/\text{rad}^2) \end{array}$$

Consideration of the Potential Energy function shows how these two sets are related,

$$\text{N/m} \quad 2V = f_{\alpha} (r_{\overset{\circ}{O}} R_{\overset{\circ}{O}}) \beta_i \alpha_i$$

$$\text{Nm/rad}^2 \quad 2V = f'_{\alpha} (\beta_i \alpha_i)$$

$$\therefore f'_{\alpha} = f_{\alpha} \cdot (r_{\overset{\circ}{O}} R_{\overset{\circ}{O}})$$

Table 4.1

FORCE CONSTANT UNITS N/m	MULTIPLICATION FACTOR	UNITS
$R_i, (R_i R_{i+1})$ etc.	1	10^2 N/m
$r_i, (r_i r_{i+1})$ etc.	1	
$(r_i R_i)$ etc.	1	
$(\alpha_i R_i), (\alpha_i r_i)$	R_o	10^{-8} N/rad
$(\beta_i R_i), (\beta_i r_i)$	r_o^s	
$\alpha_i, (\alpha_i \alpha_{i+1})$ etc.	R_o	10^{-18} Nm/rad ²
$\beta_i, (\beta_i \beta_{i+1})$ etc.	$r_o^s \cdot r_o^s$	
$(\beta_i \alpha_{i+1})$	$r_o^s \cdot R_o$	

Because the Benzene geometry is assumed for all molecules

$$(R_{i-1} \cdot R_i)^{\frac{1}{2}} = R_o \quad (\text{for an } \alpha_i \text{ deformation})$$

S is H or F as appropriate.

It is convenient to multiply the value of the force constants by 10^2 .

Thus the units used in this work are

$$\text{N/m}, 10^{-10} \text{ N/rad}, 10^{-20} \text{ Nm/rad}^2$$

This set was chosen because when the effect is compared of different environments on the deformation of an angle bend, or the difference between the force required to deform a C-H bond, and the force required to deform a C-F bond in the same environment, units of force per unit angular displacement are preferable to units of force per unit length.

Section 4.3 Absolute/Percentage Weighting

As explained in sections 2.2 and 2.3, the true vibrational frequency may differ from the observed for two main reasons, anharmonicity of vibrations and random errors in measurements. There seems to be some controversy concerning the weighting of the frequencies, done by including a weight matrix, P , in the equations to be solved to obtain corrections to the force constants.

Duinker maintained that, as Brodersen and Langseth^[25] had found that in Benzene the errors due to anharmonicity were small, then, since the anharmonicity of a vibration is strongly correlated with the amplitude of motion in that vibration, the replacement of light Hydrogen atoms with much heavier Fluorine atoms would be expected to cause a reduction in the anharmonicity of vibration. He therefore used percentage weighting.

Aldous and Mills^[49] expressed the view that if the frequencies are not corrected for anharmonicity, then since the differences between observed and calculated frequencies are not due to experimental error but to anharmonicity, these errors will be greater for the higher frequencies, and so percentage weighting should be used.

Overend and Scherer^[50] considered that anharmonic effects are not random, and as the experimental errors are evenly distributed, absolute weighting should be used. In favour of their arguments, it should be noted that harmonic corrections are almost always positive, whereas the effect of the weight matrix is to give an unbiased dispersion each side of the calculated frequency.

To make allowances for a larger than normal uncertainty in a particular frequency, the corresponding entry in P may be decreased by a fractional entry in W , a numerical diagonal matrix. Λ° are the eigen values, so the matrices $\Lambda^{\circ-1}$ and $\Lambda^{\circ-2}$ are diagonal.

For an absolute fit

$$P = (\Lambda)^{-1} W$$

For a percentage fit

$$P = (\Lambda)^{-2} W$$

Section 4.4 Statistical Dispersion

The dispersion on the force constants is given by the following formula.

$$\sigma \{f_j\} = K \frac{1}{\sqrt{2}} \left(\frac{u}{r-s} \right)^{\frac{1}{2}} \quad j = 1 \dots r$$

provided the elements of the F matrix are free variables so that $|K| \neq 0$.

The symbols are defined as follows:-

$$K = [J'PJ]^{-1} \quad \text{where}$$

J is the Jacobian matrix with elements $\partial \Lambda_p^i / \partial f_m^i$

P is the weighting matrix, which, as described previously, is $[\Lambda_p^{-1}]$ for absolute weighting and $[\Lambda_p^{-2}]$ for percentage weighting.

r is the number of force constants.

s is the number of frequencies.

and $u = ePe'$ is the weighted sum of the squares of the residual errors

where the error vector $e = \Delta fJ - \Delta \Lambda$.

If the statistical dispersion of a force constant is of the same order of magnitude as the force constant itself, it may not be set equal to zero and neglected completely. The calculations show that although the force constant is extremely ill-defined, its value lies somewhere within the range, not at the arbitrary point zero.

Because the method of deriving the expression for the Jacobian is based on first order perturbation theory, the term "perturbation" should be used to describe the derivation of the Jacobian rather than the entire process of force constant evaluation.

[14,49,100,101]

Section 4.5 Problems arising during the Force Constant Refinement Process

The refinement process minimises some function of the difference between the calculated and observed frequencies, chosen to be

$$\chi = \sum_i P_i [f(\nu_i^c) - f(\nu_i^o)]^2$$

where $f(\nu_i)$ is a function of the i^{th} frequency in a set and P_i is an appropriate weighting factor (Section 4.3).

To minimise χ with respect to adjustments in the n^{th} set of m force constants, χ is expressed in terms of the Δf^n by relating the change $\Delta \lambda_i^n$ in the i^{th} eigen value to the changes in the force constants through a Taylor series expansion

$$\Delta \lambda_i^n(f_1^n, \dots, f_m^n) = \sum_j \left| \frac{\partial \lambda_i}{\partial f_j} \right| \Delta f_j^n + \frac{1}{2} \sum_{j,k} \left| \frac{\partial^2 \lambda_i}{\partial f_j \partial f_k} \right| \Delta f_j^n \Delta f_k^n + \text{higher order terms} \quad (1)$$

$J_{i,j} = \left| \frac{\partial \lambda_i}{\partial f_j} \right|$ is the Jacobian matrix.

If all second and higher order terms are neglected, the $\Delta \lambda_i^n$ are linearly related to the Δf^n by the matrix equation

$$[\Delta \lambda^n] = J^n [\Delta f^n]^{-2} \quad (2)$$

Non-linearity

If the corrections Δf^n are very small, the second order terms in Eq (1) can be neglected and Eq (2) is a good approximation. If, however, the initial force field is not close to the final force field, this approximation does not necessarily hold, and second and higher order terms become important. Eq (2) is no longer valid, so the fit may get worse, and the calculations become unstable.

If the condition of linearity is not upheld, and the Δf are too large, or would lead to unreasonable f 's, the corrections are scaled down such that

$$f^{n+1} = f^n + a\Delta f^n \quad 0 < a < 1$$

and second and higher order terms can again be neglected.

Singularity

The normal equation to be solved to obtain the changes which have to be made to the force constants is

$$\Delta F = (J^t W J)^{-1} J^t W \Delta \Lambda$$

where $\Delta \Lambda$ is a column matrix whose i^{th} element $\Delta \lambda_i$ is the change in the i^{th} eigen value.

If the determinant of the matrix $(J^t W J)$ is equal to zero, the matrix is singular and cannot be inverted. With a computer, and a good numerical method, however, apparently satisfactory solutions to the normal equation can be obtained even when the matrix is very close to being singular.

Singularity in $(J^t W J)$ can be tested for by comparing the determinant of the matrix with the product of the diagonal elements - if the determinant is small by this standard, then the equations are ill-conditioned. Since the matrix is symmetric and positive definite, it must be dominated by its diagonal elements. The determinant will be made smaller by off-diagonal elements. If these are small, the product and the diagonals will be of the

same order of magnitude and the correlation coefficients remain unimportant, but as they get larger, $(J^t W J)$ approaches singularity, and some of the correlation coefficients start to approach unity. Usually in this case, one of the diagonal elements of $(J^t W J)^{-1}$ will be large, giving rise to a high uncertainty in the associated force constants.

These near-linear dependencies can be removed either by the introduction of more data, or by constraining to a fixed value those force constants which have large rms errors, choice being made on physical rather than mathematical grounds.

Chapter FiveDiscussion of the Force FieldsSection 5.1 Selection of the Parameters for the Modified ValenceForce Field

A number of constraints were placed on the quadratic force field.

The stretching of the ring C-C bond depends on the two substituents on the carbon atoms involved. A linear relationship was introduced

$$R^{HF} = \frac{1}{2} \{ R^{HH} + R^{FF} \}$$

The stretching of the C-X bond, where X = H or F, depends on the ortho-substituents, but not on those in the meta or para positions.

Two linear relationships were introduced

$$r^{HF}(H) = \frac{1}{2} \{ r^{HH}(H) + r^{FF}(H) \}$$

and

$$r^{HF}(F) = \frac{1}{2} \{ r^{HH}(F) + r^{FF}(F) \}$$

The angle bend depends on the substituent on the central carbon atom.

The in-plane angle bend of the C-X bond is ortho dependent only.

Two linear relationships were introduced.

$$\beta^{HF}(H) = \frac{1}{2} \{ \beta^{HH}(H) + \beta^{FF}(H) \}$$

$$\beta^{HF}(F) = \frac{1}{2} \{ \beta^{HH}(F) + \beta^{FF}(F) \}$$

The interaction force constants depend only on the atoms involved in the deformation.

Following Scherer and Overend^[5], the Kekulé type C-C/C-C interaction relation was assumed.

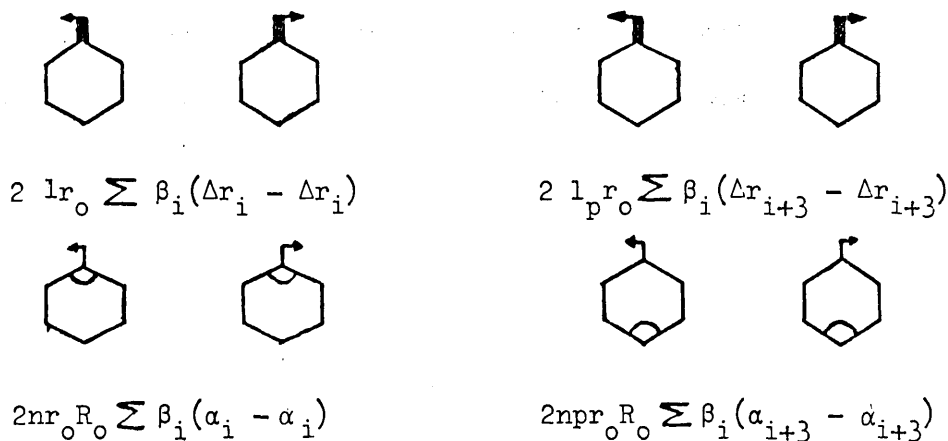
$$(R_i R_{i+1}) = -(R_i R_{i+2}) = (R_i R_{i+3})$$

The assumptions already made can be summarised as follows

- the Harmonic Oscillator approximation was used to derive the potential function
- the frequencies were not corrected for anharmonicity
- all the Fluorine substituted Benzenes were assumed to be planar
- the C_6 framework was assumed to be a regular hexagon with Benzene geometry
- all the C-F bonds were assumed to make 120° angles with the C-C bonds of the C_6 ring
- all C-F bonds were assumed to be of equal length.

The aim, therefore, was to introduce the fewest interaction force constants necessary for the average frequency deviation to be $10-15 \text{ cm}^{-1}$.

Because of the directional character of β , non-zero values of the terms



in the potential energy expression are inconsistent with the symmetry of the molecule.

There are also three independent relationships between the internal coordinates (Section 1.4). Since they are expected to be small, explicit mention was removed of the terms

$$(\alpha_i \alpha_{i+2}), \quad (\alpha_i \alpha_{i+3})$$

$$(\alpha_i r_{i+3})$$

As this still left a very large number of force constants, more arbitrary restrictions were imposed. The following interaction force constants were set equal to zero.

$$(\alpha_i R_{i+2}), \quad (\alpha_i R_{i+3})$$

$$(\beta_i R_{i+3})$$

$$(r_i r_{i+2}), \quad (r_i r_{i+3})$$

$$(\alpha_i r_{i+2})$$

$$(\beta_i r_{i+2})$$

$$(\beta_i \alpha_{i+2})$$

All involve internal coordinates which are non-adjacent.

Certain constants which were expected to be small were introduced later to explore the effects on the field.

$$(r_i(H) r_{i+1}(H))$$

$$(\beta(H) R_{i+1}), \quad (\beta(F) R_{i+1})$$

$$(r_i(H) R_i)$$

Section 5.2 The Force Fields Obtained using the Constraint

$$\underline{(R_i R_{i+1}) = -(R_i R_{i+2}) = (R_i R_{i+3})}$$

Initial guesses for the force constants were inspired by Duinker and Mills^[9, 10] for Benzene, and Steele and Whiffen^[122] for Hexafluoro Benzene. Convergence was smooth and rapid.

There was no significant effect when certain ill-defined terms such as $(\beta_i(F) r_{i+1})$, $(r_i(F) R_{i+1})$, $(r_i(F) R_{i+2})$ (Table 5.1, 37(ABS), 37(%)) were constrained to zero.

The parameters $(r_i(H) R_i)$ and $(\alpha_i r_i(H))$ are strongly correlated. Constraining one produces a significant value for the other, but the values cannot be fixed by the data available. Constraining both force constants to zero has negligible effect on the field.

The relative merits of absolute and percentage weighting have been discussed (Section 4.3). It can be seen from Table 5.1 that the effect of changing the weighting is insignificant.

Because the frequency data are affected with errors (Section 2.3), the values of the force constants can be changed slightly without significant changes to the fit.

It was found that two or three erroneous assignments had little effect on the field. This greatly increases confidence in the converged results.

A serious problem with force constant calculations is that the converged values for the force constants depend upon the initial guesses^[100]. Using the 37 parameter field, and minimising the least squares of the absolute errors of the frequencies, a new set of initial values was chosen. Whiffen's values^[2] were given to those parameters which occur in Benzene. The diagonal force constants involving Fluorine atoms were given the values

obtained in this work, and all the other interaction force constants were set to zero. Convergence onto the values given in Table 5.1 37(ABS) was very rapid.

One of the tests for transferability is that those force constants in the M.V.F.F. applied to all the Fluorine substituted Benzenes which occur in Benzene, are in reasonable agreement with the values calculated separately for Benzene. Table 5.3 compares the relevant force constants of the 37(ABS) field with Duinker's force field^[10] for the in-plane vibrations of Benzene. It must be remembered that his values were used as the initial guesses, and the models were similar, but the transferability condition is a severe extra constraint, and the extent of agreement is most encouraging.

Section 5.3 The Effects of lifting the Constraint

$$\underline{(R_i R_{i+1}) = -(R_i R_{i+2}) = (R_i R_{i+3})}$$

One of the most important constraints placed on the general quadratic force field was that

$$(R_i R_{i+1}) = -(R_i R_{i+2}) = (R_i R_{i+3})$$

The vibrational problem was re-examined, without this restriction. The difficulties encountered are discussed in Section 4.5. A large number of interaction force constants were selectively constrained to zero, but the calculations remained unstable. Considering only the diagonal force constants, comparison of Tables 5.1 and 5.2 show the trends.

$$r^{HH}(H) < r^{FF}(H) < r^{HH}(F) < r^{FF}(F)$$

$$\alpha(H) < \alpha(F)$$

$$\beta^{HH}(H) > \beta^{FF}(H)$$

$$\beta^{HH}(F) > \beta^{FF}(F)$$

to be the same in both sets of calculations. When the constraint on the C-C/C-C interactions is removed, the C-C diagonal stretching force constants

are ill-defined, which affects all interaction force constants involving the C-C stretch, and, though to a smaller extent, every parameter in the field.

The opportunity was taken to explore the effects of constraining $(r_i(E)\alpha_i)$ to different values, but it appears to have very little significance on the convergence.

Scherer^[6] obtained a M.V.F.F. for the in-plane vibrations of the Chlorine substituted Benzenes, where $(R_i R_{i+1})$, $(R_i R_{i+2})$, $(R_i R_{i+3})$ were separate parameters. Because his concept of an in-plane angle bend is derived from the Urey-Bradley mode, direct comparison of his field with ours is not really possible.

His calculations show that $R^{HH} > R^{ClCl}$. Our calculations show that $R^{HH} > R^{FF}$, or $R^{HH} < R^{FF}$, depending upon which interaction force constants are constrained.

Our calculations do not indicate

$$(R_i R_{i+1}) > |(R_i R_{i+2})| > (R_i R_{i+3})$$

The latter two appear to be of comparable magnitude, and only slightly smaller than $(R_i R_{i+1})$ only as the calculations are unstable, one would not like to be dogmatic about this, but we do not find Scherer's field acceptable in the light of this work. It is felt that the mathematical difficulties encountered when the restriction is raised, and all the uncertainties which this introduces involve more error than retaining the constraint.

Table 5.1 (i) $(R_i R_{i+1}) = - (R_i R_{i+2}) = (R_i R_{i+3})$ - the Kekulé-typeC-C/C-C interaction relation

FORCE CONSTANT	39(ABS)		FIELD		37(ABS)		37(%)	
R^{HH}	694.6	(5.3)	697.5	(5.7)	698.0	(7.8)		
R^{FF}	734.6	(13.4)	733.8	(13.5)	727.8	(15.7)		
$(R_i R_{i+1})$	52.9	(1.2)	53.3	(1.2)	53.2	(1.6)		
$r^{HH}(H)$	507.7	(1.6)	507.3	(1.6)	508.4	(4.2)		
$r^{FF}(H)$	517.3	(1.6)	517.0	(1.6)	517.8	(4.2)		
$r^{HH}(F)$	594.0	(7.9)	599.2	(5.4)	601.6	(6.0)		
$r^{FF}(F)$	664.2	(9.7)	670.8	(6.5)	669.2	(7.6)		
$(r_i(H)r_{i+1}(H))$	3.9	(.9)	2.6	(1.4)	3.6	(3.3)		
$(r_i(F)r_{i+1}(F))$	19.6	(6.8)	18.8	(6.5)	20.4	(7.6)		
$\alpha(H)$	108.7	(1.5)	108.6	(1.5)	108.1	(1.5)		
$\alpha(F)$	124.7	(20.6)	123.9	(17.8)	125.2	(15.7)		
$(\alpha_i \alpha_{i+1})$	-10.5	(.8)	-10.3	(.8)	-10.4	(.8)		
$\beta^{HH}(H)$	103.4	(.4)	103.5	(.4)	103.9	(.5)		
$\beta^{FF}(H)$	89.9	(.7)	90.3	(.7)	89.7	(.8)		
$\beta^{HH}(F)$	193.8	(1.8)	194.0	(1.8)	193.4	(1.3)		
$\beta^{FF}(F)$	175.9	(2.0)	174.8	(1.9)	175.4	(1.1)		
$(\beta_i(H)\beta_{i+1}(H))$	2.2	(.3)	2.2	(.3)	2.4	(.4)		
$(\beta_i(H)\beta_{i+1}(F))$	5.8	(.8)	5.9	(.8)	6.5	(.9)		
$(\beta_i(F)\beta_{i+1}(F))$	5.1	(1.3)	5.7	(1.3)	6.6	(.8)		
$(\beta_i(H)\beta_{i+2}(H))$	-1.1	(.3)	-1.1	(.3)	-1.6	(.4)		
$(\beta_i(H)\beta_{i+2}(F))$.4	(.8)	.4	(.8)	-.6	(.9)		
$(\beta_i(F)\beta_{i+2}(F))$	-5.5	(1.2)	-5.0	(1.2)	-4.4	(.9)		
$(\beta_i(H)\beta_{i+3}(H))$	-4.2	(.4)	-4.3	(.4)	-3.9	(.5)		
$(\beta_i(H)\beta_{i+3}(F))$	-7.6	(1.2)	-7.8	(1.2)	-5.1	(1.4)		
$(\beta_i(F)\beta_{i+3}(F))$	-6.7	(1.4)	-6.9	(1.4)	-9.8	(1.0)		

Table 5.1 (ii)

FORCE CONSTANT	FIELD					
	39 (ABS)		37 (ABS)		37 (%)	
$(r_i(H)R_i)$			-6.3 (5.1)		-1.5 (9.7)	
$(r_i(F)R_i)$	36.2	(3.5)	37.3	(2.3)	38.0	(2.6)
$(r_i(F)R_{i+1})$	-1.3	(2.7)				
$(r_i(F)R_{i+1})$ $(\alpha_i R_i)_{i+2}$	36.7	(2.7)	38.0	(2.6)	38.5	(3.3)
$(\beta_i(H)R_i)$	35.0	(.8)	35.0	(.8)	34.6	(1.0)
$(\beta_i(F)R_i)$	58.7	(3.4)	55.7	(3.4)	55.3	(3.7)
$(\beta_i(H)R_{i+1})$	-4.2	(.7)	-4.4	(.7)	-3.6	(.8)
$(\beta_i(F)R_{i+1})$	-15.5	(2.0)	-15.7	(1.9)	-14.8	(2.3)
$(\alpha_i r_i(H))$	10.6	(3.1)	6.9	(2.9)	8.3	(7.9)
$(\alpha_i r_i(F))$	-59.4	(6.6)	-64.4	(4.1)	-63.0	(4.9)
$(\alpha_i r_{i+1}(F))$	11.3	(3.0)	9.2	(1.8)	10.3	(2.2)
$(\beta_i(F) r_{i+1}(F))$	-6.4	(2.4)				
$(\beta_i(H) \alpha_{i+1})$	2.6	(.7)	2.8	(.7)	3.4	(.7)
$(\beta_i(F) \alpha_{i+1})$	12.6	(.9)	11.6	(.9)	11.4	(.7)

VARIANCE $\times 10^{-6}$

157

158

320

 $\prod_i a_{ii}$ 3.44×10^{29} 6.95×10^{28} 3.25×10^{34}

DET[A]

 1.75×10^{15} 5.4×10^{15} 1.58×10^{23} DET[A] / $\prod_i a_{ii}$ 5.07×10^{-15} 7.76×10^{-14} 4.82×10^{-12} UNITS - Nm^{-1} , $10^{-10} \text{Nrad}^{-1}$, $10^{-20} \text{Nm rad}^{-2}$ AS APPROPRIATE

Table 5.2 (i) $(R_i R_{i+1}), (R_i R_{i+2}), (R_i R_{i+3})$ included as separate parameters

FORCE CONSTANT	42(37) (ABS)		FIELD 42(36) (ABS)		42(36) (ABS)	
R^{HH}	672.8	(12.6)	707.4	(3.9)	701.8	(3.6)
R^{FF}	664.6	(18.1)	705.7	(12.2)	738.4	(8.1)
$(R_i R_{i+1})$	61.9	(2.2)	64.7	(2.0)	60.8	(1.7)
$(R_i R_{i+2})$	-34.4	(6.4)	-52.2	(1.9)	-50.0	(1.9)
$(R_i R_{i+3})$	48.1	(3.6)	42.8	(3.0)	50.5	(2.3)
$r^{HH}(H)$	506.5	(1.2)	506.3	(1.2)	506.8	(1.5)
$r^{FF}(H)$	516.4	(1.2)	516.2	(1.2)	516.5	(1.5)
$r^{HH}(F)$	607.3	(5.6)	598.6	(4.6)	598.5	(4.8)
$r^{FF}(F)$	685.9	(7.3)	673.1	(5.5)	669.2	(5.5)
$(r_i(H)r_{i+1}(H))$	-		-		-	
$(r_i(F)r_{i+1}(F))$	21.8	(6.6)	24.1	(5.5)	10.8	(5.1)
$\alpha(H)$	122.4	(12.5)	108.7	(5.3)	109.4	(5.4)
$\alpha(F)$	137.9	(11.2)	126.7	(6.3)	123.9	(6.0)
$(\alpha_i \alpha_{i+1})$	-2.9	(6.3)	-9.7	(3.0)	-9.2	(3.1)
$\beta^{HH}(H)$	101.8	(.6)	102.0	(.6)	102.8	(.6)
$\beta^{FF}(H)$	89.5	(.8)	89.6	(.8)	89.9	(.9)
$\beta^{HH}(F)$	189.8	(5.0)	189.9	(5.1)	192.8	(5.2)
$\beta^{FF}(F)$	172.9	(5.5)	173.9	(5.6)	173.6	(5.7)
$(\beta_i(H)\beta_{i+1}(H))$	1.9	(.4)	2.0	(.4)	2.1	(.4)
$(\beta_i(H)\beta_{i+1}(F))$	4.9	(1.5)	5.1	(1.5)	5.2	(1.5)
$(\beta_i(F)\beta_{i+1}(F))$	6.8	(3.3)	6.9	(3.4)	4.9	(3.5)
$(\beta_i(H)\beta_{i+2}(H))$	-1.0	(.4)	-1.0	(.4)	-1.1	(.4)
$(\beta_i(H)\beta_{i+2}(F))$	-.4	(1.5)	-.3	(1.5)	.2	(1.5)
$(\beta_i(F)\beta_{i+2}(F))$	-8.2	(3.3)	-8.5	(3.3)	-5.3	(3.2)
$(\beta_i(H)\beta_{i+3}(H))$	-2.1	(.6)	-2.5	(.6)	-3.4	(.6)
$(\beta_i(H)\beta_{i+3}(F))$	-3.4	(2.4)	-3.8	(2.5)	-4.9	(2.5)
$(\beta_i(F)\beta_{i+3}(F))$	-1.2	(4.2)	-1.4	(4.3)	-4.2	(4.2)

Table 5.2 (ii)

FORCE CONSTANT	42(37) (ABS)		FIELD 42(36) (ABS)		42(36) (ABS)	
	$(r_i(H)R_i)$	-15.0	(2.8)	-16.8	(2.7)	-15.8
$(r_i(F)R_i)$	40.3	(2.3)	38.6	(2.1)	36.5	(2.0)
$(r_i(F)R_{i+1})$	-		-		-	
$(r_i(F)R_{i+2})$	-		-		-	
$(\alpha_i R_i)$	14.8	(10.1)	36.7		36.7	
$(\beta_i(H)R_i)$	33.0	(1.0)	32.8	(1.0)	33.8	(1.0)
$(\beta_i(F)R_i)$	42.2	(6.0)	42.7	(6.2)	55.1	(4.5)
$(\beta_i(H)R_{i+1})$	-3.0	(.8)	-3.5	(.8)	-4.2	(.8)
$(\beta_i(F)R_{i+1})$	-2.4	(4.2)	-4.4	(4.1)	-15.5	
$(\alpha_i r_i(H))$	-1.0		-1.0		-1.2	(3.9)
$(\alpha_i r_i(F))$	-57.2	(8.2)	-59.0	(8.0)	-69.2	(6.9)
$(\alpha_i r_{i+1}(F))$	13.1	(3.5)	11.3	(3.4)	9.2	(2.9)
$(\beta_i(F)r_{i+1}(F))$	-		-		-	
$(\beta_i(H)\alpha_{i+1})$	5.2	(1.6)	4.2	(1.4)	3.5	(1.5)
$(\beta_i(F)\alpha_{i+1})$	15.6	(3.1)	14.2	(3.0)	11.8	(2.8)

VARIANCE $\times 10^{-6}$

125

130

141

 $\prod_{i,ii} a_{ii}$ 1.22×10^{11} 5.02×10^{10} 2.27×10^{10}

DET [A]

 3.0×10^{-4} 2.17×10^{-2} 5.19×10^{-2} DET [A]/ $\prod_{i,ii} a_{ii}$ 2.45×10^{-15} 4.33×10^{-13} 2.33×10^{-12} UNITS - Nm^{-1} , $10^{-10} \text{Nrad}^{-1}$, $10^{-20} \text{Nm rad}^{-2}$ AS APPROPRIATE

Table 5.3 Comparison of the Force Constants for the In-Plane Vibrations of Benzene of Eaton and Duinker [9, 10]

Force constant	Eaton		Duinker	
R^{HH}	697.5	(5.7)	701.5	(7.1)
* $(R_i R_{i+1})$	53.3	(1.2)	53.1	(1.7)
$r^{HH(H)}$	507.3	(1.6)	512.5	(3.1)
$\alpha(H)$	108.6	(1.5)	109.9	(5.1)
$(\alpha_i \alpha_{i+1})$	-10.3	(0.8)	-9.8	(3.3)
$\beta^{HH(H)}$	103.5	(0.4)	103.5	(0.8)
$(\beta_i(H) \beta_{i+1}(H))$	2.2	(0.3)	2.8	(0.5)
$(\beta_i(H) \beta_{i+2}(H))$	-1.1	(0.3)	-2.2	(0.5)
$(\beta_i(H) \beta_{i+3}(H))$	-4.3	(0.4)	-3.2	(0.8)
$(\alpha_i R_i)$	38.0	(2.6)	44.1	(5.7)
$(\beta_i(H) R_i)$	35.0	(0.8)	36.4	(0.9)
$(\alpha_i r_i(H))$	6.9	(2.9)	-1.4	(2.2)
$(\beta_i(H) \alpha_{i+1})$	12.6	(0.9)	6.4	(1.8)
$(\beta_i(H) R_{i+1})$	-4.2	(.7)		

$$* (R_i R_{i+1}) = -(R_i R_{i+2}) = (R_i R_{i+3})$$

UNITS $-\text{Nm}^{-1}$, $10^{-10} \text{ N rad}^{-1}$ OR $10^{-20} \text{ Nm rad}^{-2}$ AS APPROPRIATE

Section 5.4 Choice between the Two Alternative Solutions for the
B_{2u} Species

In the B_{2u} species, the force constant display graphs show two distinct solutions to the force field (see Section 1.3) for Benzene.

$$\begin{array}{ll}
 F_{14-14} = 3.94 \text{ md/\AA} & F_{14-14} = 4.34 \text{ md/\AA} \\
 \text{(I) } F_{14-15} = +0.30 \text{ md/\AA} & \text{OR (II) } F_{14-15} = +0.66 \text{ md/\AA} \\
 F_{15-15} = 0.822 \text{ md/\AA} & F_{15-15} = 0.824 \text{ md/\AA}
 \end{array}$$

where

$$\begin{aligned}
 F_{14-14} &= R^{HH} - 2(R_i R_{i+1}) + 2(R_i R_{i+2}) - (R_i R_{i+3}) \\
 F_{14-15} &= 2(\beta_i(H)R_i) - 2(\beta_i(H)R_{i+1}) + 2(\beta_i(H)R_{i+2}) \\
 F_{15-15} &= \beta^{HH}(H) - 2(\beta_i(H)\beta_{i+1}(H)) + 2(\beta_i(H)\beta_{i+2}(H)) - (\beta_i(H)\beta_{i+3}(H))
 \end{aligned}$$

Whiffen^[2] chose solution I.

$$\begin{aligned}
 F_{14-14} &= 5.553 - 2 \times 0.633 + 2 \times 0.113 - 0.573 \\
 &= 3.94 \text{ md/\AA} \\
 F_{14-15} &= 2 \times 0.049 - 2 \times (-0.050) + 2 \times 0.049 \\
 &= 0.296 \text{ md/\AA} \\
 F_{15-15} &= 0.866 - 2 \times 0.016 + 2 \times (-0.013) - (-0.015) \\
 &= 0.823 \text{ md/\AA}
 \end{aligned}$$

Duinker and Mills^[9, 10] chose solution II

$$\begin{aligned}
 F_{14-14} &= 7.015 - 5 \times 0.531 [(R_i R_{i+1}) = -(R_i R_{i+2}) = (R_i R_{i+3})] \\
 &= 4.36 \text{ md/\AA} \\
 F_{14-15} &= 2 \times 0.336 [(\beta_i(H)R_{i+1}) \text{ and } (\beta_i(H)R_{i+2}) \text{ set to zero}] \\
 &= 0.672 \text{ md/\AA} \\
 F_{15-15} &= 0.881 - 2 \times 0.024 + 2 \times (-0.019) - (-0.027) \\
 &= 0.822 \text{ md/\AA}
 \end{aligned}$$

This work seems to favour solution II

$$F_{14-14} = 6.975 - 5 \times 0.533 [(R_i R_{i+1}) = -(R_i R_{i+2}) = (R_i R_{i+3})]$$

$$= 4.31 \text{ md}/\overset{\circ}{\text{A}}$$

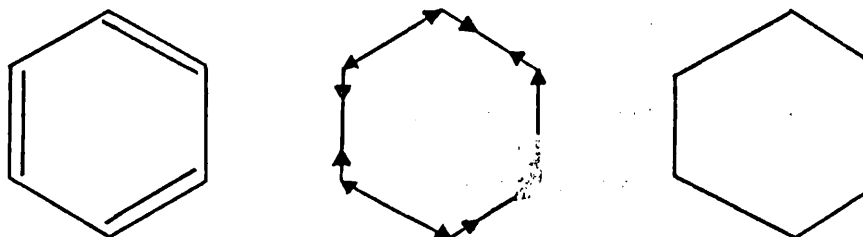
$$F_{14-15} = 2 \times 0.323 [(\beta_i(H)R_{i+1}) \text{ and } (\beta_i(H)R_{i+2}) \text{ set to zero}]$$

$$= 0.646 \text{ md}/\overset{\circ}{\text{A}}$$

$$F_{15-15} = 0.881 - 2 \times 0.0185 + 2(-0.0096) - (-0.0369)$$

$$= 0.86 \text{ md}/\overset{\circ}{\text{A}}$$

S_{14} is the vibration which leads to alternate long and short C-C bonds, so that in the distorted position, the molecule resembles a single Kekulé structure for Benzene,



and this is expected to have a lower energy than other arrangements with the same total degree of distortion. The value of the Kekulé C-C stretching constant F_{14-14} depends significantly on which solution is chosen (although in either case, the value of F_{14-14} is found to be appreciably smaller than for the other C-C stretching constants - $F_{1-1} \sim F_{8-8} \sim 7.55 \text{ md/\AA}$).

The form of the normal coordinates in the B_{2u} species is very different for the two solutions.

L matrix elements for the B_{2u} normal coordinates of Benzene calculated

- from Whiffen's force field
- from Calc. II of Mills
- from this work.

	(a)		(b)		(c)	
ν_{calc}	1307	1147	1312	1139	1315	1147
S_{14}	[+0.456 +0.205]		[+0.446 -0.225]		[+0.4095 -0.2865]	
S_{15}	[-0.672 +0.790]		[+0.190 +1.019]		[+0.3345 +0.9816]	

Again, this work seems to favour solution II.

PART 2

The Dihedral Angle of Biphenyl
and some of its Derivatives

CHAPTER SIXThe Dihedral Angle of Biphenyl and some of its DerivativesSection 6.1 Introduction

The Biphenyl molecule, which consists of two Benzene rings joined by a single C-C bond, changes geometry with physical state, and this has prompted a large number of investigations (thorough literature survey^[75]). Earlier studies of the vibrational spectra of Biphenyl^[76 - 83] left many of the assignments in doubt, and failed to give convincing evidence of spectral changes accompanying a change of state, partly because the far infra red and low frequency Raman spectra in different physical states had been inadequately determined or else obscured by solvent bands. The only report^[83] of such evidence bases the spectral interpretation on qualitative reasoning.

Experimental evidence for the conformation of Biphenyl in different physical states, using many different techniques, can be summarised as follows.

a) Crystal

Recent experimental evidence indicates that the molecule crystallizes in a monoclinic cell, space group $P_2 1/a$. X-ray studies^[84 - 86] show that the molecule is planar, within the limits of error of the experimental results. Attempts have been made to evaluate a possible non-planarity of the whole molecule, but the standard deviations on these calculated values of the displacements from the plane were large^[85, 86]. Significantly different values for the length of the ring C-C bond are suggested, especially the inter-ring C-C bond. A previous value of $1.48 \overset{\circ}{\text{A}}$ for the latter^[84] has been used in most of the subsequent experimental works and

theoretical speculations on the electronic structure of Biphenyl^[87]. The more recent accurate determinations give a value of 1.507 Å^[86] and 1.506 Å^[85] which should cause a revision of some of the previous theoretical conclusions.

b) Solution

U.V. studies^[88, 89] suggest that the most probable conformation is non-planar, with a dihedral angle of 20-25°^[89], assuming that the change in spatial configuration about a single bond in conjugated systems may affect the π - π interaction (conjugation) across the C-C inter-ring bond and so alter the position and intensity of the so-called "conjugation band" at 247 m μ . The assignment of this band is not certain, and there is evidence^[86] which suggests that there is no conjugation in the planar case, where it should be a maximum. The NMR spectrum suggests both a dihedral angle of 40°^[90] and a molecule which undergoes free rotation. ESR studies suggest a dihedral angle of 38°^[91].

c) Vapour

Electron Diffraction studies^[92] give unequivocal evidence for a non-planar structure, with a dihedral angle of about 45° ± 10°. U.V. spectra^[89], based on the assumption indicated above, suggest that the degree of deviation from planarity should be larger in the vapour state than in solution.

Theoretical studies^[93], using "molecular mechanics" gave values for the inter-ring C-C bond length, dihedral angle, and $\widehat{C_1 C_2 H_2}$ angle χ for the isolated molecule $r = 1.51 \text{ \AA}$, $\chi = 121^\circ$, $\theta = 35^\circ$ and for the crystal $r = 1.51 \text{ \AA}$, $\chi = 123^\circ$, $\theta = 0^\circ$.

Calculations^[87] of the electronic energy levels using the method due to Pariser, Parr and Pople indicates a dihedral angle of considerably less than 45° in solution.

Section 6.2 Theoretical Predictions

Spectral changes can arise from changes in restoring forces, and changes in coupling conditions resulting from different geometries. As the dihedral angle changes, the π orbital overlap will vary and possibly lead to changes in bond orders and restoring forces on the nuclei. Zerbi and Sandroni^[81] sought evidence for coupling between the rings by carrying out a perturbation analysis of planar Biphenyl using a U.B.F.F. and a S.V.F.F. Their results indicate that the extent of delocalisation of π bonds across the inter-ring C-C bond must be very small. They also concluded that steric interactions between ortho hydrogens on the two rings was small. Thus it is predicted that the restoring forces will be changed by very little when Biphenyl loses its planarity. It is assumed that a change in geometry leaves the force field unaffected, so all the large frequency shifts on twisting arise from interaction terms in the G matrix.

Perturbations in the eigen values and eigen vectors on change of conformation can be expected from the following phenomena.

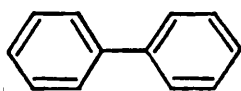
(i) Steric Interactions

The normal modes which are most affected by possible steric interactions between the ortho hydrogens can be picked out from the cartesian displacement calculations^[81]. The Van der Waal's radius of the hydrogen atom (1.24 \AA) is large compared with the equilibrium distance

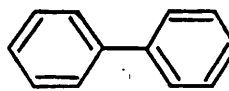
between the two ortho hydrogen nuclei (1.75 \AA) for planar Biphenyl and since the largest displacement is approximately 0.3 \AA , strong repulsion should occur. In the a_g motions both pairs of ortho hydrogens are bouncing against one another and in the b_{2u} modes only one pair is colliding. Hence the a_g and b_{2u} fundamentals involving strong β deformations will be more affected than the corresponding b_{1g} and b_{3u} modes on steric relaxation. However, the frequency shifts observed from the liquid to the crystal are very small and of the order of magnitude of the shifts generally ascribed to changes of aggregation, so that steric interactions, if they exist, must be very small and cannot be detected in the infra red, unless other phenomena take place. It has been suggested^[85, 94, 86] that in order to avoid steric hindrances, the equilibrium geometry is somewhat distorted by opening the $\widehat{C-C-H}$ angle. It could also be postulated that during the vibrations which bring the hydrogens closer, the molecule is somewhat twisted out of the plane to reduce strain. Steric repulsion could account for the increased bond length in the solid state.

(ii) Resonance Interaction between the two Rings

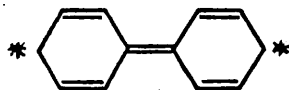
It is generally assumed that the Biphenyl molecule is a resonance hybrid of several canonical structures^[95] one of which involves the



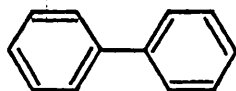
I



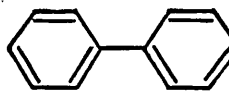
II



V



III



IV

inter-ring double bond. Zerbi and Sandroni^[81] showed that the b_{1g} and b_{2u} modes are greatly affected by the extent of delocalisation and the extent of resonance could be obtained from the values of the Kekulé resonance parameter (ρ) in their perturbed U.B.F.F. or by the values and signs of the C-C/C-C interactions in their S.V.F.F. for the planar conformation. The possible existence of a small contribution to the hybrid from the double-bonded structure was shown in the signs of certain inter-ring force constants, although their values were small. To support this, they repeated their calculations omitting these inter-ring force constants in the S.V.F.F. and inserting only one ρ parameter in the U.B.F.F. only to find that a very satisfactory fit was still obtained.

A small delocalisation of π electrons across the inter-ring bond (1.51 Å) accounts for the almost normal length of 1.54 Å for a C-C single bond. The vapour phase value of 1.48 Å may imply a slightly higher bond order.

The double bond structure (V) will contribute even less on twisting and this would be reflected in a force constant change. Calculations show that R^{CC} drops from 639.2 (55.3) Nm^{-1} in the solid phase to 593.5 (35.5) Nm^{-1} in the solution phase. Obviously, with such large variances, it is impossible to estimate the magnitude of the force constant change, but it certainly implies a slightly weaker bond. When Biphenyl is considered as two mono-substituted Benzene molecules, (C_{2v} symmetry) each of the C_{2v} motions of Biphenyl giving rise to a splitting of the original degenerate levels, a_1 modes (C_{2v}) split into a_g (in-phase) and b_{3u} (out-of-phase) parallel modes whilst b_2 modes (C_{2v}) split into b_{1g} (in-phase) and b_{2u} (out-of-phase) perpendicular modes. The amount of splitting and the eventual frequency shifts will depend on the strength of the C-C bond

joining the two rings, on the possible steric interactions and on the extent of kinetic coupling between the two rings.

Spectral Predictions based on Symmetry Considerations

As the dihedral angle is rotated from 0° to 90° , so the nuclear geometry changes from D_{2h} through D_2 to D_{2d} . In the D_{2h} configuration, the in-plane and out-of-plane vibrations do not interact if high order effects such as Coriolis coupling are ignored. For a significant rotation about the central bond - one large enough to change the shape of the potential wells - the centre of symmetry is effectively lost and the symmetry classes of the D_{2h} group coalesce in pairs. Each pair is constituted from a gerade and an ungerade species, and from an in-plane and an out-of-plane species of the D_{2h} configuration. Thus, provided the in-plane and out-of-plane vibrational wavefunctions mix, the vibrations constituting the pairs of classes will push one another apart and the mixing of the wavefunctions will lead to a relaxation of the spectral activities.

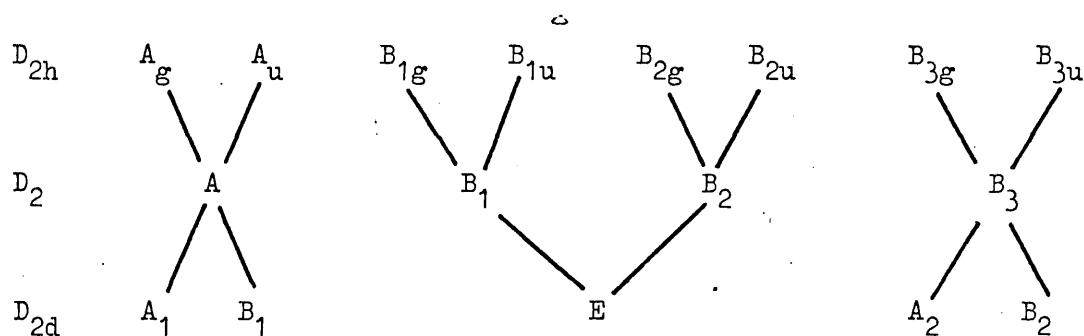


Figure 6.1 Relationships between vibrations of different symmetry species for Biphenyl in the D_{2h} , D_2 and D_{2d} configurations

No interaction occurs between the a_g and a_u , nor between the b_{3g} and b_{3u} vibrations on reduction of the symmetry, though this is formally allowed.

In the a_u and b_{3g} vibrations, the nuclei lying on the C_2 axis passing through C_1 and C_1' cannot move without violating the appropriate transformation properties of the species. Coupling can only occur through the C_2 and C_6 carbon atoms. The cartesian coordinates of these nuclei for

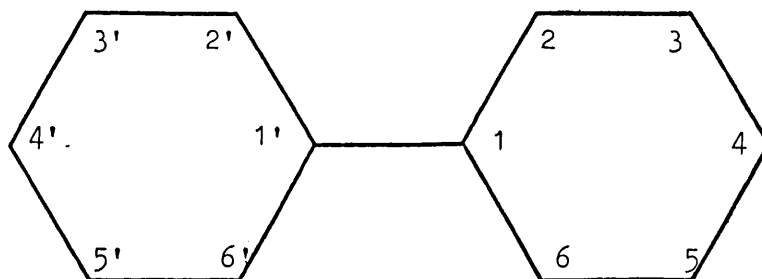


Figure 6.2 Numbering of the Carbon Atoms

A_u , A_g , B_{3u} and B_{3g} representations rotate with the rings and hence remain orthogonal for all dihedral angles. Only the a_g vibrations are affected by the value of the C-C inter-ring force constant.

In first order perturbation theory, the interaction between levels depends

- (i) on the interaction integral $\langle \psi_a | H_{ab} | \psi_b \rangle$; rotation of the rings with respect to one another will not affect this integral if the vibrational wavefunctions are localised in the rings.
- (ii) inversely on the difference between the energy levels. This implies that interaction will be weak unless there are similar vibrational frequencies in the species which coalesce.

The in-plane fundamentals lie between 3000 cm^{-1} to about 70 cm^{-1} whilst the out-of-plane modes occur only below 1000 cm^{-1} . It follows from (ii) that the perturbations will lie below 1000 cm^{-1} . This range can be narrowed. Coupling can only occur through those modes which span the ring. Since interaction cannot occur in the A species, this precludes any interactions through the C-C stretch. Other internal deformations which span the ring and may lead to coupling are γ_c (out-of-plane

deformation of the C_1 external to the ring), β_c (in-plane deformation of C_1) and δ or ϕ (ring torsion). The natural frequency of the γ_{CH} deformation lies well above that of the only in-plane deformation coordinate to span the ring, β_c , being about 900 cm^{-1} compared to 300 cm^{-1} . Again interaction is predicted to be weak. The primary perturbations arise from ϕ , β_c interactions.

Section 6.3 The Initial Calculations [96]

The aromatic rings were assumed to be regular hexagons, and the bond lengths were taken as

$$\begin{aligned} \text{C-C} &= 1.40 \text{ \AA} \\ \text{C}_1\text{-C}'_1 &= 1.48 \text{ \AA} \\ \text{C-H} &= 1.084 \text{ \AA} \end{aligned}$$

An approximate force field was composed as follows. The Benzene force field of Duinker and Mills [9] was used for the in-plane deformation coordinates. The inter-ring stretching force constant was assumed to be 4.9 md/\AA - a value chosen on the basis of the known bond length and a simple force constant/bond length relation for C-C bonds. No inter-ring coupling constants were introduced in view of the uncertainty concerning any resonance interaction. All out-of-plane force constants were transferred directly from derived fields for Benzene and mono- and p-dihalogeno Benzenes [98]. As no data was available on values for angle bending constants for a carbon substituent on a ring, it was assumed that the energy required for a unit angular deformation was independent of the substituent.

Only 59 normal modes were computed. The missing fundamental is attributed to the lowest a_u mode, and is known as the "butterfly" torsion. This deformation was omitted because the nature of the torsion in solution is uncertain. It is not known whether the torsion occurs about a fixed dihedral angle if the vibration becomes a rotational degree of freedom. Because the frequency of this mode is low, the approximation is justified as there is little mixing with other normal coordinates.

Section 6.4 A Discussion of the Observed and Calculated Frequency Shifts for Biphenyl on a Change of State [96, 97]

The frequencies calculated for the A_g and A_u species did not vary with dihedral angle. Except for the lowest A_g mode, the changes observed were small, and are probably associated with small variations in the C-C force constants. An examination of the eigen vectors for the lowest mode showed about 30% of the energy to be associated with stretching of the central C-C bond and a further $27\frac{1}{2}\%$ arising from the adjacent ring angle deformation, indicating that a reduction in these force constants is involved for a phase change from solid to liquid to gaseous phase. These changes in the values of the force constants must be quite large, perhaps as high as 30%, to account for the 7% variation in the observed frequency. It was felt that a study of the deuterated Biphenyls might elucidate the problem of the relative contributions of the two internal deformations.

The frequencies calculated for the B_{3u} and B_{3g} species did not vary with dihedral angle.

For those frequencies of the B_{1g} and B_{2u} species above 1000 cm^{-1} the calculations showed a small dependence on dihedral angle due to changes in the G matrix, coupling terms between symmetry coordinates which, for the planar molecule, are in-plane.

It was predicted that the most important angle dependence arises from interaction between the lowest b_{1g} and the second lowest b_{1u} modes, both of which exhibit about a 20% shift on change of dihedral angle from 0° to 90° .

Experimentally, the b_{1u} band is shifted 28 cm^{-1} from a strong infra red band at 458 cm^{-1} in the solid state spectrum to a strong infra red band at 486 cm^{-1} in the liquid.

The b_{1g} band in the solid was not observed in the Raman spectrum, but in the liquid occurs as a moderate infrared band at 367 cm^{-1} .

The observed frequency shift of the b_{1u} band corresponds to a dihedral angle in solution of around 40° , but as the b_{1g} and b_{1u} frequencies were calculated to be about 50 and 30 cm^{-1} high respectively, and since the interaction between the levels is sensitive to their frequency separation, the uncertainty is at least 10° .

Interaction is predicted between the two lowest b_{2u} and b_{2g} modes, though smaller than that between the b_{1u} and b_{1g} modes.

The b_{2u} band is shifted 6 cm^{-1} from a very strong infra red band at 118 cm^{-1} in the solid state spectrum to a very strong infra red band at 112 cm^{-1} in the liquid.

The b_{2g} band is shifted 18 cm^{-1} from a moderate Raman band at 251 cm^{-1} in the solid to a moderate Raman band at 269 cm^{-1} in the liquid.

If this shift is attributed entirely to G matrix effects, then it corresponds to a dihedral angle just over 60° in solution. However, since the frequency shift from melt to vapour is 4 cm^{-1} in the opposite direction, this estimate was considered too high, and preference was given to the value deduced from the shift in the B_1 species.

Section 6.5 The Frequency Shifts Observed for D₂-Biphenyl and D₁₀-Biphenyl on a Change of State [96]

The spectral shifts observed in the deuterated derivatives of Biphenyl show the same trends as those observed in Biphenyl.

Considering D₂ - Biphenyl first, the second lowest b_{1u} band is shifted 28 cm⁻¹ from a moderate infra red band at 449 cm⁻¹ in the solid state spectrum to a strong infra red band at 477 cm⁻¹ in the liquid.

The b_{1g} band in the solid was not observed in the Raman spectrum, but in the liquid occurs as a weak infra red band at 359 cm⁻¹.

The lowest b_{2g} band is shifted 21 cm⁻¹ from a moderate Raman band at 241 cm⁻¹ in the solid to a moderate Raman band at 262 cm⁻¹ in the liquid.

Interferometric studies were not done on this derivative, so the behaviour of the second lowest b_{2u} band was not observed.

For D₁₀-Biphenyl, the second lowest b_{1u} band is shifted 27 cm⁻¹ from a moderate infra red band at 410 cm⁻¹ in the solid state spectrum to a strong infra red band at 437 cm⁻¹ in the liquid.

The b_{1g} band in the solid was not observed in the Raman spectrum, but in the liquid occurs as a strong infra red band at 334 cm⁻¹.

The lowest b_{2g} band is shifted 18 cm⁻¹ from a moderate Raman band at 225 cm⁻¹ in the solid to a moderate Raman band at 243 cm⁻¹ in the liquid.

The second lowest b_{2u} band is shifted 7 cm⁻¹ from a very strong infra red band at 112 cm⁻¹ in the solid to a very strong infra red band at 105 cm⁻¹ in the liquid.

Section 6.6 A Discussion of the Observed and Calculated Frequency Shifts for 4,4' Difluoro Biphenyl [96, 97]

There is little detailed analysis in the literature of the spectra of 4,4' difluoro Biphenyl, but they are very similar to those of Biphenyl and can be interpreted accordingly.

For the calculations

$$\begin{aligned} \text{C-F} &= 1.30 \text{ \AA} \\ m_{\text{F}} &= 19.000 \text{ amu} \end{aligned}$$

The force field used was transferred from work on mono- and p-di-halogeno Benzenes [9, 98].

As with Biphenyl, the frequencies calculated for the A_g and A_u species did not vary with dihedral angle. Except for the lowest a_g mode, the changes observed were small. The potential distribution is similar to that for Biphenyl. Much of the energy of the lowest a_g mode is derived from inter-ring stretching deformation, which reflects a change in bond order due to twist.

Again, the frequency shifts observed for the B_2 and B_3 species are small.

The strongest interactions on change of dihedral angle are predicted between the two lowest b_{1g} modes, and the second and third lowest b_{1u} modes.

The lowest b_{1g} band is shifted 18 cm^{-1} from a very weak infra red band at 340 cm^{-1} in the solid phase spectrum to a moderate infra red band at 358 cm^{-1} in the liquid.

The second lowest b_{1g} band is shifted 10 cm^{-1} from a very weak infra red band at 464 cm^{-1} in the solid to a moderate infra red band 454 cm^{-1} in the liquid.

The second lowest b_{1u} band is shifted 28 cm^{-1} from a moderate infra red band at 283 cm^{-1} in the solid to a moderate infra red band at 255 cm^{-1} in the liquid.

The third lowest b_{1u} band is shifted from a very strong infra red doublet at $499/505 \text{ cm}^{-1}$ in the solid to a strong infra red band at 515 cm^{-1} in the liquid.

The observed frequency change of the 283 cm^{-1} band would indicate a dihedral angle of about 32° in the solution.

Table 6.1 The 20 parameter S.V.F.F. used to calculate the in-plane vibrational frequencies of Biphenyl [81]

	I		II	
R^{HH}	649.1	(33.4)	631.2	(19.0)
R^{CC}	440.0	(29.1)	457.7	(25.5)
$(R_i R_{i+1})$	73.2	(8.1)	72.5	(4.3)
$(R_i R_{i+2})$	-41.8	(12.6)	-34.6	(9.5)
$(R_i R_{i+3})$	30.3	(7.5)	29.9	(6.1)
$(R_i R_i^{CC})$			49.4	(12.6)
$(R_i R'_{i+1})_{cis}$	-31.9	(14.6)		
$(R_i R'_{i+1})_{trans}$	-34.1	(14.1)		
$r^{HH}(H)$	(511.6)*		(511.6)*	
$\alpha(H)$	93.2	(5.4)	95.9	(4.3)
$\alpha(C)$	96.4	(17.1)	100.2	(15.5)
$\beta^{HH}(H)$	48.1	(1.1)	48.2	(1.0)
$\beta^{HC}(H)$	57.4	(3.3)	56.9	(3.2)
$\beta^{HH}(C)$	75.0	(5.5)	75.5	(5.0)
$(\alpha_i(H)R_i)$	22.6	(20.4)	11.3	(12.5)
$(\alpha_i(C)R_i)$	71.2	(18.9)	30.9	(18.2)
$(\beta_i(H)R_i)$	8.8	(0.8)	8.8	(0.7)
$(\beta_i(C)R_i)$	12.3	(5.3)	10.8	(4.0)

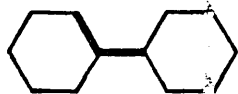
UREY-BRADLEY DEFINITION OF β CO-ORDINATES

* NOT PERTURBED

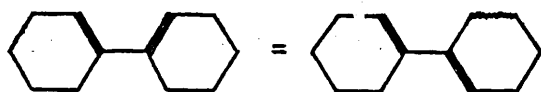
UNITS - Nm^{-1} , $10^{-10} N rad^{-1}$ OR $10^{-20} Nm rad^{-2}$ AS APPROPRIATE

$(R_{i+1} R_i^{CC}) = (R_{i+2} R_i^{CC}) = 0$

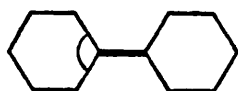
Figure 6.3 Demonstrating the motions associated with certain interaction force constants



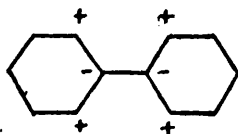
$$(R_i R_i^{CC})$$



$$(R_i R'_{i+1})$$



$$(\alpha_i R_i^{CC})$$



$$(\gamma_i(c) \gamma'_i(c))$$

Scaling of Force Constants

All angular deformations are scaled by multiplication by a bond length.

For α and ϕ this scaling factor is the ring C-C bond length. For β and γ coordinates the bond length used is that of the substituent to the ring bond.

Table 6.2 The initial values of the 37 parameter M.V.F.F. for Biphenyl,
 D_2 Biphenyl and D_{10} Biphenyl - taken from [96]

1	R^{HH}	701.5	20	$(\beta_i(C)R_i)$	36.4
2	R^{CC}	490.0	21	$(\alpha_i r_i)$	-1.4
3	$(R_i R_{i+1})$	53.1	22	$(\beta_i(H)\alpha_{i+1})$	6.4
* 4	$(R_i R_i^{CC})$		23	$(\beta_i(C)\alpha_{i+1})$	6.4
* 5	$(R_i R'_{i+1})$		24	$\gamma^{HH(H)}$	30.7
* 6	$(\alpha_i R_i^{CC})$		25	$\gamma^{HH(C)}$	30.7
7	$r^{HH(H)}$	512.5	26	$(\gamma_i(H)\gamma_{i+1}(H))$	1.53
8	α	110.3	27	$(\gamma_i(C)\gamma_{i+1}(H))$	1.53
9	$(\alpha_i \alpha_{i+1})$	-9.8	28	$(\gamma_i(H)\gamma_{i+2}(H))$	-1.29
10	$\beta^{HH(H)}$	103.5	29	$(\gamma_i(C)\gamma_{i+2}(H))$	-1.29
11	$\beta^{HH(C)}$	103.5	30	$(\gamma_i(H)\gamma_{i+3}(H))$	-1.41
12	$(\beta_i(H)\beta_{i+1}(H))$	2.8	31	$(\gamma_i(C)\gamma_{i+3}(H))$	-1.41
13	$(\beta_i(C)\beta_{i+1}(H))$	2.8	* 32	$(\gamma_i(C)\gamma_{i'}(C))$	
14	$(\beta_i(H)\beta_{i+2}(H))$	-2.2	33	$\left\{ \begin{array}{l} \phi(HH) \\ \phi(HC) \end{array} \right\} = \phi$	7.06
15	$(\beta_i(C)\beta_{i+2}(H))$	-2.2	34		
16	$(\beta_i(H)\beta_{i+3}(H))$	-3.2	35	$(\phi_i \phi_{i+1})$	-1.37
17	$(\beta_i(C)\beta_{i+3}(H))$	-3.2	36	$(\gamma_i(H)\phi_i)$	1.82
18	$(\alpha_i R_i)$	44.2	37	$(\gamma_i(C)\phi_i)$	1.82
19	$(\beta_i(H)R_i)$	36.4			

* INTERACTION FORCE CONSTANTS INTRODUCED LATER TO IMPROVE THE FIT. UNITS -

Nm^{-1} , $10^{-10} N rad^{-1}$ OR $10^{-20} Nm rad^{-2}$ AS APPROPRIATE.

Table 6.3 The convergence of the in-plane force field

		I	II	III	IV
		Perturb diagonals	Perturb selected off- diagonals	Perturb both sets simult- aneously	and again
1	R^{HH}	681.7 (12.1)		690.9 (10.8)	691.3 (8.0)
2	R^{CC}	504.0 (54.4)		636.0 (72.9)	639.2 (55.3)
3	$(R_i R_{i+1})$		51.0 (2.8)	52.7 (3.1)	52.8 (2.3)
4	$(R_i R_i^{CC})$		21.6 (15.0)	30.1 (15.8)	30.1 (11.8)
5	$(R_i R'_{i+1})$		34.6 (20.8)	26.2 (22.3)	25.6 (16.5)
6	$(\alpha_i R_i^{CC})$		-87.9 (12.2)	-124.0 (29.8)	-124.2 (22.8)
8	α	112.9 (3.1)		111.9 (2.4)	111.9 (1.8)
10	$\beta^{HH}(H)$	104.1 (2.1)		104.6 (1.5)	104.7 (1.2)
11	$\beta^{HH}(C)$	157.5 (9.6)		160.3 (7.2)	160.6 (5.3)

UNITS - Nm^{-1} , $10^{-10} N rad^{-1}$ OR $10^{-20} Nm rad^{-2}$ AS APPROPRIATE

Table 6.4 (i) The convergence of the out-of-plane force field

		I	II	III
		Perturb diagonals	Perturb selected off-diagonals	Perturb both sets simult- aneously
24	$\gamma^{HH}(H)$	30.6 (.8)		30.6 (.7)
25	$\gamma^{HH}(C)$	24.1 (1.8)		23.7 (1.3)
26	$(\gamma_i(H) \gamma_{i+1}(H))$		1.8 (.5)	1.8 (.5)
27	$(\gamma_i(C) \gamma_{i+1}(H))$			
28	$(\gamma_i(H) \gamma_{i+2}(H))$			
29	$(\gamma_i(C) \gamma_{i+2}(H))$			
30	$(\gamma_i(H) \gamma_{i+3}(H))$			
31	$(\gamma_i(C) \gamma_{i+3}(H))$			
32	$(\gamma_i(C) \gamma_i'(C))$			
33	$\left\{ \begin{array}{l} \phi(HH) \\ \phi(HC) \end{array} \right\} = \phi$	7.6 (.4)		7.8 (.6)
34				
35	$(\phi_i \phi_{i+1})$		-1.4 (.2)	-1.2 (.4)
36	$(\gamma_i(H) \phi_i)$			
37	$(\gamma_i(C) \phi_i)$			

UNITS - Nm^{-1} , $10^{-10} N rad^{-1}$ OR $10^{-20} Nm rad^{-2}$ AS APPROPRIATE

Table 6.4 (ii) The convergence of the out-of-plane force field

	IV		V		VI		VII	
	Introduce ($\gamma_i(c)\phi_i$)				Introduce ($\gamma_i(c)\gamma_i'(c)$)		Introduce ϕ (HC)	
24	29.5	(.5)	31.8	(1.5)	31.3	(1.4)	28.9	(1.0)
25	28.3	(1.5)	27.2	(1.5)	27.4	(1.5)	32.4	(1.5)
26	1.3	(.4)	1.2	(.5)	1.1	(.5)	.9	(.4)
27			3.2	(1.6)	2.4	(1.4)	.3	(1.0)
28			-1.6	(.7)	-1.6	(.7)	-.1	(.6)
29			-2.7	(2.1)	-2.9	(1.8)	-5.0	(1.3)
30			-2.0	(1.3)	-2.0	(1.0)	-1.4	(.7)
31			1.6	(2.1)	1.6	(1.6)	2.2	(1.0)
32					-2.2	(.9)	-7.7	(.9)
33	8.9	(.6)	7.7	(1.0)	7.9	(.8)	8.6	(.8)
34							11.0	(1.0)
35	-.6	(.4)	-1.4	(.6)	-1.2	(.6)	-.08	(.4)
36			2.4	(.3)	2.3	(.3)	1.8	(.2)
37	4.8	(.2)	4.1	(.4)	3.9	(.4)	4.8	(.4)

UNITS - Nm⁻¹, 10⁻¹⁰ N rad⁻¹, 10⁻²⁰ Nm rad⁻² AS APPROPRIATE.

Table 6.5 The final values of the 37 parameter M.V.F.F. for Biphenyl,
D₂ Biphenyl and D₁₀ Biphenyl

1	R^{HH}	691.3	24	$\gamma^{HH}(H)$	31.3
2	R^{CC}	639.2	25	$\gamma^{HH}(C)$	27.4
3	$(R_i R_{i+1})$	52.8	26	$(\gamma_i(H) \gamma_{i+1}(H))$	1.1
4	$(R_i R_i^{CC})$	30.1	27	$(\gamma_i(C) \gamma_{i+1}(H))$	2.4
5	$(R_i R'_{i+1})$	25.6	28	$(\gamma_i(H) \gamma_{i+2}(H))$	-1.6
6	$(\alpha_i R_i^{CC})$	-124.2	29	$(\gamma_i(C) \gamma_{i+2}(H))$	-2.9
7	$r^{HH}(H)$	512.5	30	$(\gamma_i(H) \gamma_{i+3}(H))$	-2.0
8	α	111.9	31	$(\gamma_i(C) \gamma_{i+3}(H))$	1.6
9	$(\alpha_i \alpha_{i+1})$	-9.8	32	$(\gamma_i(C) \gamma_i'(C))$	-2.2
10	$\beta^{HH}(H)$	104.7	33	$\left\{ \begin{array}{l} \phi(HH) \\ \phi(HC) \end{array} \right\} = \phi$	7.9
11	$\beta^{HH}(C)$	160.6	34		
12	$(\beta_i(H) \beta_{i+1}(H))$	2.8	35	$(\phi_i \phi_{i+1})$	-1.2
13	$(\beta_i(C) \beta_{i+1}(H))$	2.8	36	$(\gamma_i(H) \phi_i)$	2.3
14	$(\beta_i(H) \beta_{i+2}(H))$	-2.2	37	$(\gamma_i(C) \phi_i)$	3.9
15	$(\beta_i(C) \beta_{i+2}(H))$	-2.2			
16	$(\beta_i(H) \beta_{i+3}(H))$	-3.2			
17	$(\beta_i(C) \beta_{i+3}(H))$	-3.2			
18	$(\alpha_i R_i)$	44.2			
19	$(\beta_i(H) R_i)$	36.4			
20	$(\beta_i(C) R_i)$	36.4			
21	$(\alpha_i r_i)$	-1.4			
22	$(\beta_i(H) \alpha_{i+1})$	6.4			
23	$(\beta_i(C) \alpha_{i+1})$	6.4			

UNITS - Nm^{-1} , $10^{-10} N rad^{-1}$ OR $10^{-20} Nm rad^{-2}$ AS APPROPRIATE

Table 6.6 The Calculated Frequencies for the B_{1g} , B_{1u} , B_{2u} , B_{2g} Species
of Biphenyl at each stage of the Perturbation

obs ν		I	II	III	IV	V	VI	VII
B_{1g}	1592	1615	1613	1626	1626			
	1462	1459	1459	1466	1466			
	1333	1349	1351	1354	1355			0
	1263	1272	1283	1285	1285			
	1165/1149	1152	1156	1160	1160			
	1097	1077	1076	1082	1082			
	610	613	613	610	611			
	-	404	404	407	407			
B_{1u}	968	998	993	992	988	982	982	978
	903	904	905	907	904	897	899	897
	729	723	728	728	726	733	726	725
	695	705	704	703	707	706	705	701
	458	423	422	422	454	459	456	459
	73	86	86	86	80	79	78	73
B_{2u}	1568	1590	1587	1500	1599			
	1428	1429	1428	1334	1434			
	1344	1318	1322	1225	1325			
	1268	1280	1290	1293	1293			
	1154/1169	1158	1161	1165	1165			
	1075/1090	1050	1049	1055	1055			
	626	631	631	629	629			
	118	118	118	120	120			
B_{2g}	978	998	992	992	988	985	985	986
	-	911	911	913	905	898	903	916
	779/786	743	747	747	742	718	732	787
	-	692	691	689	705	712	708	699
	546	483	483	481	505	519	532	544
	251	242	242	242	229	230	233	241

Table 6.7 (i) The Observed Frequencies used in the Calculations

	A Species			4,4'difluoro Biphenyl
	Biphenyl D ₂	Biphenyl D ₁₀	Biphenyl	
A _g	-	-	-	-
R active	-	-	-	-
	-	2276	-	1603
	1610	1600	1563	1529
	1513	1509	1411	1323
	1276	1274	1186	1277
	1205	1209	965	1169
	1036	1031	880	1017
	1002	988	846	846
	743/739	734	690	660
	330	324	312	277
A _u	-	-	-	-
Inactive	-	-	-	-
	-	-	-	-

Table 6.7 (ii) The Observed Frequencies used in the Calculations

	B ₁ Species			4,4' difluoro Biphenyl
	Biphenyl D ₂	Biphenyl D ₁₀	Biphenyl	
B _{1g}	-	-	-	-
R active	-	-	-	-
	1592	1593	1533	1554
	1462	-	1347	-
	1333	1313	1280	1257
	1263	1283	-	1245
	1165/1149	1110/1117	850	1098
	1097	876	831	627
	610	605	583	* 464
	* -	* -	* -	* 340
B _{1u}	968	954	818	-
I.R. active	903	841	742	822
	729	716	620	702
	695	-	538	* 499/505
	* 458	* 449	* 410	* 283
	73	-	83	71

* bands which are observed to shift on phase change.

Table 6.7 (iii) The Observed Frequencies used in the CalculationsB₂ Species

	Biphenyl	D ₂ Biphenyl	D ₁₀ Biphenyl		4,4 difluoro Biphenyl
B _{2u}	-	-	-		-
I.R.active	-	-	-		-
	1568	1555	1522		1585
	1428	1393	1317		1393
	1344	1322	1260		1317
	1268	1262	1024		1288
	1169/1153	1115/1113	844		1124/1108
	1090/1075	862	818		642
	626	-	594		414
	* 118	-	* 112		84
B _{2g}	978	-	816		938
R active	-	865	-		-
	786/779	743/738	651		722
	-	597	539		540
	546	538	459		395
	* 251	* 241	* 225		180

* bands which are observed to shift on phase change.

Table 6.7 (iv) The Observed Frequencies used in the Calculations

	<u>B₃ Species</u>				4,4 difluoro Biphenyl
	Biphenyl	D ₂ Biphenyl	D ₁₀ Biphenyl		
B _{3u} I.R. active	-	-	-	-	-
	-	-	-	-	-
	-	2296	-	-	1600
	1597	1596/1587	1566	-	1495
	1480	1471	1343	-	1235
	1181	1180	981	-	1158
	1041	1034	950	-	1016
	1006	1007	854	-	1007
	985	-	813	-	804
	610	604	588	-	518
B _{3g} R active	-	975	-	-	966
	-	845	657/655	-	-
	-	408	354	-	-

Section 6.7 The Perturbation of Vibrational Energy Levels

Two vibrational levels of the same electronic state belonging to different vibrations may have nearly the same energy. Mixing of the eigen functions of the two vibrational levels produces a perturbation of the energy levels and they "repel" each other - the higher level is shifted up and the lower one down so that the separation of the two levels is much greater than expected. The interaction is stronger the smaller the difference in energy.

The interaction term in the Hamiltonian is given by

$$H_{ni} = \int \psi_n^{\circ} H \psi_i^{\circ} d\tau$$

where ψ_n° and ψ_i° are the eigen functions of the two vibrational levels that perturb each other. Since \hat{H} (where $H = GF$) is totally symmetric, ψ_n° must have the same symmetry type as ψ_i° in order to give a non-zero value to H_{ni} , and therefore to the magnitude of the perturbation.

In a simple treatment, the interaction is taken as arising predominantly through the G matrix, and it is the magnitude of the off-diagonal terms

$$g_{ij} = \sum_m \frac{\partial R_i}{\partial q_m} \cdot \frac{\partial R_j}{\partial q_m} \mu_m$$

which determines the magnitude of the perturbation..

It was observed some years ago that the conjugation of π electron systems has a very pronounced effect on the intensities of infra red absorption bands of certain valence vibrations. Calculations based on the assumption that charges remain fixed during motion are inadequate to account for the intensities of the infra red band. The redistribution of delocalised electrons in a distorted molecule for a vibrational mode, contribute to the induced electric vector in a very important way for this mode.

Sournia^[75] studied the effect of phase change - solid - liquid - gaseous - on the intensities of some of the bands of the Biphenyl spectrum. He showed that if

$$A(\nu_i) = \frac{8\pi^3 N \nu_i}{3hc} \left| M_{g_0 g_i} \right|^2$$

where $\left| M_{g_0 g_i} \right|^2$ is the transition moment between the states g_0 and g_i then this can be split into two terms.

M_s - the dipole moment of the skeleton, and

M_π - the term for the delocalisation of the π electrons.

It is the variation of the M_π with change of state which causes differences in the intensities.

Section 6.8 The refining of the force field for Biphenyl, D₂ Biphenyl and D₁₀ Biphenyl, and the estimate for the dihedral angle

When the first order force field was used to estimate the dihedral angle for Biphenyl, the error margin was far too high - hardly surprising since $(\nu_{\text{obs}} - \nu_{\text{calc}})$ was quite large. It was therefore decided to carry out a force constant refinement, using the frequency data of the solid state for Biphenyl, D₂ Biphenyl and D₁₀ Biphenyl (Table 6.7 (i), (ii), (iii), (iv)). The geometry, masses and the initial values of the force constants were those described in Section 6.3 and Table 6.2.

Obviously, since there are so many parameters, and a relative paucity of data, even with a set of three molecules, the problem is under-determined, and it is not possible to refine all the parameters simultaneously. The problem of ill-conditioning did not arise during

the series of calculations, but there were difficulties because the interaction terms $(\gamma_i \gamma_{i+1})$ and $(\phi_i \phi_{i+1})$ were insensitive to refinement. The convergence of the force fields is summarised in Tables 6.3 and 6.4 (i) and (ii).

In the first run, only the diagonal force constants were varied. There was significant improvement in the calculated frequencies, but certain modes, such as the higher ring modes (e.g. a_g - calc 1685 cm^{-1} , obs 1610 cm^{-1}) and the angle sensitive b_{2g} modes (e.g. calc. 483 cm^{-1} , obs 546 cm^{-1}) were badly predicted. When the interaction force constants defined by $(R_i R_{i+1})$, $[(R_i R_i^{CC})$, $(R_i R'_{i+1})$, $(R_i R'_{i+1})$, $(\alpha_i R_i^{CC})$, - see figure 6.3], $(\gamma_i \gamma_{i+1})$ and $(\phi_i \phi_{i+1})$ were introduced, there was a considerable improvement. The highest a_g ring mode dropped to 1626 cm^{-1} , and the overall error vector was considerably reduced. However, there was no improvement in the b_{2g} modes. It was necessary to allow all of the out-of-plane force constants to vary, and to introduce a new parameter $(\gamma_i(c) \gamma_i'(c))$. This had the effect of greatly improving the b_{2g} modes whilst adjusting the values of the parameters by only a small amount. All force constants had values in the range expected from comparison with Benzene, and from molecular orbital predictions.

It is important to stress certain features arising from the calculations.

An improvement in the calculated frequencies for the highest ring modes was made by introducing two interaction force constants $(R_i R_i^{CC})$ and $(\alpha_i R_i^{CC})$. It is the latter term which is of special importance. Duinker^[10] experienced great difficulties with the refinement of the $(\alpha_i r_i)$ parameter in the Benzene force field, as it is ill-defined by the frequency data since the C-H stretches are almost completely separated

from the other modes. Consequently, use of his value^[96] leads to considerable errors in analogous modes. Mills H.O.F.F.^[11] predicts that this parameter should be large and negative. It is very gratifying therefore, that the calculations produced a well-defined value that fulfilled these conditions.

The inter-ring stretching force constant is not well-defined, but clearly its value is significantly higher than was originally supposed. The rather long inter-ring bond length of 1.50 Å would suggest a bond order of about 1.14 whereas the value of the force constant suggests a bond order nearer 1.4. This discrepancy is probably due to steric repulsions between the 2,2' hydrogen atoms. The effects of this repulsion are evident in the frequency shift of the a_g β mode near 1200 cm^{-1} which occurs when the dihedral angle increases. In Biphenyl, the frequency drops about 13 cm^{-1} and the band is broad. In D_2 Biphenyl, the analogous drop is 20 cm^{-1} .

All intra-ring parameters have values close to their Benzene counterparts.

Having observed that any further variation of the parameters, whilst appearing to decrease ($\nu_{\text{obs}} - \nu_{\text{calc}}$), in fact tended to give unrealistic values, (Table 6.4 (ii) VII), the force field was used to calculate the frequencies for a number of different geometries - D_2 configuration with dihedral angle 30°, 45°, and 60°, and D_{2d} configuration (90°). Since in the D_{2d} configuration, the b_1 and b_2 frequencies pair to form degenerate e modes, the calculations show a variation in frequency with geometry for these two species.

For the eight frequency shifts observed (Sections 6.4 and 6.5) a graph was plotted of calculated frequency vs dihedral angle. The experimental frequency shifts are thought to be accurate to $\pm 2 \text{ cm}^{-1}$. In view of phase shifts, these uncertainties are increased to $\pm 3 \text{ cm}^{-1}$. This may still be an underestimate, but it does give some idea of the error margin associated with the deduced dihedral angle. Taking each graph in turn, the observed shift was marked - this is shown as the mid-point of the hatched areas, whilst the hatching shows the spread of values compatible with the $\pm 3 \text{ cm}^{-1}$ error.

The small observed shift in the lowest b_2 mode in Biphenyl gives an estimate for Θ which is too low compared with the estimate derived from the lowest b_2 mode in D_{10} Biphenyl (the corresponding mode was not observed in D_2 Biphenyl, see Section 6.5). The two estimates for given by D_2 Biphenyl do not overlap in their uncertainties ($25 - 29^\circ$ and $39 - 46^\circ$). Nevertheless, the extent of the agreement is generally very satisfactory.

The final estimate of the dihedral angle and its uncertainty was based on a weighted average of the values from the different observed shifts, and the scatter of values about this optimum estimate. Since the uncertainty in the angle derived from the lower b_2 modes of Biphenyl and D_{10} Biphenyl was high, these two estimates were given half weight. The estimates for the dihedral angle derived from the eight observed frequency shifts give a mean value for Θ of $32.2^\circ \pm 2^\circ$.

The causes of the spread of estimates for the dihedral angle are as follows:-

- a) the analysis assumed that the molecular force field remains invariant with change of dihedral angle. Since the only significant frequency shifts were those predicted in the absence of force field changes, this appears to be a minor factor.

b) errors in the eigen vectors due to force field uncertainties. Force constant calculations^[96] and the work described in Chapter 5 suggest that the Benzene force field is reasonably well-determined, and is transferable, except for certain diagonal terms referring to motions in the region of substitution. The major uncertainties, then, are believed to concern motions in the region of the inter-ring bond. A 5% error in calculated frequencies using transferred force fields is not unreasonable, but for the present purpose, this is far too large. Thus b_{1g} and b_{1u} modes of Biphenyl occur in the solid at 458 cm^{-1} and at about 390 cm^{-1} . A 20 cm^{-1} error in each in opposite directions would lead to a gross error in the interaction as a consequence of the inverse dependence of the interaction on the energy difference.

Figures 6.4 and 6.5 show plots of calculated frequency vs dihedral angle, for the following frequency shifts.

Figure 6.4

- 1 Biphenyl, b_1 mode calculated at 456 cm^{-1} for $\Theta = 0$.
- 2 Biphenyl, b_1 mode calculated at 407 cm^{-1} for $\Theta = 0$.
- 3 Biphenyl, b_2 mode calculated at 233 cm^{-1} for $\Theta = 0$.
- 4 Biphenyl, b_2 mode calculated at 120 cm^{-1} for $\Theta = 0$.
5. D_2 Biphenyl, b_1 mode calculated at 430 cm^{-1} for $\Theta = 0$.

Figure 6.5

- 6 D_2 Biphenyl, b_2 mode calculated at 224 cm^{-1} for $\Theta = 0$.
- 7 D_{10} Biphenyl, b_1 mode calculated at 407 cm^{-1} for $\Theta = 0$.
- 8 D_{10} Biphenyl, b_1 mode calculated at 378 cm^{-1} for $\Theta = 0$.
- 9 D_{10} Biphenyl, b_2 mode calculated at 217 cm^{-1} for $\Theta = 0$.
- 10 D_{10} Biphenyl, b_2 mode calculated at 110 cm^{-1} for $\Theta = 0$.

As explained in Sections 6.4 and 6.5, experimental values for the frequency shifts to which graphs 2 and 8 refer are not known at present.

Due to the high uncertainty in the angle obtained from graphs 4 and 10, these estimates were given half weight.

Figure 6.4

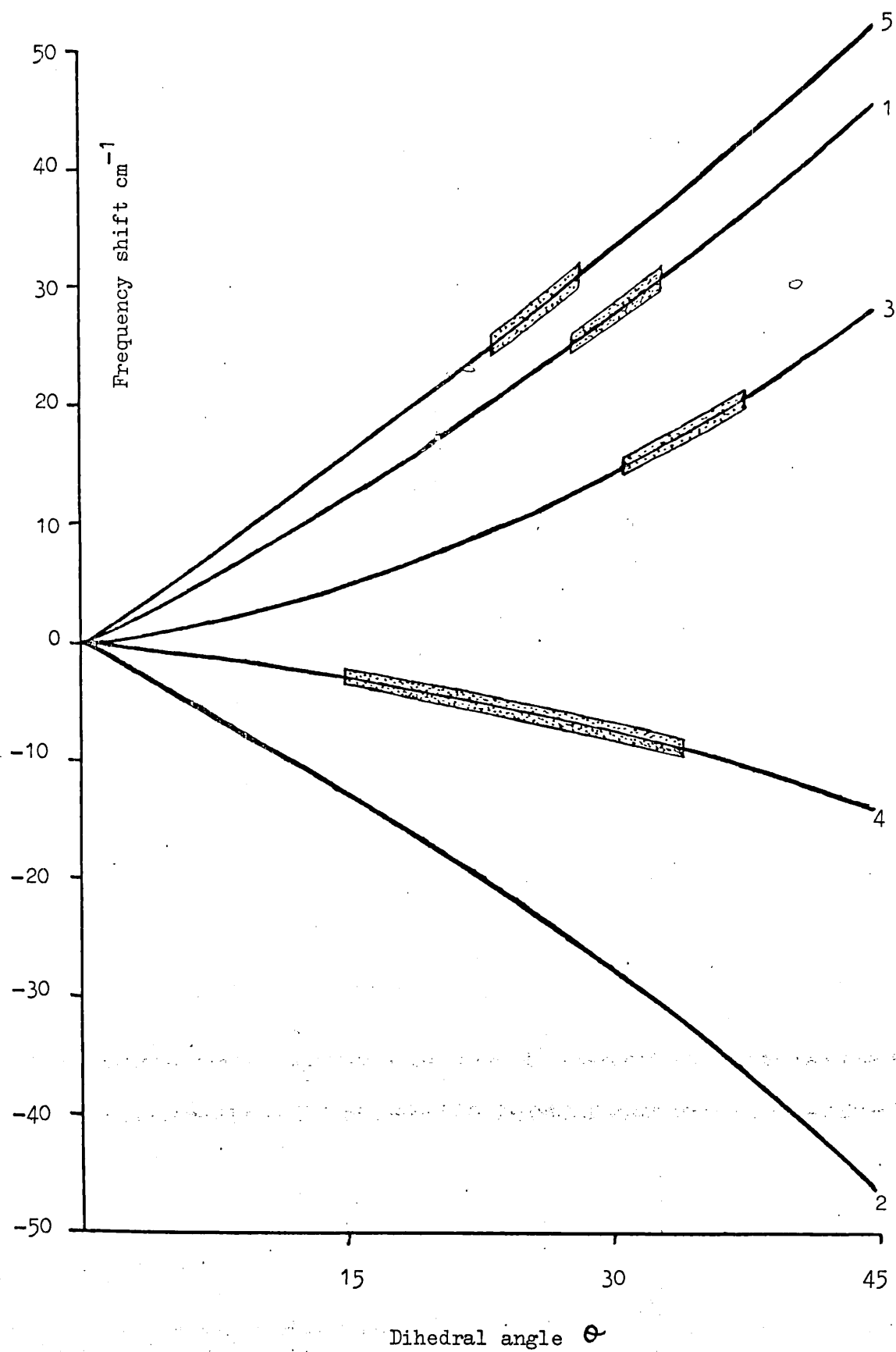
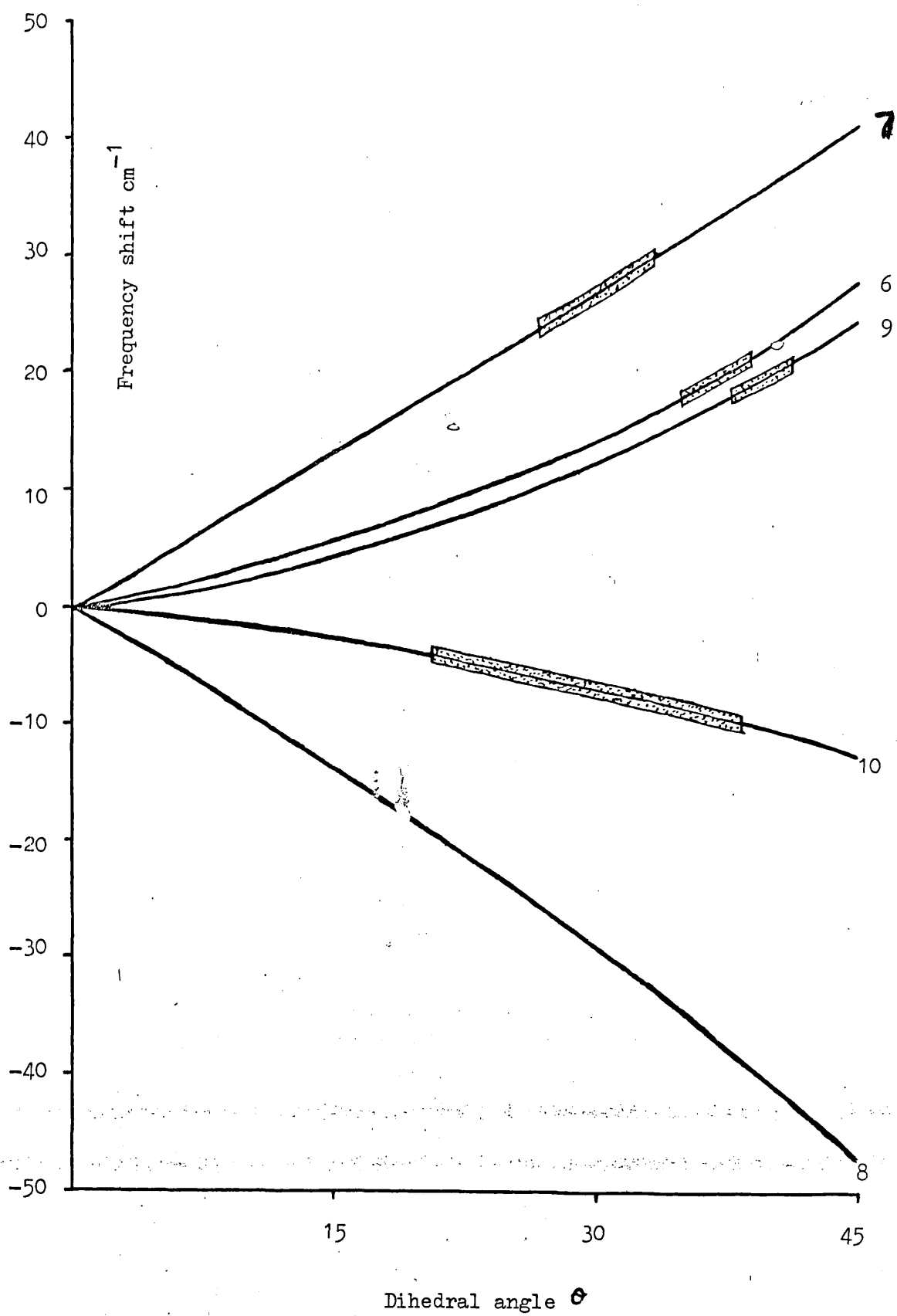


Figure 6.5



Section 6.9 The Refining of the Force Field for 4,4' Difluoro Biphenyl

A force constant refinement was attempted for 4,4' difluoro Biphenyl. The observed frequencies used are listed in Table 6.7. The molecule was assumed to have the same geometry as Biphenyl, with a C-F bond length of 1.327 Å. The atomic weights used were (in atomic mass units)

Hydrogen 1.00797

Carbon 12.01115

Fluorine 18.9984

The initial values of the force constants were those of the 37 parameter force field derived for Biphenyl, D_2 Biphenyl and D_{10} Biphenyl, and are given in Table 6.3 column IV and Table 6.4 (ii) column IV.

ϕ_i is the twisting of both the carbon and the substituent atoms about $C_i - C_{i+1}$. There are two ϕ diagonal force constants included in the 37 parameter field. A distinction is made between those deformations which involve the inter-ring bond, and those which do not.

The initial values used for the parameters

r^{HH} (F)

α (F)

β^{HH} (F)

and given in Table 5.1. The values for the out-of-plane parameters.

γ^{HH} (F)

ϕ (HF)

were taken from [14].

Inspection of the eigen values of the 283 cm^{-1} band of the B_{1u} species, which is observed to shift on change of state, suggests strong interaction between the out-of-plane deformation of the C-F bond and the ϕ torsion involving the fluorine atom. The parameter ($\gamma^{\text{HH}}(\text{H})\phi(\text{HH})$) was replaced by ($\gamma^{\text{HH}}(\text{F})\phi(\text{HF})$) where appropriate, and there was a decrease in ($\nu_{\text{obs}} - \nu_{\text{calc}}$) for this frequency.

The 340 cm^{-1} and 464 cm^{-1} bands of the B_{1g} species are also observed to shift. The second lowest mode arises from the in-plane deformation of the C-F bond, the in-plane deformation of the inter-ring bond, and the coupling between them. [As this coupling is represented at present by ($\beta_i(\text{c}) \beta_{i+3}(\text{H})$), which was not refined in the Biphenyl calculations and has the value taken from the Benzene force field of Duinker [10], it may be necessary to introduce a new term ($\beta_i(\text{c}) \beta_{i+3}(\text{F})$)]. The lowest mode arises predominantly from the in-plane deformation of the inter-ring bond. The parameter ($\beta_i(\text{c}) \beta'_i(\text{c})$) was included, and although poorly defined, did improve the fit. This behaviour is paralleled by its out-of-plane counterpart ($\gamma_i(\text{c}) \gamma'_i(\text{c})$) in the Biphenyl calculations.

The frequency data for one molecule is insufficient to successfully refine even a few carefully selected parameters. The preparation attempted of D_8 4,4' difluoro Biphenyl, by the classical Friedel-Crafts technique, has so far been unsuccessful. In the meantime, however, the calculations have given some indication of how the presence of a fluorine atom in the para position alters the distribution of the electron cloud, and which interaction force constants need to be included.

PART 3

Absolute Infra Red Intensities for some
Combination Bands of the Fluorine
Substituted Benzenes

CHAPTER SEVENAbsolute Infra Red Intensities for some Combination Bands of the
Fluorine Substituted BenzenesSection 7.1 Introduction

The dipole moment μ of an electrically neutral molecule is a vector quantity whose direction is that of a line joining the centre of charge of the negative charges with the centre of charge of the positive charges and whose magnitude is the length of that line multiplied by the total negative charge or the total positive charge, these being equal. It has the components μ_x , μ_y and μ_z given by the expressions

$$\mu_x = \sum_{\alpha} e_{\alpha} x_{\alpha}$$

$$\mu_y = \sum_{\alpha} e_{\alpha} y_{\alpha}$$

$$\mu_z = \sum_{\alpha} e_{\alpha} z_{\alpha}$$

where e_{α} is the charge and x_{α} , y_{α} and z_{α} are the cartesian coordinates (space fixed axes) of the α^{th} particle, the sum being over all particles.

Unless there is a change in the dipole moment of the molecule during a vibration there can be no interaction with electromagnetic radiation and hence no infra red band.

The intensity of absorption of infra red radiation is usually defined as

$$\int_i = \frac{1}{c l} \int_{\text{band}} \ln \left(\frac{I_0(\nu)}{I(\nu)} \right) d\nu$$

where c is the absorbent concentration

l is the path length of the beam through the absorbing material

$I_0(\nu)$ and $I(\nu)$ are the initial and final intensities of the beam of frequency ν (expressed in cm^{-1})

Alternatively, intensity can be defined as

$$A_i = \frac{1}{cl} \int_{\text{band}} \ln \left(\frac{I_0(\nu)}{I(\nu)} \right) d\nu$$

It can be shown that [17]

$$A_i = \frac{1}{\nu_i} \frac{N\pi}{3c} \left(\frac{\partial \mu}{\partial Q_i} \right)^2$$

assuming electrical harmonicity i.e. that the dipole moment μ can be expanded as a Taylor series in terms of displacements from the equilibrium positions, and all but the first derivatives neglected.

$$\mu = \mu_0 + \sum_j \left(\frac{\partial \mu}{\partial Q_j} \right)_0 Q_j + \text{higher terms (negligible)}$$

where $\frac{\partial \mu}{\partial Q_j}$ is the change in dipole moment with respect to the change

in the j^{th} normal coordinate, Q_j . In this approximation, the intensity

of an infra red combination band ought to be zero, which is certainly not so,

but unless a combination band gains intensity from a fundamental of the same symmetry, by resonance, its intensity is far less than that of a

fundamental, so the assumption is valid to a first approximation. The

error involved in the electrical harmonic approximation is much smaller

than the present experimental errors, and those arising from the

uncertainty in the normal coordinate Q_j . When considering the potential

function (Section 2.1), mechanical harmonicity was assumed, so this is a

double harmonic oscillator approximation.

For a symmetric molecule, the symmetry of Q_j , and hence of $\frac{\partial \mu}{\partial Q_j}$, is known. The experiments determine the absolute magnitude of $\frac{\partial \mu}{\partial Q_j}$ but not the direction in which the dipole moment change is produced.

Not only is it extremely difficult to make accurate intensity measurements, which imposes an obvious limitation, but the results are then limited by the accuracy of the coefficients $L_{i,j}^{-1}$ which specify the form of the normal vibration. The computed intensities are often sensitive to the smaller elements of the L^{-1} matrices, which in turn are sensitive to small, off-diagonal force constants. By contrast, the frequencies are insensitive to these terms, especially the C-H stretching frequencies above 3000 cm^{-1} .

Provided all $\frac{\partial \mu}{\partial Q_j}$ values for the infra red bands of a given symmetry species, and the eigen vectors, which relate changes in the symmetry coordinates to changes in the normal coordinates, are known, then the $\frac{\partial \mu}{\partial S_i}$ values, the change in dipole moment with respect to the change in symmetry coordinate, for that symmetry species can be calculated.

$$\frac{\partial \vec{\mu}}{\partial S_i} = \sum_j L_{i,j}^{-1} \left(\frac{\partial \vec{\mu}}{\partial Q_j} \right)$$

Because of the sign indeterminacy of each $\frac{\partial \mu}{\partial Q_j}$ term, there are 2^n different possible solutions, yielding 2^{n-1} different absolute values for $\frac{\partial \mu}{\partial S_i}$, where n is the number of normal vibrations of the symmetry type under consideration.

If isotopic data is available, a second 2^n sets of solutions can be calculated, and the correct set will have the same values for the corresponding $\frac{\partial \mu}{\partial S_i}$ terms in the two molecules. The invariance of the dipole moment function under isotopic substitution leads to isotope rules (c.f. Section 2.8) as the amount of extra data that can be obtained by

isotopic substitution is limited, but these rules can provide a useful check on the accuracy of intensity measurements.

If Coriolis data can be measured for an interaction between two vibrations of the same symmetry type, it is possible to deduce the relative signs of the two dipole transition states [104].

However, the $\frac{\partial \mu}{\partial S_i}$ values still relate to the molecule as a whole, whilst an interpretation is required of $\frac{\partial \mu}{\partial Q_j}$ in terms of the dipole moments of bonds (bond moments) and the changes in dipole moments of bonds with respect to a deformation of that bond (bond moment derivatives).

A basic tenet of Physical Chemistry is the idea of transferability, or that similar molecules display similar properties, and so theories have been postulated which allow for the transfer of bond moments and bond moment derivatives between similar molecules.

The Zero Order Bond Moment Hypothesis

In order to reduce the measured quantities $\frac{\partial \mu}{\partial S}$ to quantities characteristic of individual bonds, three further assumptions are made [105].

- (1) When a bond is stretched by dr , a moment $\frac{\partial \mu}{\partial r} dr$ is produced in the direction of the bond.
- (2) When a bond is bent through an angle $d\theta$, a moment $\mu_0 d\theta$, where μ_0 is the "effective bond moment", is produced in the plane of bending and perpendicular to the direction of the bond.
- (3) When any one bond is bent or stretched, no moments are produced in other bonds.

With these assumptions, the total moment resulting from an arbitrary distortion is just the vector sum of the moments produced by each individual bond. (1) and (2) are based on the assumption that the bond

moment lies directly along the bond and continues to do so when the molecule is deformed by vibration. If the assumptions are valid, the following criteria should hold.

- (i) values of the deduced bond moments and gradients in different molecules are comparable.
- (ii) values of given gradients and moments derived from different symmetry classes of the same molecule are equal.
- (iii) the perpendicular gradients to any bond are negligible.
- (iv) values of the bond dipoles derived are comparable with the static dipoles as measured by other methods.

The values calculated for bond moments and bond moment derivatives are generally not even transferable between different symmetry species of the same molecule. It appears that the "effective bond moments" obtained with the assumption of independent bond dipoles are not the same physical quantities as the static bond dipole moments. Because the rigid-bond model of the molecule is inadequate, since factors other than μ and $\frac{\partial \mu}{\partial r}$ are ignored, $\frac{\partial \mu}{\partial S}$ is a more meaningful quantity in which to report conclusions.

Coulson^[106] reviewed the factors which cause the breakdown of the bond moment hypothesis.

- (i) lone pairs of electrons which have dipole moments which can change during a vibration, but which are not incorporated into any bond moments.
- (ii) hybridisation changes during the deformation of a bond, which affect the molecule as a whole and not just the bond being deformed.
- (iii) the dipole is not orientated along the bond.

Sverdlov^[107] assumed that the bond moment vector departs from the bond direction during a vibration, under the influence of atoms not connected with that bond. This necessitates the introduction of components of the change in bond moment with respect to each type of bond distortion, perpendicular to that bond. Therefore the number of parameters is increased by a factor of three, and since they cannot all be determined, even for the simplest molecules, the theory has no practical advantages. This approach was used for Benzene by Kovner and Snegirev^[108].

The Electro Optical Theory of Gribov.^[109,110,111]

This gives a general expression for the dipole moment derivative in terms of the bond properties, bond moment and bond moment derivatives, referred to by Gribov as electro-optical parameters.

The dipole moment of a molecule $\vec{\mu}$ can be split into a series of components

$$\vec{\mu} = \vec{\mu}_{up} + \vec{\mu}_{pol} + \sum_R \vec{\mu}_R$$

where $\vec{\mu}_k$ is the bond moment of the k^{th} bond and these bond moments are considered to be transferable between molecules. $\vec{\mu}_{up}$ represents the contribution to the dipole moment of the molecule from unpaired electrons and $\vec{\mu}_{pol}$ represents the contribution to the dipole moment of the molecule from off-axis polarisation of the bonds.

If \vec{e}_k is a unit vector directed along the k^{th} bond and μ_k is the magnitude of the k^{th} bond moment, then

$$\vec{\mu} = \vec{\mu}_{up} + \vec{\mu}_{pol} + \sum_R \mu_R \vec{e}_R$$

If it is assumed that the contributions to the dipole moment from unpaired electrons and off-axis polarisation can be resolved into components along the bonds, then

$$\vec{\mu}_{\text{up}} + \vec{\mu}_{\text{pol}} = \sum_{\mathbf{R}} \mu'_{\mathbf{R}} \vec{e}_{\mathbf{R}}$$

and

$$\vec{\mu} = \sum_{\mathbf{R}} (\mu_{\mathbf{R}} + \mu'_{\mathbf{R}}) \vec{e}_{\mathbf{R}}$$

The two components of the dipole along the k^{th} bond can be combined so that

$$\vec{\mu} = \sum_{\mathbf{R}} \mu_{\mathbf{R}} \vec{e}_{\mathbf{R}}$$

but $\mu_{\mathbf{R}}$ can no longer be considered as a transferable bond moment.

In the case of planar molecules, in which there are no bonds perpendicular to the plane of the molecule, it may be necessary to consider certain electron orbitals as constituting a bond perpendicular to this plane.

If all the terms in the matrices $\left| \frac{\partial \mu}{\partial R} \right|$ and $|\mu|$ are retained, the number of unknowns greatly exceeds the number of observables, and can result in only being able to calculate linear combinations of certain terms, which cannot be resolved into individual components. If in the matrix $\left| \frac{\partial \mu}{\partial R} \right|$ only the terms for the change in a bond moment with respect to the stretching of that bond are retained, all terms can be calculated, but the theory reverts to being the bond moment hypothesis^[112, 113].

Steele and Wheatley^[114] examined the infra red active vibrations of Benzene and Hexafluoro Benzene, and concluded that for the out-of-plane vibrations, besides the contribution to the change in the dipole due to reorientation of the bond moments as the atoms move, there is a

contribution from the redistribution of electronic charge in the p_z orbitals of the carbon atoms forming the Benzene ring. This "rehybridisation moment" is of the same magnitude in both Benzene and Hexafluoro Benzene.

For a planar molecule, the component of the \vec{e} vector, the unit vector directed along a bond, in the direction perpendicular to the plane of the molecule, (arbitrarily defined as the z direction) is zero. π electron rehybridisation is assumed to be restricted to the p_z orbitals of the carbon atom to which the moving substituent is attached. In a γ deformation, as the substituent moves out of the molecular plane, rehybridisation at the carbon atom introduces some sp^3 character into the sp^2 σ -bonding orbitals of the planar molecule. If this rehybridisation were complete, then the fourth "bond" in the sp^3 configuration would be a lone pair of electrons and although complete rehybridisation does not occur, there is some electron flow producing an increase of electron density on the opposite side of the ring to the substituent. There is a flow of electrons in the z direction, and this will cause a change in dipole moment along the z axis in the opposite direction to the electron flow. The effect is to make the substituent appear less negative. To allow for this, the p_z orbital of each carbon atom in the ring is defined as a bond, each with a bond moment which is zero when the molecule is planar but which has a value during an out-of-plane vibration. These pseudo-bonds are orientated along the z axis so that the components of the \vec{e} vectors in the z direction all have the value one. Since an in-plane deformation cannot involve the p_z orbital, there can be no rehybridisation associated with this motion. For the Benzene molecule, the hydrogen atom is known^[115] to be at the positive end of the CH dipole, as the numerical value of the effective dipole should be greater for a γ_{CH} than for a β_{CH} deformation.

Spedding and Whiffen^[116] have interpreted the Benzene intensity data in terms of bond properties on the basis of the simple bond moment hypothesis. They obtained two different values for the effective CH bond moment, namely 0.31D for the β_{CH} deformation, and 0.61D for the γ_{CH} deformation. The net effect is to make the effective CH dipole more positive in the γ_{CH} motions by an amount 0.3D. For Hexadeutero Benzene, the value for the effective β_{CH} bond moment is less than the γ_{CH} bond moment by an amount 0.3D.

A rehybridisation moment of the same order of magnitude as in the case of Benzene is expected for Hexafluoro Benzene since such a moment will involve only the π electrons associated with the carbon nucleus and will therefore be almost independent of a substituent of the Benzene ring. In Benzene, it is known that the hydrogen atom is at the positive end of a moving CH dipole, and it seems most likely that in Hexafluoro Benzene, the fluorine atom is at the negative end of a moving CF dipole. In Benzene, because the effect of rehybridisation is to make the hydrogen atom appear less negative, the effective dipole is greater for a γ_{CH} than for a β_{CH} deformation. In Hexafluoro Benzene, the effect of rehybridisation is to make the fluorine atom appear less negative also, so we expect the effective dipole for a γ_{CF} to be less than for a β_{CF} deformation.

The interpretation chosen^[114] of the intensity data of Hexafluoro Benzene gives a value for the effective dipole for the β_{CH} deformation which is 0.3D greater than that for the γ_{CH} deformation. The opposite direction of the moment is due to the different direction of a CF dipole.

Section 7.2 Absolute Intensities of Combination Bands

Symmetry considerations show that μ_z is responsible for the infra red absorption resulting from the out-of-plane fundamentals, and μ_x and μ_y are responsible for that resulting from their binary combinations.

If ψ_1 and ψ_2 are the eigen functions corresponding to the two different states characterised by quantum numbers ν_1 and ν_2 respectively, and ψ_c is that corresponding to the state $\psi_1 \psi_2$, then the effect of a symmetry operation, S, is given by

$$\psi_c (\equiv \psi_1 \psi_2) \xrightarrow{S} \chi_1(S) \chi_2(S) \psi_1 \psi_2 \equiv \chi_1(S) \chi_2(S) \psi_c$$

Thus the character of ψ_c for an operation S is given by the product of the corresponding characters for ψ_1 and ψ_2 - the character representation of ψ_c is the direct product representation of the constituent wavefunctions. If ψ_1 and ψ_2 are non-degenerate states then ψ_c will be nondegenerate. If the fundamental states are degenerate then the representation of the multiply excited state may be reducible and the constituent irreducible representations may be deduced using

$$\sum_S a_i \chi_i^{\Gamma_i}(S) \chi_j^{\Gamma_j}(S)$$

where a_i is the number of times the i^{th} irreducible representation Γ_i appears in the reduced form.

$\chi_i^{\Gamma_i}(S)$ is the character for the element S in the irreducible representation

Γ_i .

$\chi_j^{\Gamma_j}(S)$ is the character for the element S in the reducible representation.

The combination bands of the γ_{CH} vibrations of Benzene are strong. They appear in the region of about $1700\text{--}2000\text{ cm}^{-1}$, which is relatively free from fundamental absorptions, and their interpretation is well known [117, 118, 119]. The intensity measurements of such combination bands, however, have been reported by only a few authors [120, 121]. A full and exact treatment of the intensities of these combination bands would involve the introduction of a wide variety of cubic potential constants and second derivatives of the dipole moment function. The combination bands agree quite closely with the sum of the fundamental frequencies, which suggests that the potential function does not contain exceptionally large cubic constants, so these are neglected. Their unimportance is due to the facts

- (i) that none of the combining fundamentals (antisymmetric to the ring plane) can have the same symmetry as the combination level (symmetric to the ring plane).
- (ii) there are no fundamentals of the correct symmetry in the range $1700\text{--}2000\text{ cm}^{-1}$ which could interact with the combination level (Fermi resonance). This effect may be present below 1700 cm^{-1} .

From quantitative measurements on Benzene it has been suggested that the important quantity governing the intensity of the combination bands is a very high value of the second derivative of the dipole moment with respect to the out-of-plane CH deformation $\frac{\partial^2 \mu}{\partial \gamma^2}$.

It would also be inappropriate for interpreting results of the present accuracy to retain all seven relevant second derivatives of the dipole moment function. Those involving explicitly distortion of the carbon skeleton are therefore omitted. The carbon substituent bond moves with very small amplitude during a γ_{CH} vibration - the carbon substituent

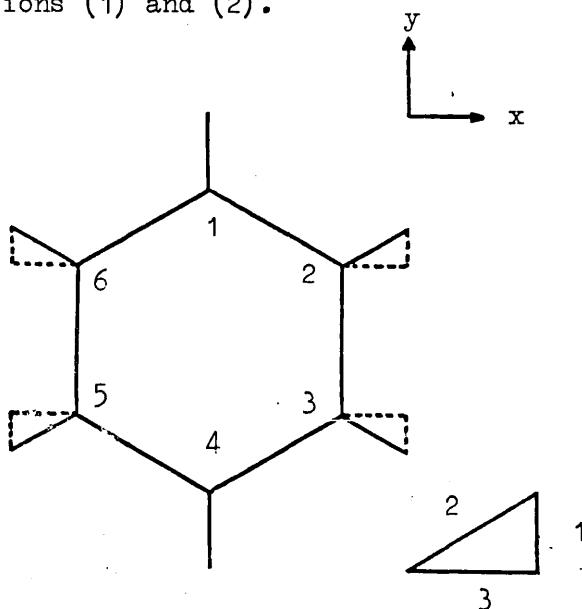
bond moment contributes mainly to the constant terms of μ_{x_0} and μ_{y_0} , and has almost no effect upon the absorption intensities. Above 1500 cm^{-1} , absorption arises predominately from the C-H distortion.

This leaves three terms proportional to the second order of the C-H bendings. The distortion is measured from the external bisector of the ring angle, and the coefficients retained are of the form

$$\frac{\partial^2 \mu}{\partial \gamma_j \partial \gamma_k} \quad \text{with } \gamma \text{ defined by}$$

$$r_0 \gamma_j = (z_j - z_j) + \rho (z_{j-1} - 2z_j + z_{j+1})$$

Symmetry requires that the dipole arising from the terms in $\frac{\partial^2 \mu}{\partial \gamma_j \partial \gamma_k}$ lie along the bisector of the angle between the j and k position and the ring centre. Added vectorially, the retained terms contribute to the dipole as in equations (1) and (2).



$$\begin{aligned} \mu_x = & \dots + 3^{\frac{1}{2}} \cdot 2^{-1} (\gamma_2^2 + \gamma_3^2 - \gamma_5^2 - \gamma_6^2) \left(2^{-1} \frac{\partial^2 \mu}{\partial \gamma_j^2} \right) \\ & + 2^{-1} (\gamma_1 \gamma_2 + 2\gamma_2 \gamma_3 + \gamma_3 \gamma_4 - \gamma_4 \gamma_5 - 2\gamma_5 \gamma_6 - \gamma_6 \gamma_1) \left(\frac{\partial^2 \mu}{\partial \gamma_j \partial \gamma_{j+1}} \right) \\ & + 3^{\frac{1}{2}} \cdot 2^{-1} (\gamma_1 \gamma_3 + \gamma_2 \gamma_4 - \gamma_4 \gamma_6 - \gamma_5 \gamma_1) \left(\frac{\partial^2 \mu}{\partial \gamma_j \partial \gamma_{j+2}} \right) \dots \quad (1) \end{aligned}$$

$$\begin{aligned}
\mu_y = & \dots 2^{-1} (2\gamma_1^2 + \gamma_2^2 - \gamma_3^2 - 2\gamma_4^2 - \gamma_5^2 + \gamma_6^2) \left(2^{-1} \frac{\partial^2 \mu}{\partial \gamma_j^2} \right) \\
& + 3^{\frac{1}{2}} \cdot 2^{-1} (\gamma_1 \gamma_2 - \gamma_3 \gamma_4 - \gamma_4 \gamma_5 + \gamma_6 \gamma_1) \left(\frac{\partial^2 \mu}{\partial \gamma_j \partial \gamma_{j+1}} \right) \\
& + 2^{-1} (\gamma_1 \gamma_3 - \gamma_2 \gamma_4 - 2\gamma_3 \gamma_5 - \gamma_4 \gamma_6 + \gamma_5 \gamma_1 + 2\gamma_6 \gamma_2) \left(\frac{\partial^2 \mu}{\partial \gamma_j \partial \gamma_{j+2}} \right) \dots
\end{aligned}$$

... (2)

To compute the transition moment, these must be transformed into the symmetry coordinates.

It can be shown [17] that, neglecting anharmonicity, band area/
molecule = $\frac{h}{24\pi c} \cdot \frac{\nu_i + \nu_j}{\nu_i \nu_j} \left(\frac{\partial^2 \mu}{\partial q_i \partial q_j} \right)^2$

This is readily transformed into an expression involving the symmetry coordinates, since

$$\begin{aligned}
\frac{\partial^2 \mu}{\partial q_i \partial q_j} &= \sum_{m,n} \left(\frac{\partial^2 \mu}{\partial s_m \partial s_n} \right) \left(\frac{\partial s_m}{\partial q_i} \right) \left(\frac{\partial s_n}{\partial q_j} \right) \\
&= \sum_{m,n} l_{i,m} l_{j,n} \left(\frac{\partial^2 \mu}{\partial s_m \partial s_n} \right)
\end{aligned}$$

Section 7.3 A Discussion of the γ_{CH} Combination Bands Observed
for the Fluorine Substituted Benzenes

Since both the out-of-plane and the in-plane force field for a series of fluorine substituted Benzenes have been successfully derived by assuming that similar internal coordinate deformations in similar environments in different molecules require the same force, an obvious approach to the analysis of the γ_{CH} combination bands of this series would be to assume that bond moments and bond moment derivatives are transferable between similar molecules.

The χ -matrix data provided by the normal coordinate analysis of the out-of-plane vibrations of the fluorine substituted Benzenes^[14] can be used with confidence. Three molecules of this series were not studied in the present work.

Hexafluoro Benzene has no C-H bonds.

Pentafluoro Benzene has only one C-H bond, so the only combination band is the overtone of the fundamental.

Because 1,2,4 trifluoro Benzene has C_2 symmetry, the spectra are complex.

Of the nine molecules to study

- * Benzene
- 1,2 difluoro Benzene
- 1,3 difluoro Benzene
- * 1,4 difluoro Benzene
- * 1,3,5 trifluoro Benzene
- 1,2,3,4 tetrafluoro Benzene
- 1,2,3,5 tetrafluoro Benzene
- * 1,2,4,5 tetrafluoro Benzene.

the four marked with an asterisk are of high symmetry, which limits the possibilities for γ_{CH} combination bands, and greatly simplifies the spectra.

Benzene is the only molecule to have been investigated thoroughly. The absolute intensity of the γ_{CH} combination bands have been measured in both gas and liquid phases.

Gas phase measurements were made by Dunstan and Whiffen^[120], using a 1-metre folded-path cell. Nitrogen to a pressure of 700 mm was added to give sufficient pressure broadening. Some difficulty was experienced with absorption of Benzene vapour inside the cell, so that the pressure gradually fell after the cell was filled. This trouble was reduced by allowing the cell to come to equilibrium with Benzene vapour before a brief pumping and filling to the desired pressure. Measurements at five or more pressures were taken for each band.

Measurements in CS_2 solution were made by Kakiuti^[121] using a liquid cell with KBr plates.

Verification of these intensity values was not considered necessary.

In this work, the intensities were measured on a Perkin-Elmer 325 grating spectrometer, using a spectral slit width of 0.6 cm^{-1} for gas phase, and 0.75 cm^{-1} for liquid phase spectra.

A gas cell was constructed which consists of a glass cylinder 9.79 cm long, with KBr windows sealed with selastomer. The cell is evacuated and filled via a greaseless tap.

The sample is contained on a glass vacuum line. Before loading it into the cell, it is degassed, by freezing to liquid nitrogen temperature, pumping on the frozen sample, and then allowing it to warm to room temperature. The sample is repeatedly frozen, pumped on, then warmed until no gas bubbles appear while it is warming. It is then allowed to evaporate into the gas cell, and the temperature and pressure are noted. The pressure is measured using a mercury manometer, with a travelling microscope, open to the gas on one side, while the other is under continual vacuum pumping.

Firstly, a spectrum of the evacuated cell is recorded, then that of the sample plus cell, and finally, the sample beam is blocked off and the 100% absorption trace recorded. A very important point to note is that as the cell has to be removed from the spectrometer to introduce the sample, it is necessary to ensure that it is always replaced in the same position.

The liquid cell used throughout consisted of two KBr plates, with a cell thickness of .508 mm, precisely determined by the usual interference method.

Spectra in the range 2500-1500 cm^{-1} were recorded for the pure liquid - the regions of interest have been redrawn [Figures 7.1 - 7.8].

Spectra were recorded for each sample in CCl_4 solution at two concentrations.

Other workers have observed that these spectra alter when CH_3CN is added to the solution. For those bands which arise from a γ_{CH} deformation, the contour is flattened and broadened, and the position of the band shifts, usually to higher frequency. The effect is most pronounced in molecules of high symmetry. Because this phenomenon is not yet fully understood - it could be explained as complexing of some form - one must exercise caution where one has seemingly negative evidence. Until the nature of the effect is known, it is difficult to decide how many moles of CH_3CN to add per mole of sample. If one visualises a π -complex, with a CH_3CN molecule above and below the ring plane, then a ratio of two moles of CH_3CN to one mole of sample is suitable for a trial run. Spectra of sample + CH_3CN + CCl_4 were recorded, at various concentrations of CH_3CN , for every sample.

The spectra of Fluoro Benzene, 1,2 and 1,3 difluoro Benzene are similar. [Figures 7.1, 7.2, 7.3]. The relatively high number of possibilities for the combination of bands arising from γ_{CH} deformation - due to the number

of CH bonds and the low symmetry - results in complex spectra, with much overlapping of bands. Addition of CH_3CN to the solution causes all the strong bands to shift, but because the molecules have only C_{2v} symmetry, the effect is small.

In 1,2,3,4 tetrafluoro Benzene, a small shift in frequency is observed for the two γ_{CH} combination bands on addition of CH_3CN , but it will be difficult to measure the intensity of the band at 1743 cm^{-1} [Figure 7.6].

The spectra recorded for 1,4 difluoro Benzene are discussed fully later.

Superimposition of spectra at three concentrations of CH_3CN shows no shift in frequency for the bands of interest in 1,3,5 trifluoro Benzene, 1,2,3,5 tetrafluoro Benzene and 1,2,4,5 tetrafluoro Benzene [Figures 7.5, 7.7, 7.8]. In each case, the combination band is overlapped by very strong bands of lower frequency. Not only will it be difficult to approximate to the band contour, but if the wavefunction of the combination band is of the same symmetry as the wavefunction of a fundamental, then provided the difference in energy of the two vibrational levels is small, there will be a perturbation of the energy levels, and the weaker band may gain intensity from the stronger [see Section 6.7]. This feeling that the intensity of these 'combination bands' is enhanced by resonance, is borne out by a consideration of the weight of sample needed. The concentration of sample per ml of solution is carefully calculated, so that the value of $\log(I_0/I)$ at the maximum of the strongest band is the same, within reason, for each spectrum. It is thus meaningful to compare the molar concentrations.

Fluoro Benzene	=	3.231×10^{-2}	moles ml ⁻¹
1,2 difluoro Benzene	=	1.879×10^{-2}	
1,3 difluoro Benzene	=	2.224×10^{-2}	
1,4 difluoro Benzene	=	1.226×10^{-2}	
1,3,5 trifluoro Benzene	=	4.679×10^{-3}	
1,2,3,4 tetrafluoro Benzene	=	2.242×10^{-2}	
1,2,3,5 tetrafluoro Benzene	=	7.616×10^{-3}	
1,2,4,5 tetrafluoro Benzene	=	1.148×10^{-2}	

Liquid cells can be filled very rapidly, whilst there is a time delay involved in allowing the gas cell to come to equilibrium with the vapour of the sample, before filling to the desired pressure. Also, comparison of solution spectra with spectra of solution + CH₃CN yields valuable information. For these reasons, all the exploratory work was done in the liquid phase.

The most accurate values for the absolute intensities of the combination bands, however, come from measurements in the gas phase. In addition, vapour phase contours are of considerable importance in assigning the symmetry species of a band.

Band areas of spectra recorded using a path length of 10 cm and a concentration dependent upon the vapour pressure of the sample at room temperature are too small for accurate work. Consideration of the equation

$$\frac{1}{c l} \log \left(\frac{I_0}{I} \right) = \text{constant}$$

shows two ways of improving the (I_0/I) ratio. The concentration can be increased by loading the cell and keeping the sample chamber of the spectrometer at a higher temperature. Vapour pressure data for these molecules would be useful, but it appears to be available only for Benzene and Fluoro Benzene. Use of heating jackets, etc, can lead to uncertainties in the concentration. The path length can be increased by using a 1-metre

folded-path cell.

It is desirable to make measurements at a maximum of five pressures. Taking the 1736 cm^{-1} band of 1,4 difluoro Benzene as an example, one needs to be able to increase the (I_0/I) ratio by a factor of 7.5 to allow sufficient latitude to make all of these measurements.

IN THE TABULATIONS OF THE COMBINATION BANDS POSSIBLE IN A GIVEN RANGE FOR EACH MOLECULE, THE ASTERISK DENOTES $\gamma_{\text{CH}} + \gamma_{\text{CH}}$, and OUT-OF-PLANE FREQUENCIES ARE UNDERLINED.

Table 7.1

The observed frequencies in cm^{-1} used for the out-of-plane vibrations [14]

Fluoro Benzene			1,2 difluoro Benzene			1,3 difluoro Benzene			1,4 difluoro Benzene		
A ₂	970	1.0	A ₂	982	0.8	A ₂	879	1.0	B _{1g}	800	1.0
	826	1.0		840	0.8		599	1.0	B _{2g}	928	1.0
	405	1.0		703	1.0		251	1.0		692	1.0
B ₁	997	1.0		(555)	0.0	B ₁	978	1.0		375	1.0
	894	1.0		198	1.0		853	1.0	A _u	943	1.0
	754	1.0	B ₁	929	1.0		769	1.0		405	1.0
	685	1.0		749	1.0		672	1.0	B _{3u}	836	1.0
	500	1.0		450	1.0		458	1.0		508	1.0
	242	1.0		298	1.0		235	1.0		157	1.0
1,3,5 trifluoro Benzene			1,2,3,4 trifluoro Benzene			1,2,3,5 trifluoro Benzene			1,2,4,5 trifluoro Benzene		
A ₂ "	847	1.0	A ₂	922	0.5	A ₂	838	0.8	B _{1g}	417	1.0
	664	1.0		717	0.5		(558)	0.0	B _{2g}	835	0.8
	206	1.0		537	0.8		258	1.0		(685)	0.0
E"	858	0.5		374	1.0	B ₁	843	1.0		295	1.0
	595	1.0		169	1.0		706	1.0	A _u	(679)	0.0
	253	1.0	B ₁	802	1.0		610	1.0		(120)	0.0
				596	1.0		368	0.8	B _{3u}	868	1.0
				286	0.8		205	0.8		457	1.0
				154	1.0		139	1.0		194	1.0

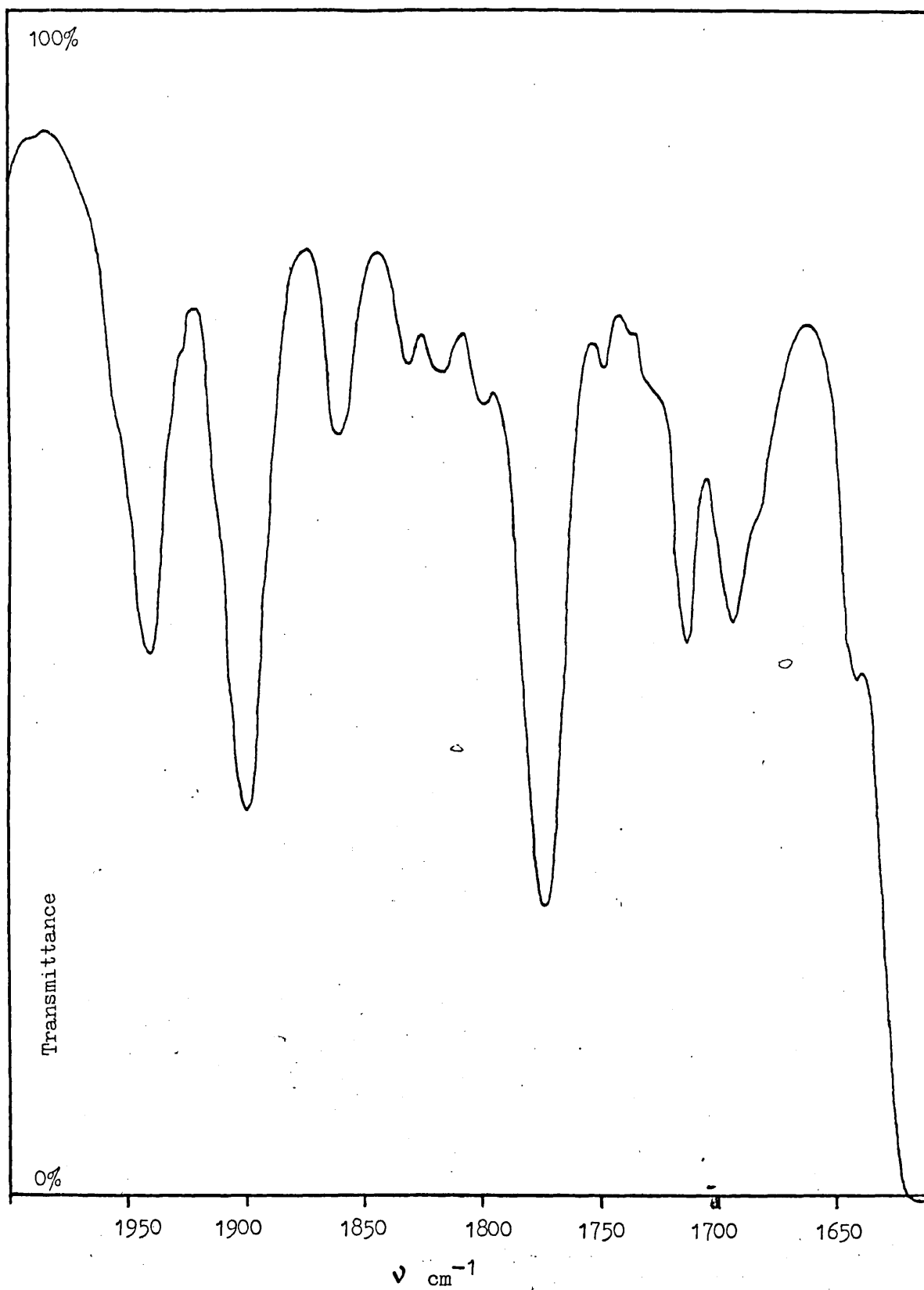
Infra red active combinations

$$\begin{array}{ll}
 A_1 \times A_1 = A_1 & A_1 \times B_1 = B_1 \\
 A_2 \times A_2 = A_1 & A_2 \times B_2 = B_1 \\
 B_1 \times B_1 = A_1 & A_1 \times B_2 = B_2 \\
 B_2 \times B_2 = A_1 & A_2 \times B_1 = B_2
 \end{array}$$

Combination bands possible for Fluoro Benzene in the range 1985 - 1660 cm⁻¹

<u>826</u> + 1156 = 1982	B ₁	* <u>826</u> + <u>997</u> = 1823	B ₂
520 + 1460 = 1980	B ₂	806 + 1009 = 1815	A ₁
<u>754</u> + 1220 = 1974	B ₁	520 + 1290 = 1810	B ₂
* <u>970</u> + <u>997</u> = 1967	B ₂	<u>997</u> + 806 = 1803	B ₁
806 + 1156 = 1962	A ₁ , B ₂	* <u>970</u> + <u>826</u> = 1796	A ₁ } Fermi
* <u>970</u> + <u>970</u> = 1940	A ₁	* <u>894</u> + <u>894</u> = 1788	A ₁ } Resonance?
615 + 1323 = 1938	A ₁	<u>754</u> + 1020 = 1774	B ₁
<u>894</u> + 1020 = 1914	B ₁	615 + 1156 = 1771	A ₁ , B ₂
<u>754</u> + 1156 = 1910	B ₁	<u>754</u> + 1009 = 1763	B ₁
<u>685</u> + 1220 = 1905	B ₁	<u>242</u> + 1499 = 1741	B ₁
615 + 1290 = 1905	A ₁	520 + 1220 = 1740	A ₁
405 + 1499 = 1904	B ₂	<u>405</u> + 1323 = 1728	A ₁ , B ₁
894 + 1009 = 1903	B ₁	* <u>754</u> + 970 = 1724	B ₂ } Fermi
<u>826</u> + 1066 = 1892	B ₁	* <u>826</u> + <u>894</u> = 1720	B ₂ } Resonance?
806 + 1066 = 1872	B ₂	<u>500</u> + 1220 = 1720	B ₁
<u>405</u> + 1460 = 1865	A ₁ , B ₁	<u>685</u> + 1020 = 1705	B ₁
* <u>970</u> + <u>894</u> = 1864	B ₂	<u>894</u> + 806 = 1700	B ₁
520 + 1323 = 1843	B ₂	<u>405</u> + 1290 = 1695	A ₁ , B ₁
<u>685</u> + 1156 = 1841	B ₁	<u>685</u> + 1009 = 1694	B ₁
<u>242</u> + 1597 = 1839	B ₁	615 + 1066 = 1681	A ₁
615 + 1220 = 1835	B ₂	520 + 1156 = 1676	A ₁ , B ₂
806 + 1020 = 1826	A ₁		

Figure 7.2

1,2 DIFLUORO BENZENE

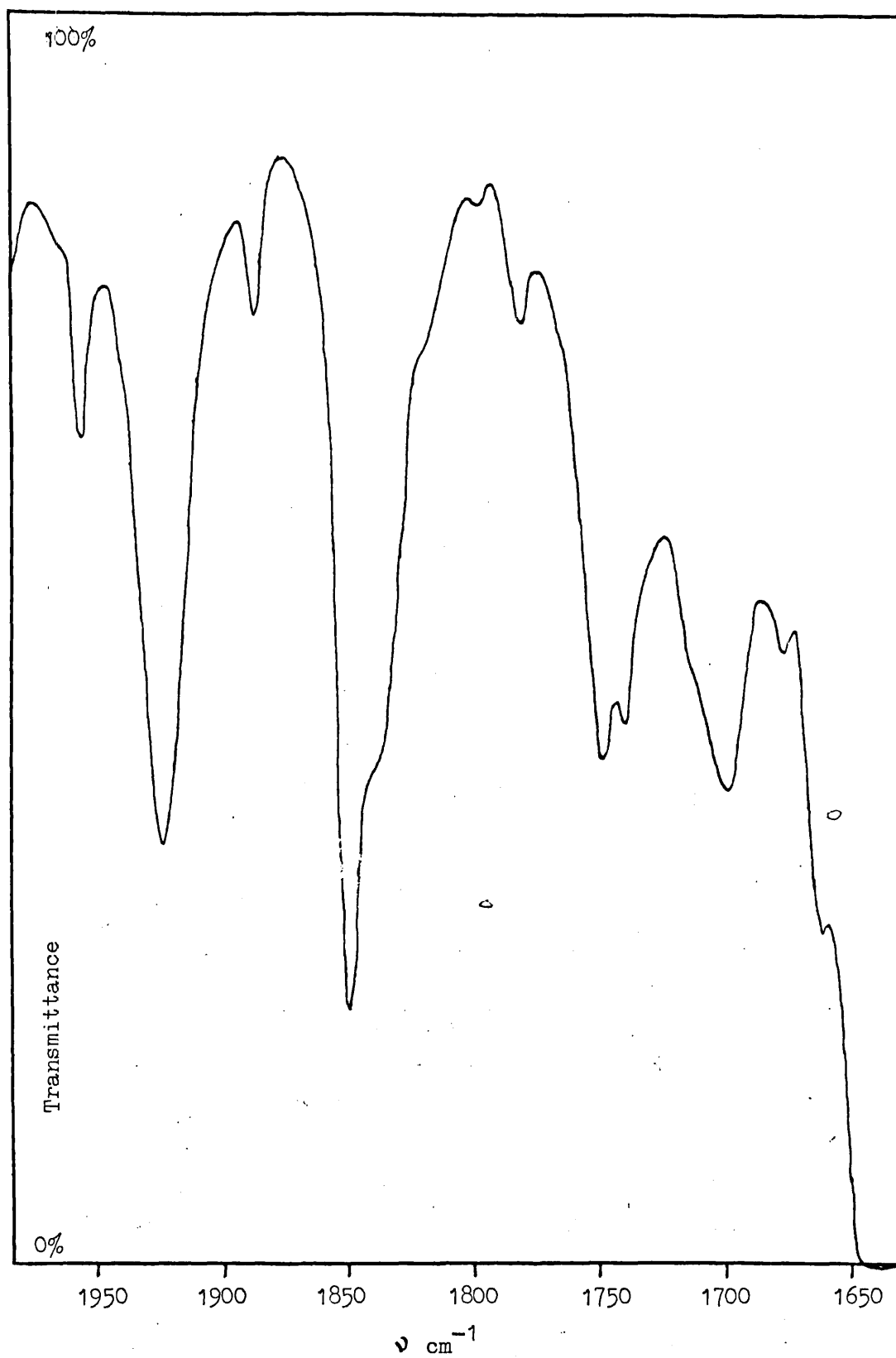
Infra red active combinations

$$\begin{array}{ll}
 A_1 \times A_1 = A_1 & A_1 \times B_1 = B_1 \\
 A_2 \times A_2 = A_1 & A_2 \times B_2 = B_1 \\
 B_1 \times B_1 = A_1 & A_1 \times B_2 = B_2 \\
 B_2 \times B_2 = A_1 & A_2 \times B_1 = B_2
 \end{array}$$

Combination bands possible for 1,2 difluoro Benzene in the range 1965-1660 cm⁻¹

<u>450</u> + 1514 = 1964	B ₁	<u>298</u> + 1514 = 1812	B ₁
* <u>982</u> + <u>982</u> = 1964	A ₁	<u>198</u> + 1609 = 1807	B ₁
857 + 1103 = 1960	A ₁	<u>703</u> + 1103 = 1806	B ₁
440 + 1514 = 1954	B ₂	287 + 1514 = 1801	A ₁
<u>929</u> + 1025 = 1954	B ₁	762 + 1025 = 1787	A ₁
<u>840</u> + 1103 = 1943	B ₁	565 + 1214 = 1779	B ₂
<u>298</u> + 1625 = 1923	B ₁	<u>749</u> + 1025 = 1774	B ₁
<u>703</u> + 1214 = 1917	B ₁	(<u>555</u>) + 1214 = (1769)	B ₁
762 + 1155 = 1917	A ₁	<u>450</u> + 1313 = 1763	B ₁
287 + 1625 = 1912	A ₁	440 + 1313 = 1753	B ₂
* <u>982</u> + <u>929</u> = 1911	B ₂	287 + 1464 = 1751	B ₂
<u>749</u> + 1155 = 1904	B ₁	440 + 1292 = 1732	A ₁
440 + 1464 = 1904	A ₁	* <u>982</u> + <u>749</u> = 1731	B ₂
287 + 1609 = 1896	B ₂	<u>450</u> + 1277 = 1727	B ₁
857 + 1025 = 1882	B ₂	565 + 1155 = 1720	A ₁
565 + 1313 = 1878	A ₁	440 + 1277 = 1717	B ₂
762 + 1103 = 1865	B ₂	857 + 857 = 1714	A ₁
546 + 1313 = 1859	B ₂	546 + 1155 = 1701	B ₂
565 + 1292 = 1857	B ₂	<u>840</u> + 857 = 1697	B ₁
(<u>555</u>) + 1292 = (1847)	B ₁	762 + <u>929</u> = 1691	B ₁
565 + 1277 = 1842	A ₁	* <u>703</u> + <u>982</u> = 1685	A ₁) Fermi
<u>982</u> + 857 = 1839	B ₁	* <u>840</u> + 840 = 1680	A ₁ } Resonance?
546 + 1292 = 1838	A ₁	565 + 1103 = 1668	B ₂
546 + 1277 = 1823	B ₂	<u>198</u> + 1464 = 1662	B ₁
* <u>982</u> + <u>840</u> = 1822	A ₁		

Figure 7.3

1,3 DIFLUORO BENZENE

Infra red active combinations

$$A_1 \times A_1 = A_1 \quad A_1 \times B_1 = B_1$$

$$A_2 \times A_2 = A_1 \quad A_2 \times B_2 = B_1$$

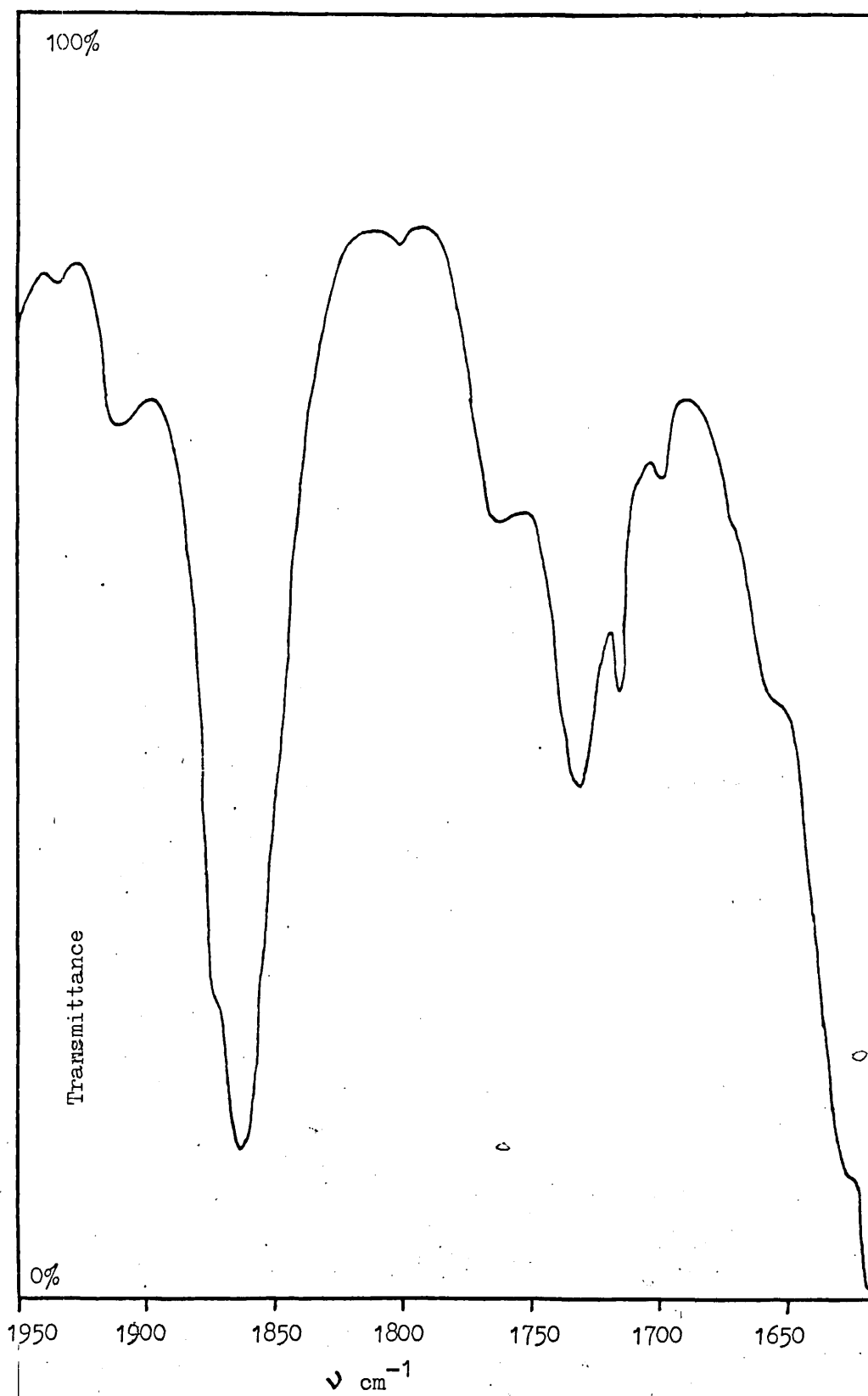
$$B_1 \times B_1 = A_1 \quad A_1 \times B_2 = B_2$$

$$B_2 \times B_2 = A_1 \quad A_2 \times B_1 = B_2$$

Combination bands possible for 1,3 difluoro Benzene in the range1980 - 1680 cm⁻¹

954 + 1008 = 1962	B ₂	735 + 1066 = 1801	A ₁
<u>672</u> + 1286 = 1958	B ₁	514 + 1286 = 1800	B ₂
* <u>978</u> + <u>978</u> = 1956	A ₁	331 + 1456 = 1787	A ₁
331 + 1608 = 1939	A ₁ , B ₂	478 + (1307) = (1785)	A ₁
478 + 1456 = 1934	B ₂	524 + (1260) = (1784)	B ₂
<u>853</u> + 1066 = 1919	B ₁	<u>769</u> + 1008 = 1777	B ₁
<u>458</u> + 1456 = 1914	B ₁	514 + (1260) = 1774	A ₁
954 + 954 = 1908	A ₁	478 + 1286 = 1764	B ₂
<u>599</u> + (1307) = (1906)	B ₁	* <u>879</u> + <u>879</u> = 1758	A ₁
735 + 1158 = 1893	B ₂	599 + 1158 = 1757	B ₁
* <u>879</u> + <u>978</u> = 1875	B ₂	* <u>769</u> + <u>978</u> = 1747	A ₁
853 + 1008 = 1861	B ₁	<u>251</u> + 1493 = 1744	B ₁
<u>599</u> + (1260) = (1859)	B ₁	<u>458</u> + 1286 = 1744	B ₁
<u>251</u> + 1608 = 1859	B ₁	735 + 1008 = 1743	A ₁
735 + 954 = 1858	B ₂	478 + (1260) = (1738)	A ₁
<u>235</u> + 1608 = 1843	B ₁	<u>672</u> + 1066 = 1738	B ₁
<u>769</u> + 1066 = 1835	B ₁	* <u>853</u> + <u>879</u> = 1732	B ₂
<u>879</u> + 954 = 1833	B ₁	<u>599</u> + 1123 = 1722	B ₁
524 + (1307) = (1831)	B ₂	<u>978</u> + 735 = 1713	B ₁
331 + 1493 = 1824	B ₂	* <u>853</u> + <u>853</u> = 1706	A ₁
514 + (1307) = (1821)	A ₁	235 + 1456 = 1691	B ₁
524 + 1286 = 1810	A ₁	735 + 954 = 1689	B ₂

Figure 7.4

1,4 DIFLUORO BENZENE

Infra red active combinations

$$A_{1g} \times B_{1u} = B_{1u}$$

$$A_u \times B_{1g} = B_{1u}$$

$$B_{2g} \times B_{3u} = B_{1u}$$

$$B_{3g} \times B_{2u} = B_{1u}$$

$$A_{1g} \times B_{2u} = B_{2u}$$

$$A_u \times B_{2g} = B_{2u}$$

$$B_{1g} \times B_{3u} = B_{2u}$$

$$B_{3g} \times B_{1u} = B_{2u}$$

$$A_{1g} \times B_{3u} = B_{3u}$$

$$A_u \times B_{3g} = B_{3u}$$

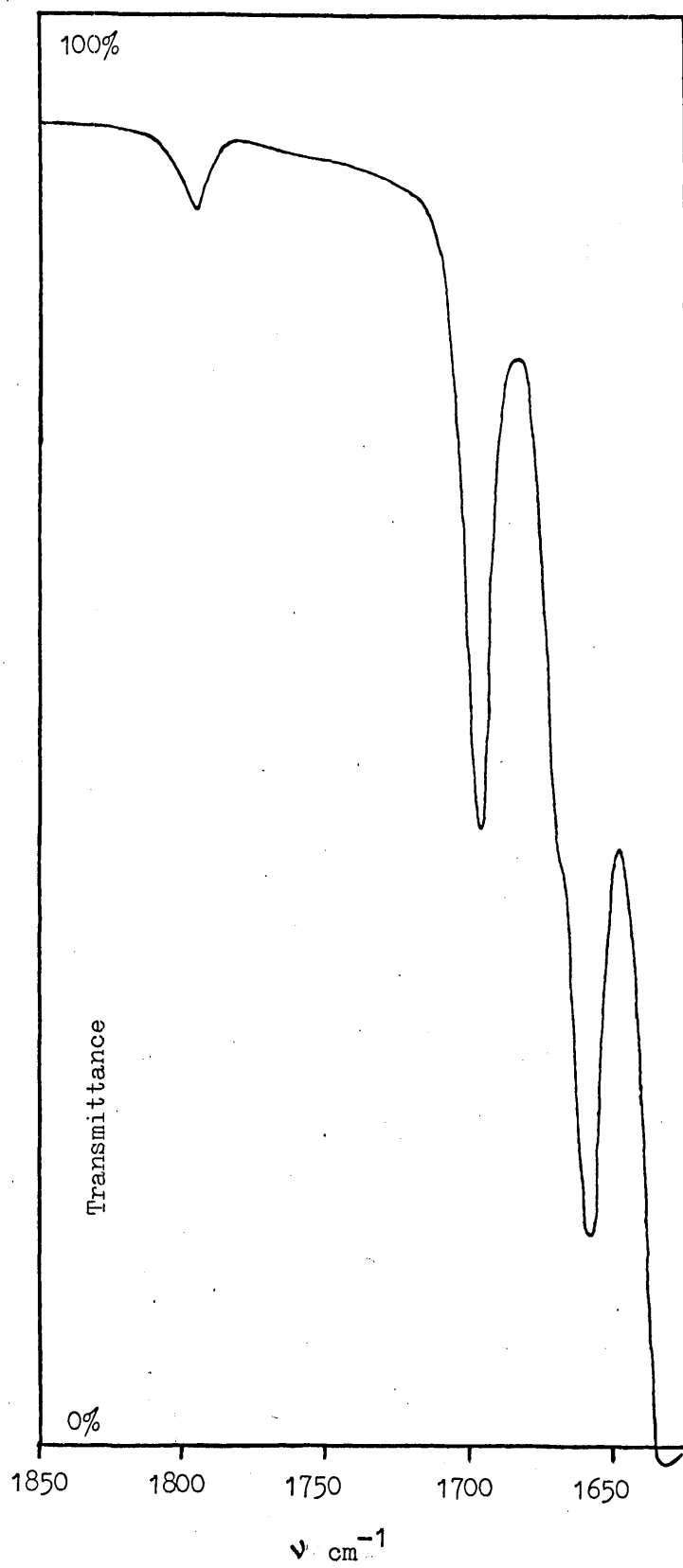
$$B_{1g} \times B_{2u} = B_{3u}$$

$$B_{2g} \times B_{1u} = B_{3u}$$

Combination bands possible for 1,4 difluoro Benzene in the range 1950-1665 cm⁻¹

<u>928</u> + 1012 = 1940	B _{3u}	<u>157</u> + 1617 = 1774	B _{3u}
(849) + 1083 = (1932)	B _{2u}	* <u>836</u> + <u>928</u> = 1764	B _{1u}
<u>692</u> + 1225 = 1917	B _{3u}	<u>508</u> + 1245 = 1753	B _{3u}
<u>375</u> + 1511 = 1886	B _{3u}	* <u>800</u> + <u>943</u> = 1743	B _{1u}
<u>800</u> + 1083 = 1883	B _{3u}	(451) + 1285 = (1736)	B _{2u} , B _{1u}
740 + 1142 = 1882	B _{1u}	635 + 1083 = 1718	B _{1u}
(451) + 1425 = (1876)	B _{1u} , B _{2u}	<u>692</u> + 1012 = 1704	B _{3u}
* <u>928</u> + <u>943</u> = 1871	B _{2u}	405 + 1285 = 1690	B _{3u}
(849) + 1012 = (1861)	B _{1u}	<u>836</u> + (849) = (1685)	B _{3u}
635 + 1225 = (1860)	B _{2u}		

Figure 7.5

1,3,5 TRIFLUORO BENZENE

Infra red active combinations

$$A_1' \times A_2'' = A_2''$$

$$A_1' \times E' = E'$$

$$A_2' \times E' = E'$$

$$A_2'' \times E'' = E''$$

$$E' \times E'' = E'' + A_1'' + A_2''$$

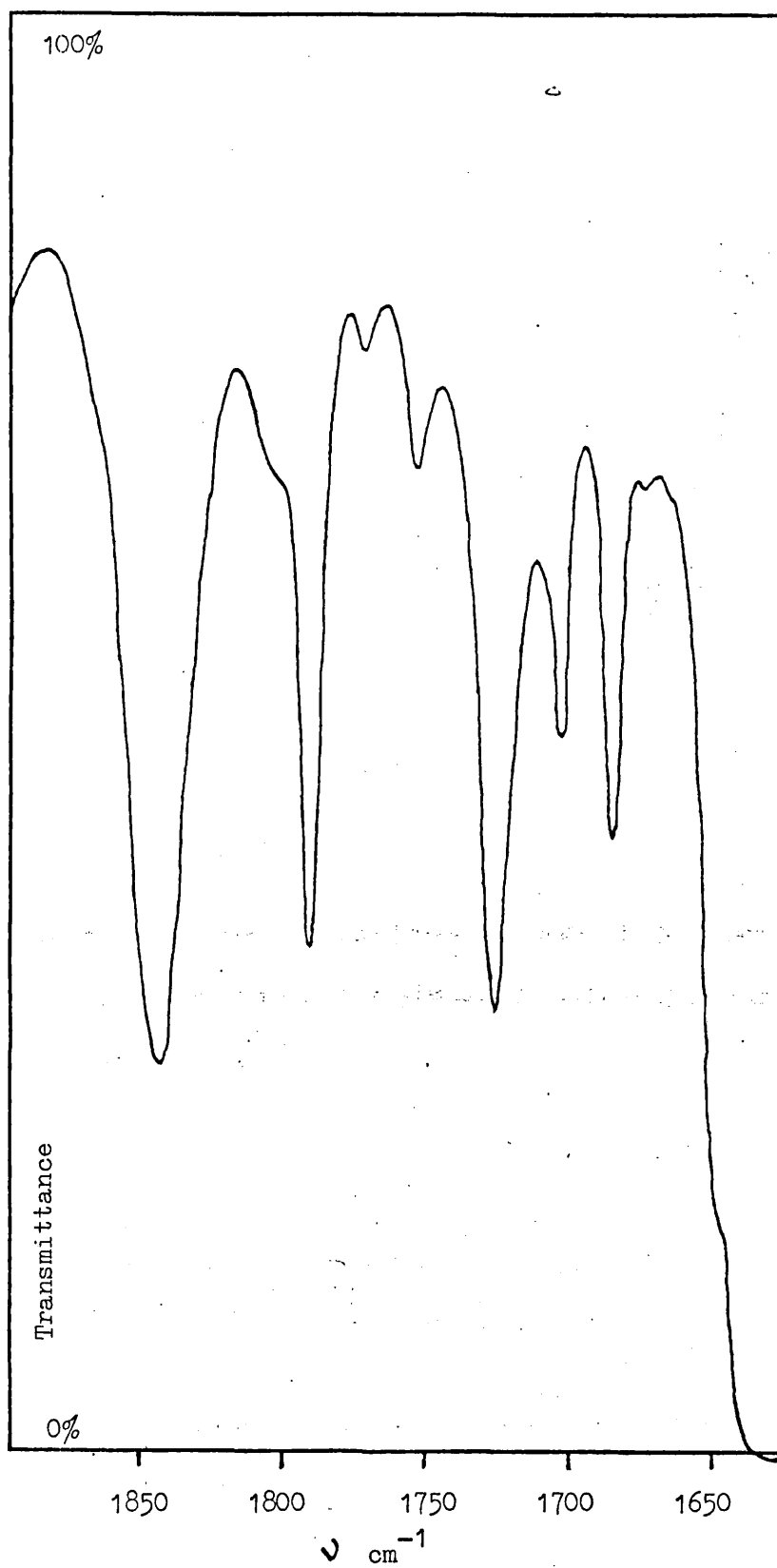
$$E'' \times E'' = E' + A_1' + A_2'$$

$$E' \times E' = E' + A_1' + A_2'$$

Combination bands possible for 1,3,5 trifluoro Benzene in the range1820 - 1620 cm⁻¹

326 + 1475 = 1801	E' + A ₁ ' + A ₂ '
500 + (1300) = (1800)	E'
<u>253</u> + 1475 = 1728	E'' + A ₁ '' + A ₂ ''
<u>595</u> + 1122 = 1717	E'' + A ₁ '' + A ₂ ''
* (<u>858</u>) + (<u>858</u>) = (1716)	E' + A ₁ ' + A ₂ '
* <u>847</u> + (<u>858</u>) = (1705)	E'
578 + 1122 = 1700	E'
500 + 1180 = 1680	E'
326 + 1350 = 1676	E'
<u>664</u> + 1010 = 1674	A ₂ ''

Figure 7.6

1,2,3,4 TETRAFLUORO BENZENE

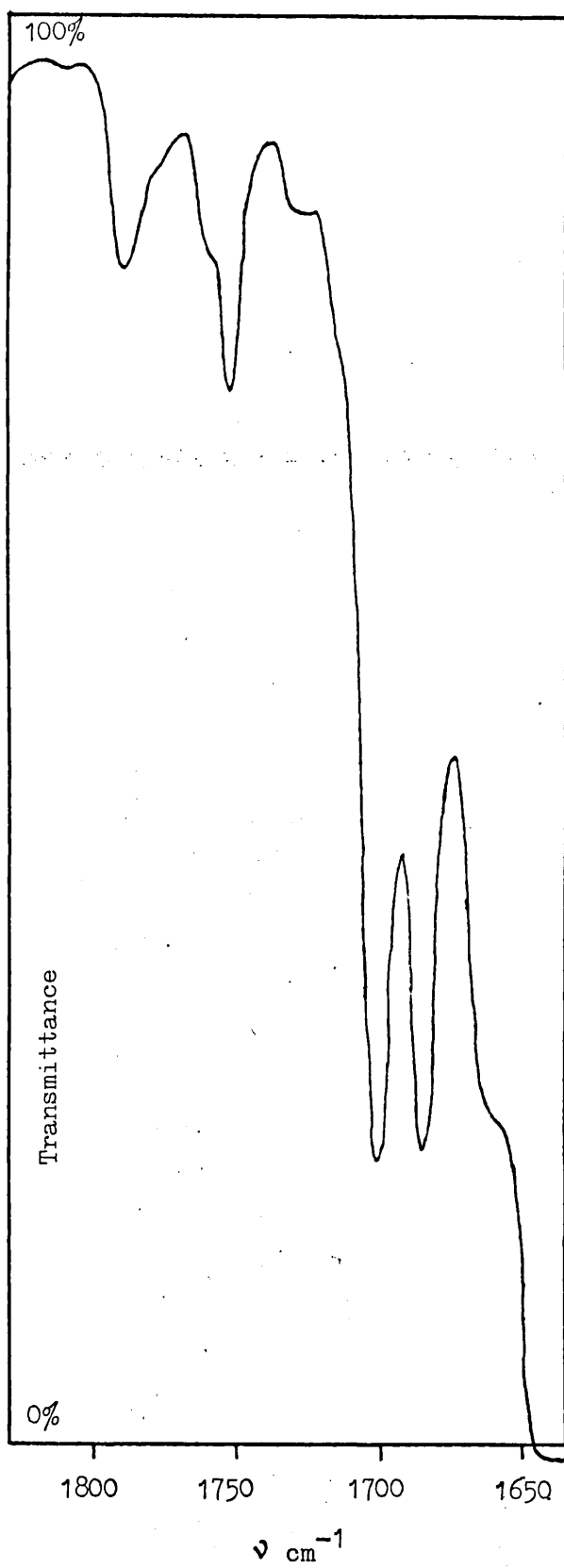
Infra red active combinations

$$\begin{array}{ll}
 A_1 \times A_1 = A_1 & A_1 \times B_1 = B_1 \\
 A_2 \times A_2 = A_1 & A_2 \times B_2 = B_1 \\
 B_1 \times B_1 = A_1 & A_1 \times B_2 = B_2 \\
 B_2 \times B_2 = A_1 & A_2 \times B_1 = B_2
 \end{array}$$

Combination bands possible for 1,2,3,4 tetrafluoro Benzene in the range1880 - 1670 cm⁻¹

604 + 1271 = 1875	B ₂	(537) + 1243 = (1780)	B ₁
<u>596</u> + 1271 = 1867	B ₁	604 + 1165 = 1769	B ₂
<u>802</u> + 1050 = 1852	B ₁	490 + 1278 = 1768	A ₁
684 + 1165 = 1849	A ₁	<u>596</u> + 1165 = 1761	B ₁
604 + 1243 = 1847	A ₁	490 + 1271 = 1761	B ₂
*(<u>922</u>) + (<u>922</u>) = (1844)	A ₁	748 + 991 = 1739	A ₁
325 + 1517 = 1842	B ₂	458 + 1278 = 1736	B ₂
490 + 1331 = 1821	B ₂	684 + 1050 = 1734	A ₁
291 + 1525 = 1816	B ₂	490 + 1243 = 1733	A ₁
(537) + 1278 = (1815)	B ₁	458 + 1271 = 1729	A ₁
(<u>286</u>) + 1525 = (1811)	B ₁	* <u>802</u> + (<u>922</u>) = (1724)	B ₂
291 + 1517 = 1808	A ₁	(<u>717</u>) + 991 = (1708)	B ₁
279 + 1525 = 1804	A ₁	458 + 1243 = 1701	B ₂
169 + 1634 = 1803	B ₁	<u>169</u> + 1517 = 1686	B ₁
748 + 1050 = 1798	B ₂	<u>154</u> + 1525 = 1679	B ₁
279 + 1517 = 1796	B ₂	684 + 991 = 1675	B ₂
458 + 1331 = 1789	A ₁	748 + (<u>922</u>) = (1670)	B ₁
<u>154</u> + 1634 = 1788	B ₁		

Figure 7.7

1,2,3,5 TETRAFLUORO BENZENE

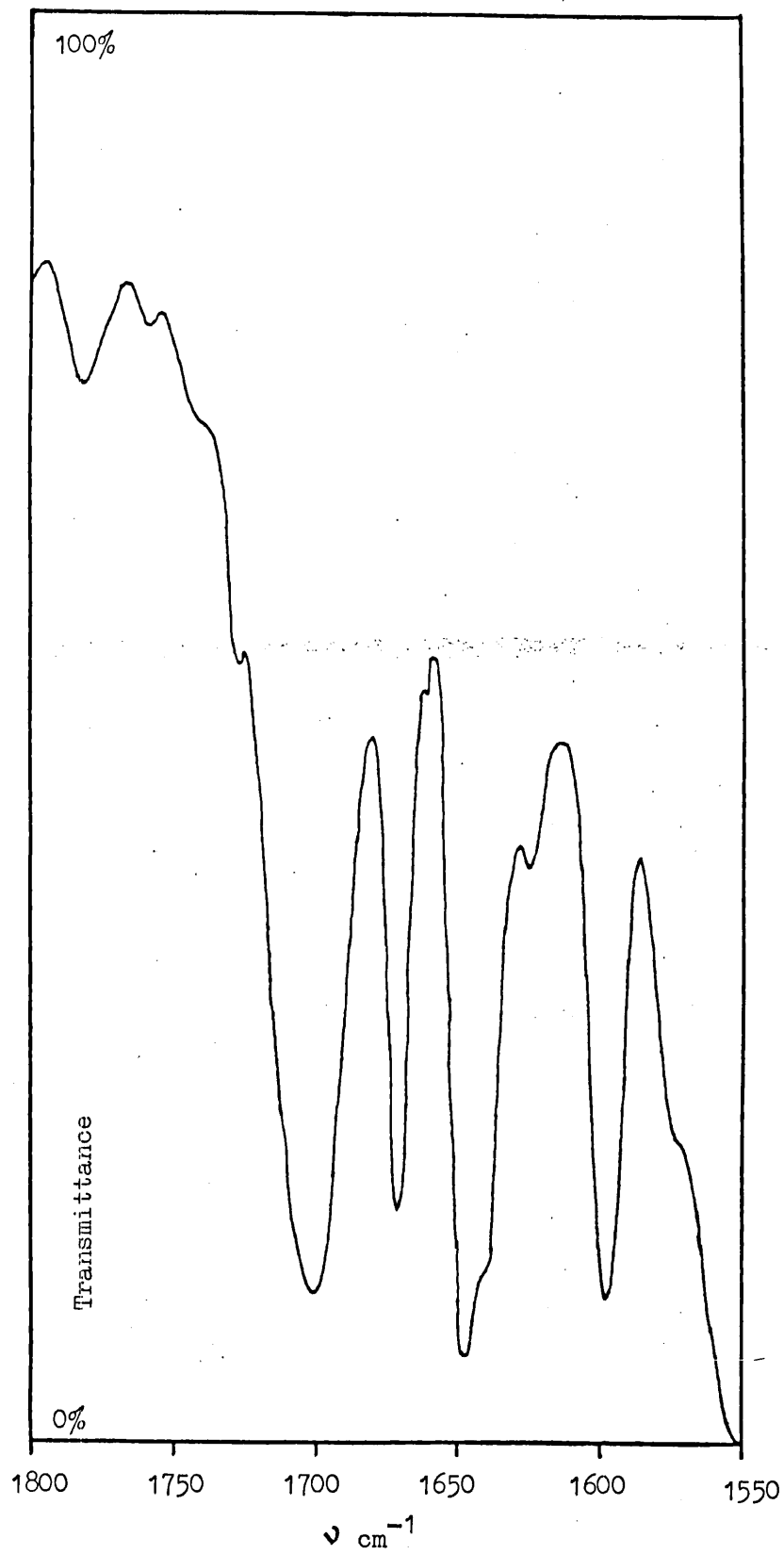
Infra red active combinations

$$\begin{array}{ll}
 A_1 \times A_1 = A_1 & A_1 \times B_1 = B_1 \\
 A_2 \times A_2 = A_1 & A_2 \times B_2 = B_1 \\
 B_1 \times B_1 = A_1 & A_1 \times B_2 = B_2 \\
 B_2 \times B_2 = A_1 & A_2 \times B_1 = B_2
 \end{array}$$

Combination bands possible for 1,2,3,5 tetrafluoro Benzene in the range1810 - 1680 cm⁻¹

(277) + 1531 = (1808)	B ₂	(558) + 1179 = (1737)	B ₁
334 + 1466 = 1800	A ₁	(205) + 1531 = (1736)	B ₁
788 + 1002 = 1790	A ₁	<u>258</u> + 1466 = 1724	B ₁
<u>139</u> + 1642 = 1781	B ₁	445 + 1273 = 1718	B ₂
505 + 1273 = 1778	A ₁	334 + 1384 = 1718	B ₂
310 + 1466 = 1776	B ₂	578 + 1130 = 1708	A ₁
638 + 1130 = 1768	B ₂	638 + 1056 = 1694	A ₁
578 + 1179 = 1757	B ₂	310 + 1384 = 1694	A ₁
(<u>368</u>) + 1384 = (1752)	B ₁	445 + 1247 = 1692	A ₁
505 + 1247 = 1752	B ₂	* <u>843</u> + <u>843</u> = 1686	A ₁
(297) + 1466 = (1743)	A ₁	505 + 1179 = 1684	A ₁
<u>610</u> + 1130 = 1740	B ₁	*(<u>838</u>) + <u>843</u> = 1681	B ₁

Figure 7.8

1,2,4,5 TETRAFLUORO BENZENE

Infra red active combinations

$$A_{1g} \times B_{1u} = B_{1u} \quad B_{1g} \times B_{3u} = B_{2u}$$

$$A_u \times B_{1g} = B_{1u} \quad B_{3g} \times B_{1u} = B_{2u}$$

$$B_{2g} \times B_{3u} = B_{1u} \quad A_{1g} \times B_{3u} = B_{3u}$$

$$B_{3g} \times B_{2u} = B_{1u} \quad A_u \times B_{3g} = B_{3u}$$

$$A_{1g} \times B_{2u} = B_{2u} \quad B_{1g} \times B_{2u} = B_{3u}$$

$$A_u \times B_{2g} = B_{2u} \quad B_{2g} \times B_{1u} = B_{3u}$$

Combination bands possible for 1,2,4,5 tetrafluoro Benzene in the range1800 - 1670 cm⁻¹

$$637 + 1161 = 1798 \quad B_{2u}$$

$$487 + 1127 = 1764 \quad B_{1u}$$

$$(120) + (1625) = (1745) \quad B_{3u}$$

$$346 + 1374 = 1720 \quad B_{2u}$$

$$280 + 1435 = 1715 \quad B_{2u}$$

$$487 + 1224 = 1711 \quad B_{2u}$$

$$*(835) + \underline{868} = 1703 \quad B_{1u}$$

$$418 + 1277 = 1695 \quad B_{2u}$$

$$*(835) + 853 = 1688 \quad B_{3u}$$

$$299 + 1374 = 1673 \quad B_{1u}$$

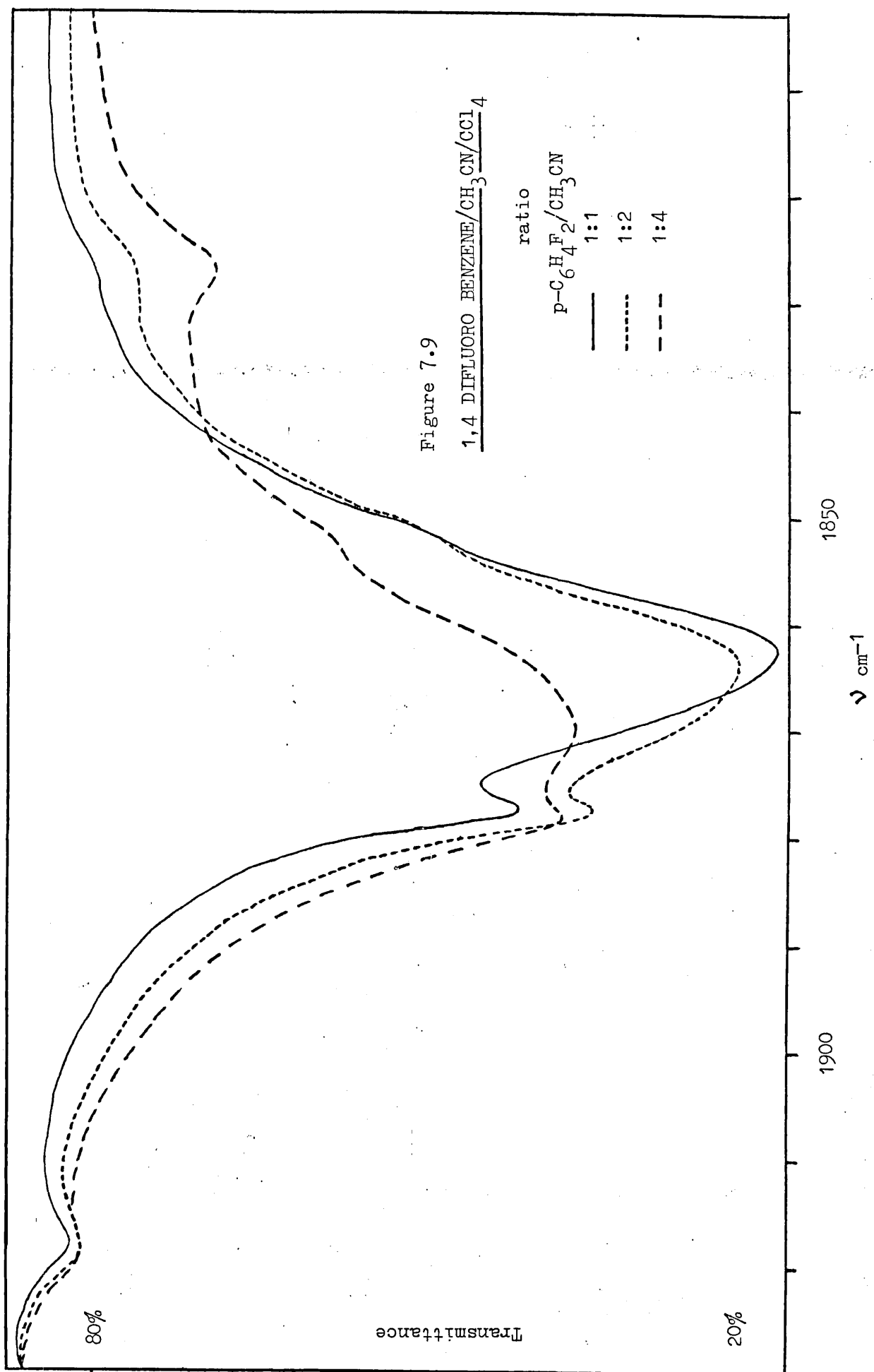
Of the eight molecules investigated, 1,4 difluoro Benzene appeared to be the most suitable for further study.

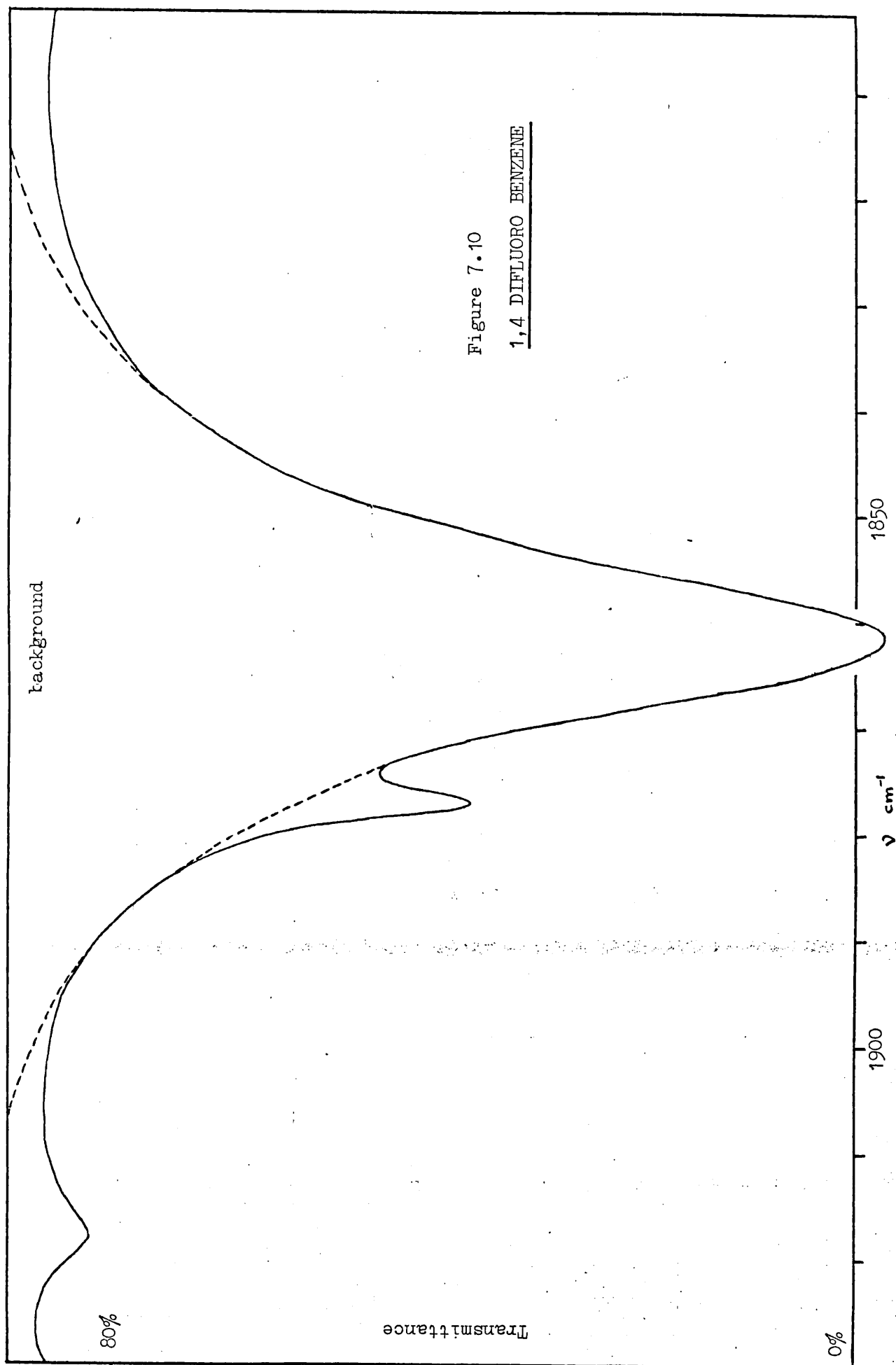
There are three γ_{CH} combination bands, but that at 1631.5 cm^{-1} was not studied very carefully because addition of CH_3CN at different concentrations did not cause the band to shift. The effects of CH_3CN on the other two bands are shown in Figures 7.9 and 7.11, which illustrate the excellence of this technique for picking out those bands which arise from a γ_{CH} deformation.

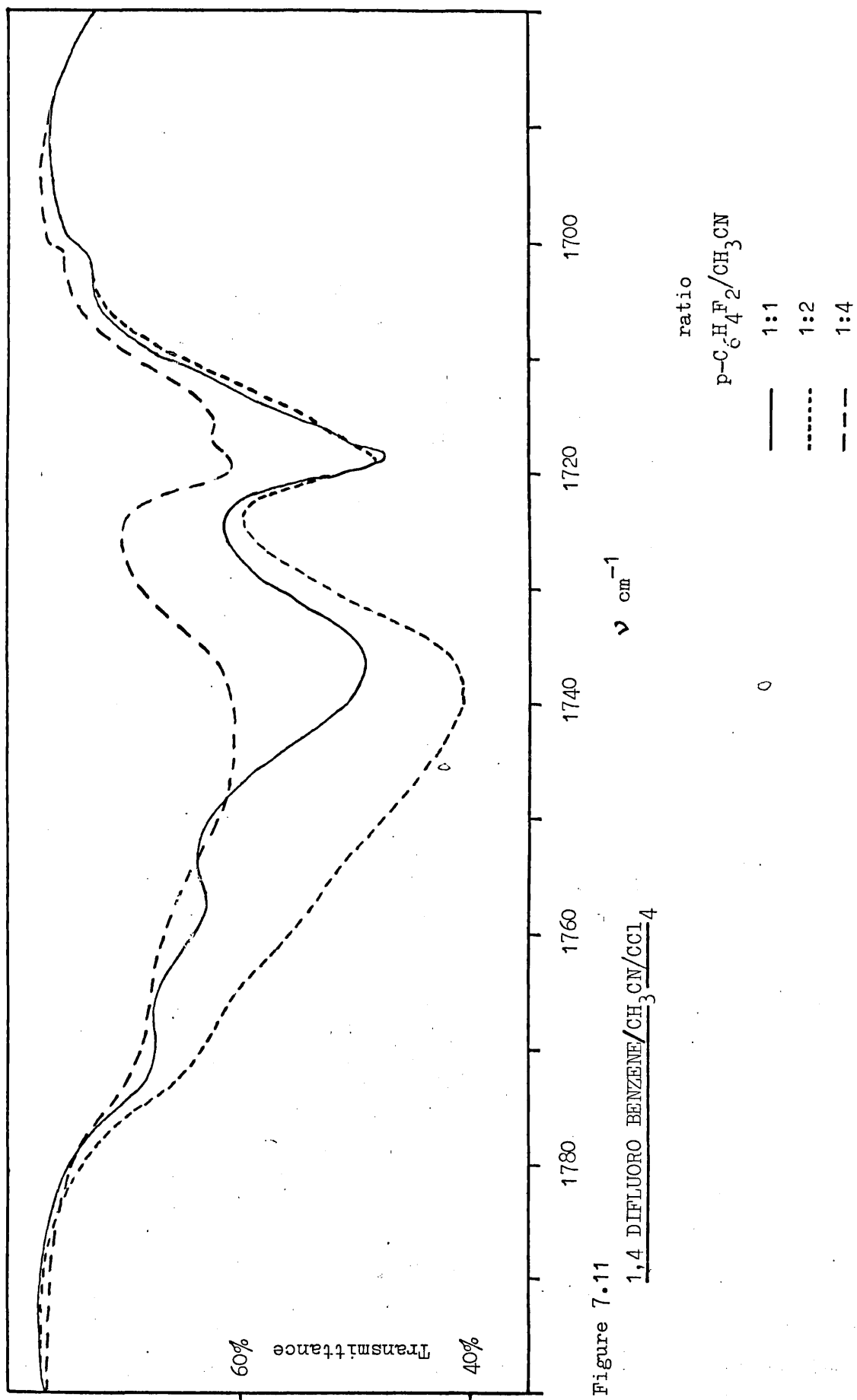
The intensities of these two bands were measured

- a) in the liquid phase, at two concentrations
- b) in the gas phase.

If the shoulder at 1877 cm^{-1} is "drawn-out", and the wings extrapolated as shown [Figure 7.10], the band at 1862 cm^{-1} can be "drawn" to approximately Gaussian form. Since intensity is a function of $\log(I_0/I)$, and the ratio of the value of $\log(I_0/I)$ at the band maximum to that at the experimentally observed wings (NOT the "drawn-in" wings) is high, this is a good approximation. The same approach cannot be employed with such confidence for the band at 1736 cm^{-1} . Because its absorption is very much weaker than that of the band at 1862 cm^{-1} , the ratio of the value of $\log(I_0/I)$ at the band maximum, and at the wings is too small for "drawing-out" of bands to be feasible. [Figure 7.12]. Indeed, in the gas phase spectrum, it is extremely difficult to "draw-out" the absorption at 1772 cm^{-1} , so it was included in the computation of the intensity.







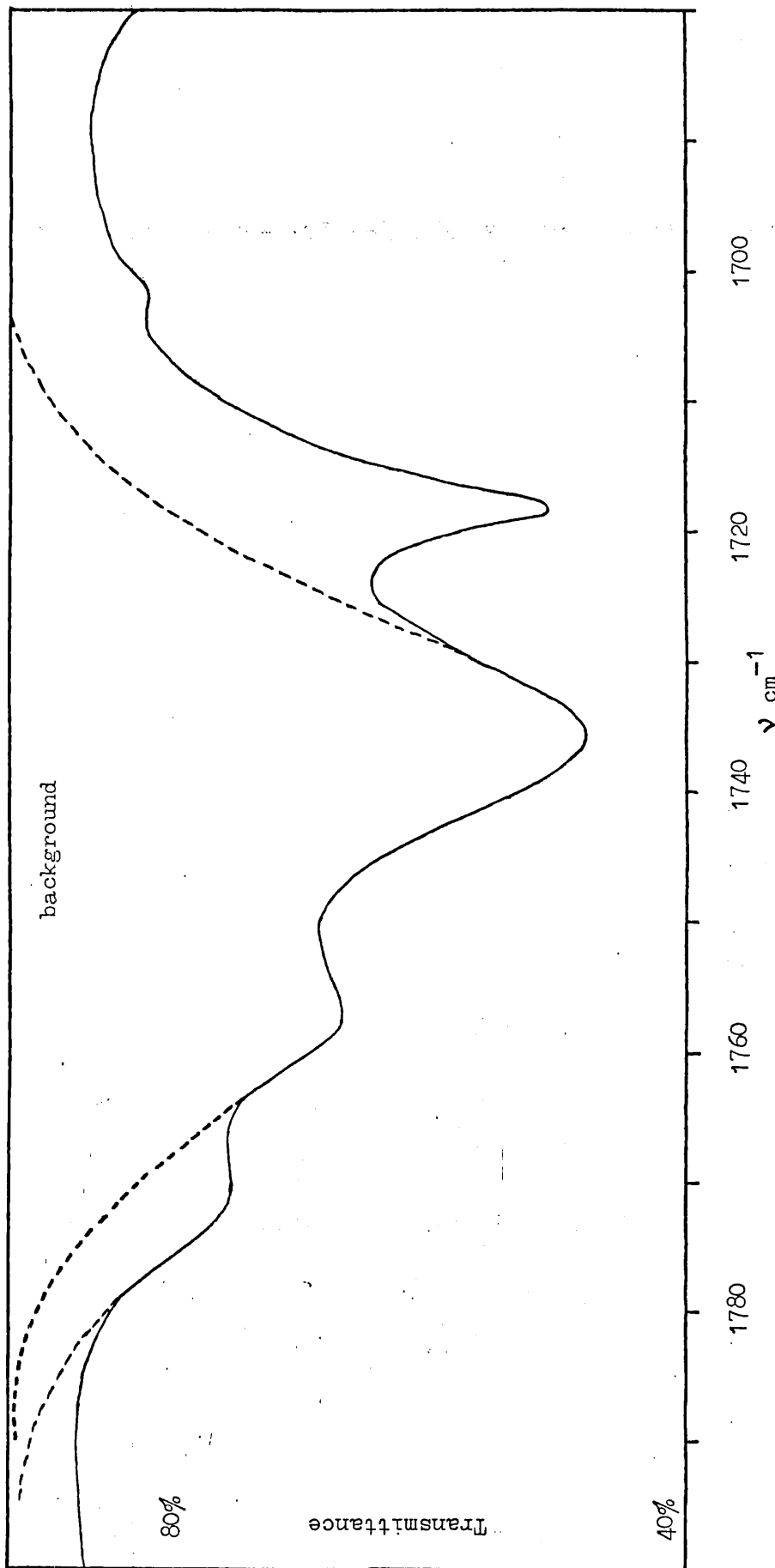


Figure 7.12 1,4 DIFLUORO BENZENE

Table 7.2

The absolute intensity of the 1862 cm^{-1} band of 1,4 difluoro Benzene

	Concentration moles cm^{-3}	$\text{mole}^{-1} \text{cm}^2$
CCl_4 (1)	1.167×10^{-3}	380.2
CCl_4 (2)	1.226×10^{-3}	353.3
gas	3.521×10^{-6}	300.0

Table 7.3

The absolute intensity of the 1736 and 1757.5 cm^{-1} bands of 1,4 difluoro Benzene

	Concentration moles cm^{-3}	$\text{mole}^{-1} \text{cm}^2$
CCl_4 (1)	1.167×10^{-3}	169.1
CCl_4 (2)	1.226×10^{-3}	182.9

Table 7.4

The absolute intensity of the 1736, 1757.5 and 1772 cm^{-1} bands of 1,4 difluoro Benzene

	Concentration moles cm^{-3}	$\text{mole}^{-1} \text{cm}^2$
CCl_4 (1)	1.167×10^{-3}	231.1
gas	3.521×10^{-6}	158.8

Table 7.5

The absolute intensity of the 1631.5 cm⁻¹ band of 1,4 difluoro Benzene

	Concentration moles cm ⁻³	mole ⁻¹ cm ²
CCl ₄ (1)	1.190 x 10 ⁻³	392.7
gas	3.521 x 10 ⁻⁶	272.8

Whilst the absolute intensity measurements are useless for estimation of bond moments and bond moment derivatives, they do give an idea of the magnitude.

The work done so far indicates that less information is available than one would have hoped. Thus the number of second derivatives of the dipole-moment function which can be retained is limited. I would suggest that important terms are

$$\left(\frac{\partial \mu}{\partial \sigma_i^H}\right)_{HH}^2$$

$$\left(\frac{\partial \mu}{\partial \sigma_i^H}\right)_{HF}^2$$

$$\left(\frac{\partial \mu}{\partial \sigma_i^H}\right)_{FF}^2$$

$$\left(\frac{\partial^2 \mu}{\partial \sigma_i^H \partial \sigma_{i+1}^H}\right)$$

$$\left(\frac{\partial^2 \mu}{\partial \sigma_i^H \partial \sigma_{i+2}^H}\right)$$

Section 7.4 is designed to show that the terrifying symbolism introduced in Section 7.2 is actually very simple to understand when translated into real numbers.

Section 7.4 Computation of

$$\left(\frac{\partial^2 \mu}{\partial Q_i \partial Q_j} \right)$$

For a combination band

$$\text{band area/molecule} = \frac{h}{24\pi c} \frac{\nu_i + \nu_j}{\nu_i \nu_j} \left(\frac{\partial^2 \mu}{\partial Q_i \partial Q_j} \right)^2$$

where

$$\frac{\partial^2 \mu}{\partial Q_i \partial Q_j} = \sum_{m,n} l_{i,m} l_{j,n} \left(\frac{\partial^2 \mu}{\partial S_m \partial S_n} \right)$$

We need L, a square matrix whose i, j^{th} element is $l_{i,j}$, the coefficient which relates the change in the i^{th} internal coordinate with the j^{th} normal coordinate. The normal coordinate calculations yield Ψ , the eigen vector matrix in symmetry coordinates. The two are related by $L = U^t \Psi$

The second derivative of the dipole moment function can be resolved along the x and y axes.

$$\frac{\partial^2 \mu_x}{\partial Q_i \partial Q_j} = L_m^t M \begin{pmatrix} x \end{pmatrix} L_n$$

$$\frac{\partial^2 \mu_y}{\partial Q_i \partial Q_j} = L_m^t M \begin{pmatrix} y \end{pmatrix} L_n$$

Consider the band at 1862 cm^{-1} in 1,4 difluoro Benzene.

$$B_{2g} + A_u = B_{2u}$$

$$928 + 943 = 1871$$

Firstly, L is computed from Ψ and U.

Symmetry Coordinates for the Out-of-Plane Vibrations of 1,4 difluoro Benzene

B_{1g}

$$\gamma_2 + \gamma_3 - \gamma_5 - \gamma_6$$

$$\phi_1 - \phi_3 - \phi_4 + \phi_6$$

B_{2g}

$$\gamma_1 - \gamma_4$$

$$\gamma_2 - \gamma_3 - \gamma_5 + \gamma_6$$

$$\phi_1 + \phi_3 - \phi_4 - \phi_6$$

$$\phi_2 + \phi_5$$

A_u

$$\gamma_2 - \gamma_3 + \gamma_5 - \gamma_6$$

$$\phi_1 + \phi_3 + \phi_4 + \phi_6$$

B_{3u}

$$\gamma_1 + \gamma_4$$

$$\gamma_2 + \gamma_3 + \gamma_5 + \gamma_6$$

$$\phi_1 - \phi_3 + \phi_4 - \phi_6$$

$$\phi_2 - \phi_5$$

U Matrices for 1,4 difluoro Benzene

B_{1g}

$$\begin{array}{c} \left| \begin{array}{cccccc} 0 & \frac{1}{2} & \frac{1}{2} & 0 & -\frac{1}{2} & -\frac{1}{2} \\ \frac{1}{2} & 0 & -\frac{1}{2} & -\frac{1}{2} & 0 & \frac{1}{2} \end{array} \right| \end{array}$$

B_{2g}

$$\begin{array}{c} \left| \begin{array}{cccccc} \frac{1}{2} & 0 & 0 & -\frac{1}{2} & 0 & 0 \\ 0 & \frac{1}{2} & -\frac{1}{2} & 0 & \frac{1}{2} & -\frac{1}{2} \\ 0 & \frac{1}{2} & 0 & 0 & -\frac{1}{2} & 0 \\ \frac{1}{2} & 0 & \frac{1}{2} & -\frac{1}{2} & 0 & -\frac{1}{2} \end{array} \right| \end{array}$$

A_u

$$\begin{array}{c} \left| \begin{array}{cccccc} 0 & \frac{1}{2} & -\frac{1}{2} & 0 & \frac{1}{2} & -\frac{1}{2} \\ 0 & \frac{1}{2} & 0 & 0 & \frac{1}{2} & 0 \\ \frac{1}{2} & 0 & \frac{1}{2} & 0 & 0 & \frac{1}{2} \end{array} \right| \end{array}$$

B_{3u}

$$\begin{array}{c} \left| \begin{array}{cccccc} \frac{1}{2} & 0 & 0 & -\frac{1}{2} & 0 & 0 \\ 0 & \frac{1}{2} & \frac{1}{2} & 0 & \frac{1}{2} & -\frac{1}{2} \\ \frac{1}{2} & 0 & -\frac{1}{2} & \frac{1}{2} & 0 & -\frac{1}{2} \end{array} \right| \end{array}$$

Matrices for 1,4 difluoro BenzeneB_{1g}

$$\begin{vmatrix} -1.1203 & 0.0 \\ 1.6647 & 0.0 \end{vmatrix}$$

B_{2g}

$$\begin{vmatrix} -.3127 & -.8104 & .3542 & 0.0 \\ 1.3612 & .3430 & .2147 & 0.0 \\ 1.7873 & -1.2832 & .0509 & 0.0 \\ -1.0528 & .9043 & .8678 & 0.0 \end{vmatrix}$$

A_u

$$\begin{vmatrix} 1.3499 & .3060 & 0.0 \\ 1.8603 & -.9689 & 0.0 \\ -1.3154 & .6851 & 0.0 \end{vmatrix}$$

B_{3u}

$$\begin{vmatrix} .6201 & .7012 & .0610 \\ -1.1129 & .3226 & .1135 \\ 1.1784 & -.8603 & .4836 \end{vmatrix}$$

DIRECTION COSINES MATRICES μ_x

	γ_1	γ_2	γ_3	γ_4	γ_5	γ_6
γ_1	0	$\frac{1}{2}$	$\frac{\sqrt{3}}{2}$	0	$-\frac{\sqrt{3}}{2}$	$-\frac{1}{2}$
γ_2		$\frac{\sqrt{3}}{2}$	1	$\frac{\sqrt{3}}{2}$	0	0
γ_3			$\frac{\sqrt{3}}{2}$	$\frac{1}{2}$	0	0
γ_4				0	$-\frac{1}{2}$	$-\frac{\sqrt{3}}{2}$
γ_5					$-\frac{\sqrt{3}}{2}$	-1
γ_6						$-\frac{\sqrt{3}}{2}$

 μ_y

	γ_1	γ_2	γ_3	γ_4	γ_5	γ_6
γ_1	1	$\frac{\sqrt{3}}{2}$	$\frac{1}{2}$	0	$\frac{1}{2}$	$\frac{\sqrt{3}}{2}$
γ_2		$\frac{1}{2}$	0	$-\frac{1}{2}$	0	1
γ_3			$-\frac{1}{2}$	$\frac{\sqrt{3}}{2}$	-1	0
γ_4				-1	$-\frac{\sqrt{3}}{2}$	$-\frac{1}{2}$
γ_5					$-\frac{1}{2}$	0
γ_6						$\frac{1}{2}$

1,4 DIFLUORO BENZENE - M MATRICES

	δ_{F_1}	δ_{H_2}	δ_{H_3}	δ_{F_4}	δ_{H_5}	δ_{H_6}
δ_{F_1}	$\frac{\delta^2}{\delta\delta_F^2}$	$\frac{\delta^2}{\delta\delta_F\delta\delta_{H_0}}$	$\frac{\delta^2}{\delta\delta_F\delta\delta_{H_m}}$	$\frac{\delta^2}{\delta\delta_F\delta\delta_{F_p}}$	$\frac{\delta^2}{\delta\delta_F\delta\delta_{H_m}}$	$\frac{\delta^2}{\delta\delta_F\delta\delta_{H_0}}$
δ_{H_2}		$\frac{\delta^2}{\delta\delta_H^2}$	$\frac{\delta^2}{\delta\delta_H\delta\delta_{H_0}}$	$\frac{\delta^2}{\delta\delta_F\delta\delta_{H_m}}$	$\frac{\delta^2}{\delta\delta_H\delta\delta_{H_p}}$	$\frac{\delta^2}{\delta\delta_H\delta\delta_{H_m}}$
δ_{H_3}			$\frac{\delta^2}{\delta\delta_H^2}$	$\frac{\delta^2}{\delta\delta_F\delta\delta_{H_0}}$	$\frac{\delta^2}{\delta\delta_H\delta\delta_{H_m}}$	$\frac{\delta^2}{\delta\delta_H\delta\delta_{H_p}}$
δ_{F_4}				$\frac{\delta^2}{\delta\delta_F^2}$	$\frac{\delta^2}{\delta\delta_F\delta\delta_{H_0}}$	$\frac{\delta^2}{\delta\delta_F\delta\delta_{H_m}}$
δ_{H_5}					$\frac{\delta^2}{\delta\delta_H^2}$	$\frac{\delta^2}{\delta\delta_H\delta\delta_{H_0}}$
δ_{H_6}						$\frac{\delta^2}{\delta\delta_H^2}$

	δ_{F_1}	δ_{H_2}	δ_{H_3}	δ_{F_4}	δ_{H_5}	δ_{H_6}
δ_{F_1}	7	6	7	7	7	6
δ_{H_2}		2	4	7	7	5
δ_{H_3}			2	6	5	7
δ_{F_4}				7	6	7
δ_{H_5}					2	4
δ_{H_6}						2

$$L_{B_{2g}} = \begin{bmatrix} \cdot & 0 & \cdot & \cdot \\ \cdot & \frac{1}{2} & \cdot & \cdot \\ \cdot & -\frac{1}{2} & \cdot & \cdot \\ \cdot & 0 & \cdot & \cdot \\ \cdot & -\frac{1}{2} & \cdot & \cdot \\ \cdot & \frac{1}{2} & \cdot & \cdot \end{bmatrix} \begin{bmatrix} -0.3127 & \cdot & \cdot & \cdot \\ 1.3612 & \cdot & \cdot & \cdot \\ 1.7873 & \cdot & \cdot & \cdot \\ -1.0528 & \cdot & \cdot & \cdot \end{bmatrix} = \begin{bmatrix} 0 \\ .675 \\ -.675 \\ 0 \\ .675 \\ -.675 \end{bmatrix}$$

$$L_{Au} = \begin{bmatrix} 0 & \cdot & \cdot \\ \frac{1}{2} & \cdot & \cdot \\ -\frac{1}{2} & \cdot & \cdot \\ 0 & \cdot & \cdot \\ \frac{1}{2} & \cdot & \cdot \\ -\frac{1}{2} & \cdot & \cdot \end{bmatrix} \begin{bmatrix} 1.3499 & \cdot & \cdot \\ 1.8603 & \cdot & \cdot \\ -1.3154 & \cdot & \cdot \end{bmatrix} = \begin{bmatrix} 0 \\ .675 \\ -.675 \\ 0 \\ .675 \\ -.675 \end{bmatrix}$$

Instead of writing out the coefficients of the second derivatives of the dipole moment function in full each time, it is convenient to refer to them by numbers

$$\left(\frac{\partial \mu}{\partial \gamma_i^H} \right)_{HH} \quad 1$$

$$\left(\frac{\partial \mu}{\partial \gamma_i^H} \right)_{HF} \quad 2$$

$$\left(\frac{\partial \mu}{\partial \gamma_i^H} \right)_{FF} \quad 3$$

$$\left(\frac{\partial^2 \mu}{\partial \gamma_i^H \partial \gamma_{i+1}^H} \right) \quad 4$$

$$\left(\frac{\partial^2 \mu}{\partial \gamma_i^H \partial \gamma_{i+2}^H} \right) \quad 5$$

$$\left(\frac{\partial^2 \mu}{\partial \gamma_i^H \partial \gamma_{i+1}^F} \right) \quad 6$$

$$0 \cdot 0 \quad 7$$

As a first approximation,

$$\left(\frac{\partial \mu}{\partial \gamma_i^F}\right)^2, \quad \left(\frac{\partial^2 \mu}{\partial \gamma_i^F \partial \gamma_{i+1}^F}\right), \quad \left(\frac{\partial^2 \mu}{\partial \gamma_i^F \partial \gamma_{i+2}^F}\right) \quad \text{are set equal to zero.}$$

All para interaction terms are zero by symmetry considerations.

To simplify the problem still further, δ can be set equal to zero.

$$M(x) = \begin{bmatrix} 7 & 6 & 7 & 7 & 7 & 6 \\ 6 & 2 & 4 & 7 & 7 & 5 \\ 7 & 4 & 2 & 6 & 5 & 7 \\ 7 & 7 & 6 & 7 & 6 & 7 \\ 7 & 7 & 5 & 6 & 2 & 4 \\ 6 & 5 & 7 & 7 & 4 & 2 \end{bmatrix}$$

$$\begin{bmatrix} 0 & 0 & 0 & 0 & 0 & 0 \\ 0 & \frac{\sqrt{3}}{2}x^2 & 1x^4 & 0 & 0 & 0 \\ 0 & 1x^4 & \frac{\sqrt{3}}{2}x^2 & 0 & 0 & 0 \\ 0 & 0 & 0 & 0 & 0 & 0 \\ 0 & 0 & 0 & 0 & -\frac{\sqrt{3}}{2}x^2 - 1x^4 & 0 \\ 0 & 0 & 0 & 0 & -1x^4 & \frac{\sqrt{3}}{2}x^2 \end{bmatrix}$$

$$M(y) = \begin{bmatrix} 7 & 6 & 7 & 7 & 7 & 6 \\ 6 & 2 & 4 & 7 & 7 & 5 \\ 7 & 4 & 2 & 6 & 5 & 7 \\ 7 & 7 & 6 & 7 & 6 & 7 \\ 7 & 7 & 5 & 6 & 2 & 4 \\ 6 & 5 & 7 & 7 & 4 & 2 \end{bmatrix}$$

$$\begin{bmatrix} 0 & 0 & 0 & 0 & 0 & 0 \\ 0 & \frac{1}{2}x^2 & 0 & 0 & 0 & 1x^5 \\ 0 & 0 & -\frac{1}{2}x^2 & 0 & -1x^5 & 0 \\ 0 & 0 & 0 & 0 & 0 & 0 \\ 0 & 0 & -1x^5 & 0 & -\frac{1}{2}x^2 & 0 \\ 0 & 1x^5 & 0 & 0 & 0 & \frac{1}{2}x^2 \end{bmatrix}$$

$$\begin{bmatrix} 0 & \frac{1}{2} & \frac{\sqrt{3}}{2} & 0 & \frac{\sqrt{3}}{2} & \frac{1}{2} \\ \frac{1}{2} & \frac{\sqrt{3}}{2}x^2 & 1 & \frac{\sqrt{3}}{2} & 0 & 0 \\ \frac{\sqrt{3}}{2} & 1 & \frac{\sqrt{3}}{2} & \frac{1}{2} & 0 & 0 \\ 0 & \frac{\sqrt{3}}{2} & \frac{1}{2} & 0 & \frac{1}{2} & \frac{\sqrt{3}}{2} \\ \frac{\sqrt{3}}{2} & 0 & 0 & \frac{1}{2} & \frac{1}{2} & -1 \\ -\frac{1}{2} & 0 & 0 & \frac{1}{2} & -1 & \frac{\sqrt{3}}{2} \end{bmatrix}$$

$$\begin{bmatrix} 1 & \frac{\sqrt{3}}{2} & \frac{1}{2} & 0 & \frac{1}{2} & \frac{\sqrt{3}}{2} \\ \frac{\sqrt{3}}{2} & \frac{1}{2} & 0 & \frac{1}{2} & 0 & 1 \\ \frac{1}{2} & 0 & \frac{1}{2} & \frac{1}{2} & -1 & 0 \\ 0 & -\frac{1}{2} & \frac{\sqrt{3}}{2} & -1 & \frac{\sqrt{3}}{2} & -\frac{1}{2} \\ \frac{1}{2} & 0 & -1 & \frac{\sqrt{3}}{2} & \frac{1}{2} & 0 \\ \frac{\sqrt{3}}{2} & 1 & 0 & \frac{1}{2} & 0 & \frac{1}{2} \end{bmatrix}$$

$$L_{B_{2g}}^t M \textcircled{x} L_{Au} = [0, .68, -.68, 0, -.68, .68] \begin{bmatrix} 0 & 0 & 0 & 0 & 0 & 0 \\ 0 & \frac{\sqrt{3}}{2} \times 2 & 1 \times 4 & 0 & 0 & 0 \\ 0 & 1 \times 4 & \frac{\sqrt{3}}{2} \times 2 & 0 & 0 & 0 \\ 0 & 0 & 0 & 0 & 0 & 0 \\ 0 & 0 & 0 & 0 & -\frac{\sqrt{3}}{2} \times 2 - 1 \times 4 & \\ 0 & 0 & 0 & 0 & -1 \times 4 & \frac{\sqrt{3}}{2} \times 2 \end{bmatrix} \begin{bmatrix} 0 \\ .675 \\ -.675 \\ 0 \\ .675 \\ -.675 \end{bmatrix}$$

$$= 4 \times .68 \times \frac{\sqrt{3}}{2} \times .675 \times 2 - 4 \times .68 \times 1 \times .675 \times 4$$

$$L_{B_{2g}}^t M \textcircled{y} L_{Au} = [0, .68, -.68, 0, -.68, .68] \begin{bmatrix} 0 & 0 & 0 & 0 & 0 & 0 \\ 0 & \frac{1}{2} \times 2 & 0 & 0 & 0 & 1 \times 5 \\ 0 & 0 & -\frac{1}{2} \times 2 & -1 \times 5 & 0 & \\ 0 & 0 & 0 & 0 & 0 & 0 \\ 0 & 0 & -1 \times 5 & 0 & -\frac{1}{2} \times 2 & 0 \\ 0 & 1 \times 5 & 0 & 0 & 0 & \frac{1}{2} \times 2 \end{bmatrix} \begin{bmatrix} 0 \\ .675 \\ -.675 \\ 0 \\ .675 \\ -.675 \end{bmatrix}$$

= 0

$$\text{Thus } \left(\frac{\partial^2 \mu}{\partial Q_i \partial Q_j} \right) = 1.59 \left(\frac{\partial \mu}{\partial \gamma_i^H} \right)_{HF} - 1.836 \left(\frac{\partial^2 \mu}{\partial \gamma_i^H \partial \gamma_{i+1}^H} \right)$$

in this simple approach.

The idea can easily be extended to include more parameters.

List of References

1. B.L. Crawford and F.A. Miller,
J. Chem. Phys. 17 (1949), 249.
2. D.H. Whiffen,
Phil. Trans. Roy. Soc. A248 (1955), 131.
3. A.C. Albrecht,
J. Mol. Spectry. 5 (1960), 236.
4. S. Califano and B.L. Crawford,
Spectrochim. Acta. 16 (1960), 889.
5. J.R. Scherer and J. Overend,
Spectrochim. Acta. 17 (1961), 719.
6. J.R. Scherer,
Spectrochim. Acta. 20 (1964), 345.
7. J.R. Scherer,
Spectrochim. Acta. 21 (1965), 321.
8. J.H. Callomon, T.M. Dunn and I.M. Mills,
Phil. Trans. Roy. Soc. A259 (1966), 499.
9. J.C. Duinker and I.M. Mills,
Spectrochim. Acta. 24A (1968), 417.
10. J.C. Duinker,
Ph. D. Thesis, University of Amsterdam (1964).
11. I.M. Mills,
Spectrochim. Acta. 19 (1963), 1585.

12. G. Herzberg,
Infrared and Raman Spectra of Polyatomic Molecules,
van Nostrand, New York (1945).
13. K. Radcliffe and D. Steele,
Spectrochim. Acta. 25A (1969), 597.
14. R.A.R. Pearce,
Ph. D. Thesis, University of London (1972).
15. R.A.R. Pearce, D. Steele and K. Radcliffe,
J. Mol. Structure 15 (1973), 409.
16. R.S. Mulliken,
J. Chem. Phys. 23 (1955), 1997.
17. E.B. Wilson, Jr., J.C. Decius and P. Cross,
Molecular Vibrations, McGraw-Hill, New York (1955).
18. D.R.J. Boyd and H.C. Longuet-Higgins,
Proc. Roy. Soc. A213 (1952), 55.
19. R.D. Mair and D.F. Hornig,
J. Chem. Phys. 17 (1949), 1236.
20. N. Herzfeld, C.K. Ingold and H.G. Poole,
J. Chem. Soc. (1946), 316.
21. D.F. Heath and J.W. Linnett,
Trans. Faraday Soc. 44 (1948), 556 and 873.
22. I.M. Mills,
Spectrochim. Acta. 19 (1963), 1585.

23. C.A. Coulson,
Victor Henri Memorial Volume, p.15, Desoer, Liege (1947).
24. C.A. Coulson, J. Duchesne and C. Manneback,
Victor Henri Memorial Volume, p.33, Desoer, Liege (1947).
See also [17].
25. S. Brodersen and A. Langseth,
Mat. Fys. Skr. Dan. Vid. Selsk, 1, (1956).
26. P. Torkington,
J. Chem. Phys. 17 (1949), 357.
27. W. Sawodny,
J. Mol. Spectry. 30 (1969), 56.
28. J.L. Duncan and I.M. Mills,
Spectrochim. Acta. 20 (1964), 1089.
29. J.L. Duncan,
Spectrochim. Acta. 20 (1964), 1197.
30. H. Eyring, J. Walter and G.E. Kimball,
Quantum Chemistry, John Wiley and Sons, New York (1944).
31. P. Torkington,
Trans. Faraday Soc. 47 (1951), 105.
32. S. Brodersen,
Pure Appl. Chem. 4 (1962), 27.
33. B. Crawford, Jr., and J. Overend,
J. Mol. Spectry. 12 (1964), 307.

34. J.H. Schachtscheider and R.G. Snyder,
Spectrochim. Acta. 19 (1963), 117.
35. D. Steele,
Theory of Vibrational Spectroscopy, W.B. Saunders,
Philadelphia (1971).
36. J.C. Decius and E.B. Wilson,
J. Chem. Phys. 19 (1951), 1409.
37. J. Heiklen,
J. Chem. Phys. 36 (1961), 721.
38. S. Brodersen and A. Langseth,
Mat. Fys. Skr. Dan. Vid. Selsk. 1, No. 5 (1958).
39. R.M. Badger and L.R. Zumwalt,
J. Chem. Phys. 6 (1938), 711.
40. S.L. Gerhard and D.M. Dennison,
Physical Review 43 (1933), 197.
41. B.P. Stoichoff,
Can. J. Phys. 32 (1954), 339.
34 (1956), 350.
42. L. Nygaard, I. Bojesen, T. Pedersen and J. Rastrup-Andersen,
J. Mol. Struct. 2 (1968), 209.
43. L. Nygaard, E.R. Hansen, R.L. Hanson, J. Rastrup-Andersen and
G.O. Sørensen,
Spectrochim. Acta. 23A (1967), 2813.
44. A. Almenningen, O. Bastiansen, R. Seip and H.M. Seip,
Acta. Chem. Scand. 18 (1964), 2115.

45. D. Peters,
J. Chem. Phys. 38 (1963), 561.
46. G.W.C. Kaye and T.H. Laby,
Tables of Physical Constants, Longmans, London (1968).
47. M. Gussoni and G. Zerbi,
J. Mol. Spectry, 26 (1968), 485.
48. S. Califano,
Molecular Spectroscopy - IX (report of Ninth European
Congress on Molecular Spectroscopy), Butterworths,
London (1969).
49. J. Aldous and I.M. Mills,
Spectrochim. Acta. 18 (1962), 1073.
50. J. Overend and J.R. Scherer,
J. Chem. Phys. 32 (1960), 1720.
51. F.A. Miller,
J. Chem. Phys. 24 (1956), 996.
52. D.C. Smith, E.E. Ferguson, R.L. Hudson, and J.R. Nielsen,
J. Chem. Phys. 21 (1953), 1475.
53. D.W. Scott et al.,
J. Am. Chem. Soc., 78 (1956), 5457.
54. D.H. Whiffen,
J. Chem. Soc. (1956), 1350.
55. D. Steele, E.R. Lippincott, and J. Xavier,
J. Chem. Phys. 33 (1960), 1242.

56. G. Nonnenmacher and R. Mecke,
Spectrochim. Acta. 17 (1961), 1049.
57. D.W. Scott et al.,
J. Chem. Phys. 38 (1962), 532.
58. J.H.S. Green, W. Kynaston and H.M. Paisley,
J. Chem. Soc. (1963), 473.
59. A. Hatta and K. Kozima,
Bull. Chem. Soc. Japan 43 (1970), 704.
60. E.E. Ferguson, R.L. Collins, and J.R. Nielsen,
J. Chem. Phys. 21 (1953), 1470.
61. E.E. Ferguson, R.L. Hudson, J.R. Nielsen and D.C. Smith,
J. Chem. Phys. 21 (1953), 1457.
62. A. Stojiljkovic and D.H. Whiffen,
Spectrochim. Acta. 12 (1958), 47.
63. D. Steele, W. Kynaston and H.A. Gebbie,
Spectrochim. Acta. 19 (1963), 785.
64. P.N. Gates, K. Radcliffe and D. Steele,
Spectrochim. Acta. 25A (1969), 507.
65. E.E. Ferguson, R.L. Hudson, J. Rud Nielsen,
J. Chem. Phys. 21 (1953), 1727.
66. J.R. Nielsen, C-Y Liang and D.C. Smith,
Disc. Faraday Soc. 9 (1950), 177.

67. E.E. Ferguson,
J. Chem. Phys. 21 (1953), 886.
68. J.R. Scherer, J.C. Evans, and W.W. Muelder,
Spectrochim. Acta. 18 (1962), 1579.
69. D. Steele,
Spectrochim. Acta. 18 (1962), 915.
70. E.E. Ferguson, R.L. Hudson, and J.R. Nielsen,
J. Chem. Phys. 21 (1953), 1464.
71. D. Steele and D.H. Whiffen,
Spectrochim. Acta. 16 (1959), 368.
72. L. Delbouille,
J. Chem. Phys. 25 (1956), 182.
73. L. Delbouille,
Bull. Acad. Roy. Sc. Belg. V. 44 (1958), 971.
74. D. Steele and D.H. Whiffen,
Trans. Faraday Soc. 55 (1959), 369.
75. A. Sournia,
Ph. D. Thesis, University of Science and Technology
of Languedoc, 1972.
76. J. Dale,
Acta. Chem. Scand. 11 (1957), 640.
77. J.E. Katon and E.R. Lippincott,
Spectrochim. Acta. 15 (1959), 627.

78. D. Steele and E.R. Lippincott,
J. Mol. Spectry. 6 (1961), 238.
79. G.V. Peregudov,
Opt. Spectry. 9 (1960), 155.
80. G. Zerbi and S. Sandroni,
Spectrochim. Acta. 24A (1968), 483.
81. G. Zerbi and S. Sandroni,
Spectrochim. Acta. 24A (1968), 511.
82. G. Zerbi and S. Sandroni,
Spectrochim. Acta. 26A (1970), 1951.
83. B. Pasquier and J.M. Lebas,
J. Chim. Phys. 64 (1966), 765.
84. J. Dahr,
Indian J. Phys. 7 (1932), 43.
85. J. Trotter,
Acta. Cryst. 14 (1961), 1135.
86. A. Hargreaves and S.H. Rizvi,
Acta. Cryst. 15 (1962), 365.
87. R. Grinter,
Mol. Phys. 11 (1966), 7.
88. J. Dale,
Acta. Chem. Scand. 11 (1957), 650.

89. H. Suzuki,
Bull. Chem. Soc. Japan 32 (1959), 1340.
90. R.A. Hoffmann and P.O. Kinell,
Arch. Sci. Geneva 11 (1958), 228.
91. K. Moebius,
Z. Naturforsch. 20a (1965), 1093.
92. O. Bastiansen,
Acta. Chem. Scand. 3 (1949), 408.
93. G. Casalone, C. Mariani, A. Mugnoli and M. Simonetta,
Mol. Phys. 15 (1968), 339.
94. C.A. Coulson,
Ind. Chim. Belge 2 (1963), 149.
95. G.B. Wheland,
Resonance in Organic Chemistry. John Wiley (1955).
96. R.M. Barrett,
Ph. D. Thesis, University of London, 1972.
97. R.M. Barrett and D. Steele,
J. Mol. Structure 11 (1972), 105.
98. K. Radcliffe and D. Steele,
Spectrochim. Acta. 25A (1969), 597.
99. M. Davies,
Infrared Spectroscopy and Molecular Structure, Elsevier,
1963.

100. D.A. Long, R.B. Gravenor and M. Woodger,
Spectrochim. Acta. 19 (1963), 937.
101. D.A. Long and R.B. Gravenor,
Spectrochim. Acta. 19 (1963), 951.
102. B.L. Crawford, Jr.,
J. Chem. Phys. 20 (1952), 977.
103. J.C. Decius,
J. Chem. Phys. 20 (1952), 1039.
104. I.M. Mills, W.L. Smith and J.L. Duncan,
J. Mol. Spectry. 16 (1965), 349.
105. D.F. Hornig and D.C. McKean,
J. Phys. Chem. 59 (1955), 1133.
106. C.A. Coulson,
in Proceedings of the Conference on Molecular Spectroscopy,
E. Thornton and H.W. Thompson (Editors), Pergamon, London
(1959), 183.
107. L.M. Sverdlov,
Opt. Spectry. (USSR) 8 (1960), 316.
108. M.A. Kovner and B.N. Snegirev,
Opt. Spectry. (USSR) 10 (1961), 165.
109. L.A. Gribov,
Intensity Theory for Infra Red Spectra of Polyatomic
Molecules, Consultants Bureau (1964).
110. L.A. Gribov and E.M. Popov,
Opt. Spectry. 12 (1962), 304.

111. L.A. Gribov,
Soviet Physics - Doklady 4 (1960), 847.
112. S. Saeki and K. Tanabe,
Spectrochim. Acta. 25A (1969), 1325.
113. K. Tanabe and S. Saeki,
Spectrochim. Acta. 26A (1970), 1469.
114. D. Steele and W. Wheatley,
J. Mol. Spectry. 32 (1969), 260.
115. R.P. Bell, H.W. Thompson and E.E. Vago,
Proc. Roy. Soc., A192 (1948), 498.
116. H. Spedding and D.H. Whiffen,
Proc. Roy. Soc. A238 (1956), 245.
117. C.W. Young, R.B. Duvall and N. Wright,
Anal. Chem. 23 (1951), 709.
118. D.H. Whiffen,
Spectrochim. Acta. 7 (1955), 253.
119. Y. Kakiuti,
J. Chem. Phys. 25 (1956), 777.
120. F.E. Dunstan and D.H. Whiffen,
J. Chem. Soc. (1960) 5221.
121. Y. Kakiuti, Y. Suzuki and M. Ondo,
J. Mol. Spectry. 27 (1968), 402.
122. D. Steele and D.H. Whiffen,
Trans. Far. Soc., 56 (1960), 5.